Investigation of the effect of preparation methods on the surface properties, dissolution rate and stability of solid dispersions

Peng KE

A thesis submitted for the degree of Doctor of Philosophy

The School of Pharmacy, University of London

29-39 Brunswick Square, London,

WC1N 1AX

2010

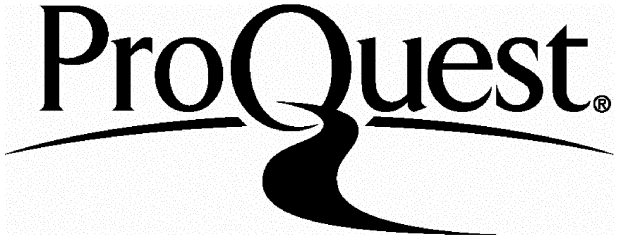

Plagiarism Statement

This thesis describes research conducted in the School of Pharmacy, University of London between 2005 and 2009 under the supervision of Professor G. Buckton and Dr. S. Gaisford. I certify that the research described is original and that any parts of the work that have been conducted by collaboration are clearly indicated. I also certify that I have written all the text herein and have clearly indicated by suitable citation any part of this dissertation that has already appeared in publication.

Peng Ke

Signature

08/02/10

Date

Abstract

Formation of solid dispersions is frequently used as an important strategy to improve the dissolution properties of poorly water-soluble drugs. In addition, the carriers used to prepare solid dispersions can help stabilise the drugs if they appear in the amorphous form. Preparation method is a key factor affecting both dissolution and stability of a solid dispersion due to difference in dispersivity and molecular arrangement of the drug and carrier. The objectives of this work were to study the effect of preparation method on the physical properties, stability and dissolution of solid dispersions containing indometacin as the model drug. The surface energy state of the solid dispersions during aging was studied. Molecular mobility at the surface and in the bulk of the solid dispersions was determined and correlated to the stability and dissolution properties. Solid dispersions with different carriers were prepared using different methods and their stability and dissolution profiles were investigated.

Solid dispersions of polyvinylpyrrolidone (PVP) and indometacin (30%:70%) were prepared using melt quenching or ball milling and subjected to physical aging. It was found that the surface energy state of the samples decreased as a function of time and this energy reduction was temperature dependent, as determined using inverse gas chromatography (IGC). A novel method which utilises the retention volume of decane (V_{max}) to measure surface relaxation by IGC was developed. The surface relaxation of PVP and indometacin solid dispersions prepared by ball milling, spray drying, and melt quenching were measured using the V_{max} method and compared to their bulk relaxation measured using step-scan differential scanning calorimetry. The surface appeared to have higher molecular mobility than the bulk irrelevant of which preparation method was used. However, preparation method appeared to have an impact on both surface and bulk molecular mobility. Relaxed samples sorbed less moisture and dissolved slower than the initial ones as determined by dynamic vapor sorption and dissolution experiments, and a faster bulk relaxation rate led to a more significant reduction in the dissolution rate of the solid dispersions after aging. The glass fragilities of the systems were obtained using the heating rate dependence of the glass transition method. The values were found to be preparation method specific. The zero mobility temperatures (T_0), of the systems were calculated using the fragility parameter. With a similar glass transition temperature (T_g) at c.a. 64 to 67 °C, the T_0 of the ball milled, spray dried and melt quenched samples were -4.2, 16.7, and 21.6 °C, respectively. Physical stability test showed that the ball milled sample was the least stable while the melt quenched one was the most, which correlated well with their T_0 values. It is suggested that T_0 might be a better indicator of stability than T_g. Carriers which were miscible or immiscible with indometacin were used to form solid dispersions with the drug prepared by ball milling and spray drying. Improved stability and dissolution rate of indometacin were noticed. Intermolecular interactions between the drug and carrier were found to be crucial to the stability of the amorphous drug no matter whether the carrier was miscible or not. The effect of preparation methods on the dissolution rate of the sample was found to be carrier dependent.

To my grandma

To my dearest parents and wife

Acknowledgements

Firstly, I would like to express my sincere gratitude to Professor Graham Buckton for his supervision. He has always provided me support when I needed it. His advice and guidance has been very important to me throughout my PhD. I would also like to acknowledge Dr. Simon Gaisford for his help, and encouragement.

I am grateful to Ms Isabel Goncalves for all her technical support and help.

Thanks must also go to the various members in the research group that I have been so lucky to work with during my PhD – Hisham, Cyrus, Naziha, Ana Caterina, Karolina, Meena, Liang, Luis, Rita and Viraj. I would also like to thank my other friends and colleagues in the School of Pharmacy: Adeline, Boom, Enosh, Fang, Felipe, Gabby, Hala, Hamid, Hanene, Jon, Ketan, Nui, Qian, Sami, Suchada and Winnie. Without their support and company, the time in the school will be inevitably less joyful. Thanks are also due to Mr Owen Shephard. The demonstration work for his practical was very enjoyable.

Special thanks to Dr. Susumu Hasegawa for his help and support on the IGC experiments. Thanks also go to Dr. Hasegawa for all the invaluable knowledge and experience that he shared with me when we worked together. I would also like to thank Dr. Hardyal Gill for his help on IGC and Mr David McCarthy for helping me taking the SEM images.

Last but most importantly, I would like to dedicate this thesis to my parents, my wife and my late grandma whom I owe so much. Without all your love, encouragement, and selfless giving, I would never have been able to come this far. I love you all forever.

Table of contents

Chapter 4 Influence of preparation methods on surface and bulk structural relaxation of solid solutions

List of figures

Chapter 1

Chapter 2

Chapter 3

Chapter 4

Chapter 5

List of tables

Chapter 1

Chapter 2

Chapter 3

Chapter 4

Chapter 5

List of abbreviations

A	Surface area
a	Interaction surface area
AFM	Atomic force microscopy
AN^*	Acid (electron acceptor) number
β	Distribution of the relaxation time constant
B	A material parameter related to its fragility
BET	Brunauer-Emmett-Teller equation
C	Concentration
C_h	Saturation solubility of the drug in the boundary layer
C_p	Heat capacity
C_s	Saturation solubility of the drug in the stationary layer
δ	Solubility parameter
ΔE_{Tg}	Activation enthalpy of structural relaxation at glass transition temperature
ΔG_{ads}	Free energy of sorption
ΔH_∞	Maximum enthalpy of relaxation
ΔH_m	Fusion of melting
D	Strength parameter
D_d	Diffusion coefficient of the drug in the solubulising fluids of the gastrointerstinal tract
DN	Base (electron donor) number
DSC	Differential scanning calorimetry
DVS	Dynamic vapour sorption
g	Constant regarding acceleration due to gravity
η	Viscosity
F	Exit flow rate of the carrier gas
FID	Flame ionised detector
FTIR	Fourier transform infrared
γ	Surface free energy
γ^d	Dispersive component of surface free energy
γ^p	Polar component of surface free energy
GIT	Gastrointestinal tract
h	Boundary layer
H	Enthalpy
HPMCAS	Hydroxypropyl methylcellulose acetate succinate
IGC	Inverse gas chromatography
IM	Indometacin
IMC	Isothermal microcalorimetry
j	The James-Martin compressibility correction factor
K_A	Acidic (electron accepting) parameter
K_D	Basic (electron donating) parameter

L	Stationary layer
m	Fragility parameter
M	Sample mass
MCC	Microcrystalline cellulose
MMP	Molecular Modeling Pro software
MSE	Modified stretched exponential function
NSAID	Non-steroidal anti-inflammatory drug
φ	Volume fraction
P	Power
PVP	Polyvinylpyrrolidone
PHPMA	Poly[N-(2-hydroxypropyl)methacrylate]
q	Heating/cooling rate
q_c	Critical cooling rate
ρ	Density
R	Gas constant
RH	Relative humidity
R_q	Root-mean-square roughness
S	Entropy
SEM	Scanning electron microscopy
SMCC	Silicified microcrystalline cellulose
τ	Relaxation time
τ_0	The shortest possible relaxation time
τ_{In}	Induction time needed to form a nucleus
t	Time
T	Temperature
T_0	zero mobility temperature
T_∞	The temperature of infinite relaxation time
T_a	aging temperature
TAM	Thermal Activity Monitor
T_b	boiling point
TCD	Thermal conductivity detector
T_g	Glass transition temperature
T_k	Kauzmann temperature
T_m	Melting point
V	Volume
V_{com}	Retention volume measured using the center mass point of the peak
V_{max}	Retention volume measured using the maximum point of peak
V_n	Retention volume
VTF	Vogel-Tammann-Fulcher equation
W_{ads}	Work of adsorption
WLF	William-Landel-Ferry equation
y_i	Distance of point i from the centre line

Chapter 1

Introduction

1.1 Introduction

Oral drug delivery is the most convenient route for drug administrations with the solid oral dosage forms being preferred over other types of dosage forms because of their smaller bulk size, better stability, accurate dose, and ease of preparation (Vasconcelos *et al.*, 2007). Drugs used in solid oral dosage forms need to have good solubility in order to result in good bioavailability. However, based on some recent estimates, about 40% of present drugs are poorly soluble in water, and even up to 60% of compounds coming directly from synthesis encounter the same problem (Merisko-Liversidge, 2002). Therefore, finding an efficient approach to increase the dissolution and solubility of the drugs is a major challenge for pharmaceutical researchers.

Formation of solid dispersions is an efficient strategy for dissolution rate improvement (Sekiguchi and Obi, 1961; Chiou and Riegelman, 1971; Serajuddin, 1999). The particle size of the drugs in a solid dispersion can reach as low as molecular level which helps to improve the dissolution rate (Vasconcelos *et al.*, 2007). In addition, the drugs can exist in the amorphous forms which in theory represent the most energetic solid state of a material, and hence they should have the biggest advantage in terms of apparent solubility (Hancock and Zografi, 1997). However, a potential risk of solid dispersions is recrystallisation of the amorphous drug resulting in an alteration of the dissolution properties of the products upon storage. Molecular mobility is considered to be the governing factor affecting the crystallisation rate of the drug from the carrier matrix; therefore, in this thesis, studies were conducted to understand molecular mobility and some other relevant properties in relation to the physical stability and dissolution properties of solid dispersions. Since crystallisation is surface initiated in many cases (Wu and Yu, 2006), focus was also placed on the study of surface molecular mobility. An efficient method for probing the surface molecular mobility is needed in the pharmaceutical research field: hence a new method regarding the use of inverse gas chromatography (IGC) was developed for this purpose. The surface molecular mobility detected using this method was compared to the bulk molecular mobility measured using differential scanning calorimetry (DSC).

Previous studies have shown that the physical properties of an amorphous material could be greatly affected by the way it is prepared (Surana *et al.*, 2004), but the understanding of the effect of preparation methods on solid dispersions is limited (Patterson *et al.*, 2007). In this thesis, emphasis was also placed on the influence of preparation methods on the physical properties, stability and dissolution of the solid dispersions. Thus studies were undertaken to prepare stable solid dispersions with rapid dissolution rate using a variety of methods and the effect of carrier type was studied. The interaction between the drug and carrier in relation to the physical stability of the solid dispersions was also investigated.

1.2 Permeability-solubility drug classification

In order for solid state drugs which are administrated orally to elicit an efficient therapeutic effect, they have to be absorbed into the systemic circulation first so as to reach the site of action. The effect of absorption is usually determined by two factors: the dissolution and solubility of the drug, and its permeability through the intestinal membrane. According to the solubility and permeability levels, drugs can be divided into four different classes (Amidon *et al.*, 1995).

	Class I	Class II	Class III	Class IV
Permeability	High	High	Low	Low
Solubility	High	Low	High	Low

Table 1.1: *The Biopharmaceutical Classification system of drugs (adapted from Amidon et al., 1995).*

According to the classification (Table 1.1), the strategies needed for different classes of drugs for absorption improvement become clear: 1) class I drugs have both high permeability and solubility, hence no special treatment is required; 2) for class II drugs, the limiting step is the dissolution and solubility of the drugs, therefore, the most effective strategy is to increase the amount of drug dissolved at the absorption site; 3) for class III drugs, permeability is the limiting step which is opposite to the class II drugs, and increasing membrane permeability of the drugs will be crucial; 4) for class IV drugs, both dissolution and permeability needed to be improved. It should be noted that for class IV drugs, improving dissolution and solubility is more efficient than improving the permeability. The drug dissolved at the absorption site can range over six orders of magnitude while permeability ranges only 50 fold (Curatolo, 1998). Therefore the potential for absorption improvement of the class IV drugs will be larger by improving their dissolution and apparent solubility.

1.3 Drug absorption

Drug absorption is closely related to bioavailability, but they are not exactly the same. Absorption is related to the movement of a drug into the bloodstream whereas bioavailability is related to drug concentration in the blood circulation. Since drug absorption is the prerequisite of bioavailability, it is necessary to briefly explain how drugs are absorbed. There is a four-step process for the successful transport of a drug from an oral dosage form into the general circulation. These are: 1) bringing the drug to its absorption site; 2) releasing the drug into the aqueous liquid in the gastrointestinal tract (GIT); 3) transport of the dissolved drug through the membranes of the GIT; and 4) movement of the drug into the general circulation from the site of absorption. The order of the first two steps is interchangeable, which means that the drug may dissolve either before or after getting to its absorption position.

1.3.1 Bringing the drug to its site of absorption

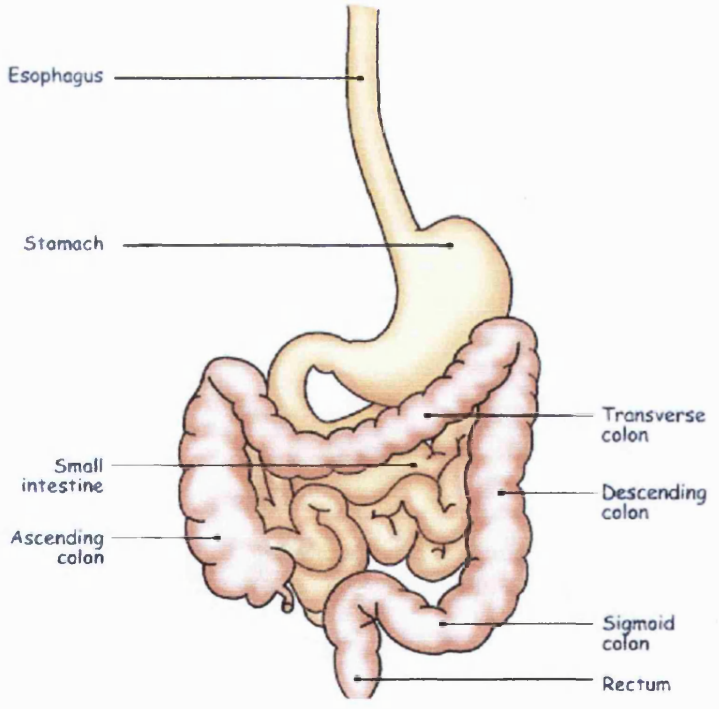

Figure 1.1: *Diagram of the gastrointestinal tract (divided into esophagus, stomach, small intestine, colon and rectum).*

The gastrointestinal tract (Figure 1.1) is the place where an oral dosage form can be absorbed after swallowing. During this passage the dosage form will encounter great anatomical and physiological variations. Among these variables, the two most important ones affecting the delivery of the drug from its oral dosage form are: 1) hydrogen ion concentration, which exhibits a 10^7 fold difference between the mucosal fluids of the stomach and the intestine (pH 1 to 3 in the stomach, pH 5 to 7 in the duodenum, and pH 7 to 8 in the jejunum and ileum); and 2) available surface area for absorption, which changes dramatically at different regions of the GIT.

The stomach acts as a barrier for protecting the intestine from extreme conditions, such as the small difference in pH, temperature, osmolarity, or viscosity from the normal conditions of the intestine. Thus, the stomach will delay emptying until these conditions become normal. Due to factors such as increased membrane surface area and decreased thickness, the intestine is a more preferable site for drug absorption than the stomach. The rate at which the drug gets to the small intestine can significantly affect its rate of absorption. Therefore, gastric-emptying rate may be one of the important factors determining the absorption rate of a drug. Factors like light physical activity will stimulate stomach emptying, but strenuous exercise will delay emptying (Bachrach, 1959; Davenport, 1971). Posture, emotional state, and numerous pathological conditions of a patient can all alter the gastric-emptying rate and hence the absorption rate of a drug in the body. Other drugs taken together may also affect the gastric-emptying rate by influencing gastrointestinal motility.

Absorption is not the only process that occurs along the GIT. The aqueous fluids of the GIT can degrade and different enzymes can metabolise a drug before it reaches the absorption site. This is especially the case for drugs that structurally resemble nutrients, such as polypeptides, nucleotides, or fatty acids which are liable to undergo enzymatic degradation. Conversely, the metabolic and degradative processes can also help to increase the bioavailability of drugs in some cases. These degradative processes play an important role for some prodrugs in aiding them to achieve their bioavailability. Hence

the metabolism and degradation of a drug can either reduce or enhance its extent of availability.

1.3.2 Getting the drug into solution

In order to be absorbed, the drug has to be in solution following release from its dosage form after it gets to the absorption site. The dissolution process of a drug is illustrated schematically in Figure 1.2 below.

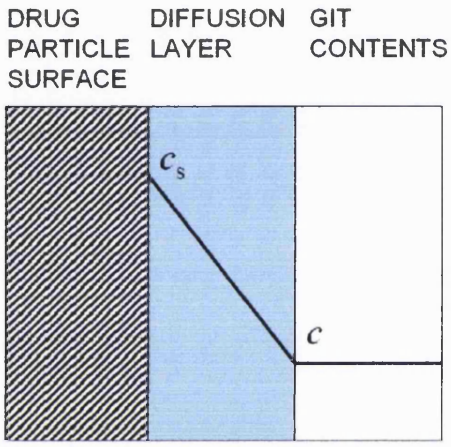

Figure 1.2: *Schematic diagram of the dissolution process.*

The Noyes-Whitney equation, which relates the rate of dissolution of solids to the properties of the solid and the dissolution, can be used here to describe this process:

$$\frac{dW}{dt} = \frac{D_d A(C_s - C)}{L} \qquad \text{Equation 1.1}$$

where $\frac{dW}{dt}$ is the rate of dissolution, A is the surface area of the drug particles, C is the concentration of drug in the bulk fluids of the gastrointestinal tract, C_s is the saturation solubility of the drug in the stationary layer, D_d is the diffusion coefficient of the drug in the solubilising fluids of the gastrointestinal tract, and L is the thickness of the stationary layer of solvent around the drug particle. This equation presupposes that the

drug dissolved uniformly from all surfaces of the particles, which are assumed to be spherical and having the same size. Additionally, L is assumed to be constant while both L and C_s are taken to be independent of particle size. Based on the equation, it is indicated that the possibilities for improving dissolution rate are to increase the surface area available for dissolution by decreasing the particle size of the solid compound and/or by optimising the wetting characteristics of the compound surface, to decrease the boundary layer thickness, to ensure sink conditions for dissolution and to improve the solubility of the drug in the gastrointestinal tract (Leuner and Dressman, 2000). Among the methods stated above, there are two which have been widely applied to improve the bioavailability of poorly soluble drugs: increasing the surface area, and increasing the solubility. These approaches will be discussed in the following section.

1.3.2.1 Effective surface area of the drug particles

It is generally accepted that the smaller the drug particles, the greater will be the surface area for a given amount of drug (i.e. a greater specific surface area). Therefore, based on the Noyes-Whitney equation, the dissolution rate will increase as particle size decreases. This is commonly applied for drugs with poor water solubility. For example, the therapeutic dose of griseofulvin was reduced to 50% by micronisation and it was also found that a more constant and reliable blood level was produced (Atkinson *et al.*, 1962). The commercial dose of spironolactone was also decreased to half by just a slight reduction of particle size (Levy *et al.*, 1963). It is shown that in many cases, enhancement of drug absorption can be increased several fold if the particle size of the drug is reduced (Bauer *et al.*, 1962).

Particle-size reduction is usually achieved by: conventional grinding, ball milling, fluid energy micronisation, controlled precipitation by change of solvents or temperature, application of ultrasonic waves and spray drying. It should be emphasised that not all the resultant fine particles can have faster dissolution and absorption behaviors. This is due to the possible aggregation and agglomeration of the particles caused by their increased surface energy and the subsequent stronger van der Waal's attraction between

nonpolar molecules. This was first demonstrated by Lin *et al.* (1968), who showed that the in vitro dissolution rates of micronised griseofulvin and glutethimide were slower than those of their coarser particles.

1.3.2.2 Solubility of the drug

The physical and chemical properties of a drug can be modified to increase its saturation or apparent solubility. Therefore, according to the Noyes-Whitney equation, improvement in dissolution rate of the drug can be achieved. Some examples are described as follow:

Salt form of drugs

In the majority of cases, the dissolution rate and solubility of the salt form of a drug is greater than that of its nonionised form. Hence the formation of the salt form of a drug is one of the alternatives to improve its dissolution, solubility and bioavailability. Indeed, many studies have been done regarding this area. For example, a weakly acidic drug p-aminosalicylic acid, having three salt forms (potassium, calcium, and sodium), was found to exhibit much higher dissolution rates in the salt forms compared to the nonionised drug. The bioavailability of the acid form was only about 77% of that of the salt forms (Pentikaninen *et al.*, 1974). In general, the solubility of the salt is related on the counterion, and the smaller the counterion, the more soluble the salt is.

Drugs in ionised forms

The ionised form of a drug is expected to be more soluble than the nonionised form in the aqueous fluids of the GIT. Since the pH of the gastrointestinal fluids will determine the ionised or nonionised state of a drug, pH should be considered as a factor for influencing the solubility of a drug. Equation 1.1 can be rewritten here as:

$$\frac{dW}{dt} = \frac{DA(C_h - C)}{L} \qquad \text{Equation 1.2}$$

All the terms are described as before, excluding C_h which is the saturation solubility of the drug in the boundary layer, h, at any pH. When C_h=C_s, the drug exists as its nonionised form after it dissolves in the aqueous fluids. In this case, for a weak acid:

$$C_h = [HA] + [A^-] = C_s \left(1 + \frac{K_a}{[H^+]}\right) \qquad \text{Equation 1.3}$$

$$\frac{dW}{dt} = \frac{DA}{L}\left\{C_s\left(1 + \frac{K_a}{[H^+]}\right) - C\right\} \qquad \text{Equation 1.4}$$

Similarly, for a weak base:

$$C_h = [HB^+] + [B] = C_s\left(1 + \frac{[H^+]}{K_a}\right) \qquad \text{Equation 1.5}$$

$$\frac{dW}{dt} = \frac{DA}{L}\left\{C_s\left(1 + \frac{[H^+]}{K_a}\right) - C\right\} \qquad \text{Equation 1.6}$$

Therefore, the dissolution rate of weak acid increases as pH increases, while that of weak base decreases as the pH decreases.

Solvate formation

The solvate of a drug is another variable which will affect its saturation solubility. It is known that the anhydrous, hydrated and alcoholated forms of a drug have different solubility and dissolution rates.

Polymorphism and amorphous state of drugs

Many materials are able to exist in different crystalline forms and this is known as polymorphism (Yu, 2001). Generally, the dissolution rate and apparent solubility of different polymorphs are different. For example, indometacin has three different

crystalline forms (γ, α, and β) and each of them exhibits different dissolution behavior, while α has the fastest dissolution rate and best apparent solubility, β is the next and γ is the worst. Polymorphism can cause variations in melting point, stability, density and other properties depending on the escaping tendency of the molecules from a particular crystalline structure. The amorphous form is the least stable form of a material and it has the highest internal energy; therefore, amorphous drug tends to exhibit better dissolution rate compared to its corresponding crystalline forms. Detailed discussion about the amorphous form will be given in the next section. Suffice to say, in most cases, the more apparently soluble form has the least thermodynamical stability. Hence, the balance between the stability and solubility of a drug is an important consideration for pharmaceutical researchers.

Complex formation

Drug-cyclodextrin complexes can be prepared by adding the drug and excipient together, and as a result solubility of a drug can be increased. Cyclodextrins, which exist in γ, α, and β forms, are a group of structurally-related cyclic oligosaccharides that have an apolar cavity and hydrophilic external surface. Complexation of a drug with cyclodextrin is purely noncovalent and occurs due to physical forces such as electrostatic interactions, van der Waals forces, hydrophobic interactions, hydrogen bonding and release of enthalpy rich water molecules (Loftsson and Brewster, 1996). The complex structure protects the drug molecule from unfavorable environments in some respects.

Solid dispersions

Preparation of solid dispersions is also a useful approach to increase the dissolution rate and apparent solubility of poorly soluble drugs (Serajuddin, 1999). More discussion about the use of solid dispersions for bioavailability improvement will be given in section 1.5.

1.3.3 Gastrointestinal membrane transport of drugs

Once a drug gets into the aqueous liquids at the absorption site in the GIT, it must cross the membrane (Figure 1.3) to reach into the general circulation. It is the membrane that keeps all of the cell contents securely inside, but which allows some materials to pass in and out the cell via several different mechanisms. One of the main mechanisms by which drugs are transported through the cell membrane is passive diffusion. This is based on the difference in the concentration of the drug outside and inside of the cell. The greater the difference is, the greater the diffusion of the drug from outside to the inside of the cell. Since the membrane is highly lipidic in structure, the partitioning ability of the drug is dependent on its lipophilic properties. Thus, the oil-water partition coefficient of the drug can be used to test whether it can move through the membrane. As mentioned above, the pH of the aqueous fluids will determine the ionised and unionised state of the drug. Since unionised molecules are more lipid-soluble and can diffuse across membranes more easily, the pH of the fluids will play an important role during passive diffusion. Besides passive diffusion, facilitated diffusion is another mechanism for transport of drugs, whereby carrier proteins will transport water soluble drugs through the membrane. The drugs are transported from a higher concentration to a lower one. The third mechanism is the one involving the transport of inorganic ions such as sodium and potassium and many drugs, which are moved through the cell membrane by active transport. In this process, a membrane pump such as sodium/potassium ATPase pump plays a role to transport chemicals against a concentration gradient into the cell. Unlike diffusion, this is an energy demanding process. The fourth mechanism involves drugs crossing the membrane via pores. This mechanism is dependent on the size of the pore and the molecular weight of the drug. Finally, the membrane can also engulf the drug, forming a vesicle and then transport it across the membrane into the cell. This process is called pinocytosis.

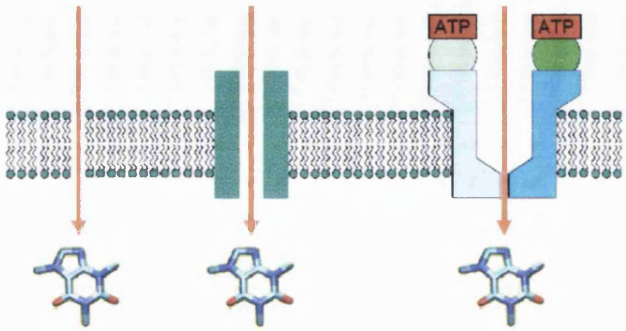

Figure 1.3: *A scheme of membrane transport of drugs.*

1.3.4 Movement of the drug into the general circulation

Moving the drug away from the site of absorption is also an important process. Drugs that have crossed the gastrointestinal membrane are primarily removed as a function of blood flow (Benet *et al.*, 1976). If there is no blood flow, the passage of a drug across the membrane will cease. If the blood flow decreases, it might decrease the rate or removal of passively absorbed drugs and also interfere with active transport systems owing to the reduction of the supply of oxygen to the tissues. Thus, the possible effect of blood flow rate (especially alterations in the flow rate) on the availability of drugs is an important factor for considerations in pharmaceutical research.

1.4 Solids in the amorphous state

Unlike crystalline solids which have three-dimensional long range order, amorphous solids exhibit short range order and the arrangement of molecules is more random (Figure 1.4). Amorphous solids can be treated as a supercooled liquid in which the molecules can vibrate and rotate as those in liquid, while in the case of crystalline solids these movements appear to a lesser extent or are even absent due to their rigid arrangement. Therefore, the molecules in amorphous solids have a higher internal energy than those in the crystal forms (Imaizumi *et al.*, 1980). In pharmaceutical research and development, the amorphous state is commonly used to improve the solubility and bioavailability of poorly soluble drugs because it is more energetic compared to the corresponding crystalline forms (Hancock and Parks, 2000).

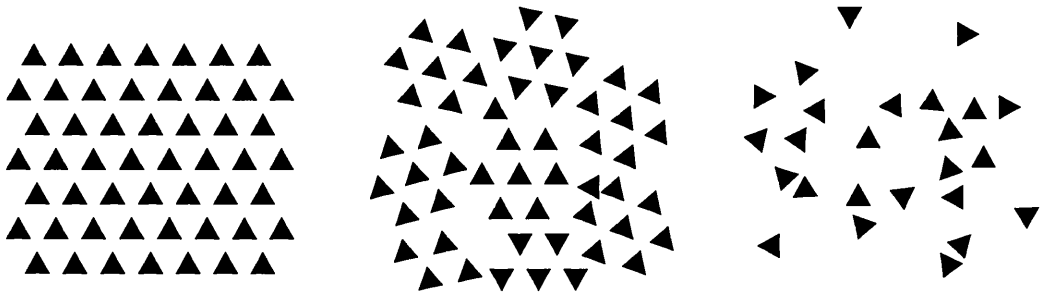

Figure 1.4: *Schematic representation of the structure of an amorphous solid (adapted from Yu, 2001).*

1.4.1 The formation of amorphous solids

In the past, the term "*glass*" has been used to refer to an amorphous solid produced by rapid quenching of a melt. In recent times, the definition for glass has been broadened (Zallen, 1983). A glass is now defined as an amorphous solid which displays a short-range order and exhibits a glass transition. An amorphous solid exists in the glassy state when below the glass transition temperature (T_g).

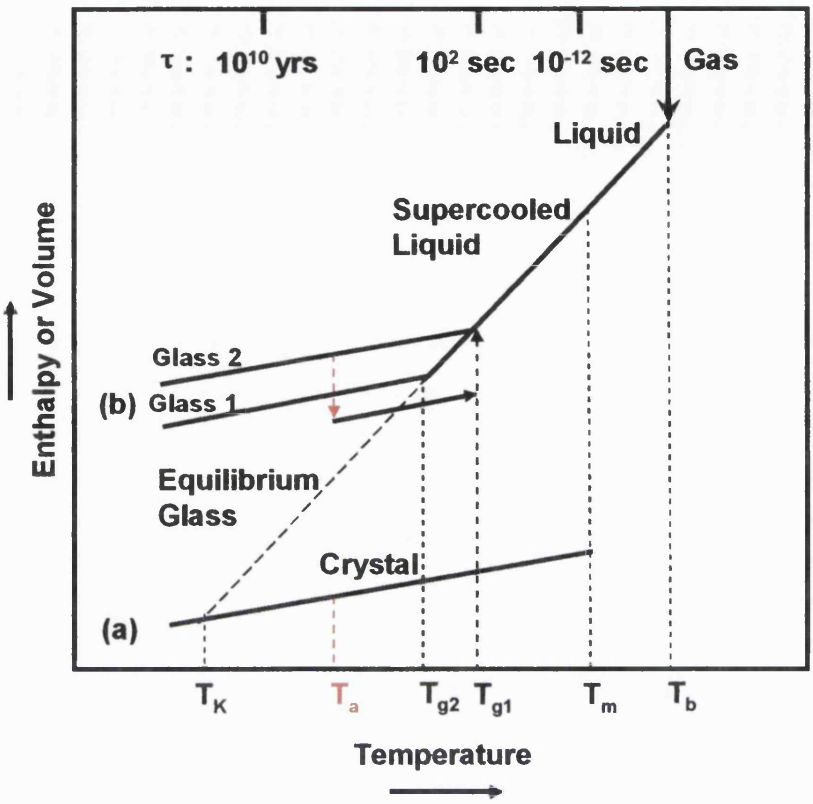

Figure 1.5: *A scheme representing the change of enthalpy and volume during cooling of a material from its gas or liquid form which can either crystallise (route a) or form a glass (route b). The thermodynamic and dynamic properties of a glass depend on the cooling rate. T_b is the boiling point, T_m is the melting point, T_g is the glass transition temperature, T_a is the aging temperature, T_k is the Kauzmann (or zero mobility) temperature and τ is the relaxation time.*

In Figure 1.5 the change of enthalpy (H) and volume (V) during the formation of a glass (or a crystal) by cooling a gas (or liquid) is shown. A sharp break or bend in H and V indicates a change of phase during the decrease of temperature. The first change of phase happens at T_b where the gas turns into liquid and abrupt changes of H and V are accompanied. Continuous cooling of the liquid decreases the H and V in a continuous way, until eventually T_m is reached. At this point, if the cooling rate is sufficiently low, the liquid would take route (a) and crystallise into a solid in a discontinuous way. Crystallisation is a first-order phase transition, and as shown in the figure, an abrupt

change in H and V is noticed. Meanwhile, if the cooling rate is sufficiently high, T_m is bypassed without incident and route (b) is taken to the solid state. The liquid that manages to get below T_m without crystallisation is called a supercooled liquid (or an amorphous solid in the rubbery state). As the liquid is further cooled, its viscosity increases and the molecules eventually rearrange so slowly that molecular configurations can not happen in the allowed timescale depending on the cooling rate. The H and V will begin to deviate abruptly (but continuously) from the equilibrium value at a certain temperature and the structure of the liquid appears 'frozen' resulting a glass. The temperature at which deviation happens is called the glass transition temperature. Below T_g, H and V of the glass continue to decrease but in a lower temperature dependence similar to the crystal state. It should be noted that the slower the liquid is cooled, the longer the time available for molecular configurations at each temperature, and hence the lower it can get before deviation from the equilibrium (Debenedetti and Stillinger, 2001). In another words, T_g increases as the cooling rate increases (Bruning and Samwer, 1992).

The critical cooling rate (q_c) for glass formation from the melt to prohibit crystallisation can be defined using the following equation (Hilden and Morris, 2004):

$$q_c = \frac{T_m - T_n}{\tau_{1n}} \qquad \text{Equation 1.7}$$

where τ_{1n} is the induction time needed to form a nucleus at temperature, T_n. Therefore, a sufficiently fast cooling rate is needed to make sure the time spent to cool from T_m to T_n is shorter than the induction time at T_n in order to avoid crystallisation. The fastest cooling rate for cooling a bulk sample or micronised droplets in quench cooling or spray freeze drying is about 10^7 Ks^{-1}. If the sample can be made into thin film with a thickness of less than 100 nm, the cooling rate can reach as fast as 10^{14} Ks^{-1} (Debenedetti, 1996).

Turnbull (1987) has used a three-step process to describe the general procedure for

preparing amorphous solids from a crystalline material, namely: 1) energising the material (such as melting, milling, etc.); 2) de-energising of the material, for example, quench cooling; and 3) kinetically trapping the amorphous form which often continues from step two. Melt quenching is a commonly used technique for the preparation of amorphous solids. This technique involves melting of a solid material into liquid followed by rapid cooling using liquid nitrogen. Other techniques for amorphous state formation include mechanical activation of a crystalline mass (such as milling), precipitation from solution and solvent evaporation (such as spray drying and lyophilisation (Hancock and Zografi, 1997; Craig *et al.*, 1999). All these techniques fall into the three-step procedure described by Turnbull (1987).

1.4.2 Physical properties of the amorphous state

The crystalline state and the liquid state above the melting temperature of a material are thermodynamically stable, but the amorphous state of the material is not. Since the amorphous solid has a higher free energy compared to its crystalline state, it will tend to crystallise into the stable form. However, the amorphous solid can be kinetically stable if the time needed for the solid to crystallise or reach an equilibrium state is significantly longer than the timeframe of the experiment or shelf life of the product. Separated by the glass transition temperature, an amorphous solid can exist in two different physical states: the glassy state and the rubbery state. The kinetic stability of the physical states is different. During the glass transition, properties such as modulus of elasticity, specific volume, enthalpy, heat capacity, viscosity and thermal expansion coefficient change dramatically. In the rubbery state, these properties exhibit high temperature dependence. The molecular mobility in the rubbery state is very high, which helps crystallisation and hastens chemical reactions, hence it is very likely that the amorphous solid is kinetically unstable. In contrast, in the glassy state, the temperature dependence of the properties stated above is less extreme and the molecular mobility of the amorphous solid is much reduced. At a sufficiently low temperature, the crystallisation and chemical reactions would be extremely slow or sometimes absent. Thus, under these conditions, the amorphous solid is kinetically stable.

1.4.3 Molecular mobility and relaxation of the amorphous solids

Molecular mobility of amorphous solids can be linked with their physical instability or crystallisation rate from the amorphous state. The temperature dependence of molecular mobility has been found to be similar to that of the degradation rate for some amorphous drugs (Shamblin *et al.*, 1999; Guo *et al.*, 2000), therefore it could be used to predict the onset of crystallisation of amorphous products (Aso *et al.*, 2000, 2004). On the other hand, in a recent study, researchers suggested a method to establish coupling between reaction rate (i.e., crystallisation onset or growth rates) and relaxation time of an amorphous solid at higher temperatures and extrapolate such correlations to lower temperatures (Bhugra *et al.*, 2006). Based on these correlations, reasonable predictions can be made for a pharmaceutical product at temperatures where reaction rates are greatly reduced, without actually running a long term stability experiment. A good correlation was found between the molecular mobility measured above and below T_g using different techniques (Bhugra *et al.*, 2006). In another study, the same group of researchers have further confirmed the coupling between crystallisation onset times and molecular mobility above T_g and it is possible to exploit the correlation to below T_g for prediction of a crystallisation onset time of the amorphous product. The predictions were found to be in good agreement with the experimental data (Bhugra *et al.*, 2008b). These examples demonstrate perfectly the important meaning of molecular mobility in relation to the stability of an amorphous solid.

Although molecular mobility can be studied according to the viscosity of an amorphous solid, it is usually quantified in terms of molecular relaxation time τ. The relaxation time is defined as the time taken for a particular motion to take place (Angell, 1995). Molecular relaxation may be classified as structural relaxation (α-relaxation) and Johari-Goldstein relaxation (β-relaxation) according to the relaxation modes (Kawakami and Pikal, 2005). Structural relaxation corresponds to the motion of the whole molecule such as diffusional motion and viscous flow, while β-relaxation is related to the intramolecular motion such as rotation of a side chain on a polymer or motion of a small group of atoms on a large molecule that is not coupled or correlated with motion of the

whole molecule (Kawakami and Pikal, 2005).

Since the relaxation time can be used to represent the rate at which the molecular configuration of the amorphous solid adapts during changes of temperature, the risk of crystallisation during glass formation is reduced if the relaxation time is longer or at least similar to the experimental timeframe (for example, in the case of spray drying and melt quenching). Also, relaxation times at the storage conditions can be used to predict the shelf life (Andronis and Zografi, 1997; Bhugra *et al.*, 2007). As discussed above in section 1.4.1, the molecular configuration of amorphous solids changes dramatically during the cooling process. On the top of Figure 1.5, an indication of this change is given separately at the T_m, T_g and a temperature well below the T_g (T_g-50 °C). The relaxation time can vary from the order of 10^{-12} seconds at T_m, 10^2 seconds at T_g to 10^{10} years at T_g-50 °C.

Relaxation time can be characterised according to many properties which include macrostructural, or bulk properties such as free volume, enthalpy, mechanical and dielectric response, as well as microstructural or molecular scale properties that can be measured using spectroscopic and scattering techniques (Hutchinson, 1995). There are many techniques available for measuring these properties for the determination of the molecular mobility below the T_g. They include enthalpy recovery experiments, which are determined by differential scanning calorimetry (Hancock *et al.*, 1995; Matsumoto and Zografi, 1999), isothermal microcalorimatry (Liu *et al.*, 2002), thermally stimulated depolarisation current spectroscopy (Shmeis *et al.*, 2004), dielectric relaxation (Bhugra *et al.*, 2008a), nuclear magnetic resonance (Aso and Yoshioka, 2006), and dynamic mechanical analysis (Andronis and Zografi, 1997). Some surface properties can be used to reflect the surface molecular mobility, such as the surface roughness and deformation which can be probed by atomic force microscopy (AFM) (Kerle *et al.*, 2001). Apart from AFM, in polymer science, some other probing techniques which focus on the surface properties can be used to detect the surface molecular mobility as well. For instance, friction force microscopy can be used to study surface viscoelastic relaxation

(Hammerschmidt *et al.*, 1999) and near-edge X-ray absorption fine structure spectroscopy can also be applied (Liu *et al.*, 1997). Relaxation is always accompanied with the loss of energy, it will be interesting to study the change of surface free energy in order to acquire molecular mobility information on the surface. The use of inverse gas chromatography to study the surface energy change during relaxation is shown and discussed in the result chapters.

A commonly used approach for the study of relaxation is through physical aging of the amorphous solids. During physical aging, the properties of an amorphous solid can change as a function of storage time. The degree and rate of the property change can be measured to obtain information on molecular mobility. An example was shown in Figure 1.5, which provides a representative scheme of the change of specific volume and enthalpy stored at an aging temperature T_a below T_g. When the glass is stored at T_a, there will be a driving force for the excess thermodynamic quantities (i.e. specific volume and enthalpy) to reduce towards equilibrium as shown by arrow A. By measuring the decreasing rate of the specific volume or enthalpy, the molecular mobility of the glass at T_a can be estimated. As the aging temperature is reduced, a longer time-scale would be needed for the glass to reach the equilibrium state. After reheating the aged glassy solid, the volume or enthalpy losses can be recovered at or near T_g (Petrie, 1972). DSC is a useful technique for the measurement of the relaxation enthalpy. The relaxation enthalpy of the glass measured after aging for different period of time can be fitted to the Kohlraush-Williams-Watts (KWW) equation to obtain the relaxation time τ and the distribution of the relaxation time constant β (the use of KWW equation for fitting of the DSC data will be explained in Chapter 3) The enthalpy recovery experiment by DSC is one of the most commonly used methods for detecting the molecular mobility of an amorphous solid in the non-equilibrium state (Six *et al.*, 2001).

Based on the behaviour of the molecular relaxation time and the viscosity above the glass transition temperature, Angell (1991) classified the amorphous solids into two types: strong glasses and fragile glasses. The strong glasses show Arrhenius behaviour

while the fragile ones exhibit significant deviation from the exponential Arrhenius relaxation in the viscosity/relaxation versus temperature plot. A study has shown that the fragile amorphous solid at temperature just above T_g would have a relaxation time decrease by one magnitude for every 3 °C temperature rise while for strong amorphous solid, 33 °C temperature rise is needed to achieve the same kind of effect (Slade and Levine, 1991). It is worth pointing out that most pharmaceutical amorphous compounds exhibit moderately fragile to fragile behaviour (Crowley and Zografi, 2001).

The non-Arrhenius temperature dependence of properties of the fragile glasses above T_g can be described by the Vogel-Tammann-Fulcher (VTF) equation:

$$\tau = \tau_0 \exp(\frac{B}{T - T_\infty}) \qquad \text{Equation 1.8}$$

where relaxation time τ can also be replaced by viscosity η, τ_0 represent the shortest possible relaxation time, B is a material parameter related to its fragility, and T_∞ is the temperature of infinite relaxation time. The empirical William-Landel-Ferry (WLF) equation is usually used to describe relaxation times or viscosity in polymers and it is mathematically equivalent to the VTF equation:

$$\log(\frac{\eta_T}{\eta_{T_g}}) = -\frac{C_1 \cdot (T - T_g)}{C_2 + (T - T_g)} \qquad \text{Equation 1.9}$$

where η_t and η_{tg} are related to the viscosity of the glass at the experimental and glass transition temperatures. For polymers with $T_m/T_g \approx 3/2$, the constants C_1 and C_2 are 17.44 and 51.6 respectively, which are usually referred to as "universal" constants (Slade and Levine, 1991).

A representative scheme indicating the relaxation time and viscosity for the strong and fragile glasses is shown in Figure 1.6. It shows the significant meaning of T_g to the

molecular mobility of a glass solid because it acts as a dividing line for high and low mobility of the glass. According to this, some studies proposed that a temperature at T_g-50 °C would be an ideal storage condition for most fragile glasses because their molecular mobility will be greatly reduce at this point. Therefore, a high T_g will be always preferred for the stability of an amorphous solid. Another thermodynamic temperature for the storage of an amorphous solid is the Kauzmann temperature which is also defined as the zero mobility temperature T_0. At this temperature, the configurational entropy of the amorphous solid would reach zero and its total entropy would approach that of a crystal. Theoretically, it should be the most ideal storage temperature for amorphous solids.

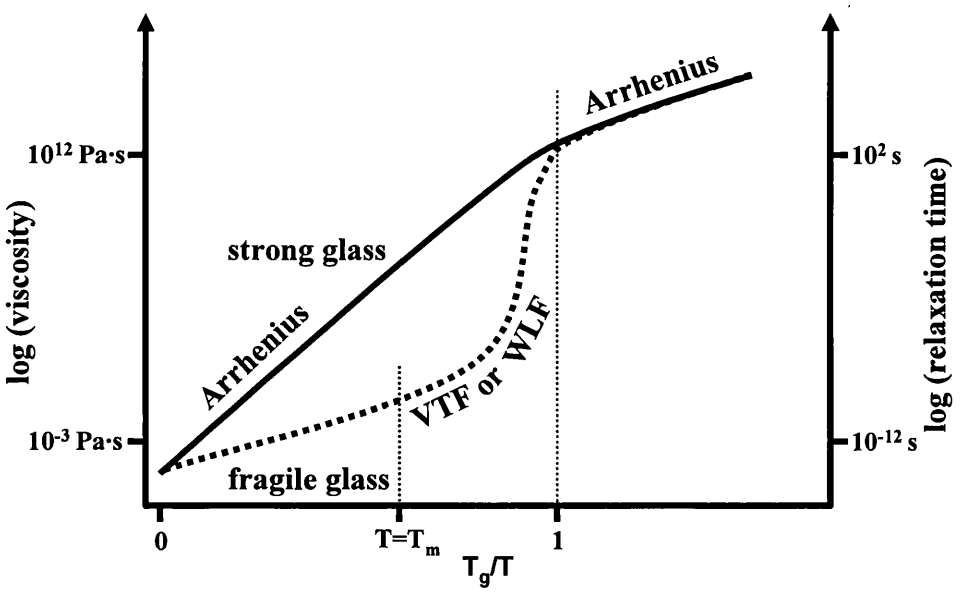

Figure 1.6: *Relaxation time and viscosity of fragile or strong glasses as a function of temperature relative to T_g (adapted from van Drooge, 2006).*

1.4.4 Plasticisation effect of amorphous solids

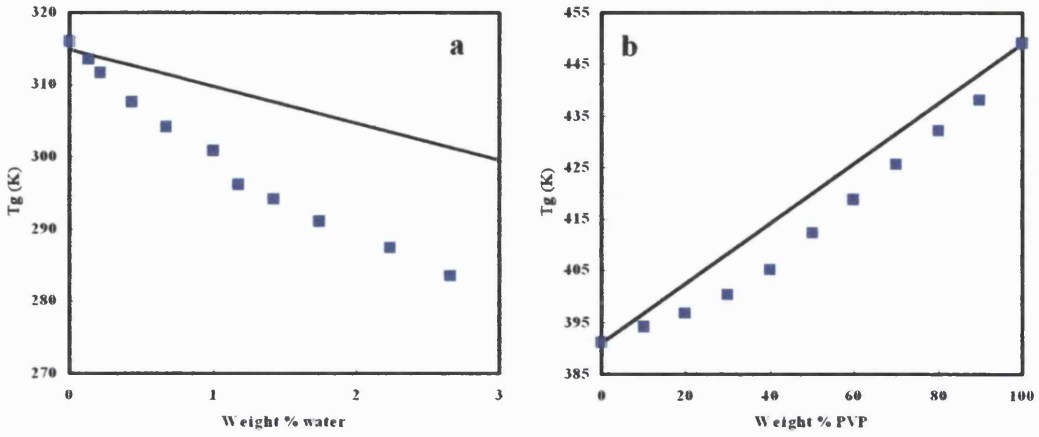

Figure 1.7: *T_g of mixtures of two components (■) in different weight percentages: a) the T_g of amorphous indometacin as a function of the percentage of water (Andronis et al., 1997); b) the T_g of amorphous sucrose as a function of the percentage of PVP (Taylor and Zografi, 1998). The solid lines represent the theoretical prediction of T_g based on the Gordon-Taylor equation.*

Amorphous solids, in most cases, would not appear alone; they always exist together with other components. The simplest example is that after an amorphous solid is stored in a humidified condition, the water sorbed to the solid would make the system become a multi-component system. Therefore, a question frequently asked in pharmaceutical research is whether the additional components affect the structures and thermodynamics, and if they cause any other unpredicted changes to an amorphous solid (Craig *et al.*, 1999; Yu, 2001). The glass transition temperature, as the most important characteristic parameter for amorphous solids, would be the main concern in this question. Small molecules such as water, methanol, ethanol can increase the molecular mobility (or viscosity) of an amorphous solid (like the effect of a lubricant) when they are mixed together, and as a result, the T_g of the solid would be lowered. The extent of the lowered T_g would depend on the concentration of the components. Figure 1.7a shows a very good example of the T_g of amorphous indometacin with different amount of water

(w/w). In contrast, if the amorphous solid is mixed with another component which has a higher T_g (usually a polymer with high molecular weight), the T_g of the solid is increased and this phenomenon is called anti-plasticisation. Figure 1.7b shows the effect of high molecular weight polymer, polyvinylpyrrolidone (PVP), on the T_g of a disaccharide, trehalose (Taylor and Zografi, 1998).

The Gordon-Taylor equation, which is based on free volume theory, was proposed to predict the T_{gmix} value of a binary mixture (Gordon and Taylor, 1952):

$$T_{g_{mix}} = \varphi_1 T_{g_1} + \varphi_2 T_{g_2} \qquad \text{Equation 1.10}$$

where T_{g1} and T_{g2} are the glass transition of the two components individually φ_1 and φ_2 are their volume fractions. The Gordon-Taylor equation is based on the assumption that no interaction between the two components exists and it can be modified into the following equation:

$$T_{g_{mix}} = \frac{(w_1 T_{g_1}) + (K w_2 T_{g_2})}{w_1 + (K w_2)} \qquad \text{Equation 1.11}$$

where:

$$K = \frac{T_{g_1} \rho_1}{T_{g_2} \rho_2} \qquad \text{Equation 1.12}$$

The constant K is related to the free volume of the two components, which can be calculated basing on the Simha Boyer rule (Simha and Boyer, 1962). The parameter ρ is the density of each component and it is in the unit of kg/m^3. It is deemed that any deviation of the experimental data from the line predicted by the Gordon-Taylor equation is a sign of non-ideal mixing between the two components (Craig *et al.*, 1999).

In a study conducted by Taylor and Zografi (1998), it was found that a negative deviation in T_g occurred because the intramolecular hydrogen bond among the individual component was more favoured than the intermolecular one between the two components. In another study (Patterson *et al.*, 2007), a positive deviation of T_g was observed when two components form strong intermolecular hydrogen bonding, while the individual component did not have enough intramolecular interaction tendency.

1.4.5 Crystal nucleation and growth

As long as stable crystalline forms exist, all amorphous solids would eventually crystallise when cooled below the melting temperature because of the thermodynamic metastability of the amorphous state. The first step in crystallisation involves nucleation. The formation of nuclei is not well understood but could be related to dust, impurities or small agglomerates of molecules of the compound normally a few nanometers in size (Byrn *et al.*, 1999). The onset of crystallisation is governed by the formation of nuclei and once the nucleation barrier is crossed, the amorphous system is physically unstable since the system is on its direction to the more stable crystalline state, which is recognised as crystal growth. During crystal growth, small crystals are formed followed by gradual incorporation of nuclei to form larger crystals. Both nucleation and crystal growth together govern the physical stability of the amorphous solids (Bhugra and Pikal, 2008).

The tendency for an amorphous solid to crystallise in an experimental time scale is determined by the characteristic time τ_1 which is related to the time required for a given volume fraction of amorphous state to crystallise at a constant temperature after a rapid cooling. If the effect of viscosity is neglected, when τ_1 increases, the probability of a critical nucleus formation decreases, and τ_1 decreases exponentially with decreasing temperature. However, in reality, viscosity would slow down nucleation because high viscosity would make the aggregation of nuclei become difficult. Hence, τ_1 is also dependant on τ_2, the average time needed for molecules to rearrange in the glass state and it is a representative of the molecular mobility. The schematic relationship between

τ_1 and τ_2 is shown in Figure 1.8. A faster nucleation rate happens at lower temperature while high molecular mobility is achieved at elevated temperatures. Therefore, the maximum crystallisation rate lies between T_g and T_m, at a point where the nucleation rate equals the molecular mobility rate (Salekigerhardt and Zografi, 1994). This is why normally in a DSC scan, the crystallisation exotherm happens between the T_g and T_m.

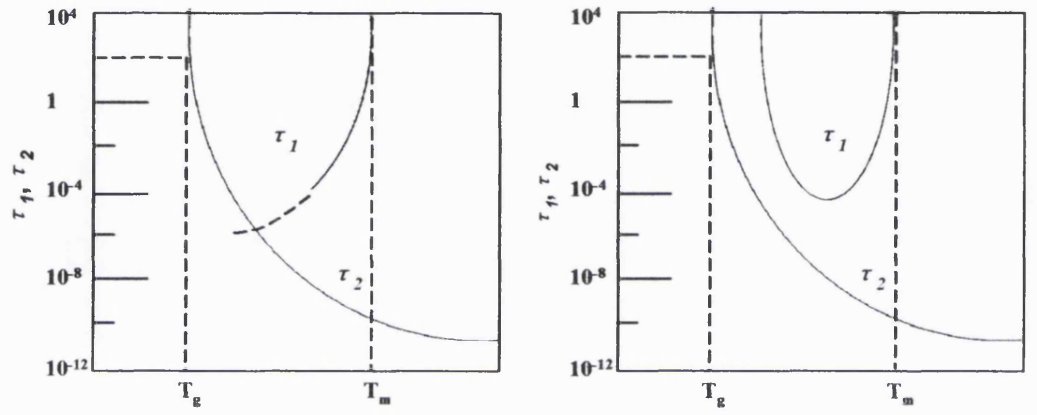

Figure 1.8: *Schematic of the relationship between τ_1 and τ_2 a) system not taken into account of viscous effects and b) realistic system with the effects of viscosity (adapted from Angell, 1988).*

1.4.6 Characterisation techniques for amorphous solids

When a liquid is cooled into the rubbery or glassy state, a multitude of physical properties of the material change including viscosity, density, heat capacity, X-ray diffraction and diffusion behaviour (Hancock and Zografi, 1997). Therefore, techniques which can measure these property changes are capable of detecting the presence of the amorphous state. Some of the most commonly used techniques are:

1. Diffraction techniques are probably the most commonly used techniques for amorphous state determination. Because the lack of long-range three-dimensional molecular order of the amorphous state, its irregular diffraction of electromagnetic radiation can be compared to that of the crystalline state which usually show sharp

diffraction peaks. There are conventional, small-angle and wide angle X-ray powder diffraction (XRPD) techniques available depending on the purpose of the measurements (Hancock and Zografi, 1997).

2. Spectroscopic techniques such as nuclear magnetic resonance, Raman, infrared, near infrared and electron spin resonance are useful for the characterisation of amorphous systems because of their high structural resolution.
3. Differential scanning calorimetry is a very powerful technique for amorphous state characterisation (Kerc and Srcic, 1995). During a DSC measurement, samples are heated using a constant heating rate, and thermal events can be detected. These thermal events include glass to rubber transition, crystallisation, melting or degradation. In recent years, the development of Hyper-DSC (Saunders *et al.*, 2004) and modulated-temperature DSC (Craig *et al.*, 2000) have helped to make the determination and quantification of amorphous contents more sensitive and accurate.
4. Isothermal microcalorimetry is useful to measure the crystallisation energy of amorphous materials as well as some other phase transitions and thermal decompositions. In an isothermal microcalorimetry experiment, samples are held at a constant temperature and any heat produced or absorbed by them is measured as a function of time (Gaisford and Buckton, 2001). It is different to the other calorimetry method, DSC, which measures the heat-flow as a function of temperature
5. Solution calorimetry works on the basis that the heat of solution is different for the crystalline and the amorphous states of a sample (Buckton and Darcy, 1999). The dissolution of crystalline materials is usually endothermic while that of the amorphous ones is exothermic.
6. Water vapour sorption is also a useful technique for amorphous content determination. The amorphous and crystalline materials usually have different water uptake patterns. Many amorphous materials are able to crystallise after sorbing a criticial amount of water because the sorbed water can help to lower their T_g and facilitate the crystallisation (Buckton and Darcy, 1999). If it is necessary,

organic solvents such as methanol, ethanol etc. can be used instead of water to trigger the crystallisation.

7. Specific volumes of the rubber and glass states are different, which could be reflected by the density values. Though accurate measurements of volume or density are difficult, gas or liquid displacement pycnometry can be used to measure the density of materials and quantify the amorphous contents (Salekigerhardt *et al.*, 1994).

In some cases, bulk analytical techniques such as DSC, XRPD or Isothermal microcalorimetry might not be useful if the amorphous content is mainly located at the surface of a solid. Therefore, techniques such as inverse gas chromatography (Newell *et al.*, 2001), microthermal anaylsis (Craig *et al.*, 2002), atomic force microscopy (Ward *et al.*, 2005) and Raman mapping (Patterson *et al.*, 2007) are all very useful for surface amorphous contents qualification or quantification.

1.5 Solid dispersions for drug delivery

As mentioned previously in section 1.3, formation of salts, particle size reduction and other methods are able to improve the bioavailability of poorly soluble drugs, but there are practical limitations for these techniques. Salt formation is only possible for some weakly acidic or weakly basic drugs (Serajuddin, 1999; Karavas *et al.*, 2006). In some cases, the salts can not increase the dissolution rate because of the reconversion into the respective acid or base forms due to hydrolysis. A major disadvantage of the salt formation method is that the newly formed salt might represent a new chemical entity which requires additional clinical trials. As far as particle size reduction is concerned, there is a practical limit to the size that can be achieved. Moreover, if the particle size is too small, the powders might become tacky and form agglomerates, which might jeopardise the dissolution property of the drug in some cases.

Solid dispersions, first developed and prepared by Sekiguchi and Obi (1961), are a useful method which can overcome the above-mentioned limitations. they are currently one of the most promising strategies for the enhancement of the oral bioavailability of poorly water-soluble drugs. Chiou and Riegelman (1971) defined a solid dispersion as a solid matrix consisting of at least two components: generally a hydrophilic carrier and a hydrophobic drug. The carrier can be either crystalline or amorphous and the drug can be dispersed molecularly, in amorphous particles (clusters) or in crystalline particles.

The dissolution advantages of solid dispersions include: 1) reduced particle size which could be as small as molecular level giving rise to a high surface area; 2) improved wettability by the use of a hydrophilic carrier; 3) higher porosity which favours a rapid drug release; and 4) drugs in amorphous state which have a higher apparent solubility compared to their crystalline forms. Moreover, the use of solid dispersions can help to prevent recrystallisation of the amorphous drugs. The stability advantages of solid dispersions will be explained in section 1.5.3.

1.5.1 Classifications of solid dispersions

After nearly 50 years of continuing research and development, many solid dispersion formulations have been prepared. According to the type of the carriers used, molecular arrangements and addition of surfactants or not, there are three generations of solid dispersions classified (Figure 1.9).

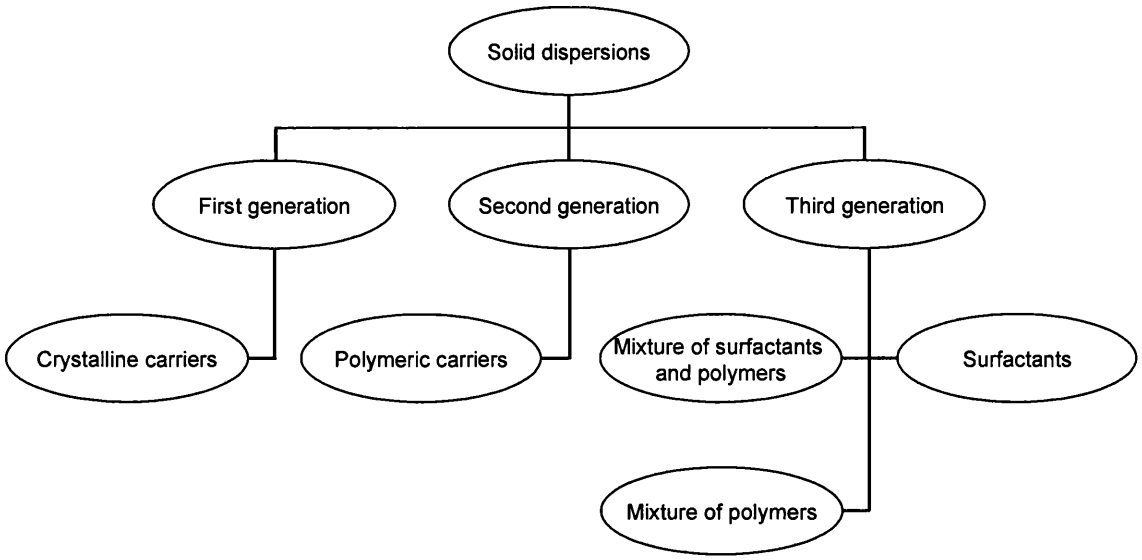

Figure 1.9: *Classification of three generations of solid dispersions (adapted from Vasconcelos et al., 2007).*

The first generation of solid dispersions is the ones prepared using crystalline carriers, and in the solid dispersions, at least one of the components (drug and carrier) exists in crystalline form. The crystalline carriers used here include urea (Sekiguchi *et al.*, 1964) and sugars (Kanig, 1964). The best example of the first generation solid dispersion is the eutectic mixture prepared by Sekiguchi and Obi (1961), the first solid dispersion prepared in the literature. In the study, sulphathiazole and urea were melted together at a temperature above the eutectic point and then cooled in an ice bath. The dispersed drugs were trapped within the carrier matrix in the resultant solid eutectic, which was then milled to reduce the particle size. A eutectic mixture usually contains two crystalline materials and it has a melting point lower than that for any other ratio of mixtures of the

same materials. Later, some other solid dispersion systems were developed by preparing solid solutions through molecular dispersions instead of eutectic mixtures (Kanig, 1964; Chiou and Riegelman, 1969). These solid dispersions also fall into the first generation category because they appeared in crystalline states.

The disadvantage of forming crystalline solid dispersions is that it makes the dissolution of drug slower than when in the amorphous state. Therefore, the second generation of solid dispersions appeared, which contain amorphous drugs and carriers. These kinds of solid dispersions are the most commonly used nowadays. The carriers used here are mostly polymeric, such as ethyl cellulose, polyvinylpyrrolidone, polyethyleneglycols, hydroxypropylmethyl cellulose and so forth. Depending on the molecular arrangement between the drug and carriers, the second generation solid dispersions could be divided into solid solution, solid suspension or a mixture of both. The differences among the three sub-groups are detailed here below:

1. In a solid solution, the drug and carrier are totally miscible (soluble) resulting as a homogeneous one phase system, which means that the crystalline drug is completely dissolved into the carriers.
2. In a solid suspension, the carrier and drug have very limited solubility. The system is still amorphous but the drug and carrier do not form a homogeneous structure, which means it is a two-phase system.
3. The third type system is a mixture of solid solution and solid suspension. A heterogeneous structure occurs as the drug is both dissolved and suspended in the carrier.

Compared to the first generation of solid dispersion, the second generation provides a better dissolution of drug since the drug particle size can be reduced to nearly a molecular level and the drug can exist in its amorphous form.

Recently, a third generation of solid dispersions has been developed by using a carrier

which has surface activity or self-emulsifying properties. The solid dispersions contain either a surfactant carrier or both polymeric and surfactant carriers. It was found that these types of systems could help to improve the bioavailability of poorly-soluble drug significantly and at the same time help to improve the stability of the drug for a long period of time (Dannenfelser *et al.*, 2004).

There is also another way to classify solid dispersions based on the miscibility between the drug and carrier. Accordingly, Augsburger and Hoag (2008) have broadly divided solid dispersions into two categories: solid dispersion and solid solution. Despite the general meaning of solid dispersion described above, herein, solid dispersion also refers to the system that amorphous drug is dispersed (immiscible) in the carrier matrix and the system is usually distinguished by two separate T_g values of the drug and the carrier respectively. Meanwhile, solid solution refers to the system that the amorphous drug is miscible with the carrier and only one T_g exists for the system. Hence forth, this classification of solid dispersions is applied in order to better distinguish the molecularly dispersed solid dispersions to the others.

1.5.2 Preparation methods for solid dispersions

There are generally two main methods for the preparation of solid dispersions, one is through the use of liquid phase such as melting and solvent methods (Serajuddin, 1999) and the other one is through the solid phase such as milling (Patterson *et al.*, 2007).

1.5.2.1 Melting method

The melting method is widely used for preparing solid dispersions and some of the first developed solid dispersions for pharmaceutical applications were prepared by this method. Generally, in a melting process, drug and carrier are melted together and the high molecular mobility of the components allows them to be incorporated into each other. Cooling is usually followed to solidify the melted mixtures and the processes include ice bath agitation, immersion in liquid nitrogen, stainless steel thin layer spreading followed by a cold draught, spreading on plates with dry ice and so forth.

Pulverisation is often needed to break down the cake into small particles after cooling.

However, there are some significant drawbacks which might limit the application of the melting method. Firstly, degradation can happen to some drugs and carriers during heating to temperatures needed to melt them. Secondly, incomplete miscibility between drug and carrier may occur because of the high viscosity of some carriers in the molten state. Therefore, some modified melting methods such as hot-stage extrusion, have been developed in order to avoid these problems (Chokshi *et al.*, 2005). In this approach, the carrier and drug used are firstly heated together to the melting temperature or a temperature lower than that for a short period of time, and then extrusion at high rotational speed is followed. Finally, the resulting materials are cooled at room temperature and milled. In some cases, the use of carbon dioxide as a plasticiser can greatly reduce the heating temperature which makes this method even more useful to thermosensitive compounds.

1.5.2.2 Solvent method

In the solvent method, drug and carrier are dissolved in a solvent (usually volatile organic solvents) and then the solvent is removed leading to the production of solid dispersions. Solvent methods are very useful for thermosensitive compounds because the solvent evaporation usually occurs at a low temperature. There are many different types of solvent methods which are determined by the solvent removal process, such as vacuum drying, heating on a hot plate, slow evaporation of the solvent at low temperature, the use of a rotary evaporator, use of nitrogen, spray drying, freeze drying and the use of supercritical fluids. Among these methods, spray drying and freeze drying are probably the most commonly used. In a spray drying process, the carrier and drug are dissolved or suspended in a certain solvent and then through an atomiser, the solution is sprayed into very small droplets which can be dried easily using a stream of heated air flow (van Drooge *et al.*, 2006). During freeze drying, the drug and carrier are dissolved in a common solvent followed by immersion in liquid nitrogen for freezing. Then the frozen samples are lyophilised. Vacuum drying is normally needed in order to

remove the solvent thoroughly. The use of super critical fluids, usually carbon dioxide, has been receiving more and more attention recently (Won *et al.*, 2005). Its advantages include reduced particle size and residual solvent content, disappearance of any degradation and high product yield (Majerik *et al.*, 2007). The co-precipitation method (Huang *et al.*, 2006) and spin-coated films (Konno and Taylor, 2006) are also two very useful solvent methods for preparation of solid dispersions. The limitation regarding the solvent methods is the use of organic solvents which increases the preparation cost and leads to great risk to the environment.

1.5.2.3 Ball milling method

Ball milling differs to the melting and solvent methods in that solid dispersions of drug and carrier are prepared in the solid state. This method has been widely used to make the amorphous phase (Willart and Descamps, 2008). During milling, strong mechanical forces occur which can help to facilitate the incorporation of drug and carrier (Gupta *et al.*, 2003). Heat might be generated in the local collision region between the balls and the wall of the pot, which could help to dissolve the drug into a carrier with good miscibility (Patterson *et al.*, 2007). Studies have shown that solid solutions can be made by using high energy milling approaches such as planetary ball milling (Patterson *et al.*, 2007). Advantages of ball milling to prepare solid dispersions include its suitability for thermosensitive materials and its ease in handling avoiding the use of large amount of solvents. However, compared to melting and solvent methods, ball milling might be difficult to scale up. Prolonged milling might also lead to potential degradation of the materials.

1.5.3 Stability of solid dispersions

A critical factor to maintaining the dissolution properties of a solid dispersion after storage is to prevent the recrystallisation of the amorphous drug. As explained above, the amorphous drug is thermodynamically unstable and it has the tendency to recrystallise into the stable form. One important reason for the preparation of a solid dispersion is to reduce the crystallisation rate of the amorphous drug by compounding it

with a carrier. However, forming a solid dispersion does not mean that the drug will inevitably stay amorphous forever. The drug in the carrier matrix may still have the tendency to recrystallise if it is stored for a certain period of time. Figure 1.10 shows the physical changes during crystallisation of a solid dispersion in which the drug is molecularly dispersed. Molecular mobility is the governing factor that influences the rate that the crystals form in the solid dispersion. If the molecular mobility is lowered, the time needed for the drug molecules to diffuse back together and start to form crystals is shortened. A useful way to reduce the molecular mobility of the drug is to increase its T_g by compounding it with a high T_g carrier through the anti-plasticisation approach.

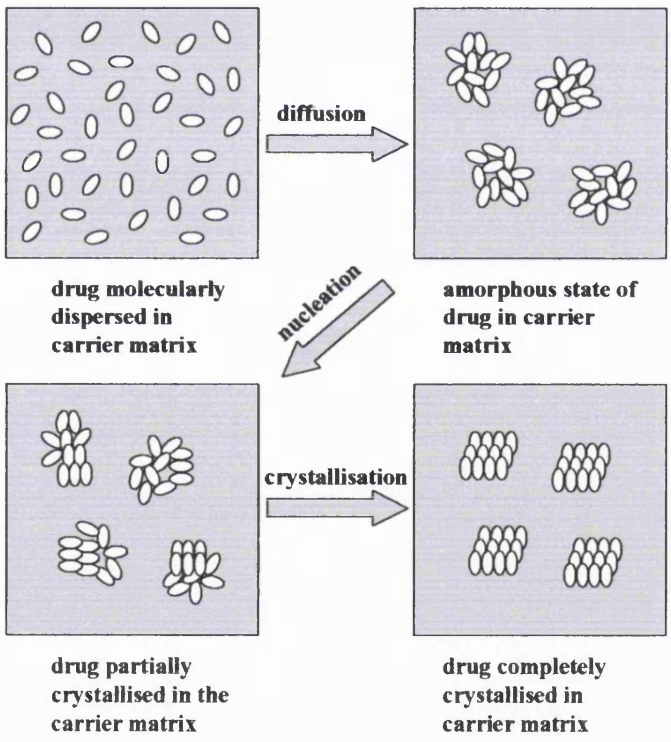

Figure 1.10: *Different stages of drug molecules in the carrier matrix of solid dispersions during crystallisation.*

There are some other issues which are important for reducing the molecular mobility or keeping the drug molecules separate. A high molecular weight carrier can help to restrict

the molecular motions of the drug because the free volume of the solid dispersion is smaller (Kaushal *et al.*, 2004). Also, a high carrier ratio is important because the diffusion distance for separate drug molecules getting back together is larger. Furthermore, when the T_g of the carrier is higher than that of the drug, a higher carrier content can help to increase the T_g of the solid dispersion further according to the Gordon-Taylor equation. Higher carrier content increases the chance of interaction between the drug and carrier molecules and also minimise the risk of the drug exceeding the solid solubility (Vasanthavada *et al.*, 2004). Carriers which can help to reduce the water uptake are also favored because plasticisation of T_g by water can be avoided or at least minimised (Augsburger and Hoag, 2008).

Compared to other types of solid dispersions in which clusters of drug molecules exist, solid solutions can be considered superior in terms of stability. This is because for this type of solid dispersions, an extra step of diffusion is needed before nucleation happens (Figure 1.10). Therefore, a good miscibility between a drug and a carrier can, in many respects, help to increase the stability of the solid dispersion. However, sometimes, high T_g and good miscibility might not be enough to guarantee a good stability (Al-Obaidi, 2007). A strong drug-carrier intermolecular interaction is also needed (Matsumoto and Zografi, 1999). There are many examples relating the drug-carrier interaction to the stability of a solid dispersion (Broman *et al.*, 2001; Forster *et al.*, 2001). The extent and type of interactions can control the dissolution, phase separation and miscibility of the solid dispersion. Furthermore, strong interactions can help to increase the T_g of the solid dispersion (Khougaz and Clas, 2000), which as a result leads to an increased stability.

1.6 Surface properties of solids

The surface properties of solids can be affected by a consequence of physical manipulation as well as the chemical structure (Buckton, 1995). The change of size, crystal habit, polymorphic form, hydrate or solvate form, degree of crystallinity and introduction of impurities can all alter the surface of a solid. The extent of crystallinity at the surface of a solid is probably the most important factor as far as variability in solid surface properties is concerned.

When the surface of a solid changes, the way the solid interacts with other phases (mostly liquid or solid phase in pharmaceutical areas) changes as a result. These interactions include sorption of moisture, wetting and spreading of a liquid over the solids, dissolution, film coating, suspension formation, tabletting, flowability, solid-solid blending, and so forth. For example, by changing the surface of the materials used in a dry powder inhaler system, the inter-particulate interactions (both cohesion and adhesion) of the materials can be altered and, thus, the performance of the system can be adjusted (Tong *et al.*, 2006). In another example, since the cohesive strength of interaction of colloidal silicon dioxide (silica, 311.5 MPa) is lower than that of microcrystalline cellulose (MCC, 386.1 MPa), the surface of MCC can be manipulated by adding silica on it to obstruct MCC-MCC bonding and lower the tablet strength during compaction (van Veen *et al.*, 2005). The dissolution improvement of many poorly soluble drugs in solid dispersions can be partly attributed to the increase of surface area after size reduction and increase of wettability on the surface after compounding with a hydrophilic carrier. Therefore, in many cases, the study of the surface behaviour of a solid is important for pharmaceutical scientists to produce an efficient formulation.

1.7 Aims of thesis

The main aim of this thesis was to study the effect of different preparation methods on the physical properties, stability and dissolution of solid dispersions. The specific objectives were to investigate: 1) the effect of aging on the surface energy of the solid dispersions; 2) differences between the surface and bulk molecular mobility of the solid dispersions; 3) correlating physical stability of the solid dispersions and their molecular mobility, fragility and zero mobility temperature; 4) the effect of aging on the water sorption and dissolution characteristics of solid dispersions; 5) approaches to prepare stable solid dispersions with rapid dissolution rate and finding the most suitable preparation method depending on the miscibility of carriers used.

The following hypotheses were established and tested:

1. Relaxation is usually accompanied by a decrease of energy; therefore, the surface energy of the solid dispersions decreases during physical aging. Furthermore, solid dispersions prepared by different methods exhibit differences in surface energy relaxation because the solid dispersions have different surface morphologies.
2. Since crystallisation is often initiated at the surface, the molecular mobility at the surface of the solid dispersions is greater than that of the bulk.
3. Crystallisation rates below T_g are orders of magnitude lower than those found above, but still very significant over the time scales employed during storage. Therefore, zero mobility temperature, T_0 can be a better indicator for prediction of the physical stability compared to T_g. When the T_g are similar, the solid dispersion with a lower T_0 tends to crystallise first.
4. Interaction between the drug and carrier is vital for the physical stability of a solid dispersion. The drug and carrier interaction happens more easily in the liquid state than the solid state. The drug and carrier of the solid dispersions which prepared through liquid state have a better interaction tendency than the ones prepared in the solid state.

Chapter 2

Materials and methods

In this chapter, the materials and methods used for the study and the instruments used for characterisation of the samples will be explained in detail.

2.1 Materials

All materials were used as received, unless otherwise stated.

Material	Grade and supplier
Indometacin	Tokyo Kasei
Polyvinylpyrrolidone (PVP)	K30, BSFE
Hydroxypropyl methylcellulose acetate succinate (HPMCAS)	AS-LG, Shin-etsu
Poly[N-(2-hydroxypropyl)methacrylate] (PHPMA)	Acros Organics
Microcrystalline cellulose (MCC)	EMCOCEL® 50M, Mendell UK
Silicified microcrystalline cellulose (SMCC)	Prosolv® 50, JRS Pharma
Magnesium aluminum silicate (Neusilin)	Neusilin® US2, Fuji Chemical
Liquid Nitrogen	BOC
Lithium Chloride (LiCl)	Analytical grade, Acros Organics
Sodium Chloride (NaCl)	AnalaR®, BDH
Ethanol	AnalaR®, BDH
Acetone	Laboratory reagent grade, Fisher Scientific
Decane	GPR^{TM}, BDH
non-hermetically sealed aluminum pans	PerkinElmer

Table 2.1: *List of the materials used with grade and supplier.*

2.1.1 Model drug: indometacin

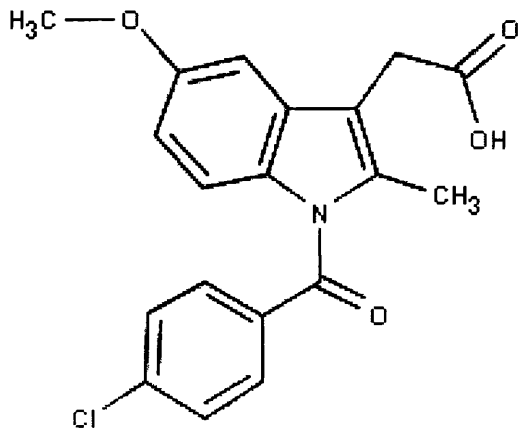

Figure 2.1: *Chemical structure of indometacin.*

Indometacin (Figure 2.1) belongs to the non-steroidal anti-inflammatory drug (NSAIDs) family which can be used to reduce inflammation, pain, and temperature. Indometacin is usually applied in the treatment of osteoarthritis, acute gouty arthritis, rheumatoid arthritis, and ankylosing spondylitis. Because of its action as a prostaglandin synthase inhibitor, indometacin has also been used to delay premature labor. Indometacin is classified as a class II drug because of its poor solubility (a water solubility of ~5 μg/L, Hancock and Parks, 2000) and high permeability. Due to these characteristics, the bioavailability of a class II drug can be improved by increasing its solubility or dissolution rate using many formulation approaches such as: co-grinding with fine porous silica particles (Watanabe *et al.*, 2001); preparation of solid dispersion with PVP by spray drying (Matsumoto and Zografi, 1999); mechanical mixing with crospovidone followed by heating to temperatures below the melting point to form a solid dispersion (Fujii *et al.*, 2005); and coprecipitating with PVP by solvent-free supercritical fluid processing (Gong *et al.*, 2005).

Indometacin was chosen as a model drug for these studies because of its excellent glass forming ability with a relatively low T_g and its well characterised crystallisation tendency above or below its T_g (Telang *et al.*, 2009). Indometacin can exist in different

polymorphic forms, the major two of which, γ- and β- forms have been systematically studied (Andronis and Zografi, 2000). It can also exist as solvates and an amorphous form. The amorphous properties of indometacin have been extensively studied with much literature available (Andronis and Zografi, 1998; Tong and Zografi, 1999).

2.1.2 Carriers

2.1.2.1 Polyvinylpyrrolidone（PVP）

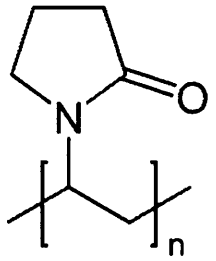

Figure 2.2: *Chemical structure of PVP.*

PVP is a hydrophilic polymer made from the monomer N-vinyl pyrrolidone and it is soluble in many polar solvents. Unlike its monomer which is toxic and carcinogenic, the pure polymer PVP is safe to be used by humans. In the pharmaceutical sciences, PVP is widely applied in the preparation of many dosage forms. In some solid formulations, PVP can be used as a binder in wet granulation, a solubilising agent for increasing dissolution rate of poorly soluble drugs or a coating substance for tablets. In suspensions, PVP can be used as a suspending agent, stabilising agent or a viscosity-increasing agent. Moreover, PVP can also be used in some injections or eye drops. Because of the tertiary amide group, PVP is known to be a strong hydrogen bond accepter, and it has been widely used in the preparation of solid dispersions. Over 60 drugs have been reported to be dispersed in this polymer according to a statistic in 1986 (Ford, 1986), and this figure is expected to be more currently. For example, PVP has been commonly used with indometacin to form solid dispersions because the amide group of PVP as a proton acceptor could interact with the hydroxyl group of indometacin as a proton donor. With this interaction, the recrystallisation of amorphous

indometacin could be inhibited. Sekikawa *et al.* (1978) have shown that the crystallisation inhibition mechanism is related to the drug and polymer interaction level. Because of its relative high T_g, PVP can act as an anti-plasticiser when compounding with many compounds with a low T_g. In the case of indometacin which has a T_g at 42 °C, its T_g can be greatly increased when compounded with PVP, hence reducing its molecular mobility as well as the tendency to crystallise. The hydrophilic nature of the polymer could also help to increase the wettability of a poorly soluble drug in a solid dispersion.

2.1.2.2 Magnesium aluminum silicate (Neusilin)

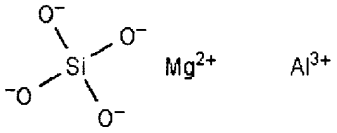

Figure 2.3: *Chemical structure of Neusilin.*

Magnesium aluminum silicate has a commercial name Neusilin and it is derived from refined and purified natural clay. In the pharmaceutical area, Neusilin is used in tablets, ointments and creams. When used alone or with other materials, Neusilin can act as a suspending agent or stabiliser in some oral or external dosage forms. In cosmetics, Neusilin can be used to thicken, emulsify and color cosmetics. Gupta *et al.* (2002) have tried to use three-component solid dispersion granules prepared by hot-melt granulation including Neusilin as a surface adsorbent to enhance drug dissolution. It was found that the drug dissolution rate of these solid dispersions increased on storage, accompanied by evidence of hydrogen bonding between the drug and the surface of Neusilin, which could act as a proton donor as well as an acceptor because of the surface silanol groups. A later study has shown that after compounding with Neusilin, the conversion from crystalline to amorphous states of four drugs was greatly reduced (Gupta *et al.*, 2003).

2.1.2.3 Hydroxypropyl methylcellulose acetate succinate (HPMCAS)

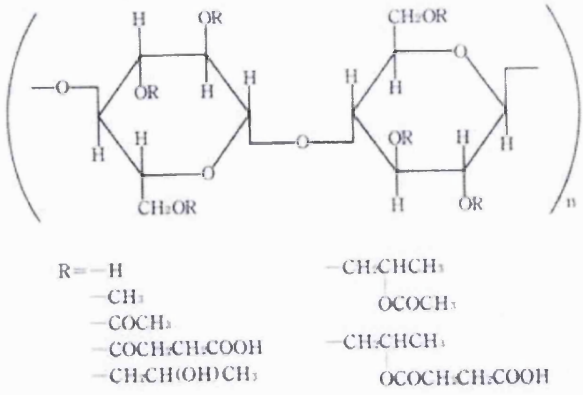

Figure 2.4: *Chemical structure of HPMCAS.*

HPMCAS is manufactured by introducing acetyl and succinoyl groups to the hydroxyl groups of HPMC which comes from highly-purified pulp from natural trees. By controlling the ratio of acetyl and succinoyl moieties, the dissolution behavior of HPMCAS in buffers with different pH values could be manipulated. Because of this special characteristic, HPMCAS can be used as an aqueous enteric coating material. Tanno *et al.* (2004) have studied the application of HPMCAS in a solid dispersion with nifedipine, a poorly soluble drug. It was shown that HPMCAS was able to increase the dissolution rate of nifedipine while preventing its recrystallisation from a supersaturated solution.

2.1.2.4 Other carriers

Silicified microcrystalline cellulose (SMCC), Poly [N-(2-hydroxypropyl)methacrylate] (PHPMA) were also used in this study in the preparation of solid dispersions because of their different characteristics. The dissolution and stability behaviour of drugs compounding with these carrierss were studied and compared.

2.2 Methods

2.2.1 Preparation of amorphous indometacin

About 3 g of crystalline indometacin was evenly distributed into 10 pieces of aluminum foil and then placed on a hot plate kept at 165 °C. Indometacin melted completely within about 10-20 seconds. By visual observation, once indometacin was all melted (this process was accompanied by a colour and phase change of the white powder to a yellow clear liquid), the foils were placed on the surface of liquid N_2 for quench cooling. Direct contact between the liquid N_2 and the melted liquid was always avoided in order to reduce the moisture content in the final product. Once the liquid turned into a glassy state, this sample was kept in a vacuumed desiccator over phosphorus pentoxide (P_2O_5) at room temperature for moisture removal. The glassy sample was firstly dried in the desiccator for one hour to allow the sample to return to room temperature (the sample would tend to sorb more moisture at a lower temperature) and then taken out and ground gently using a mortar and pestle. Ground powders were passed through a sieve with different mesh sizes as required by the experiments and kept in the desiccator drying for another one hour (the drying time was always fixed to control the thermal history). The final product would be used directly or stored at -80 °C sealed with parafilm until required.

2.2.2 Preparation of solid dispersions using ball milling

2.2.2.1 Introduction

For practical formulation purposes, milling has been frequently applied by pharmaceutical manufacturers as an important method for reducing particle sizes. For increasing the dissolution rate of a poorly soluble drug, milling can be used to decrease the crystallinity of compound until amorphisation or formation of metastable polymorphic forms occurs, which provide a higher energy for the drug to dissolve and hence increasing its bioavailability (Hancock and Zografi, 1997). Some recent studies have applied milling as a preparation method to form co-crystals (Chadwick *et al.*, 2007; Karki *et al.*, 2007). Moreover, milling a drug with some carriers such as silicates could help to enhance its physical properties and keep it stable during storage.

Ball milling is a milling method which has been used for over one hundred years. Depending on the purpose of the milling, different scales of ball mills could be used: a tumbler mill can be used for primarily large-scale industrial manufacturing with high milling energy; an attrition mill can be used for small-industry scale size reduction purpose (<100 kg); a shaker mill would be used for research-scale experiments which require a relatively high milling energy and a planetary mill is the one used during this study and it can provide medium to high milling energy for a sample size lower than 250 g.

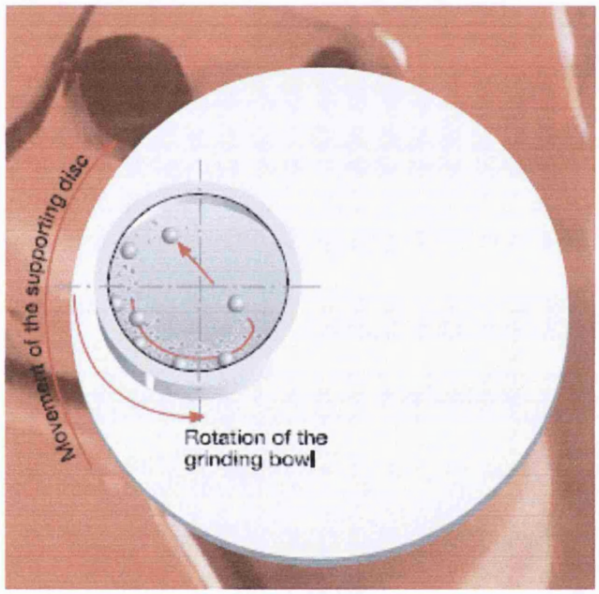

Figure 2.5: *Principal of a planetary mill (adapted from manual of Pulverisette 5, Fritsch).*

The principal of a planetary mill is to generate maximum energy impact together with friction between the balls and the wall by cascading the milling balls across the milling pot and colliding to the opposite wall. To achieve this, the milling pots with materials and balls inside rotate in one direction and the supporting disc which the pots are sitting on would rotate in the opposite direction around its central axis mimicking the revolution and rotation of the earth around the sun. A strong centrifugal force can be produced allowing the milling materials and balls rotating inside the wall of the pot

(friction force is generated) until a certain point that they start to separate from the wall and cascade across the pot at a high speed generating a huge impact force. Figure 2.5 shows a diagram of how a planetary mill works and the movement of the balls.

The milling effect could be greatly affected by many milling parameters (Table 2.2). For a planetary mill, the milling speed which means the relative speeds of pot rotation to disk revolution is a major concern for many scientific researchers (Watanabe, 1999; Mio *et al.*, 2002).

	Pot	Milling balls	Milling samples	Milling temperature	Others
Affecting parameters	Composition, size, shape, and surface	Number, size, material (density and elasticity) and surface	Weight, shape, size and composition	Temperatures of pot, ball, sample and collision point	Type of mill, speed of mill, amount of filling, and milling duration

Table 2.2: *Parameters related to a milling process.*

Rose (1957) have summarised the different stages of ball milling as the rotation speed increases: distinct avalanche, continuous avalanche, cascading motion, cataracting motion and centrifugal motion which happen in a sequence. The rotation speed that is required to achieve the final stage, i.e. centrifugal motion, is called critical rotation speed N_c which could be calculated using Equation 2.1:

$$N_c = \frac{1}{2\pi}\sqrt{\frac{2g}{D-2r}} \qquad \text{Equation 2.1}$$

where r is the radius of the balls, D is the inner diameter of the milling pot and g is a constant related to gravity with an average magnitude of 9.81 m/s^2. Therefore, by understanding the critical rotation speed, a suitable speed could be decided based on the purpose of an experiment. For example, avalanche motion and centrifugal motion gives more friction force while cascading motion and cataracting motion give more impact force. Figure 2.6 shows how the balls behave in a milling pot depending on r_s values which represents the ratio of rotation-to-revolution speed.

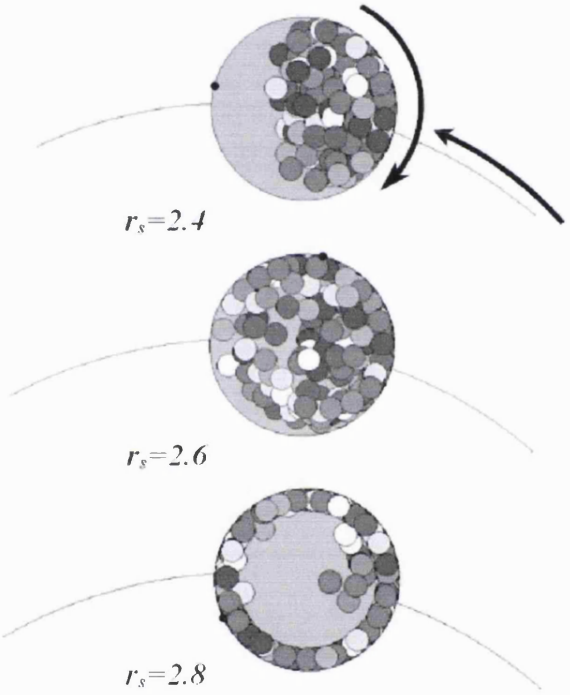

Figure 2.6: *Ball motions during milling at different speed ratios (adapted from Mio et al., 2002).*

The ball motions change from cascading (r_s =2.4), into cataracting (r_s =2.6) then to "slipping" (r_s =2.6) at the end. The specific impact energy changes following the change of the ball motions with the cataracting motion giving the highest value. The specific impact energy of balls, E_w, can be calculated using Equation 2.2:

$$E_w = \sum_{j-1}^{n} \frac{1}{2w} m v_j^2 \qquad \text{Equation 2.2}$$

where v_j is the relative velocity between two colliding balls or a ball colliding against the wall, m is a ball's mass, n is the number of collisions between a ball and other balls or the wall per second, and W is the weight of the filling sample. E_w could be related with the size reduction and the rates of conversion to amorphous state.

During milling, the temperature and the atmosphere inside the pot can be controlled. While 100% of conversion of indometacin into the amorphous state could not be achieved at room temperature, indometacin became completely amorphous when being milled at 4 °C in 4 hours (Otsuka *et al.*, 1986) or cryogenic impact milling for 1 hour (Crowley and Zografi, 2002). Adding some solvents to the powders during milling might be able to make the size reduction more efficient due to the decrease of particles' surface energy (Oguchi *et al.*, 1995).

2.2.2.2 Experimental

A Fritsch pulverisette 5 planetary mill was used for preparing ball milled solid dispersions. 5 g of powders with different drug to carrier ratios (by mass) were weighed and loaded into a 250 mL ZrO_2 jar. The sample was then milled under different milling conditions. Depending on the purpose of different experiments, the milling conditions were altered by adjusting the milling time, the number of milling balls and/or the rotation speed of the pot. These conditions including the sample compositions used will be listed in the following relevant chapters.

2.2.3 Preparation of solid dispersions using melt quenching

2.2.3.1 Introduction

Melt quenching is one of the most widely used methods for the preparation of glassy materials (Hancock and Zografi, 1997; Yu, 2001). When a crystalline material is heated, the energy given by the heat will make the solid melt into liquid (if it doesn't degrade)

and then if the liquid is cooled below its melting point (T_m), its molecular mobility would slow down. There is a balance between the tendency to crystallise and the decrease of the molecular mobility. When the cooling rate is sufficiently fast, the time is insufficient for the molecules to rearrange within the timescale and the liquid's structure would be frozen: the liquid turns into a glass as a result (Debenedetti and Stillinger, 2001). This liquid to solid transformation can only be observed if the nucleation of supercritical clusters is suppressed during cooling and the nucleation is controlled by a thermodynamic barrier. The most rapid crystallisation rate is related to the competition between the thermodynamic driving force for the transformation and the molecular mobility, therefore the effective critical cooling rate of the vitrification process is decided by the necessity to quickly pass it (Willart and Descamps, 2008). Figure 2.7 shows a time-temperature-transformation (TTT) diagram about this process.

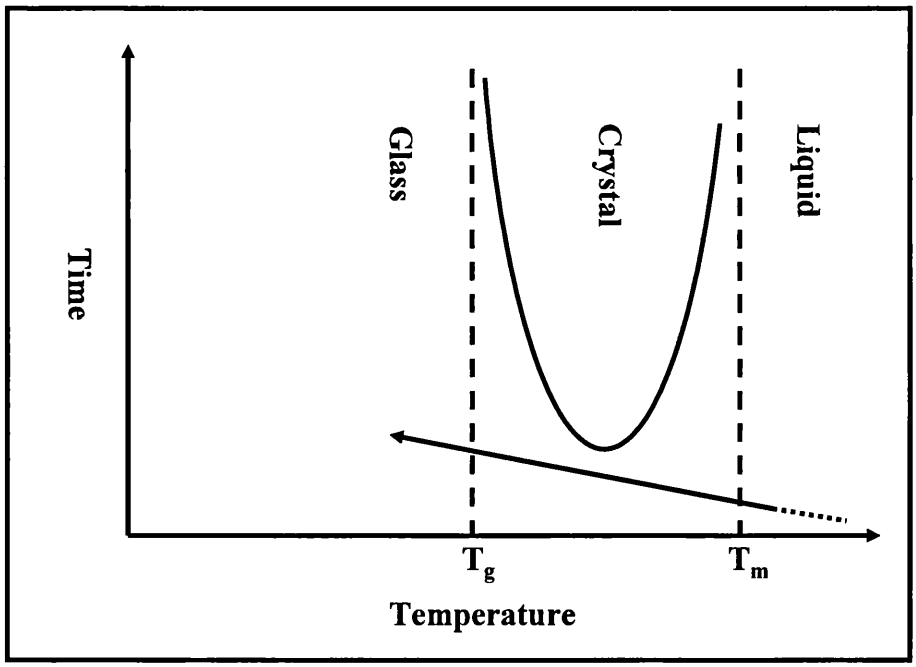

Figure 2.7: *Time-temperature-transformation (TTT) diagram (adapted from Willart and Descamps, 2008).*

Melt quenching is a useful method for preparing glasses; the drawback of it is its potential for chemical degradation of thermosensitive compounds. Therefore, the melt

quenching conditions need to be carefully considered, because the longer the duration of heating or the higher the heating temperature the greater the risk for a material to degrade. There are only a few limited ways to prevent degradation happen such as: introducing an inert gas to the heating process; the use of a twin-screw extruder to lower the heating temperature because the shear force applied could make a drug and carrier to form a solid dispersion at a lower temperature than the drug's melting point (Nakamichi *et al.*, 2002); Hasegawa *et al.* (2005) used a closed melting method for the preparation of a troglitazone and PVP solid dispersion by adding a plasticiser (water) to the physical mixture, the T_g of PVP can be lowered and the solid dispersion can be prepared without heating the sample over the melting point of the drug (Hasegawa *et al.*, 2005).

2.2.3.2 Experimental

For melt quenching, 3 g of indometacin and PVP (70%:30%) physical mixtures were weighed into a crucible and then placed in an oven which was preheated to 175 °C and stabilised. The physical mixtures were heated for 15 minutes to allow complete melting of the ingredients. In the time points of 5 and 10 minutes, the crucible was taken out and the melted liquid was stirred using a small spatula. This was to help the components to mix well and prevent phase separation. After heating, the crucible was immediately placed on liquid N_2 for quench cooling. Direct contact between liquid N_2 and the sample was avoided to reduce the possibility of moisture sorption. A glassy amorphous solid (appeared as a hard cake) was formed and it was kept in a vacuumed desiccator over P_2O_5 at room temperature for one hour for drying and to allow the cooled sample to recover to room temperature (samples would tend to sorb more moisture at a lower temperature). Grinding of the sample was followed using a pestle and mortar. The ground powders were sieved through a 90 micron sieve and the powders was dried in the desiccator (0% RH and room temperature) for another one hour to allow the same total drying time as the ball milled and spray dried sample to ensure that thermal history were the same.

2.2.4 Preparation of solid dispersions using spray drying

2.2.4.1 Introduction

Spray drying has been a commonly used technique in many industrial and laboratory applications since the late 19th century (Marshall and Seltzer, 1950). By definition, spray drying is a process of drying a liquid feed by a hot drying medium, which is a one step rapid process for the production of a dried product. The product can be powder, granules or agglomerates depending on the physical and chemical properties of the feed and the design of the spray dryer. The feed here can be a solution, colloid or suspension (Masters, 1972).

Figure 2.8 shows a scheme of four different steps included in a spray drying operation: a) atomisation of feed into a spray; b) spray-drying medium contact; c) drying of the spray and d) removal of the dried product from the drying medium (Masters, 1972). Firstly, the suitable feed (sludge, slurries or clear liquids with different viscosity) was prepared by mixing and agitation, and then pumped through an atomiser device for atomisation into a spray. The atomisers can be a rotary, single fluid, two-fluid or ultrasonic nozzle design. Secondly, the spray and hot drying air make contact which includes mixing the flow depending on the designs of the chamber. The spray and hot air can enter the chamber in a co-current or counter-current flow: a co-current flow enables a lower residence time of the particles and higher particle separation efficiency in the cyclone; a counter-current flow enables a longer residence time of the particles in the chamber giving them a better drying effect. Thirdly, drying of droplets happens immediately after the contact of spray and dry medium. It contains two periods: in the first period of drying, evaporation of moisture is at a constant rate because of diffusion of moisture from the core of the droplet maintaining surface saturation; in the second period of drying, critical point is reached when there is insufficient moisture to maintain saturated conditions, hence a dried shell starts to form at the surface of the droplet. The evaporation rate decreases because diffusion slows down caused by the increased thickness of the surface dried shell. Finally, dried particles are removed from the drying medium. There are two systems for this purpose. In system one, primary separation of

particles takes place at the base of the drying chamber (usually the coarser particles) and then the residual particles (the finer particles) are collected in a separation equipment, sometimes with bag filters. In system two, total removal of dried particles happens in the separation equipment (Masters, 1972).

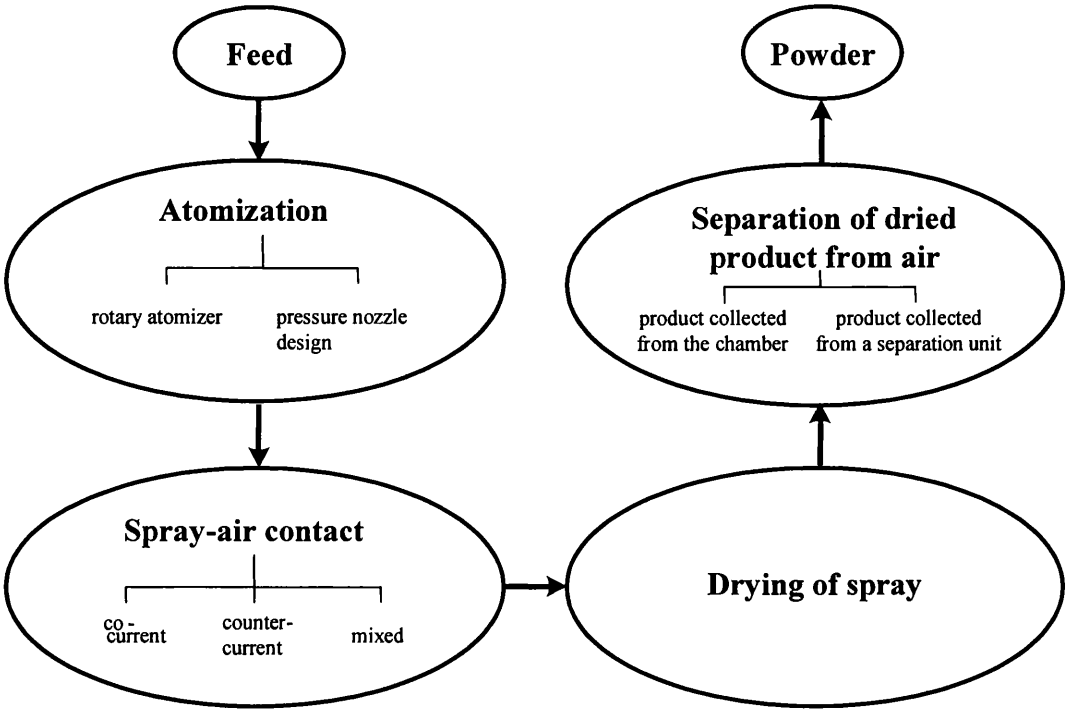

Figure 2.8: *Different process stages included in a spray drying operation.*

Spray drying is a complicated process in that there are many variables that need to be carefully considered. A higher atomiser speed and nozzle pressure usually produce a smaller spray droplet size; a higher feed viscosity and feeding rate produce a coarser spray at fixed atomisation conditions; the drying rate and different feed properties exhibit different final products, some will expand, some will collapse, fracture or disintegrate while others retain a spherical shape or contract leading to denser particles (Chidavaenzi *et al.*, 1997). The yield of spray drying increases with higher inlet temperature, and as the inlet temperature increases, a maximum powder yield is reached followed by a sharp decrease as the temperature of the chamber, or cyclone wall, go over the sticky point causing powder to deposit on it. Decreasing the liquid pumping

rate, increasing the atomising air flow rate and the dry air flow rate can all help to increase the yield (Maury *et al.*, 2005).

The spray drying technique can be utilised in food productions (such as instant coffee, milk, and soups), household commodities and pharmaceuticals. The advantages of spray drying are the effective control of certain product properties and quality values, suitability for drying of some thermosensitive materials, capability of large-scale production in a relatively economic cost and higher efficiency over other types of dryers. While at the same time, there are some drawbacks of spray drying which need to be borne in mind: products with low bulk densities are frequently obtained while often the opposite property is required; a coarse product is required while the spray dryer is designed for producing fine particles; and the materials to be spray dried need to be in a form that can be pumped to the atomiser (Marshall and Seltzer, 1950).

Figure 2.9 shows the Niro SD MICRO^{TM} spray drying unit that was used in this work. The spray drying unit comprises of an air compressor, a nitrogen generator, an operating control panel and a spray dryer. The nitrogen generator connected to the spray dryer can provide nitrogen flow as the drying medium which allows the use of flammable feeds for spray drying and this is an important feature of this system. Another advantage of the spray dryer is that the fluid dynamics of the system mimics those of an industrial scale plant; therefore it makes scale-up studies easier. Furthermore, the spray dryer contains a two-fluid nozzle atomiser (pneumatic nozzle) which can be used for production of fine particles with a size of 5-20 μm. This pneumatic nozzle can also produce a liquid film of spray with a high velocity gas (Khalid, 2006).

Figure 2.9: *A picture of the Niro SD MICRO™ spray drying unit which includes a) air compressor, b) nitrogen generator, c) operating control panel and d) spray dryer.*

2.2.4.2 Experimental

The GEA Niro SD MICRO™ was used for spray drying purpose. A Maxigas Nitrogen generator was attached to the spray dryer which can provide dry nitrogen flow through the spray dryer. 200 mL of different solvents were used to prepare drug and carrier solutions. The feed concentration in the solution was 1.5 % or 2.0 % w/v and 30 minutes were allowed for the materials to dissolve completely into the solvent. The solution was then spray dried using following parameters:

atomiser gas flow: 2.5 kg/h
chamber inlet flow: 30.0 kg/h
inlet temperature: 80 °C
feeding rate: 20%

Spray dried samples were collected from the collection bottle and cyclone and then stored in a vacuumed desiccator over P_2O_5 at room temperature before further use. The drug and carrier compositions, types of solvents and feed concentrations for different experiments will be listed in the following relevant chapters.

2.2.5 Inverse gas chromatography (IGC)

2.2.5.1 Introduction

Inverse gas chromatography (IGC) is an inverted version of the gas chromatography technique which was developed in the 1950s for the purpose of characterisation of catalyst support materials such as activated carbon, silica or alumina (Kiselev and Yashin, 1969). In contrast to the conventional analytical GC in which the solid phase is the material with known physicochemical properties and the vapour phase is the sample to be investigated, the roles of the phases in IGC are inverted.

IGC measurements can be conducted in two different techniques, pulse and frontal. In a pulse measurement, a certain amount of probe molecules are injected to a carrier gas (usually helium) and delivered to the powder sample in the column, then adsorption and

desorption occurs and the detector shows a peak indicating the clearance of the probe. In a frontal method, continuous injection of probe molecular is made and the detector would display a breakthrough curve instead of a single peak. A fast equilibration of probe molecule adsorption is required for pulse technique while the frontal technique can always achieve equilibration because of the continuous probe injection (Thielmann, 2004). Because the frontal method is independent of the retention, it is not discussed as an IGC approach (Thielmann, 2004). The pulse method is the method used for this study.

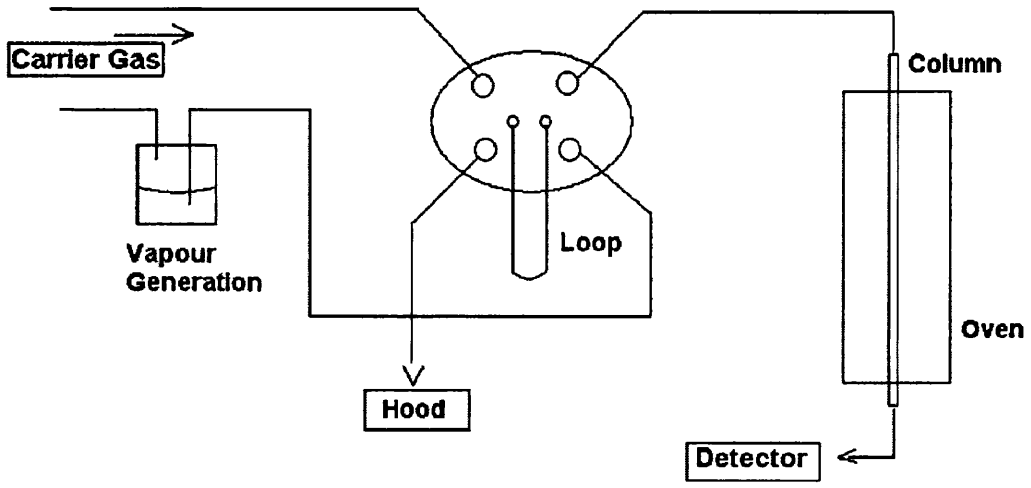

Figure 2.10: *A schematic diagram of an IGC instrument (adapted from Thielmann, 2004).*

In an IGC pulse measurement, powder samples under investigation are loaded in an empty column with glass wools on either end, followed by tapping of the column gently for a certain period of time in order to eliminate unwanted hollows or cracks in the powder body. The column is then conditioned in a column oven under a certain temperature as requested (15-120 °C) and the relative humidity (0-90%) inside the column is adjusted by a carrier gas which constantly flows through the column. A single pulse of a polar (acetone, ethanol, chloroform etc.) or non-polar (decane, nonane, octane etc.) vapour would be injected as a probe molecule and brought into the column by

helium to interact with the powders. The signal of the vapour can be detected by a flame ionised detector (FID) and a thermal conductivity detector (TCD) would be used to monitor the RH. Figure 2.10 shows a simple schematic of an IGC instrument.

It needs to be borne in mind that for the measurement of thermodynamic parameters, an infinite dilution condition must be achieved. When the probe injected is in a very low concentration, the uptake of the probe is independent of the surface coverage, and the isotherm in this range is linear. This range is called the Henry region and it is also the infinite dilution range. In this range, the interaction between the vapour phase molecule and the solid phase predominantly happens on the solid's high energy site. Therefore, the retention volume of the probes would not be affected by the size and mass of the samples.

Since the early 1990s, IGC has received more and more attention in the pharmaceutical field and the numbers of publications are increasing in recent years (Buckton and Gill, 2007). In general, IGC can be applied in pharmaceutical science to measure isotherms, surface free energy (the calculation process is discussed in Chapter 3), heat of sorption and surface heterogeneity (Newell *et al.*, 2001; Roubani-Kalantzopoulou, 2004). IGC could also be used for some specific applications: IGC was proved to be capable to study samples that contain small but differing levels of amorphous content and differentiate them (Newell and Buckton, 2004). Therefore, IGC is a very suitable technique for batch variability and routine materials characterisation. The surface dispersive energy calculated using dispersive probes can be used as an index to predict the batch and batch difference or stability on the surface of powders while the bulk techniques could not show any change. On the other hand, some materials for which surface dispersive energies show very similar values for different samples while with known differences in functionality, their polar data are often different (Ticehurst *et al.*, 1996). A very important advantage of IGC is controlling of the temperature and relative humidity. For example, Surana *et al.* (2003) studied the T_g of an amorphous sucrose-PVP mixture by increasing the oven temperature. The retention volume of

decane deviated from linear when the sample was approaching its glass transition and another deviation happened when it passed through the rubbery phase. IGC also enables the study of plasticised T_g under a certain RH. In another case, for the first time, Buckton *et al.* (2004) used a RH method to study the surface T_g of indometacin based on the retention volume calculated by the center of decane peak and the center of the peak mass. Because of the ability to detect the free energy level of a material based on the interaction between a probe and the material's surface, IGC could be used to study the surface relaxation of amorphous materials. In Chapter 3, a novel method will be developed to investigate the surface relaxation of amorphous solid dispersions by detecting the decrease of free energy during relaxation measured by the drop of retention volume of decane as a function of time.

2.2.5.2 Experimental

The IGC instrument used for this study was made by Surface Measurement Systems (London, UK). 500-800 mg of powder samples were weighted accurately and loaded into a pre-silanised glass column (internal diameter 3 mm, column length 30 cm) followed by 15 minutes of tapping. Samples with this amount of mass were able to reach infinite dilution condition. The packed column was placed in the column oven and conditioned for 4 (for surface energy measurement and the oven temperature was 30 °C) or 10 (for decane retention method and the oven temperature was 25 °C) hours in order to eliminate any moisture depending on the samples under study. Then the non-polar or polar probes with a concentration of 0.03 p/p^0 (p^0 is the saturated vapour pressure of the liquid probe at the experimental temperature) was injected to the column. For the measurement of surface dispersive energy, the non-polar probes decane, nonane, octane, heptane, and hexane were used and for the measurement of K_A/K_D values (K_A, acidic parameter and K_D, basic parameter), the polar probes acetone, chloroform, ethanol and ethyl acetate were used. For both of these experiments, the column over temperature was set at 30 °C during probe injections. On the other hand, for the measurement of surface relaxation by retention volume method, decane was continuously injected for up to 24 or 48 hours and the column oven temperature was set as 50 °C. In all cases,

methane was used as an internal reference. All solvents used were of HPLC grade. The IGC experiment was controlled by software SMS IGC controller V1.5 and data were analysed using a SMS IGC analysis macros V1.2 (Surface Measurement Systems, London, UK).

2.2.6 Differential scanning calorimetry (DSC)

2.2.6.1 Conventional DSC

Differential scanning calorimetry (DSC) is commonly used in the pharmaceutical field for the characterisation of the physical and energetic properties of a compound, because of its ability to provide an accurate, easy and quick measurement compared to other techniques. Some examples of DSC application are detection of polymorphism, characterisation of amorphous or crystalline materials, investigation of compatibility between different components in a formulation, measurement of solid-solid solubility, and investigation of reaction and decomposition kinetics. Basically, nearly all DSC measurement involves the introduction of a temperature scan in a linear way or an isothermal temperature programme and the detection of the change of heat flow (usually presented in the unit of watt) as a function of time or temperature (Coleman and Craig, 1996).

There are two main kinds of differential thermal instruments, differential thermal analysis which measures temperature difference between reference and sample pans, and differential scanning calorimetry which measures the energy difference (Clas *et al.*, 1999). Depending on the data acquisition method, DSC can be divided into two types: heat flux DSC and power-compensated DSC.

In a heat flux DSC, there is only one furnace where both the sample and reference pans are heated by the same source (a constantan thermoelectric) and the signal of temperature change is converted to heat flow using Equation 2.3:

$$\Delta Q = \frac{(T_s - T_r)}{R_t}$$ Equation: 2.3

where Q is heat, T_s is the sample temperature, T_r is the reference temperature and R_t is the cell's resistance.

In a power-compensated DSC, there are two individual furnaces for the sample and reference pans and the temperature between them is always kept the same by compensating the heat gain or lost during an exothermic or endothermic event to the pans. The power used for compensation can be calculated using Equation 2.4:

$$P = \frac{dQ}{dt} = I^2 R$$ Equation: 2.4

where P is power, R is the resistance of the heater, t is time and I is current used by the heater. Figure 2.11 shows the schematic diagram of these two types of DSC.

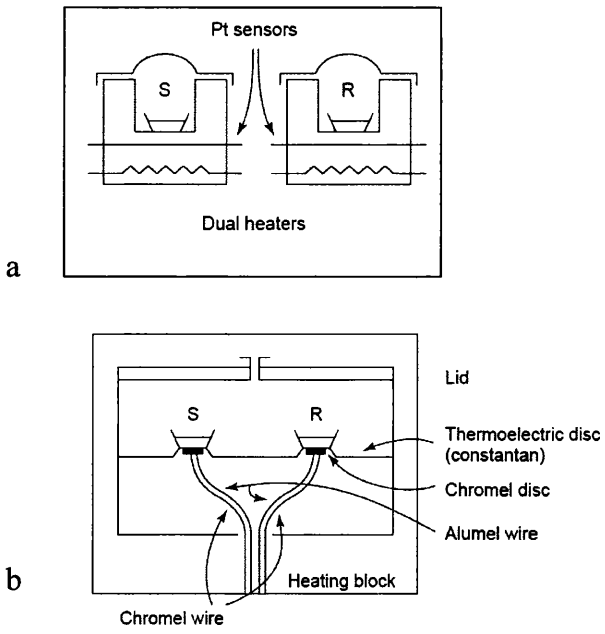

Figure 2.11: *Schematic diagrams of a power-compensated DSC (a) and a heat flux DSC (b) (adapted from Clas et al., 1999).*

2.2.6.2 Modulated temperature differential scanning calorimetry (MTDSC)

MTDSC is an extension of conventional DSC. In MTDSC, a modulation of temperature is superimposed over the underlying linear heating or cooling temperature programme to enable the separation of the total heat flow signal into the heat capacity component and the kinetic component. The kinetic component can be obtained by the difference between the total heat flow and the heat capacity component. This feature gives many advantages to MTDSC such as: a higher resolution and sensitivity, an easier way to detect a sample's heat capacity, detection of some hidden phenomena, investigation of initial crystallinity, and better discrimination of glass transitions or melting covered by moisture evaporation or other event (Coleman and Craig, 1996). For example, Royall *et al.* (1998) studied the T_g of saquinavir by MTDSC which is able to separate out the T_g appearing in the reversing signal from enthalpy elaxation endotherm appeared in the non-reversing signal providing a clear detection of T_g.

2.2.6.3 Hyper differential scanning calorimetry (Hyper DSC)

One drawback of the conventional DSC or MTDSC is their relatively slow heating rate (usually 2, 5, 10, 20 °C/min) during a measurement and this is not desirable for detecting polymorph behaviour of some substances. A slow heating rate might allow the polymorphic to recrystallise to another polymorphic form (McGregor *et al.*, 2004). Therefore, a Hyper-DSC which usually scans a sample at 100-500 °C/min (some newer models can even reach 1500 °C/min) is needed for this issue. The scanning rate is so quick that any small change of sample can be inhibited. Another advantage of Hyper-DSC is its higher detection sensitivity because of a larger heat flow per unit of time due to its fast scanning rate. This feature can help the detection of small changes in minor contents in a mixture such as a formulation easier and more accurate (Buckton *et al.*, 2006).

2.2.6.4 Experimental

A Pyris 1 DSC (PerkinElmer Instruments, Beaconsfield, UK) was used for the study, which is connected to a cooling unit (Intracooler IIP, PerkinElmer Instruments) allowing

the sample conditioned at minimum -55 °C. Measurements were performed under a N_2 gas purge at a flow rate of 20 mL/min (except for the fragility study, where a flow rate of 40 mL/min was used). Calibration was carried out using pure indium, or indium and decane together in the case of fragility study at the heating rate required by the studies. Samples (around 5 mg) were accurately weighed into non-hermetically sealed pans. In a conventional DSC study, a heating rate of 20 °C/min was used in the scan range from -20-220 °C. In a Hyper-DSC measurement, 200 °C/min was used in the scan range from -20-250 °C. Temperature modulated scans were also performed and the conditions were: starting temperature: 0 °C, heating rate: 10 °C/min, step: 2 °C, isothermal time per step: 1 min and repeats: 50-100 times. Different DSC modes were used depending on the purpose of the studies: detection of relaxation enthalpy, characterisation of samples, detecting the T_g or measuring the fragility of amorphous samples.

2.2.7 X-ray powder diffraction (XRPD)

2.2.7.1 Introduction

X-ray powder diffraction can be efficiently used for determining the degree of crystallinity of powders. The principle behind X-ray diffraction is that when an X-ray beam is applied to the sample, interference bands can be detected. The angle at which the interference bands can be detected depends on the wavelength used and the geometry of the sample with respect to periodicities in the structure (Leuner and Dressman, 2000). Figure 2.12 shows a simple diagram of an XRPD instrument. Every crystalline substance has a unique pattern which is like a fingerprint. Therefore, XRPD is very useful to detect a substance in a mixture in which the pattern is the overlap of the individual pattern of each component.

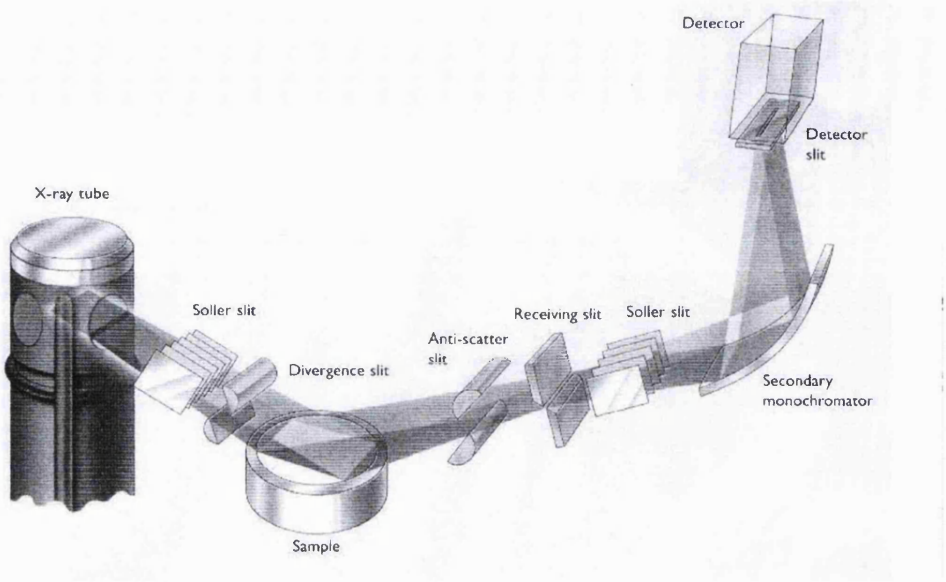

Figure 2.12: *Schematic diagram of an XRPD (adapted from PANalytical manual).*

2.2.7.2 Experimental

An X-ray diffractometer (Philip PW3710, Holland) was used for the characterisation of the amorphous or crystalline samples using copper radiation $K_{\alpha 1}$ and $K_{\alpha 2}$ with tube power of 45kV voltage and 30 mA current. The powder sample was loaded and flattened on a copper plate and placed into the detection chamber of the XRPD. The X-ray patterns were obtained using a step of 0.02° in a 2θ range of 5-40°, with a rate of one second per step.

2.2.8 Fourier transform infrared spectroscopy (FTIR)

2.2.8.1 Introduction

Spectroscopic instruments such as IR, Raman, NIR and NMR can be used to detect the interactions between drugs and carriers. For example, infrared spectroscopy can detect changes in bonding between functional groups which are led by structural changes and lack of a crystal structure. Furthermore, because the crystalline changes cannot affect all peaks in the IR spectrum, it is possible to discriminate those peaks that are sensitive to crystallinity changes from those that are not (Taylor and Zografi, 1997). Taylor and Zografi (1997) tried to use IR and FT-Raman spectra to examine the structure of binary

amorphous mixtures of indometacin and PVP at the molecular level and it was found that indometacin interacted with PVP in their solid dispersions through hydrogen bonds formed between the drug hydroxyl and carrier carbonyl resulting in disruption of indometacin dimers.

2.2.8.2 Experimental

FTIR was utilised in this study to investigate the interaction between the drug and different carriers, and the amorphous state of the drug in the solid dispersions was also confirmed by the spectra of FTIR. A FTIR (Avatar 360, Nicolet) was used and the spectra were obtained over a spectral region from 4000 to 400 cm^{-1} with a resolution of 4 cm^{-1} for 32 scans. Each sample was examined in triplicate.

2.2.9 Other methods

2.2.9.1 Thermal gravimetric analysis (TGA)

A TGA (Perkin Elmer Instruments, Beaconfield, UK) was used to detect the moisture level of the samples. About 10-20 mg of sample was used and scanned from 30-200 °C at a heating rate of 20 °C/min. Nitrogen purge was applied at a flow rate of 20 mL/min.

2.2.9.2 Scanning electron microscopy (SEM)

All samples tested were manually dispersed onto a carbon tab adhered to an aluminum stub using a micro-brush. Samples were gold-coated prior to viewing using a sputter coater (Emitech K550X, Texas, USA) and scanned using a Phillips SEM (XL30, Cambridge, UK) to study their morphology, with magnifications of 5 and 10 μm.The acceleration voltage was 10-12kV.

Chapter 3

Investigation of surface properties of solid solutions during relaxation using inverse gas chromatography

3.1 Introduction

The importance of the amorphous form in pharmaceutical products has been rapidly gaining interest (Hancock and Zografi, 1997). Amorphous material can be produced by many different ways such as milling, spray drying, freeze drying, and melt quenching. The presence of an amorphous phase in a product can be expected or unexpected. If the amorphous phase is unexpected (during preparation such as size reduction, granulation, compression and so forth) the surface properties of the product might be significantly altered leading to an undesirable performance. Newell *et al.* (2001a) have studied the surface energy difference of 100% crystalline/amorphous lactose, physical mixture of crystalline lactose (99%) and amorphous lactose (1%), and milled lactose with around 1% (w/w) of amorphous content. It was found that the milled lactose has a surface energy close to the 100% amorphous lactose. According to the authors, this phenomenon was due to the fact that amorphous content of the milled lactose is mainly located at the surface. The surface of the milled lactose might cause difficulties in wet granulation of micronised drugs and performance variability in micronised inhalation products (Newell *et al.*, 2001a). This study demonstrates clearly how the unexpected formation of an amorphous phase could sometimes be detrimental.

In many other cases amorphous content is generated deliberately. For example, amorphous solid dispersions are prepared in order to achieve improved apparent solubility and rapid dissolution rate of poorly soluble drugs. It is known that the surface energy can greatly influence some fundamental issues of a system, such as dissolution (Rowe, 1988, 1989). If the surface energy of a solid dispersion changes during storage, the dissolution properties of the solid dispersion could be affected. Furthermore, a solid dispersion can be applied in many administration routes and dosage forms. As such, it has to be mixed with other excipients. For example, during capsule filling, tabletting and preparation of dry powder inhalation, the solid dispersion might be mixed with some other relevant compounds and excipients. Whenever a solid gets in contact with another substance irrespective whether it is a solid or liquid, the surface energy of the system immediately starts to affect the interaction. Therefore, it is very important to

study the surface energy of solid dispersions, especially during storage. It is known that the amorphous state would have a different surface energy if it crystallised, but understanding of the surface energy behaviour during relaxation (where the sample is still amorphous) is limited. Hence further studies are necessary to understand this issue. The hypothesis based in this chapter is: since relaxation is accompanied by a reduction in energy, it is very likely that the surface energy of the solid dispersion would decrease as a consequence of relaxation. On the other hand, it will also be interesting to investigate if the change of surface energy could provide any information about the molecular mobility at the surface, since molecular mobility is highly related to the stability of an amorphous material. Herein, solid solutions of polyvinylpyrrolidone (PVP) and indometacin were prepared using melt quenching and ball milling and subjected to physical aging. The surface properties change during aging was monitored using inverse gas chromatography (IGC). The use of IGC has been rapidly growing in the pharmaceutical field. Its advantages over some other surface measuring methods have been discussed in Chapter 2. Basically, IGC is a versatile technique for studying influence of mechanical treatment on the surface of solid samples (York *et al.*, 1998), determination of surface (Buckton *et al.*, 2004) and bulk glass transition temperature (Surana *et al.*, 2003), effect of relative humidity (RH) on the solid surface (Newell *et al.*, 2001b), batch to batch surface variations (Ticehurst *et al.*, 1994) and so forth. IGC will be used in this study to help better understand the surface properties of solid dispersions.

3.2 Chapter outline

The outline of this chapter is 1) to prepare amorphous solid solutions of PVP and indometacin by melt quenching and ball milling and characterise them using X-ray powder diffraction (XRPD), differential scanning calorimetry (DSC) and Fourier transform infrared (FTIR); 2) to study the change of dispersive surface free energy of the solid solutions during aging; 3) to study the acid and base parameters of the solid solution; and 4) to develop an efficient and convenient method for detecting the molecular mobility at the surface of amorphous materials.

3.3 Methods

3.3.1 Preparation of physical mixtures

20 g of powders with a ratio of 30% (PVP) to 70% (indometacin) were weighed carefully into a glass bottle and mixed using a Turbula mixer for 15 min. These physical mixtures were kept at room temperature in a desiccator together with silica gel until further use for the preparation of solid dispersions.

3.3.2 Ball milling

5 g of indometacin and PVP powders with a ratio of 70%:30% was weighed carefully into a milling pot. The weighing process was conducted in a glove bag with N_2 flowing through to keep the relative humidity lower than 10% RH and the pot was wrapped with parafilm before moving out from the glove bag to prevent moisture getting inside during milling. The powders were then milled for 18 hours at 300 rpm to achieve complete amorphous state conversion as described in Section 2.2.2. Afterward, the milled powders were collected from the pot and passed through a 90 micron sieve to break down any lumps in the glove bag and then kept in a vacuumed desiccator over phosphorus pentoxide (P_2O_5) at room temperature for 2 hours to allow efficient drying. The use of a glove bag through out the experiment was intending to lower the potentiality of moisture sorption.

3.3.3 Melt quenching

Indometacin and PVP with a ratio of 70% and 30% were melt quenched using the method described in Section 2.2.3.

3.3.4 Inverse gas chromatography (IGC)

IGC measurements were performed on the ball milled and melt quenched products using the methods described in Section 2.2.5. These measurements were conducted to study the dispersive surface energy, the acidic parameter K_A and basic parameter K_D, and the decane retention volume change during aging of the products.

3.3.5 Differential scanning calorimetry (DSC)

Differential scanning calorimetry was applied to confirm the amorphous state of the ball milled and melt quenched products using the method described in Section 2.2.6 Calibration of DSC was conducted by measuring the melting temperature and heat of fusion of pure indium. After calibration, around 5 mg of samples was weighed carefully into a non-hermetically sealed pan. The sample was then heated at a heating rate of 20 °C from -20 to 220 °C under a N_2 gas purge at a flow rate of 20 mL/min.

3.3.6 X-ray Powder Diffraction (XRPD)

X-ray powder diffractions were also performed according to the method described in Section 2.2.7 in order to confirm the amorphous state of the products after ball milling and melt quenching. Also, XRPD was used to monitor the amorphicity of the samples after physical aging.

3.3.7 Fourier transform infrared spectroscopy (FTIR)

Fourier transform infrared spectroscopy was used to study the intermolecular interactions between indometacin and PVP. The experimental condition used was described in Section 2.2.8. Each sample was measured in triplicate.

3.3.8 Scanning electron microscopy (SEM)

The morphology of the samples was studied using scanning electron microscopy as described in Section 2.2.9.

3.4 Results and discussion

3.4.1 Physical properties of the solid solutions

3.4.1.1 Melt quenched solid solutions

Indometacin is a white powder when it is in the crystalline form. After melt quenching with PVP, indometacin turned into yellow indicating the presence of the amorphous state. The change of color during crystalline-amorphous transition could be attributed to the rearrangement of molecules in different forms. The drug to carrier ratio chosen here is 70% to 30%. In this ratio the dimer form of indometacin is completely eliminated by PVP and the molar ratio of indometacin to the monomer unit of PVP is close to 1:1, which means the hydrogen bonding between the indometacin carboxyl and the PVP carbonyl group is substantial (Matsumoto and Zografi, 1999). The surface morphology of the solid solution was characterised by scanning electron microscopy (SEM) which showed that the melt quenched particles have irregular shapes with a size around 10-20 μm (Figure 3.1). Complete formation of amorphous indometacin was achieved according to the XRPD result, as the XRPD pattern (Figure 3.2) showed a halo shape (which is typical for an amorphous material) and lack of any characteristic peak of crystalline indometacin. Moreover, the DSC study has confirmed that indometacin was in the amorphous form since no melting peak was observed during a conventional scan of the sample (Figure 3.3).

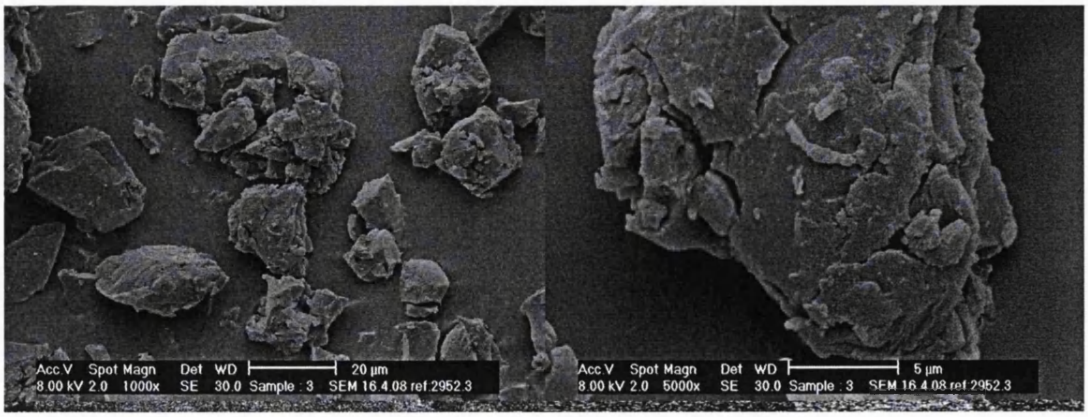

a b

Figure 3.1: *SEM images of melt quenched indometacin:PVP (70%:30%) solid solution (a, 20 μm and b, 5 μm).*

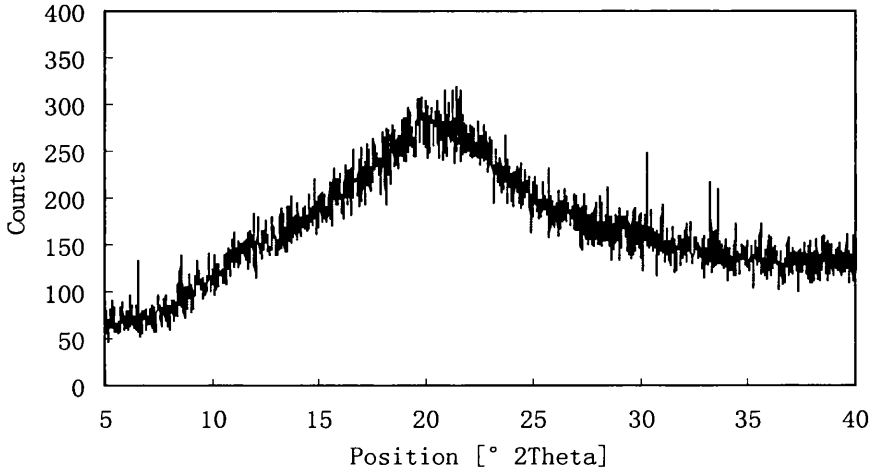

Figure 3.2: *XRPD pattern of melt quenched indometacin:PVP (70%:30%) solid solution.*

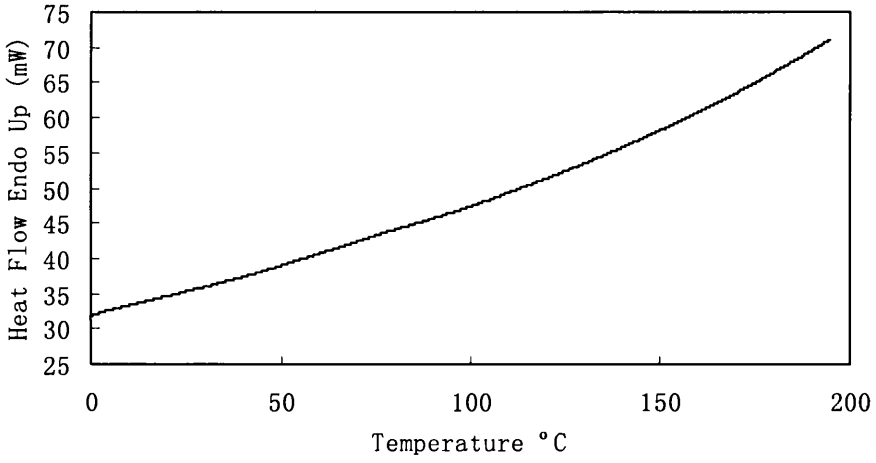

Figure 3.3: *Conventional DSC scan of melt quenched indometacin:PVP (70%:30%) solid solution.*

3.4.1.2 Ball milled solid solutions

Ball milling is one of the commonly used methods for the preparation of amorphous forms. However, some previous reports showed that it is difficult to achieve complete crystalline to amorphous transition in the absence of any excipient (Patterson *et al.*, 2007). Indometacin on its own is very difficult to be milled into a completely amorphous form at room temperature. Figure 3.4 shows that after being milled

continuously for 48 hours without any additive, indometacin still exhibited characteristic peaks of its γ-form, albeit with reduced peak intensities.

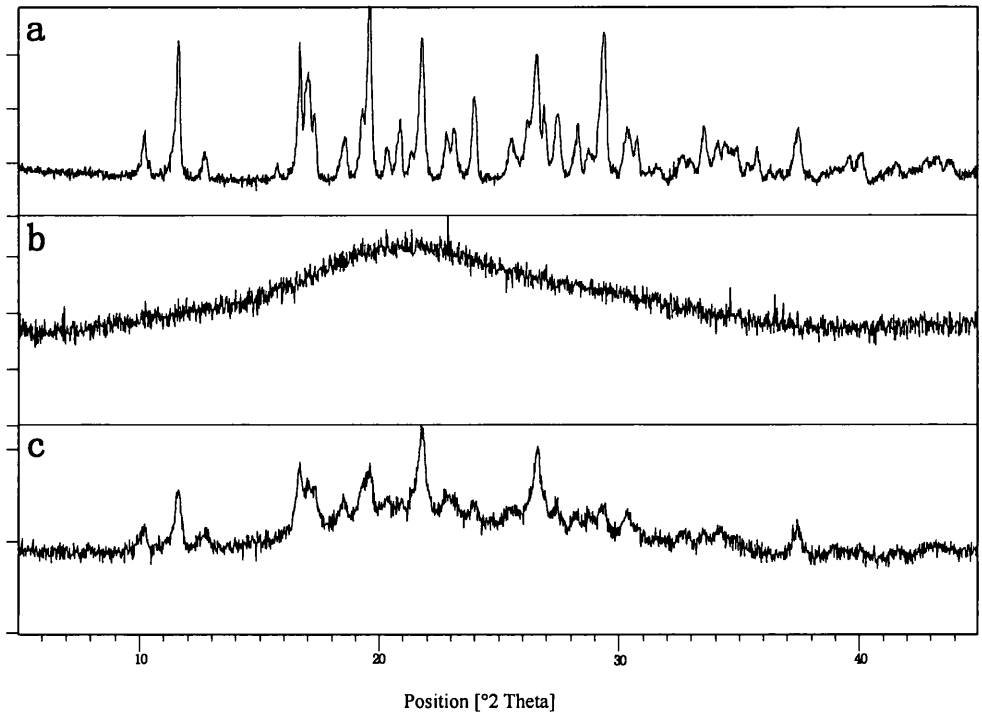

Figure 3.4: *XRPD patterns of a) γ-indometacin, b) melt quenched (amorphous) indometacin and c) γ-indometacin milled continuously for 48 hours.*

Some studies have shown that high-energy milling is capable of producing solid solutions (Boldyrev *et al.*, 1994) or form miscible drug-excipient regions (Friedrich *et al.*, 2005). The same ratio of indometacin and PVP as the melt quenched sample was milled here in order to achieve complete amorphous form. In order to decide a suitable milling time, the physical mixture was milled by a planetary mill and at the time points of 0.5, 1.5, 3, 6, 12, 18 hours a small amount of sample was collected for characterisation by Hyper DSC studies. Figure 3.5 shows that during milling, the enthalpy of melting decreased gradually and completely vanished after 18 hours. Based on the DSC results, it was found that indometacin could be turned amorphous when milled with PVP. The hydrogen bond interaction between PVP and indometacin might be the main reason facilitating the amorphous state conversion of indometacin. FTIR

studies of the interaction between PVP and indometacin will be discussed in the next section. The XRPD pattern has also shown a typical halo shape for the ball milled sample confirming its amorphous nature.

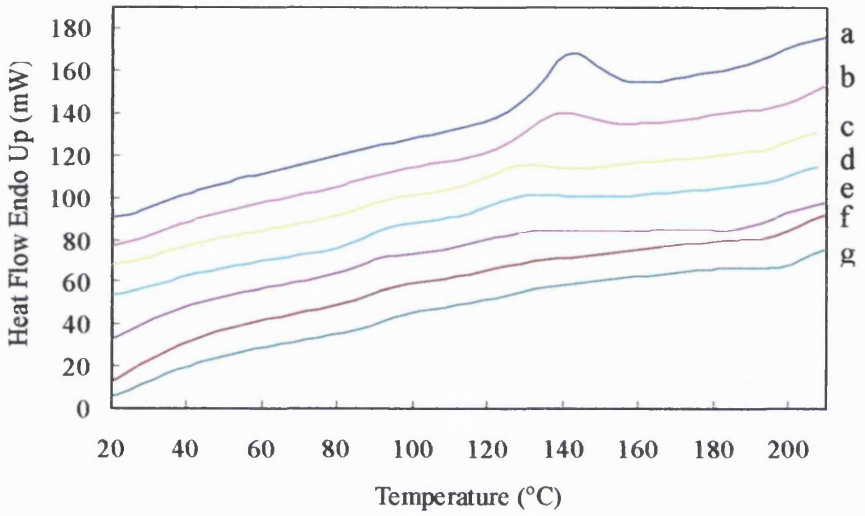

Figure 3.5: *Hyper-DSC traces of indometacin and PVP (70%:30%) physical mixture milled for 0.5 (a), 1.5 (b), 3 (c), 6 (d), 9 (e), 12 (f), and 18 (g) hours.*

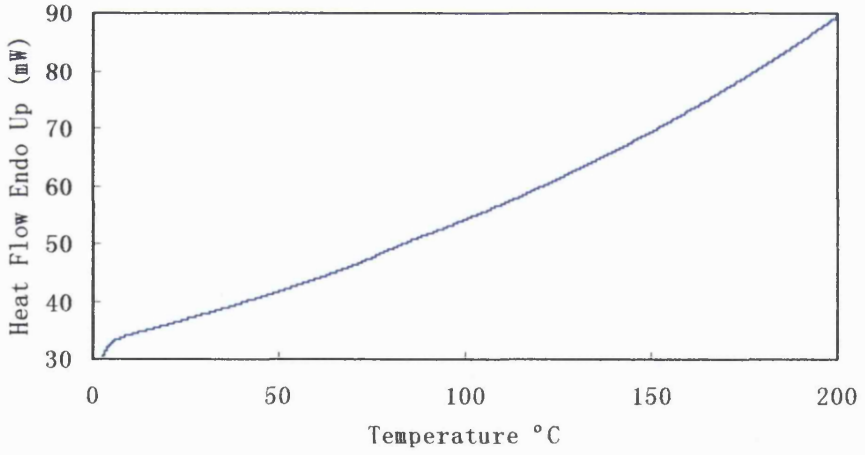

Figure 3.6: *Conventional DSC scan of ball milled indometacin:PVP (70%:30%) solid solution (18 hours of milling).*

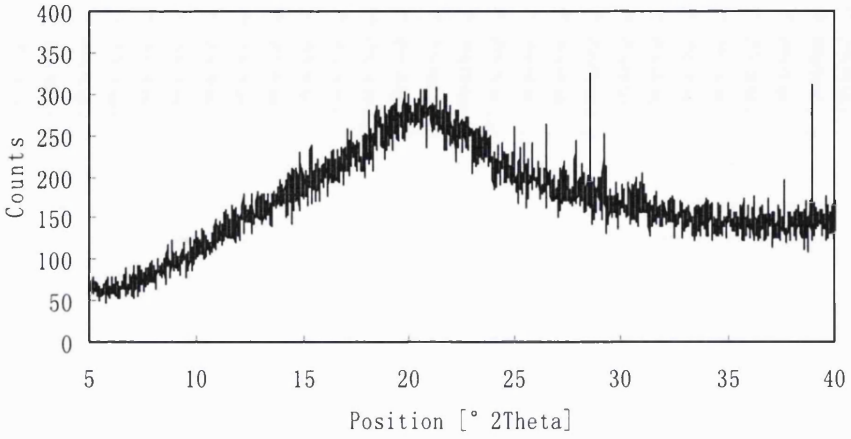

Figure 3.7: *XRPD pattern of ball milled indometacin:PVP (70%:30%) solid solution (18 hours of milling).*

SEM images of the ball milled solid solution are shown in Figure 3.8. Compared to the melt quenched sample, the ball milled sample has a smaller particle size (5-10 μm).

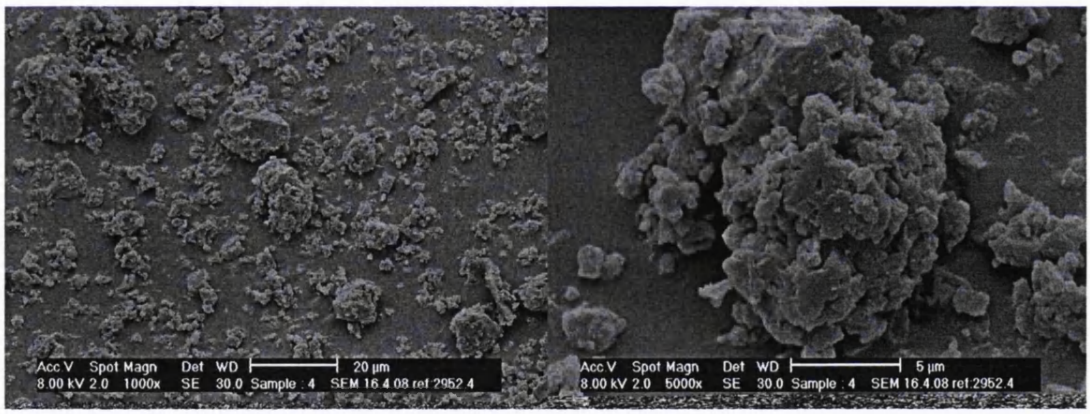

a b

Figure 3.8: *SEM images of ball milled indometacin:PVP (70%:30%) solid solution (a, 20 μm and b, 5 μm).*

3.4.1.3 Hydrogen bonding between indometacin and PVP

A hydrogen bond is a chemical bond in which a hydrogen atom of one molecule is attached to an electronegative atom (usually nitrogen, oxygen, or fluorine atom) of another molecule. Hydrogen bonding can occur within different functional groups of a single molecule, or between different molecules (Taylor and Zografi, 1998). The

strength of a hydrogen bond can range from as weak as van der Waals forces to so strong that they can hardly be distinguished from covalent bonds. The energy of a hydrogen bond is around 5 to 30 kJ/mole, close to some weak covalent bonds which only have about 20 times stronger energy. Therefore, the hydrogen bond is often deemed to be the most important of all directional intermolecular interactions (Serajuddin, 1999). In pharmaceutical research, intermolecular hydrogen bonding interaction is frequently utilised in order to improve the stability of an amorphous material. When hydrogen bonding to a certain carrier, the molecular mobility of an amorphous compound is reduced, therefore, its crystallisation tendency is hindered. There are many examples from the literature (Taylor and Zografi, 1998; Watanabe *et al.*, 2003). In a study done by Al-Obaidi (2007), it was found that phase separation happened very quickly in a griseofulvin-PVP solid dispersion because there was no hydrogen bonding interaction detected in this system. In contrast, griseofulvin-pHPMA solid dispersion could remain stable for more than 18 months because of the strong intermolecular hydrogen bonding between them (Al-Obaidi, 2007).

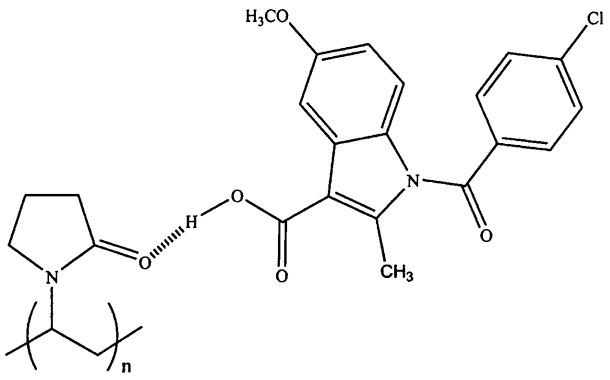

Figure 3.9: *Hydrogen bonding between PVP and indometacin.*

Taylor and Zografi (1997) have used spectroscopic methods to examine the structure of binary amorphous mixtures of indometacin and PVP at the molecular level. The study suggested that drug and carrier interact in the solid dispersions through hydrogen bonds formed between the hydroxyl of indometacin and carbonyl of PVP resulting in

disruption of indometacin's dimmer structure. The geometry structure of indometacin and PVP is shown in Figure 3.9.

The interactions between indometacin and PVP of both the melt quenched and ball milled solid solutions were studied using FTIR (Figure 3.10). In the physical mixture, the peak at 1715 cm^{-1} relates to the dimer form of indometacin while the peak at 1692 cm^{-1} relates to its carbonyl peak. The ball milled and melt quenched solid solutions show similar spectra indicating the preparation methods did not give a significant influence to the hydrogen bonding of the components. In the spectra of the solid solutions, the dimer peak at 1715 cm^{-1} has disappeared, a new peak started to show at around 1724 cm^{-1}, and the carbonyl peak of PVP at 1692 cm^{-1} shifted to a lower wavenumber. These changes of the peaks indicate that indometacin and PVP are forming a strong hydrogen bond.

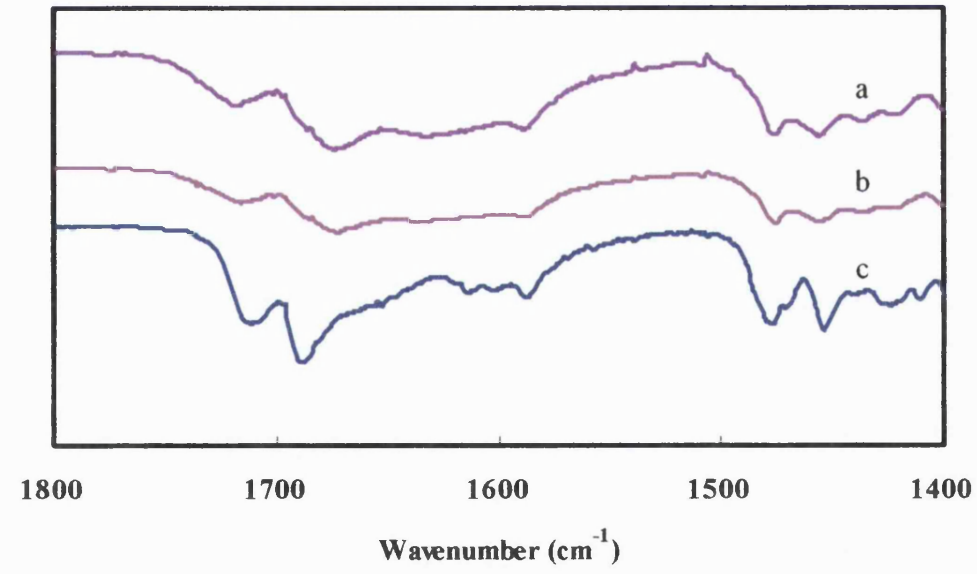

Figure 3.10: *FTIR spectra of indometacin and PVP (70%:30%): a) ball milled solid solution, b) melt quenched solid solution and c) physical mixture.*

3.4.2 Changes of surface free energy of the solid solutions during physical aging

In order to make a bulk cleave into two surfaces, energy is needed to disrupt any intermolecular bonds and this energy is quantified as surface free energy. Therefore, surface free energy is usually defined as the energy needed to generate a unit area of surface. It is one of the most important parameters used to represent the energetic level on the surface of a solid material because when a solid gets into close contact with another solid or liquid, their surface energetic level will affect the interaction. For example, wetting of some liquids on a solid would be easier on the high energy surface such as glass, ceramics, and metals (held together by covalent, ionic, or metallic chemical bonds) while for some crystals, where the molecules are held together by weak molecule force such as van der Waals force or hydrogen bonding, wetting would become more difficult.

Depending on the nature of the forces such as dispersive (non-polar) forces, or polar forces (acid base or hydrogen bonding), the surface free energy (γ) can be divided into dispersive (γ^d) and polar (γ^p) components. There are several techniques suitable to determine the surface free energy, such as contact angle measurements and IGC. It has been discussed that there are some drawbacks with the contact angle methods: 1) when compressing powders onto a plate or a disk, the compression force applied might alter the surface properties or surface roughness; 2) Although the powder can be attached to a glass slide with an adhesive, it still can not solve the problem regarding the surface roughness (Grimsey *et al.*, 2002); and 3) Measuring the rate of liquid penetration through powder beds does not require compression of the powders, but the measurements can be affected by the particle size, pore geometry and etc (Buckton, 1995). Therefore, IGC as an alternative method drew more interest for surface free energy determination. Ticehurst *et al.* (1994) showed that result of the IGC and contact angle methods might not be the same. IGC at infinite dilution condition is probably only measuring a small part of the powder surface. So with a heterogeneous surface, probes would tend to interact with the more energetic surface sites first giving a bias result of the whole sample. However, many studies have shown that these two methods are well

correlated (Dove *et al.*, 1996; Planinsek *et al.*, 2001).

It has been discussed in Chapter 2 that the dispersive surface free energy or polar component data obtained by IGC can be used as a very useful index to detect batch variability or to predict interfacial interaction. In this section the dispersive surface energy and acid-base parameters of the indometacin solid solutions are measured as a function of time at different temperatures in order to understand how structure relaxation affects the surface properties.

Calculation of the surface free energy

Samples under characterisation need to be packed into a glass column, and minimum concentration of polar or non-polar probes are injected and carried through the column in the flow of an inert gas (helium). The time required for the probe to elute out (t_r) can be used as an indicator of the interaction level between the probe and the solid surface. After correcting the effect of the void space by subtracting t_r with t_m (retention time of an inert probe, such as methane), net retention time t_n can be obtained. Therefore, the net retention volume, which means the amount of carrier gas required to elute out all the probe molecules, can be calculated using Equation 3.1:

$$Vn = \frac{j}{M} \cdot F \cdot (t_r - t_m) \cdot \frac{T}{273.15} \qquad \text{Equation 3.1}$$

where V_n is the net retention volume, T is the column temperature, M is the sample mass, F is the exit flow rate of the carrier gas at 1 atm and 273.15K, and j is the James-Martin compressibility correction factor for correction of the retention time affected by the pressure drop in the column.

According to Equation 3.2, the net retention volume can be related to the free energy of sorption ΔG_{ads}:

$$\Delta G_{ads}^{D} = -RT\ln(V_n) + K \qquad \text{Equation 3.2}$$

where R is the gas constant and K is a constant to compensate the effect of the vapour pressure, weight and surface area of probes in the gas state (Schultz *et al.*, 1987).

The relation of the free energy and the work of adhesion W_{ads} between probe molecule and solid is shown in Equation 3.3:

$$\Delta G_{ads}^{D} = N \cdot a \cdot W_{ads} \qquad \text{Equation 3.3}$$

where a is the interaction surface area of the liquid probe molecules and N is the Avogadro constant. W_{ads} is the work of adsorption which can be split into a dispersive and a specific interaction component according to Fowkes (1964):

$$W_{ads} = W_{ads}^{D} + W_{ads}^{S} \qquad \text{Equation 3.4}$$

where W_{ads}^{D} is the work of adsorption due to the van der Waals forces and W_{ads}^{S} is the specific work of adsorption due to polar interactions. As for the calculation of dispersive surface free energy, only non-polar probes are used, the W_{ads} can be expressed only by the dispersive interactions:

$$W_{ads} = 2(\gamma_s^d \cdot \gamma_l^d)^{1/2} \qquad \text{Equation 3.5}$$

where γ_s^d is the surface tension of the solid and γ_l^d is that of the probe. Combining Equation 3.3 and 3.5 leads to:

$$RT\ln(V_n) = 2N \cdot (\gamma_s^d)^{1/2} \cdot a \cdot (\gamma_l^d)^{1/2} \qquad \text{Equation 3.6}$$

Schultz *et al.* (1987) described a method basing on Equation 3.6 to calculate the dispersive component of the solid sample (γ_s^d). The values of interaction surface (a) and dispersive free energy of the probe (γ_l^d) can be found from the literature (Schultz *et al.*, 1987; Nardin and Papirer, 1990), therefore, after obtaining the V_n value by IGC experiment, γ_s^d can be obtained from the slope of Equation 3.6 according to a plot of $RTlnV_n$ versus $a \cdot (\gamma_l^d)^{1/2}$ for a series of alkane (non-polar probes).

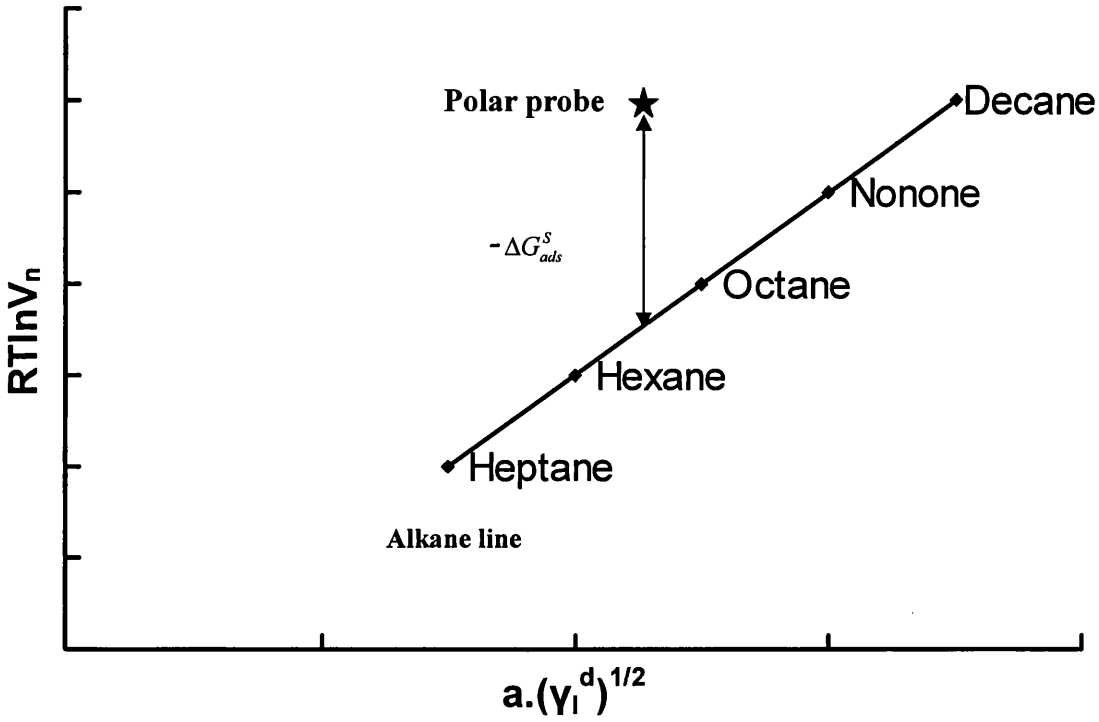

Figure 3.11: *An example of a plot of* $RTlnV_n$ versus $a \cdot (\gamma_l^d)^{1/2}$ *for alkanes: decane, nonane, octane, heptane and hexane.*

When a polar probe such as chloroform or ethanol is used, its $RTlnV_n$ value would lie above the alkane line, and the vertical distance between the point of the polar probe and the alkane line is the specific free energy of adsorption of the probe and the solid surface ($-\Delta G_{ads}^S$). According to Equation 3.7, after obtaining ΔG_{ads}^S at different temperatures, the specific enthalpy and the specific entropy of adsorption can be

obtained:

$$\Delta G_{ads}^{S} = \Delta H_{ads}^{S} - T\Delta S_{ads}^{S} \qquad \text{Equation 3.7}$$

The value of ΔG_{ads}^{S} can be related to the acidic (electron accepting) parameter K_A and the basic (electron donating) parameter K_D as shown in Equation 3.8:

$$-\Delta G_{ads}^{S} = K_A \cdot DN + K_D \cdot AN^{*} \qquad \text{Equation 3.8}$$

where DN is a base (electron donor) number characterised according to Gutmann (1978), and AN^{*} is an acid (electron acceptor) number (Riddle and Fowkes, 1990). After plotting $-\Delta G_{ads}^{S}/AN^{*}$ versus DN/AN^{*}, the values of K_A and K_D of the solid sample can be acquired from the intercept and the gradient of the line. The DN and AN^{*} values can be found from the literature (Gutmann, 1978; Riddle and Fowkes, 1990).

3.4.2.1 Dispersive surface free energy of melt quenched solid solutions

Step-scan DSC studies were conducted and it was shown that the T_g of the solid solution is around 67 °C (with a ΔC_p of 0.25 J/g), which is close to the T_g value of 68 °C reported by Matsumoto and Zografi (1999) on a spray dried solid solution with the same component ratio. There was only one T_g detected over the entire scanning range which indicates that a single miscible amorphous phase was formed. Based on the T_g value, the aging temperature was decided to be 7, 17 and 27 °C lower than the T_g (i.e. 60, 50 and 40 °C). The solid solution was therefore split into 3 groups and stored at these three temperatures in 0 % RH for 2, 4, 6, 9, 12 and 18 days. To check that whether the solid solution could remain amorphous during the aging period, FTIR, XRPD and DSC (Figures 3.12-3.14) studies were conducted in order to test any recrystallisation of these samples. Results showed that the solid solution remained amorphous during storage at each temperature. The XRPD patterns did not show any features of crystalline

indometacin, DSC did not show any melting of the crystals and the FTIR spectra remained the same at 60 °C for up to 18 days. These results gave evidence that any surface free energy change measured after aging would be the result of structure relaxation of the samples rather than recrystallisation.

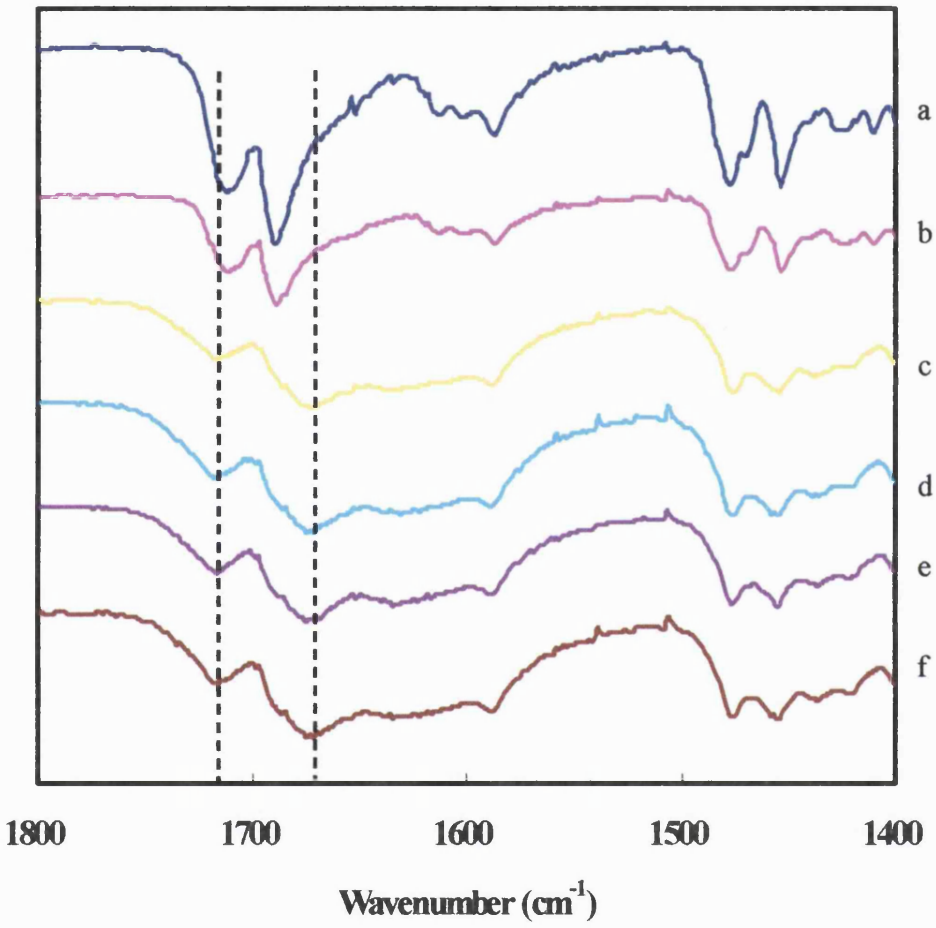

Figure 3.12: *FTIR spectra of crystalline indometacin (a), physical mixture (b), and melt quenched solid solution of indometacin and PVP (70%:30%) aged for 0 (c), 6 (d), 12 (e) and 18 (f) days at 60 °C.*

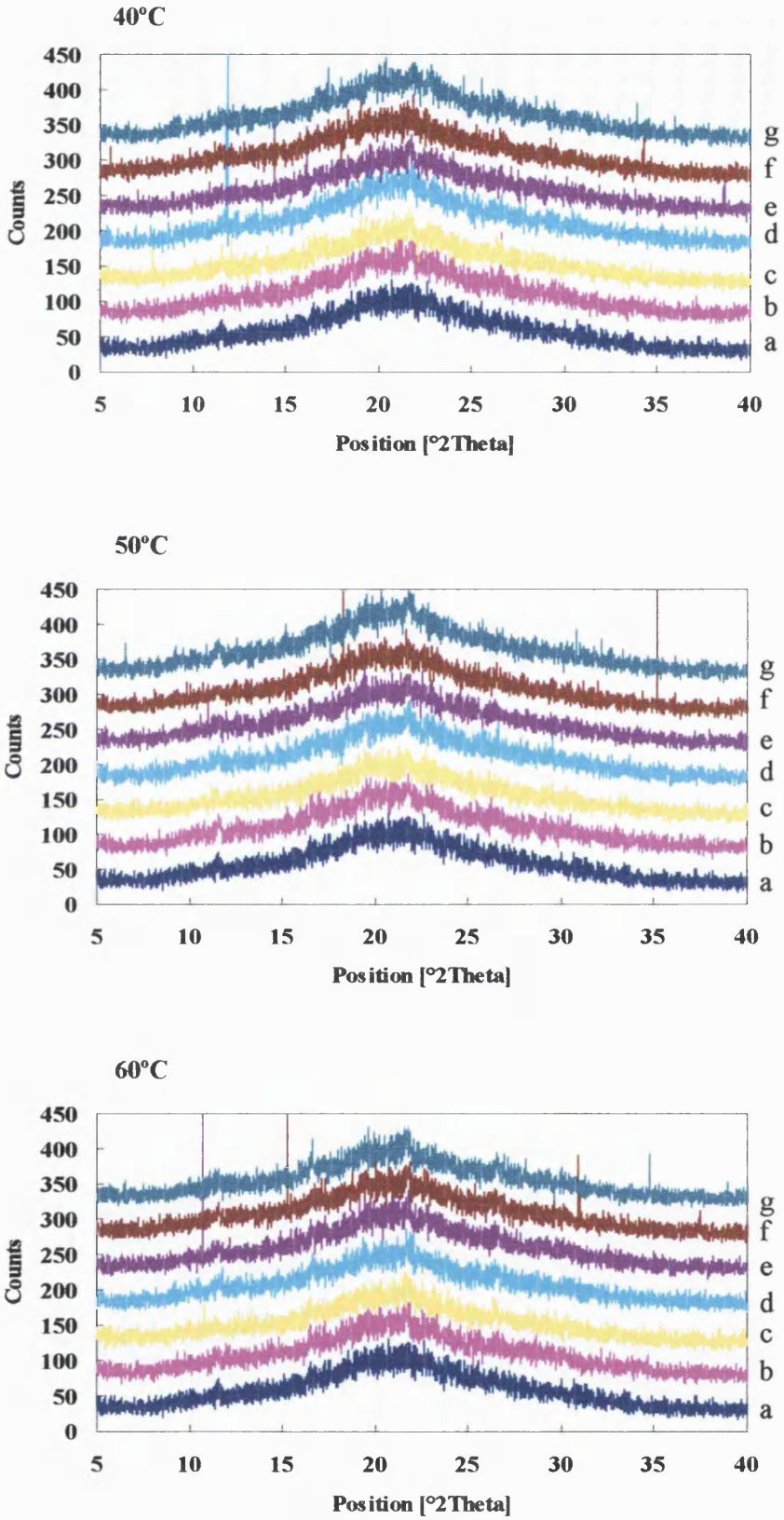

Figure 3.13: *XRPD patterns of the melt quenched indometacin:PVP (70%:30%) aged at 40, 50 and 60 ℃ for 0 (a), 2 (b), 4 (c), 6 (d), 9 (e), 12 (f) and 18 (g) days.*

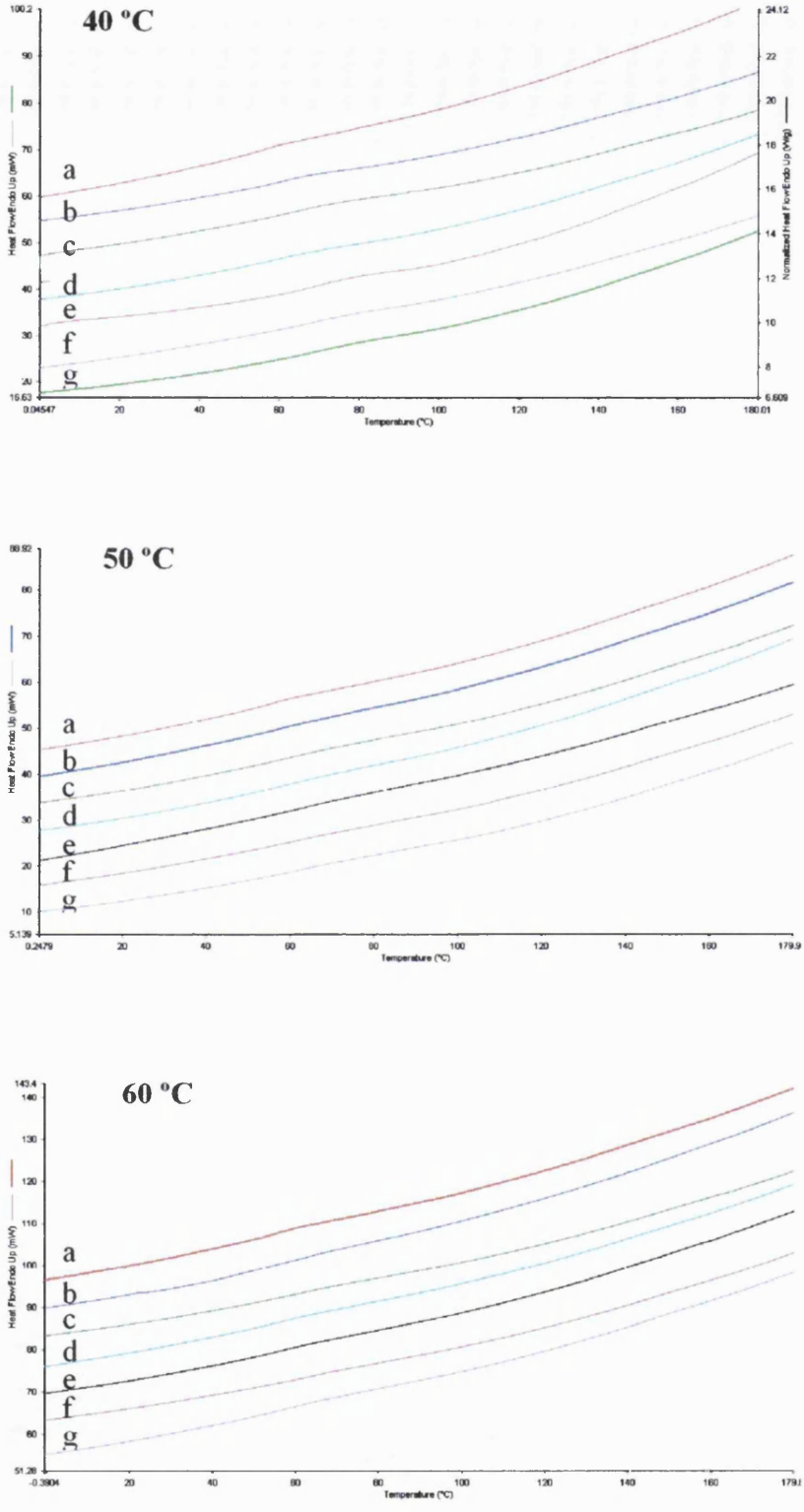

Figure 3.14: *Conventional DSC scans of the melt quenched indometacin:PVP (70%:30%) solid solutions aged at 40, 50 and 60 °C for 0 (a), 2 (b), 4 (c), 6 (d), 9 (e), 12 (f) and 18 (g) days.*

Table 3.1 shows the γ^d of indometacin, PVP, and melt quenched indometacin-PVP solid solution (the γ^d values were means of 4 repeats on the same batch of samples). The γ^d of indometacin is close to the literature value which is 39.65 mJ/m^2 (Bajdik *et al.*, 2004) determined according to Wu's method (Wu, 1971). The γ^d of PVP is also in good correlation with the one (48.0 mJ/m^2) reported by Planinsek *et al.* (2001) using IGC. PVP as received from the manufacturer and the one just freshly melt quenched are close to each other, which means that any change of γ^d of PVP caused by relaxation during storage is negligible in the laboratory timescale. This is probably because of the slow relaxation rate of PVP at room temperature benefiting from its relatively high T_g value (c.a. 170 °C). The γ^d of the freshly prepared solid solution is 47.2 mJ/m^2, higher than that of the pure indometacin. This result indicates the surface of indometacin was in a higher energy state after compounding with PVP. It is interesting to note that the dispersive surface free energy of most pharmaceutical compounds is usually greater than 40 mJ/m^2 as determined by means of either IGC or contact angle measurement. This is probably due to the reason that the testing materials usually consist of oxygen, hydrogen, and carbon (Planinsek *et al.*, 2001).

	Indometacin	PVP (as it is)	PVP (melt quenched)	Solid solution of indometacin:PVP (70%:30%) day 0
γ^d (mJ/m^2)	42.24±0.45	47.45±0.48	48.17±0.66	47.20±0.39

Table 3.1: *Dispersive surface free energy of the pure components and the melt quenched solid solution (indometacin:PVP, 70%:30%) measured by IGC (values are mean ± s.d., n=4).*

As shown in Figures 3.15-3.17, the γ^d of the solid solution decreases as a function of time for all the temperature tested, indicating the high energy sites of the sample were

relaxing toward a lower energy state. The initial γ^d of the solid solution is 47 mJ/m^2 and the difference between the initial and the minimum γ^d is 3.05 mJ/m^2 at 40 °C, 5.51 mJ/m^2 at 50 °C and 6.64 mJ/m^2 at 60 °C after aging for 18 days. These results indicate different decreasing rates of γ^d at different temperatures. It can be seen that though at each time point the solid solution samples were measured 4 times, at some particular points a deviation of the γ^d value from the overall decreasing trend is shown. This is not a surprising result. In a previous study, Newell *et al.* (2001b) used IGC to measure the γ^d of amorphous lactose which was 37.1 ± 2.3 mJ/m^2 based on 12 measurements. From the standard deviation, it is shown that the range of the surface energy may vary significantly (4.6 mJ/m^2). It is logical to expect that the random orientation of amorphous material would give a wide range of surface energies obtained from different measurements.

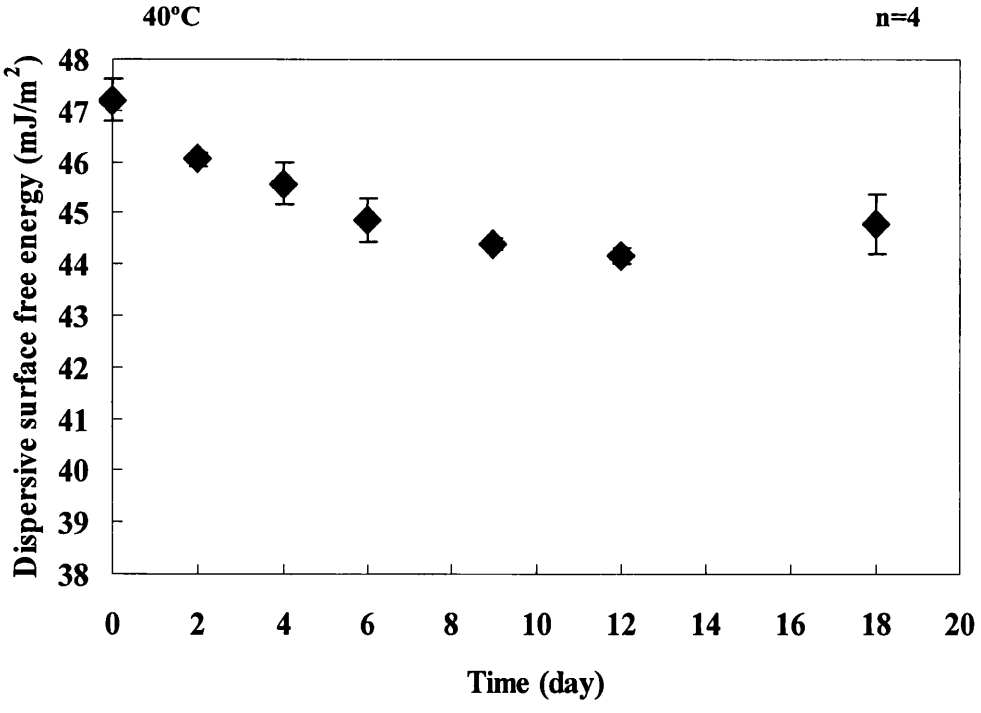

Figure 3.15: *Changes of dispersive surface free energy of the melt quenched solid solution (an indometacin to PVP ratio of 70%:30%) aged at 40 °C.*

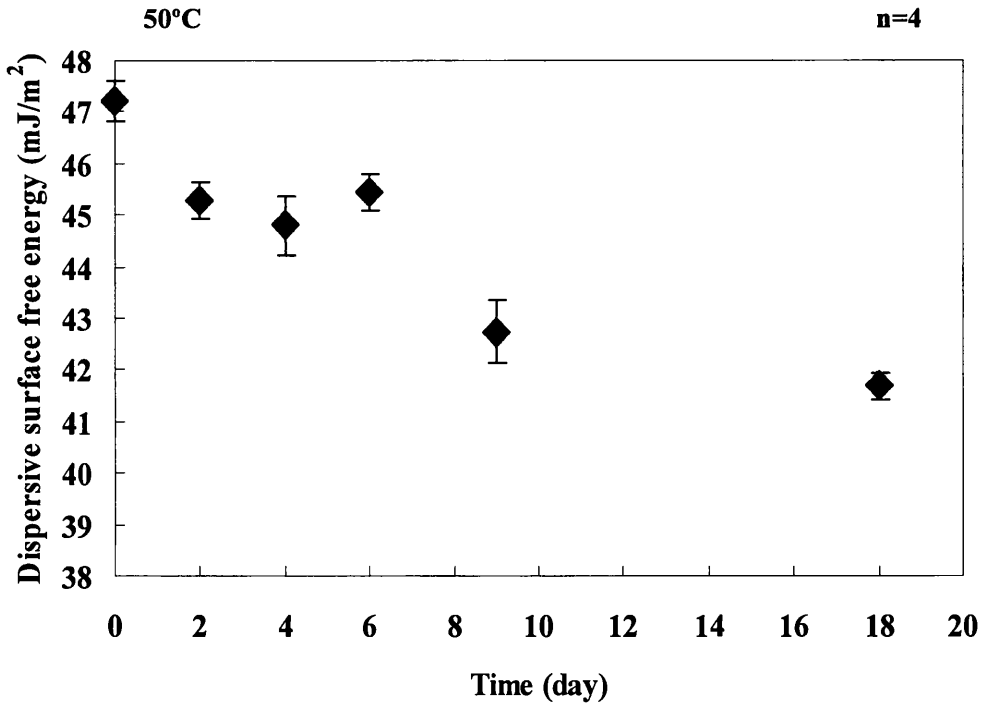

Figure 3.16: *Changes of dispersive surface free energy of the melt quenched solid solution (an indometacin to PVP ratio of 70%:30%) aged at 50 °C.*

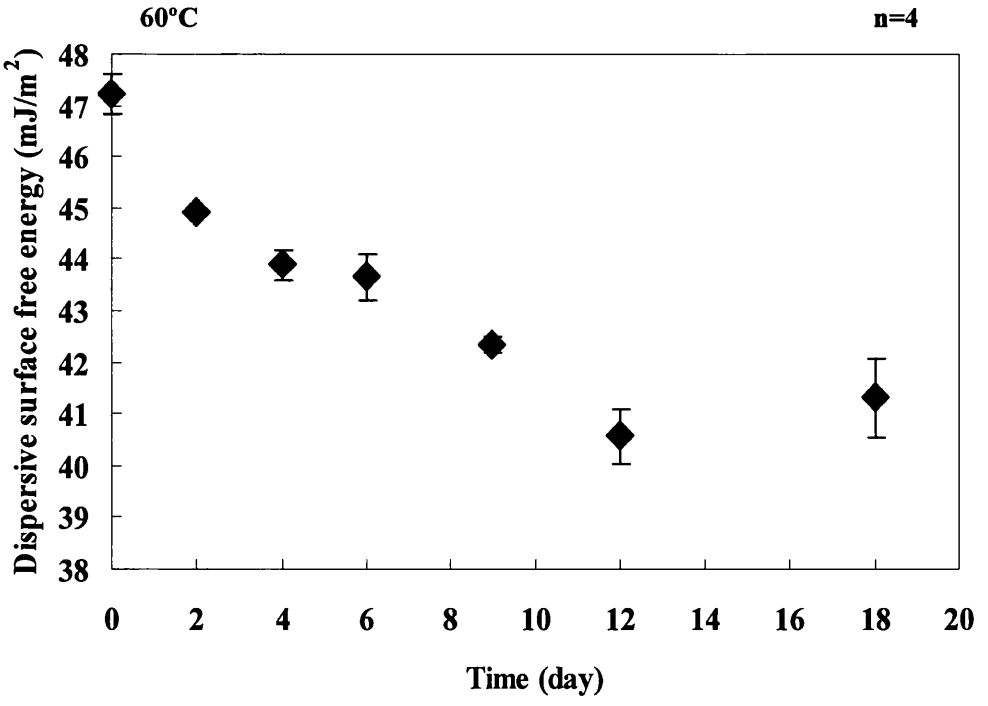

Figure 3.17: *Changes of dispersive surface free energy of the melt quenched solid solution (an indometacin to PVP ratio of 70%:30%) aged at 60 °C.*

Relaxation in the glassy state is often referred to as structural relaxation, which means the changes in atomic/molecular arrangements that occur during relaxation (Hilden and Morris, 2004). In a study, Hogan and Buckton (2001) have found that amorphous raffinose particles start to show the external shape of crystals prior to crystallisation. Therefore, the relaxation process of an amorphous state will lead to changes in the physicochemical properties of the amorphous form prior to any crystallisation event happening. The change in the physicochemical properties often associates with the change of free volume and enthalpy in the bulk while at the surface this change might be represented by the surface energy, as relaxation is often associated with a loss of energy. It is reasonable to believe that the decrease of γ^d indicates the surface relaxation of the solid solution.

The γ^d data were fitted to an empirical Kohlraush-Williams-Watts (KWW) equation in order to obtain the relaxation parameters of the solid solution. The KWW equation is a stretched exponential equation containing two adjustable relaxation time constants, τ and β:

$$\phi(t) = \exp(-(\frac{t}{\tau})^{\beta}) \qquad \text{Equation 3.9}$$

where t is time and $\Phi(t)$ is a relaxation function. The parameter τ is the relaxation time while β is regarded as the extent to which the relaxation process deviates from exponential behavior and is often called a "stretching parameter" (Shamblin *et al.*, 2000). The KWW equation is usually applied to the relaxation data including those obtained by measuring volume relaxation (Cowie *et al.*, 1998), dielectric relaxation (Stickel *et al.*, 1995), light scattering (Carroll and Patterson, 1985) and enthalpy relaxation (Hancock *et al.*, 1995). In DSC studies, relaxation can be estimated from the relaxation enthalpy, ΔH. First of all, the maximum enthalpy of relaxation at any storage temperature ΔH_{∞} must be calculated using Equation 3.10:

$$\Delta H_{\infty} = (T_g - T) \cdot \Delta C_p \qquad \text{Equation 3.10}$$

where T_g is the glass transition temperature of the sample, C_p is the heat capacity and T is the aging temperature. The relaxation enthalpy of DSC can be normalised using the following equation:

$$\phi(t) = 1 - \frac{\Delta H}{\Delta H_{\infty}} \qquad \text{Equation 3.11}$$

Therefore these normalised data can be fitted using the KWW equation to obtain the relaxation parameters τ and β. The KWW equation should also be appropriate for the fitting of the IGC data as well, but an important issue needs to be addressed is to obtain a minimum value which can reflect the lowest energy state that the sample's surface can relax to (like ΔH_{∞} in DSC). In the next section of this chapter, a modified KWW equation will be explained and applied in the calculation of this lowest energy point. Whereas in the case of the surface free energy study, the IGC data have a relatively high deviation and also the data points are not enough for the equation to obtain a reasonable value using this equation. Hence the minimum γ^d obtained during experiment was used accordingly for the normalisation of the IGC data (Equation 3.12):

$$\phi(t) = 1 - \left(\frac{\gamma^d - \gamma^d_{\min}}{\gamma^d_{\max} - \gamma^d_{\min}}\right) \qquad \text{Equation 3.12}$$

where $\gamma^d_{\max}$ is the initial surface free energy and $\gamma^d_{\min}$ is the minimum surface free energy. The normalised data were fitted using the KWW equation. Figure 3.18 shows a plot of the KWW fitting on the IGC data.

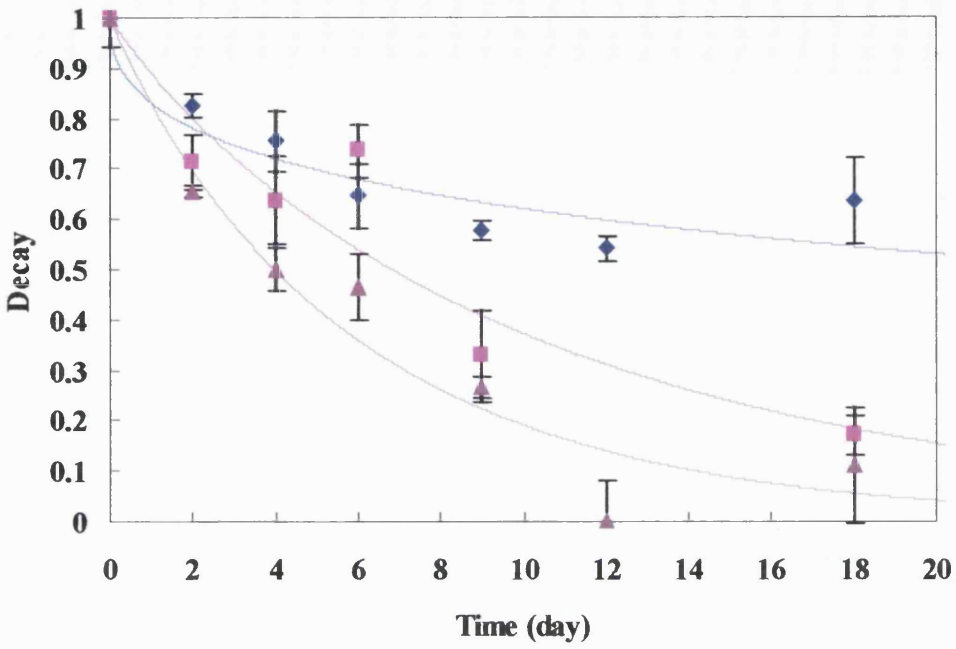

Figure 3.18: *Structural relaxation decay function determined from IGC data (n=4). The aging temperatures are: 40 ℃ (◆),50 ℃ (■) and 60 ℃ (▲) with KWW fitting (—).*

From the relaxation parameters shown in Table 3.2, it can be seen that as expected, τ values decreased as the aging temperature increased. This is because as the aging temperature increases, the molecular mobility of the solid solution increases, and the time needed for the molecules to totally relax would become less. Mirroring the decrease of τ, the β values increased as the aging temperature increased. In a previous study, Bhugra *et al.* (2007) have shown the temperature dependence of β as the aging temperature increased, β increased correspondingly. The parameter β is used to represent the distribution of relaxation times with a value close to one indicating a system with homogenous relaxation and a value close to zero indicating a large distribution of the relaxing substrates (Shamblin *et al.*, 2000). As already explained, the infinite relaxation enthalpy (ΔH_∞) can be calculated based on the aging temperature. From Equation 3.10, it can be seen that ΔH_∞ values increase if T_g-T increases (i.e. a lower aging temperature). A higher ΔH_∞ gives the possibility to the molecules to relax further away from the equilibrium stage, hence the relaxation level of the molecules at a

given time point would have a wider distribution potential comparing to a smaller ΔH_∞ at a higher aging temperature. In many studies, τ^β has been used for comparison of the relaxation rate because the τ^β value is more robust due to its lower sensitivity to experimental error (Liu *et al.*, 2002). It is rational to think that 40 °C, as the lowest aging temperature should have the longest relaxation time. However, Table 3.2 shows that at the temperature of 40 and 60 °C the τ^β values are similar while at 50 °C the τ^β is the highest. These results might be due to the scattering γ^d values at some time points which affect the KWW fitting. Therefore, the wide range of variation of the surface energy of amorphous sample might be a potential drawback for the use of surface free energy to accurately detect surface molecular mobility. Table 3.2 also shows R^2 which represents the coefficient of determination, and Chi^2/DoF representing the reduced Chi^2 value which was used to quantify the deviation of predicted values from the actual values. A Chi^2/DoF value close to zero indicates a perfect fit.

	40 °C	50 °C	60 °C
τ (day)	62.55	10.42	6.02
β	0.409	0.922	0.945
τ^β (day)	5.43	8.67	5.45
Chi^2/DoF	0.00376	0.0131	0.0074
R^2	0.8789	0.8835	0.9467

Table 3.2: *Relaxation parameters obtained from IGC data for the indometacin:PVP (70%:30%) melt quenched sample after KWW fitting (R^2, coefficient of determination, and Chi^2/DoF, reduced Chi^2 value).*

In order to study the effect of carrier ratio on the surface relaxation, the indometacin to PVP ratio was increased to 50%:50%. It was expected that if the aging temperature is the same, the dispersive surface free energy relaxation rate will be slower in this ratio,

because due to the anti-plasticisation effect, when the concentration of PVP increases, the T_g of the solid solution increases as well resulting a slower molecular mobility. The T_g of the (indometacin:PVP 50%:50%) solid solution was 78 °C as detected by DSC, about 10 °C higher than the one with 30% of PVP. XRPD and DSC studies have confirmed that the sample was in amorphous state. The aging temperatures used were 40, 60 and 70 °C. After the solid solution was aged for 3, 6, 9, 12 and 18 days, samples were removed for IGC studies to detect any change of the γ^d value.

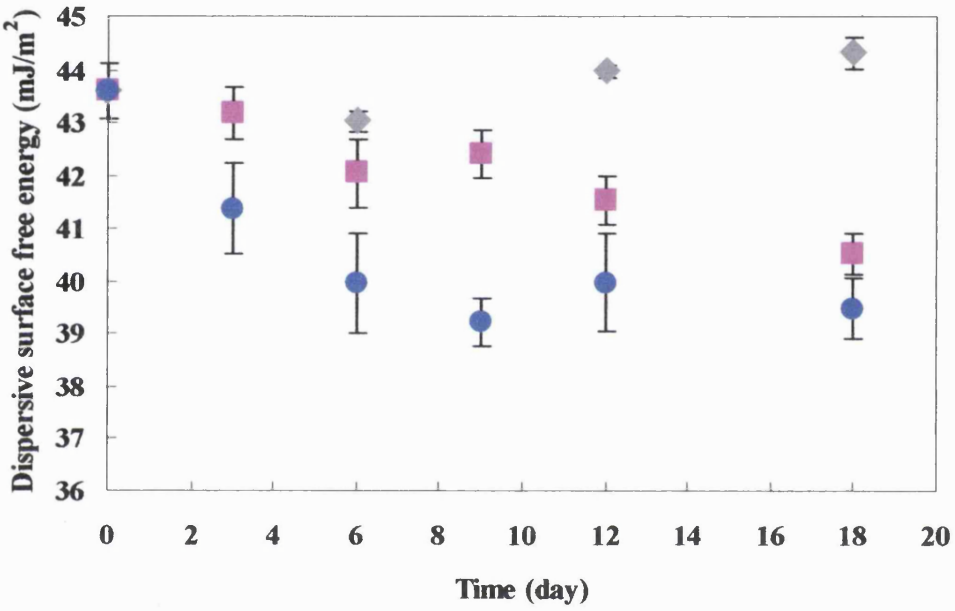

Figure 3.19: *A plot of dispersive surface free energy changes of melt quenched solid solutions (an indometacin to PVP ratio of 50%:50%) stored at 40 (◆), 60 (■) and 70 (●) °C (n=4).*

Figure 3.19 shows how γ^d decreased with time, and the degree of the relaxation is depending on the aging temperature. At the highest aging temperature 70 °C, the γ^d decreased most significantly with a difference of 4.13 mJ/m^2 between the initial and the end points. At 60 °C the difference is 3.08 mJ/m^2. This is because the sample would tend to relax in a higher extent at a temperature closer to its T_g due to the higher molecule mobility. The γ^d remained relatively the same at 40 °C after 18 days. In a study conducted by Hancock *et al.* (1995), it was observed that sucrose, PVP and indometacin

relax significantly even at temperatures well below their T_g, however, the authors find out that the molecular mobility seemed to be greatly reduced to a level which would not affect the life-time of the samples when they were stored at 50 °C below the T_g. When the solid solution was aged at 40 °C, about 38 °C lower than its T_g which was close to the 50 °C general limit, it is reasonable to consider that its relaxation rate would be very slow at this temperature. Therefore, the studied timeframe 18 days might not be long enough for the solid solution to show any significant energy reduction.

In order to study the effect of carrier on the γ^d relaxation more directly, the KWW equation was also applied here to obtain the relaxation parameters. As already explained previously, the minimum γ^d value was used for normalisation of the data to enable the fitting (Figure 3.20).

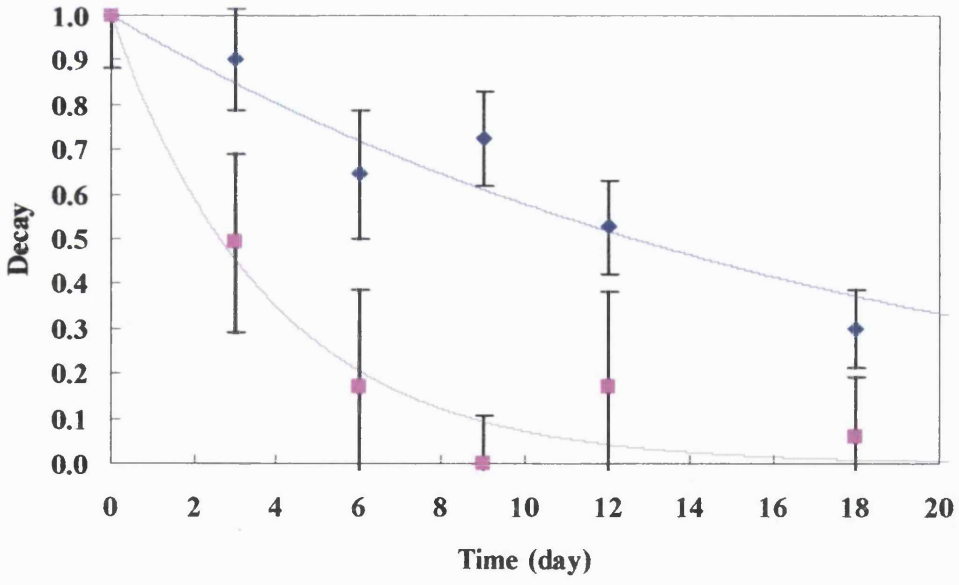

Figure 3.20: *Structural relaxation decay function determined from IGC data (n=4). The aging temperatures are: 60 °C (◆) and 70 °C(■) with KWW fitting (—).*

Since the data for γ^d at 40 °C did not show any significant change, KWW fitting at this temperature was not performed. For the temperatures at both 60 and 70 °C, KWW

fitting was able to performed, however the β sometimes was over 1 (1.0-1.15) which is physically impossible, because theoretically the β value is usually between 0 and 1 indicating the distribution of the relaxation. Therefore, during the fitting, the β value was fixed to 1 in order to obtain the τ values. Ramos (2006) has tried to use dispersive surface free energy to study the surface relaxation of amorphous lactose at 100, 65 and 50 °C, the β values the author obtained were ranging from 0.9 to 1.1 which are similar to the ones obtained in this study. The KWW equation is an empirical equation which has been mostly applied to enthalpy relaxation and dielectric relaxation. The suitability of using KWW equation for the fitting of the dispersive surface free energy relaxation still needs to be proved by further studies (Ramos, 2006). Furthermore, the high variation of the normalised values as shown in Figure 3.20 also indicates that γ^d is probably not sensitive enough for measuring the energy change during surface relaxation, therefore, the accuracy of fitting using the γ^d data might be affected.

	60 °C	70 °C
τ (day)	18.18	3.79
β	1	1
τ^{β} (day)	18.18	3.79
Chi^2/DoF	0.0053	0.0061
R^2	0.9176	0.9572

Table 3.3: *Relaxation parameters obtained from IGC data for the indometacin:PVP (50%:50%) melt quenched sample after KWW fitting (R^2, coefficient of determination, and Chi^2/DoF, reduced Chi^2 value).*

The relaxation parameters are shown in Table 3.3. A temperature dependence of the γ^d relaxation is indicated by the τ values while the solid solution at 60 °C has a much longer relaxation time than the one at 70 °C. At 60 °C, the solid solution containing 30

% of PVP has a relaxation time of 6.02 days and the one containing 50 % of PVP here has a relaxation time of 18.18 days. This fits with the hypothesis that the PVP could help to reduce the molecule mobility of the solid solution as a result of reducing its relaxation rate.

In this section, it has been shown that during aging, the energy on the surface of a melt quenched solid solution relaxed to a lower state according to the decrease of dispersive surface energy determined by IGC. This surface relaxation happened prior to the crystallisation of the surface as confirmed by XRPD, DSC and FTIR measurements. The surface relaxation has shown temperature dependence as the aging temperature gets closer to the T_g of the sample, the relaxation time is shorter, and the surface relaxation can be affected by the amount of carrier PVP which has been proven to be able to increase the relaxation time of the bulk of indometacin-PVP solid solution (Matsumoto and Zografi, 1999).

3.4.2.2 Dispersive surface free energy of ball milled solid solutions

Many researchers have shown that preparation method plays a very important role on the pharmaceutically relevant properties of the final amorphous products, such as the crystallisation rate (Surana *et al.*, 2004), the apparent solubility (Zhang *et al.*, 2009) and the dissolution behaviour (Patterson *et al.*, 2007) etc. Therefore, it would be interesting to study the effect of preparation method on the dispersive surface free energy of the indometacin-PVP solid solution. In this section, a ball milled solid solution with an indometacin to PVP ratio of 70%:30% was made and studied using IGC to monitor its dispersive surface free energy during aging. The characterisation of the solid solution by DSC, XRPD and FTIR has been shown in the previous section. The solid solution was confirmed to be in an amorphous form and the FTIR study has confirmed that there was hydrogen bonding between the drug and carrier, similar to the one prepared by melt quenching method. Step-scan mode DSC studies detected that the T_g of the ball milled sample was 64 °C which is close to that of the melt quenched one. There was only one T_g detected for the sample which might indicate the formation of a one-phase system.

The aging temperatures here were chosen to be 50 and 60 °C, and after aging for certain periods of time, a portion of sample was taken out for IGC characterisation.

The initial surface free energy of the ball milled solid solution was 44 mJ/m². Different to the melt quenched solid solution which showed an obvious decrease in γ^d during aging, the ball milled one remained relatively the same after 14 days at 50 and 60 °C (Figure 3.21). The γ^d ranged between 44-45 mJ/m² at each sampling point during the aging period and did not show any significant increase or decrease tendency. XRPD and DSC results indicated that the solid solution did not crystallise even after 14 days at 60 °C which is very close to its T_g. For the samples which were under measurement of γ^d, the sample column would be conditioned at 30 °C for 4 hours under a helium flow prior to the pulse injection methods were conducted. A concern is that the sample has relaxed thoroughly during this conditioning period. This concern is reasonable, but considering that the conditioning temperature is about 34 °C lower than the T_g of the sample, it is unlikely that the sample has relaxed significantly

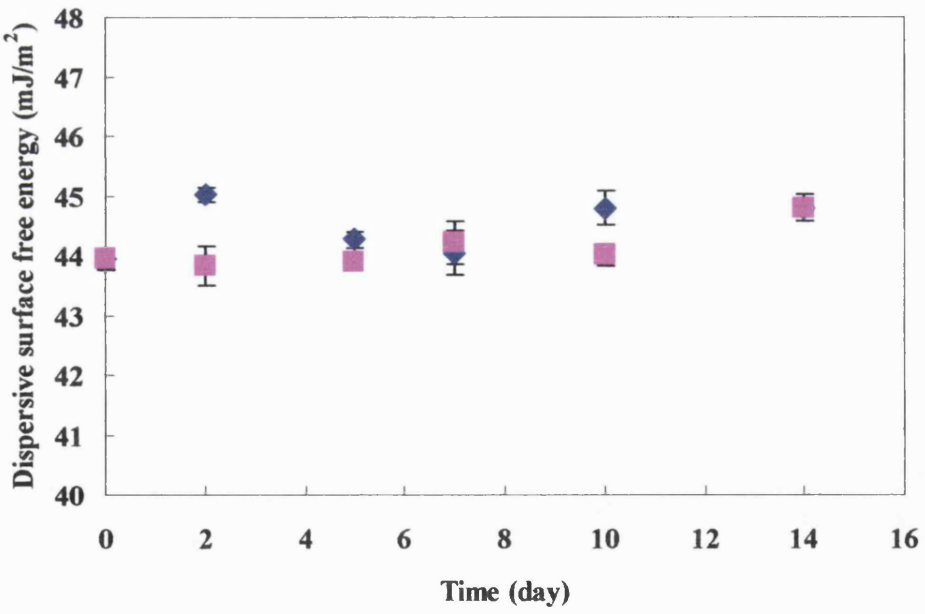

Figure 3.21: *A plot of dispersive surface free energy changes of ball milled solid solutions (an indometacin to PVP ratio of 70%:30%) stored at 50 °C (■), and 60 °C (◆) (n=4).*

In order to study this issue further, the retention volume (V_{max}, calculated by the time of the peak's maximum point) of the probes were investigated, as based on Equation 3.2, the V_{max} is related to the energy of adsorption of the probe. In another words, V_{max} might be able to provide some information of the energy on the surface of the sample. Figure 3.22 shows the V_{max} change of decane during aging and it is clear to see that V_{max} decreases as a function of time. Moreover, the drop of V_{max} at 60 °C is more significant than the one at 50 °C indicating a temperature dependence of this decreasing tendency.

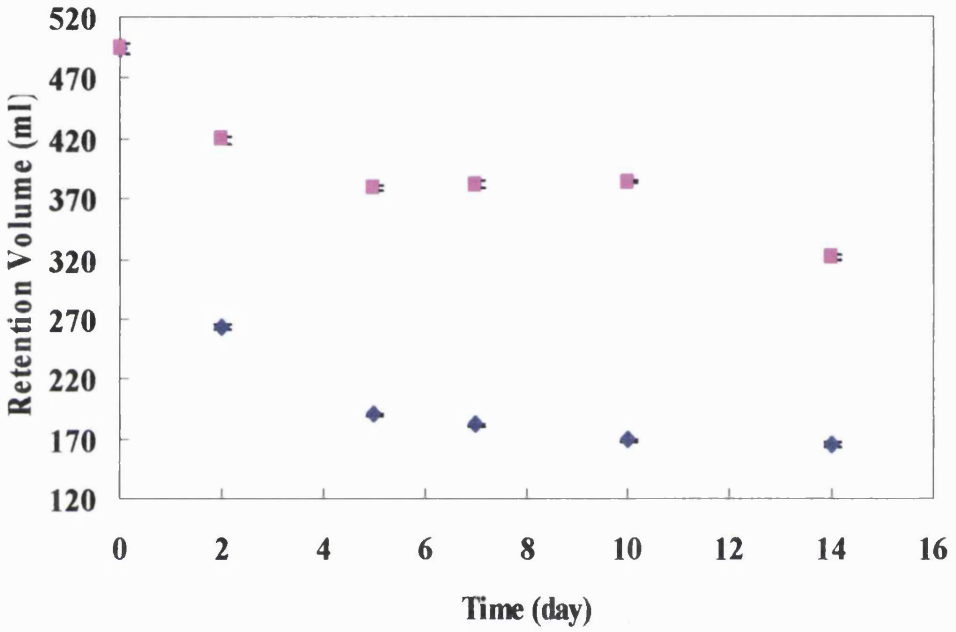

Figure 3.22: *A plot of decane retention volume changing as a function of time (■, 50 °C; and ◆, 60 °C, n=4).*

Retention volume is the volume of helium needed to elute out all the probe molecules. Therefore the higher extent of the interaction between the probe molecules and the surface energy sites, the more helium is needed (a bigger V_{max}). Hence V_{max} can be used to indicate the surface energy state. During aging, the V_{max} values decreased indicating the interaction ability between decane and the surface of the solid solutions decreased (and also the energy state decreased) as a function of time. Decane as a bigger alkane molecule can interact with surface to a larger extent compared to nonane and octane (the

retention time for decane is usually much longer than the others). In another words, decane is more sensitive to any change that occurred to the surface energy sites. The use of the retention volume of decane to measure the surface energy state of the solid solution would therefore provide higher sensitivity than the surface free energy method which also takes into account the sensitivity of smaller molecule probes. This finding led to consideration of using decane on its own for the surface relaxation study in order to eliminate the compromise of accuracy caused by the poor sensitivities of the other probes. The decane V_{max} study will be the focus of a later section.

3.4.2.3 The acid-base contributions to the surface free energy during aging

The acidic (electron accepting) parameter K_A and the basic (electron donating) parameter K_D can be obtained based on the surface energy data using the method described previously. By studying the K_A and K_D, it is possible to understand the acid and base properties on the surface of the materials. The K_A, K_D and the basic to acidic parameter ratios K_D/K_A of indometacin, PVP and the ball milled solid solution are shown in Figure 3.23. Values of K_D/K_A of greater than 1 indicate a basic nature, and values of less than 1 imply an acidic nature (Ohta and Buckton, 2004). It is surprising to see that crystalline indometacin has a negative K_D value. A reasonable explanation for this observation cannot be given. However, the low K_D/K_A values for both the amorphous and crystalline indometacin indicate the acid nature on their surfaces. Indometacin is a weak acid drug with a *pKa* of 4.5 and it is known that the surface of indometacin can be acidic. Watanabe *et al.* (2003) discovered that the acid-base reaction between indometacin and SiO_2 mediated by the OH groups at their interface could help to immobilise the indometacin molecules leading to suppression of crystallisation. In a more recent study, Telang *et al.* (2009) utilised the acid-base interaction on the surface of indometacin and a base meglumine to keep the drug stable in its amorphous form. The K_D/K_A value of PVP is the highest compared to the others indicating a least acidity of PVP notwithstanding the K_D/K_A value is less than 1 suggesting an overall acid nature on its surface.

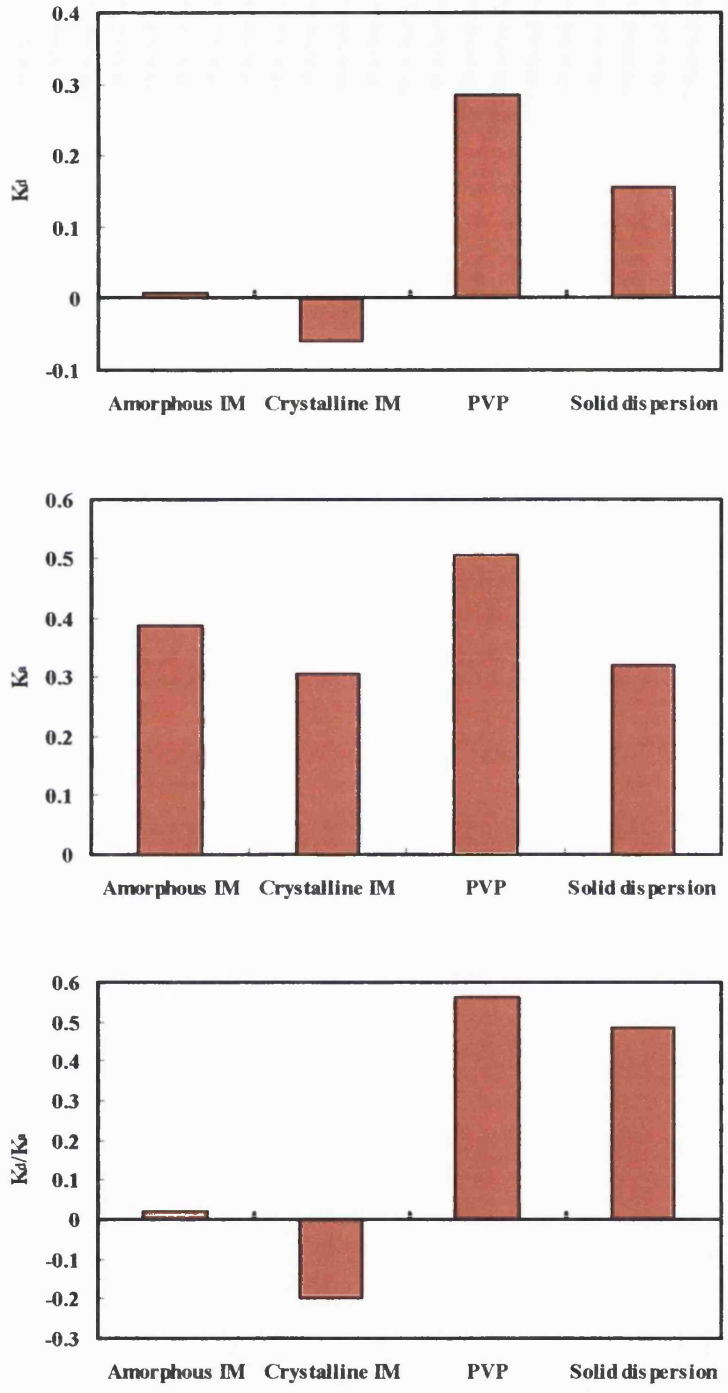

Figure 3.23: *K_A, K_D and K_D/K_A values of amorphous and crystalline indometacin, PVP and the ball milled solid solution (an indometacin to PVP ratio of 70%:30%).*

The acid-base parameters of the ball milled solid solution were studied to observe changes during relaxation. The K_D and K_A values were obtained after 2, 7 and 14 days.

The basicity on the surface of the solid solution decreased (or surface acidity increased) as the aging time increased as illustrated by the K_D/K_A ratio in Figure 3.24. This might indicate a reorientation of polar surface groups of the sample and thereby affecting its adhesion-cohesion force balance. Hence it is concluded that the surface relaxation might have an impact on the polar properties of the solid solution surface.

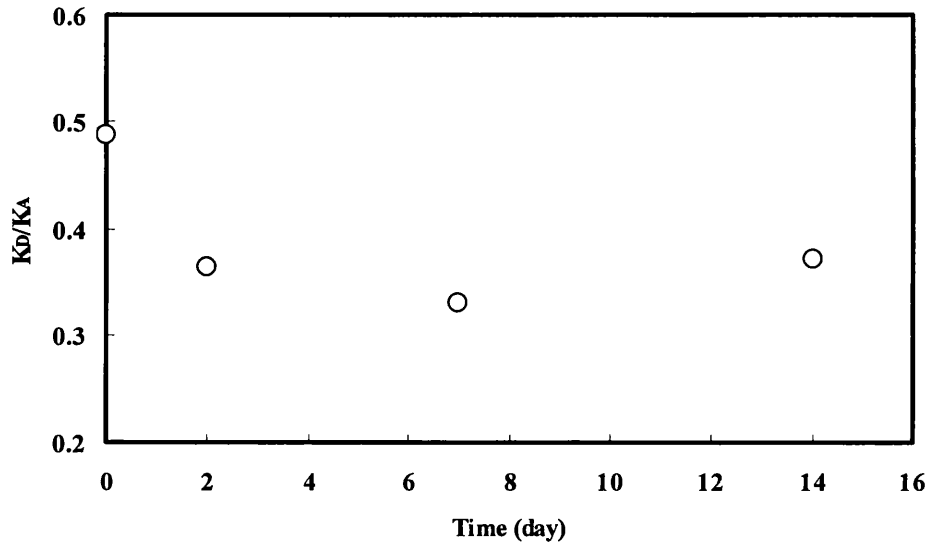

Figure 3.24: *Gutmann K_D/K_A ratio of the ball milled solid solution of indometacin and PVP (70%:30%) as a function of time at 60 °C.*

3.4.3 Detecting surface relaxation using the retention volume of decane

Melt quenched indometacin-PVP (70%: 30%) solid solution was used in this section as a model system for the development of a new method which includes the use of retention volume (V_{max}) of decane to study the surface relaxation. The sample was firstly purged under helium flow at 25 °C for 10 hours in order to remove moisture and any potential organic solvent sorbed. After purging for about 4 hours, both the flame ionised detector (FID) and thermal conductivity detector (TCD) signals have decreased to the minimum point and stabilised indicating that water and organic solvents were eluted. Purging was still carried on for up to 10 hours in order to ensure this process was sufficiently complete. Because if there is any water or organic solvent remained, their molecules would occupy the potential surface interaction sites at the surface. This in return will reduce the probability of the interaction between decane and the surface, leading to a variation of V_{max} value. Therefore, complete removal of water and organic solvent is crucial for the decane V_{max} method.

Decane was chosen as the only probe to be injected for the acquisition of the relaxation profile because of its higher interaction potential in comparison with the other probes (nonane, octane, heptane or hexane). Immediately after conditioning finished, continuous injections of decane and methane were performed for a period of 48 hours. Each decane injection was followed by a methane one in order to obtain the information of the void space for the correction of decane's net retention volume. 45 minutes were allowed between each injection (15 minutes of signal recording time and 30 minutes of sample conditioning before next injection was performed). Consequently, only 90 minutes lapsed between each data point (this time interval can be further shortened depending on the retention time of the probe), instead of 3-4 hours needed for the dispersive surface energy data. This method provides more data points for the detection of the surface relaxation trend and it is especially useful for those samples which relax at a fast rate.

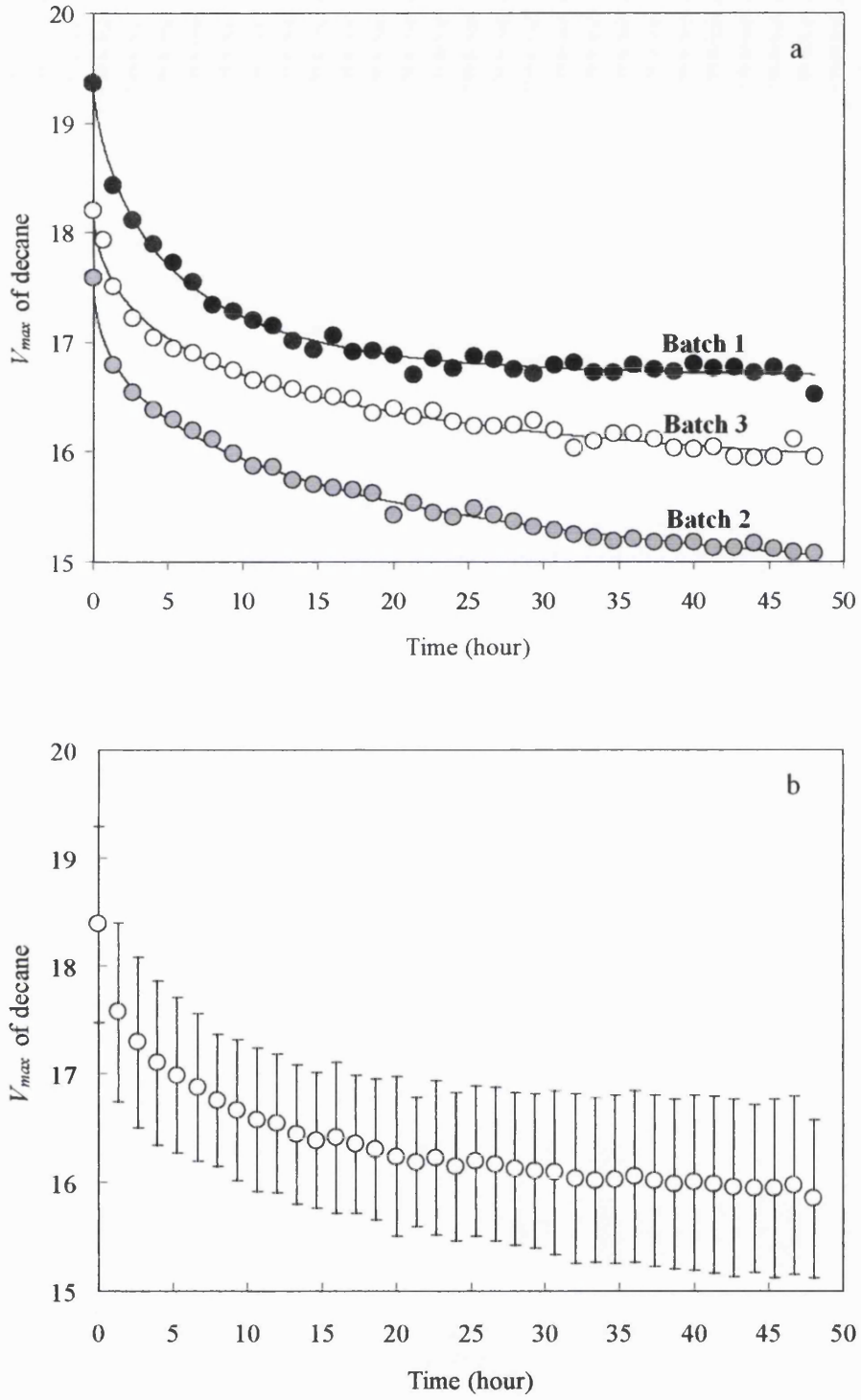

Figure 3.25: *Decrease of decane V_{max} on three different batches of melt quenched indometacin and PVP (70%:30%) solid solution as a function of aging time at 50 °C. a) traces of measurements on three different batches and b) trace of the mean of three measurements ± s.d.).*

It has been discussed in section 3.4.1 and 3.4.2 that the dispersive surface free energy of the amorphous solid solution sample decreased as the surface relaxation occurred and also the V_{max} of decane dropped indicating a decrease of the interaction capability between the probe and the surface. Figure 3.25 shows how the V_{max} of decane altered as a function of time when the solid solution was aged at 50 °C. Three different batches of solid solutions were studied and they showed a very similar relaxation trend, though their absolute values were different to each other. This difference is attributed to variation in the surface area and morphology of different batches of samples and also the tapping condition between different columns. These factors can affect how fast the inert gas can run through the column (i.e. different retention times), therefore, the retention volumes are different. In addition, the slight difference of sample weight for each measurement can influence the time that the vapour probe and helium gas need to pass through a column, hence the retention volume can be altered. The relaxation rate or relaxation parameters obtained are based on the trend of the relaxation behaviour rather than its absolute value, therefore, this difference in the absolute values between each batch would not affect the accuracy of the result as long as their trends are similar.

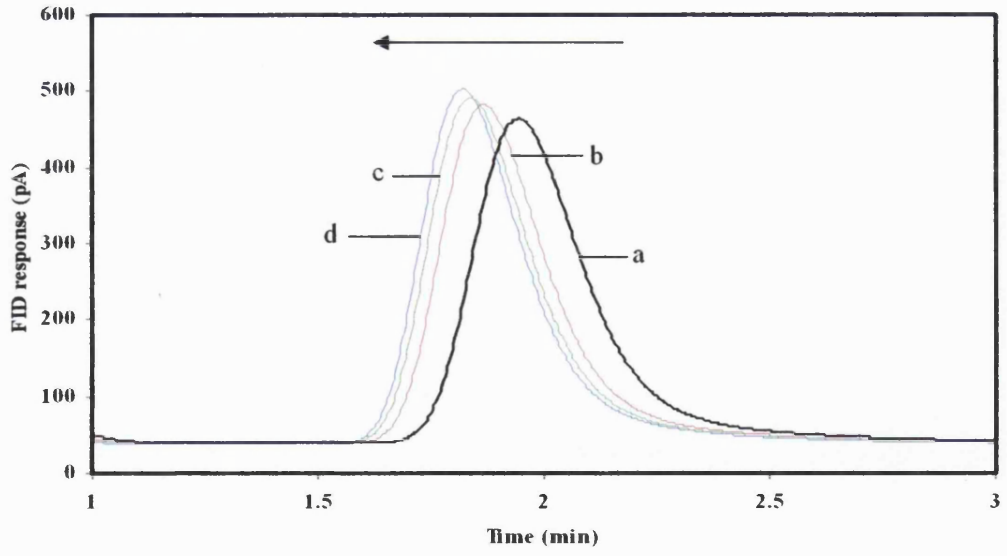

Figure 3.26: *The FID responses showing the decane peaks at different time point during measurement for the melt quenched solid solution containing indometacin and PVP with a ratio of 70%:30% (a, 0 min; b, 90 min; c, 180 min and d, 270 min).*

By plotting the decane peaks obtained as a function of time, a clear shift of the maximum peak position to the left hand side can be observed indicating a decrease in the retention time (Figure 3.26). Because the sample mass in the column remained unchanged during the measurement, this decrease in the retention time is solely due to the change of the interaction capability between the probe and the solid surface. In other words, the energy state of the surface decreased to a lower level. By DSC and XRPD measurement, the sample after measurement only showed an amorphous response (also previous DSC and XRPD studies confirmed that melt quenched solid solution could remain amorphous even after 18 days stored at 60 °C), therefore this change in energy is caused by the surface relaxation.

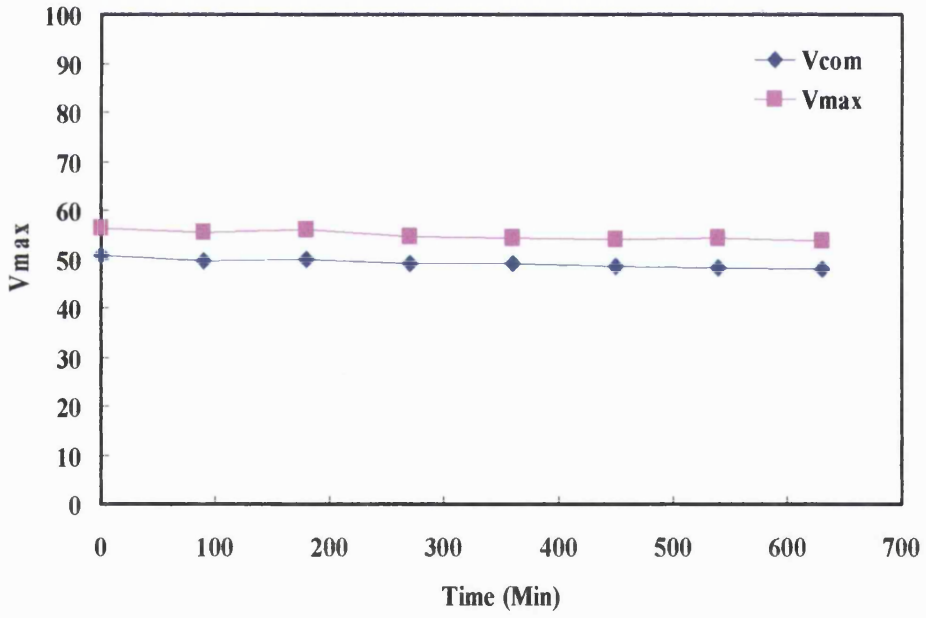

Figure 3.27: *The net retention volume of indometacin:PVP (70% : 30%) physical mixtures at 50 °C (V_{com}, net retention volume calculated using the time point at centre of mass of the peak and V_{max}, the one calculated using the time point at the maximum of the peak).*

In order to further prove the decrease of decane V_{max} was related to the surface relaxation, the decane V_{max} of a physical mixture of indometacin:PVP with the same ratio as the solid solution was measured at 50 °C to be used as a controlled experiment. As shown in Figure 3.27, no matter which method was used to calculate the net retention volume of decane (by the maximum point of the peak or its center of mass), the retention volume of the sample remained the same during the measurement. In the physical mixture, indometacin was used at its stable γ-form so that no polymorphic transformation or any physical changes (at 50 °C) can occur. PVP was expected to be stable at this studied temperature because of its high T_g. Therefore, it is rational to see that the decane retention volume remained unchanged for the physical mixture, which indicates that the decane retention method is measuring the surface relaxation.

One further possibility for the solid solution that the decrease of decane V_{max} was due to the gradual occupation of the energy sites by decane on the solid surface which leads to a decrease of decane V_{max} and solid surface interaction. To examine this, fresh solid solution sample was kept in the column oven at 50 °C for the initial 12 hours without any injection of decane probe after conditioning and thereafter decane and methane were injected. The decane V_{max} value after 12 hour was found identical to the same batch of sample which had been exposed to repeated injections of decane from the very beginning. This indicated that the decane drop was not a result of the continuous probe injection.

There are two ovens in an IGC instrument, one is for the columns and the other one is used to keep the probe vapour at a certain temperature (in order for an accurate injection of vapour probes, the probes need to be kept at a stable temperature condition). The default temperature for the probe oven is 30 °C. A potential concern was that during the relaxation study, when the probe was injected to the sample column which was kept at 50 °C, the sudden increase of temperature would give an influence on the retention volume of decane and cause it to decrease. Therefore a set of experiment was carried out to study the effect of probe oven temperature on the decane retention volume during

relaxation. During the experiment, the probe oven was fixed at 50 °C which was the same as the column oven temperature. After 10 hours conditioning at 25 °C, the solid solution was aged at 50 °C and decane was injected continuously. The retention volume of decane during relaxation was obtained. As shown in Figure 3.28, both the V_{max} and V_{com} of decane decreased as relaxation was occuring. This result clarified that the sudden increase of the temperature of the probes is not the reason causing the retention volume of decane to decrease.

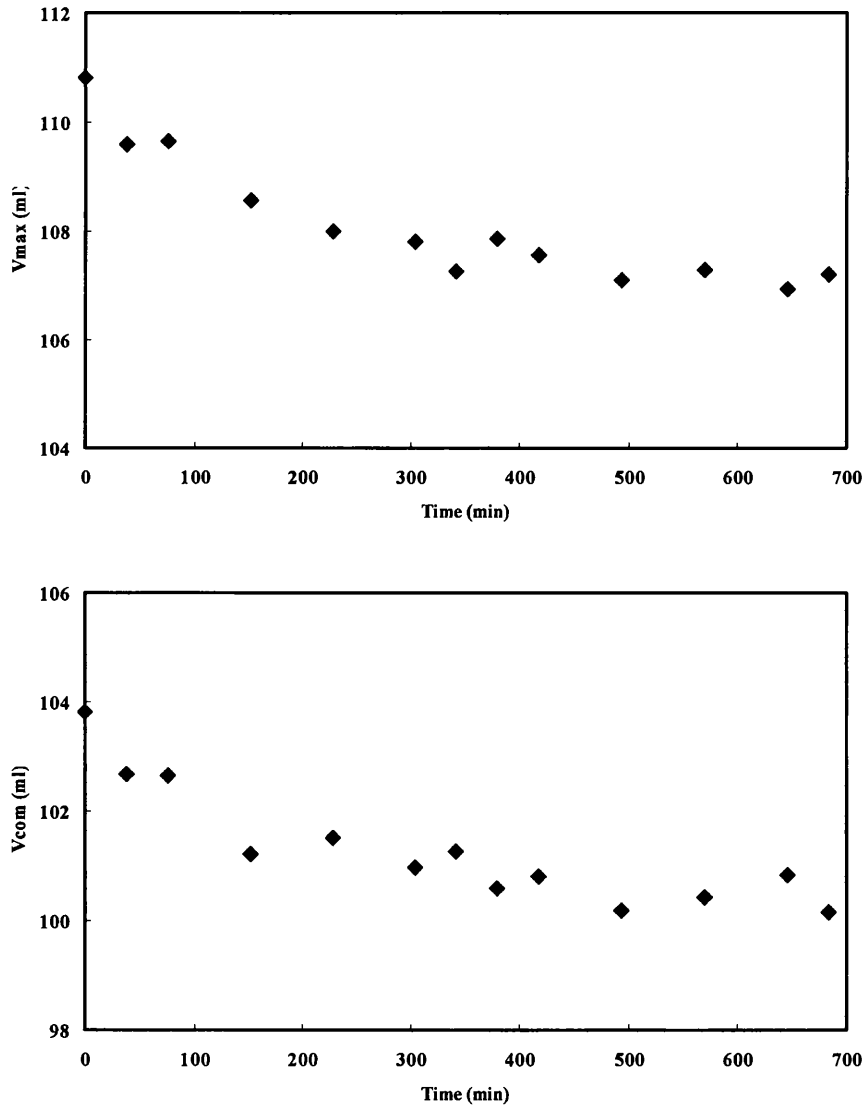

Figure 3.28: *Time course of V_{max} and V_{com} of decane kept at 50 °C during measurement for the indometacin-PVP (70%:30%) solid solution.*

In order to compare the difference of using decane (V_{max}) and dispersive surface energy as an indicator for surface relaxation determination, the solid solution sample was kept at the column oven (50 °C) and continuous injections of decane, nonane, octane and methane were conducted for up to 32 hours. This allowed the possibility to acquire the dispersive surface energy as a function of time. As shown in Figure 3.29, during the experiment, 9 points of dispersive surface energy as well as decane V_{max} could be obtained. These data points of relaxation were far less than simply injecting a single probe, decane. A few hours were needed before a second round of measurement started. From the plot, it can be seen that dispersive surface energy decreased in the initial 14 hours and then started to scatter accompanied with slight increase on further storage. This phenomenon was probably due to experimental error associated with variability in the measurement of lower alkanes such as nonane and octane which elute from the column too quickly. Hence, the accuracy of measurements was jeopardised. From the plot of decane V_{max} (which has a longer retention time), a smooth decreasing trend up to 32 hours can be seen and the V_{max} values have a tendency to decrease further. The sensitivities of using decane V_{max} to evaluate the surface structural relaxation is higher than dispersive surface energy. Furthermore, in the first few hours of aging, the relaxation of the amorphous sample was very fast and the retention volume of any probe was changing rapidly. As a consequence, the order of probe injection would probably influence the results of the dispersive surface energy. All these issues demonstrate that decane V_{max} method is better than the dispersive surface free energy method in probing surface molecular mobility.

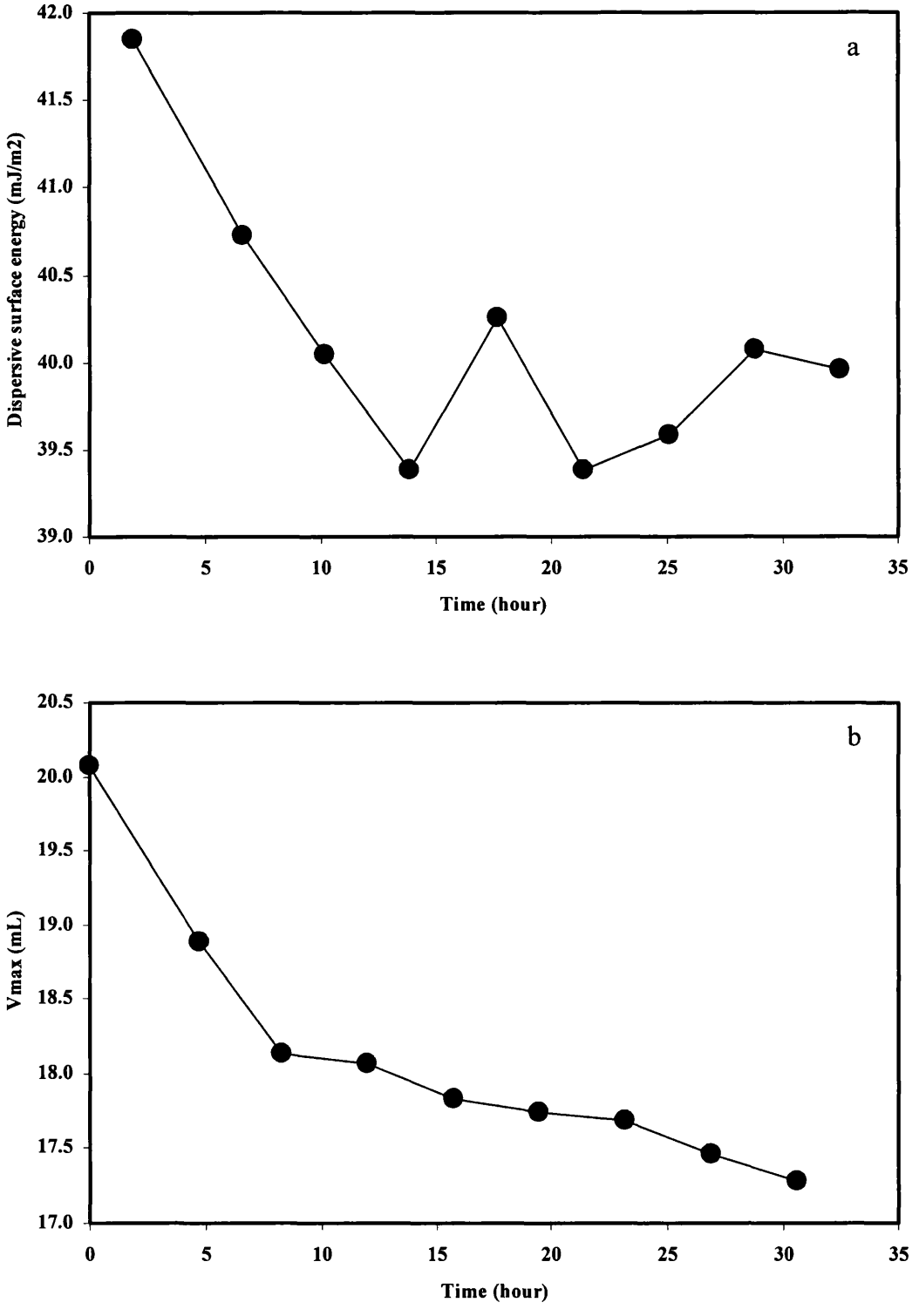

Figure 3.29: *Plots of dispersive surface energy and V_{max} (decane) as a function of aging time for the melt quenched indometacin and PVP (70%:30%) solid solution at 50 °C. a) dispersive surface energy calculated using three probes, decane, nonane and octane; and b) V_{max} of decane.*

In a previous secion, KWW fitting was conducted to obtain the τ and β values of the melt quenched solid solution using the dispersive surface energy data. However, unlike a DSC relaxation study where the infinite enthalpy can be calculated according to the glass transition temperature and apparent heat capacity of the sample, the dispersive energy of the surface when it relaxes completely is unknown and there is no existing equation available to calculate this value. Experimental measurements could be a possible way to obtain the minimum dispersive surface energy, but only when complete relaxation achieved within the laboratory timeframe. For a relatively stable sample which could take months or even years to relax, the time course of experimental measurements would be problematic and unrealistic. Accordingly, the smallest dispersive energy value obtained during the experiment was used to make the KWW fitting feasible.

For the decane V_{max} study, the minimum point of V_{max} was also unknown. As decane V_{max} can generate relatively more sufficient data points, a modified KWW thereby was proposed and used to estimate the convergent retention volume (V_{min}) after long aging (Equation 3.13):

$$V = V_{\min} + A\exp(-(\frac{t}{\tau})^{\beta}) \qquad \text{Equation 3.13}$$

where V, t, τ, β are the same as stated before, and A is a pre-exponential factor. As shown in Equation 3.13, when t is infinite, $Aexp(-(t/\tau)^{\beta})$ gets close to zero, then V_{min} can be defined as a convergent retention volume. Using Equation 3.14, the decane V_{max} data were normalised and fitted to the KWW equation.

$$\phi(t) = 1 - \frac{(V - V_{\min})}{(V_{\max} - V_{\min})} \qquad \text{Equation 3.14}$$

The V_{min} of batch 1, 2 and 3 were 16.68 ± 0.03, 14.39 ± 0.18 and 15.64 ± 0.15 mL

respectively and using these values the retention volume of decane can be plotted into a decay function (Figure 3.30). Moreover, the relaxation parameters of the solid solution are shown in Table 3.4.

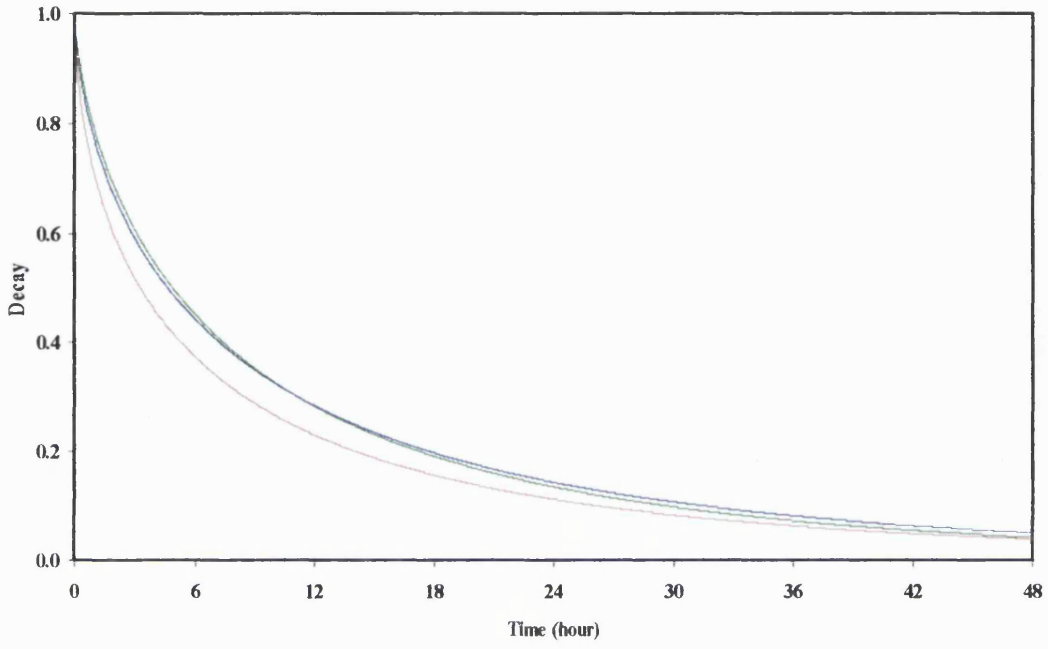

Figure 3.30: *Decay function of the retention volume of decane of the melt quenched solid solution (an indometacin to PVP ratio of 70%:30%) aged at 50 ℃ (n=3).*

	τ (hour)	β	τ^{β} (hour)
Solid solution	13.1	0.60	4.6

Table 3.4: *Structural relaxation parameters of the melt quenched solid solution (an indometacin to PVP ratio of 70%:30%) obtained from decane V_{max}.*

In this section, a new method using the retention volume of decane to evaluate the structural relaxation on the surface of an amorphous system was developed and verified. The repetition of injecting a single probe can provide more data points of the relaxation

compared to the dispersive surface free energy method for which at least three probes are needed to be injected in order to obtain one value. Furthermore, the long retention time of decane is able to eliminate the negative effect caused by the rapid clearance of the lower alkanes and increase the sensitivity of the system. A modified KWW equation was used to obtain the relaxation parameters based on the V_{max} values of decane.

3.5 Conclusion

PVP and indometacin (30%:70%) solid solutions were prepared by ball milling and melt quenching. DSC, XRPD and FTIR studies showed that they were completely amorphous. For each solid solution system, there was only one T_g shown indicating the formation of a one-phase system. PVP and indometacin was found to form a one phase system with a higher ratio of PVP (Patterson *et al.*, 2007). The planetary ball mill used here was able to generate complete miscibility of PVP and indometacin with a concentration of PVP as low as 30%.

After forming a solid solution with PVP, the dispersive surface free energy of indometacin increased no matter which preparation method was used. IGC studies showed that the dispersive surface free energy of the melt quenched solid solution decreased during physical aging at a temperature lower than its T_g. This relaxation temperature dependence is because the sample aged at a temperature closer to the T_g showed the shortest relaxation time and the one further from the T_g showed the longest. This relaxation was also found to depend on the carrier concentration, as when the concentration of PVP was increased to 50%, a slower relaxation time was noticed at the same aging temperature.

In the case of the ball milled solid solution, no change of dispersive surface free energy was noticed after aging. However, by measuring the retention volume of an individual probe, decane, decrease of energy state of the surface was observed and this decrease was also temperature dependent. It was considered that the value of dispersive surface energy could be affected by the sensitivity of the individual probe used. Sometimes, even though the energy of the surface has changed, it might not be accurately represented by the dispersive surface free energy values. The use of decane retention time led to the development of a novel method for monitoring the energy state change on the surface of a material and it has some advantages over the surface energy method such as a short data collecting time and higher sensitivity. A modified KWW equation was proposed for the fitting of the decane V_{max} data in order to obtain the relaxation

parameters of the sample.

Furthermore, the studies of the acid and base contribution on the surface of ball milled solid solution provided evidence that a reorientation of surface molecular functional groups could happen during aging. The studies in this chapter have confirmed that the relaxation process of an amorphous state will lead to changes in the physicochemical properties of the amorphous form prior to any crystallisation event happens. Also the studies have confirmed the importance of monitoring the surface properties of solid dispersions during storage.

Chapter 4

Influence of preparation methods on surface and bulk structural relaxation of solid solutions

4.1 Introduction

Stability has been a major concern for many pharmaceutical researchers when preparing amorphous materials. In many cases, physical stability test is used as an important method to acquire stability data of the amorphous products. However, this method could sometimes be problematic and time consuming. Therefore, some alternative methods have been used to predict the stability of the products instead. Among these methods, relaxation assessment has been conventionally used since it can provide useful information about the molecular mobility of the product and therefore its shelf-life can be predicted. There are several techniques which are very powerful in measuring bulk relaxation such as differential scanning calorimetry (DSC) and isothermal microcalorimetry (IMC). DSC and IMC obtain the relaxation information through different ways: DSC measures the enthalpy recovery of the product after aging for different time periods, while IMC measures the instant rates of enthalpy relaxation during aging. Both of these techniques were used in this study to investigate relaxation of indometacin and polyvinylpyrrolidone (PVP) solid solution systems prepared by ball milling, melt quenching and spray drying. The effect of preparation method on the stability of the systems was evaluated.

On the other hand, some studies on polymers have shown that the molecular mobility on the surface should be differentiated from the bulk because their mobility is different (Tanaka *et al.*, 1996; DeMaggio *et al.*, 1997; Kajiyama *et al.*, 1997). The study of surface is important because the mobility at a surface or interface can affect the surface wetting, diffusion and interaction between different materials. Crowley and Zografi (2003) have shown that crystallisation of amorphous indometacin is surface-initiated; Wu and Yu (2006) found that the surface crystallisation of indometacin is at a faster rate than the bulk; and Wu *et al.* (2007) used nano-coating to inhibit crystallisation of indometacin. All these studies demonstrate that surface molecular mobility would be critical for developing a stable amorphous formulation. However, in the pharmaceutical field, the lack of efficient technique for determination of surface molecular mobility has limited understanding of the molecular mobility on the surface. Thereby, the decane

(V_{max}) method developed in the former chapter was applied here to study the relaxation on the surface of the solid solutions and in comparison to that of the bulk determined by DSC and IMC. The hypothesis is that since the crystallisation commonly starts from the surface, the surface would have a higher molecular mobility than the bulk.

Glass fragility of the solid solutions prepared by different methods was studied using DSC to understand how the molecular mobility of the amorphous samples changes with temperature, especially when they undergo a glass transition. Glass transition temperature, T_g is often used to correlate the stability of an amorphous material. A higher T_g is always favoured to stabilise the product at a given storage temperature. Because when the storage temperature is very close to or even higher than the T_g, the glassy sample will deform into rubber state which gives rise to physical collapse, crystallisation or even degradation (te Booy *et al.*, 1992). But a high T_g might not be enough to necessitate good stability. Some studies have shown that degradation could still happen below the glass transition temperature (Pikal *et al.*, 1991; Kerr *et al.*, 1993). Therefore, in this study, zero mobility temperature, T_0 was used as another indicator to predict the stability of the solid solutions. The zero mobility temperature was used to describe the temperature at which configuration entropy (molecular mobility) reaches zero and it can be calculated according to the fragility parameters of the solid solutions. In addition, the solid solutions were stored at room temperature, 75% relative humidity (RH) to obtain the actual physical stability data. These data were used to verify the prediction made from T_0 and the relaxation data.

Crystallisation of an amorphous product would frequently lead to slower dissolution rate. But a relationship between relaxation and the dissolution properties of the product has not been established. Hence dynamic vapour sorption and dissolution studies were conducted to investigate the effect of aging on the water uptake and dissolution rate of the samples. The effect of preparation methods on the dissolution rate after aging was also studied.

4.2 Chapter outline

The aim of the work related in this chapter was to apply the single probe injection method developed in the previous chapter to study the surface structural relaxation of solid solutions prepared by different techniques (melt quenching, ball milling and spray drying). Step-scan DSC was used to study these solid solution systems to obtain the relaxation information in the bulk and compared to the one determined by inverse gas chromatography. Furthermore, isothermal microcalorimetry was also used to study the relaxation of these solid solutions. Glass fragility was measured and the zero mobility temperature was calculated in order to predict the stability of these solid solutions. The effect of relaxation on the dissolution behaviour and physical stability of the solid solutions were investigated.

4.3 Methods

4.3.1 Spray drying

Indometacin and PVP with a ratio of 70% to 30% was spray dried using the method described in Section 2.2.4. 200 mL of ethanol was used to dissolve indometacin and PVP. The feed concentration in the solvent was 1.5 % w/v and 30 minutes were allowed for the drug and carrier to dissolve completely into the solvent. The solution was then spray dried using the following parameters: atomiser gas flow 2.5 kg/h; chamber inlet flow 30.0 kg/h; inlet temperature 80 °C; and feeding rate 20%. The spray dried samples collected were passed through a 90 micron sieve and then dried in a vacuumed desiccator over phosphorus pentoxide (P_2O_5) at room temperature for 2 hours before any further study.

4.3.2 Ball milling

Indometacin and PVP (70%:30%) were milled according to the method described in Section 2.2.2 and Section 3.3.2.

4.3.3 Melt quenching

Indometacin and PVP (70%:30%) were melt quenched using the method described in Section 2.2.3.

4.3.4 Differential scanning calorimetry (DSC) for enthalpy recovery measurement

About 5 mg of fresh solid solution was loaded in a non-hermetically sealed aluminum pan (PerkinElmer Instruments, Beaconsfield, UK) and stored in a desiccator over P_2O_5 at 50 °C. After different periods of aging time (up to 48 hours), the pans were taken out and their enthalpy of relaxation was determined using a Pyris 1 DSC (PerkinElmer Instruments, Beaconsfield, UK) with step-scan mode. After equilibration at 0 °C for 5 min, samples were heated in a step of 2 °C at 10 °C/min. The isothermal time at each step was 1 min and 50 to 100 steps were conducted allowing samples to be heated to 100 to 200 °C. For each aging time point, 3 sample pans were prepared and measured. Indium was used as the reference for DSC calibration.

4.3.5 Differential scanning calorimetry for fragility measurement

A Pyris 1 DSC instrument (PerkinElmer Instruments, Beaconsfield, UK) with an intracooler IIP cooling system (Intracooler IIP, PerkinElmer Instruments) was used for this study. Dry, high purity N_2 gas with a flow rate of 40 mL/min was purged through the sample. A two-point temperature calibration was performed at each heating rate (2, 5, 10, 20 and 40 °C/min) using the extrapolated onset of melting temperature T_m and fusion of melting (ΔH_m) of indium (T_m =156.6 °C) and n-decane (T_m = -29.7 °C). Frequent calibration checks were conducted during the experiment.

All samples were sieved using a 90 μm sieve to minimise the particle size effect on the T_g. About 5-6 mg of samples was accurately weighed into non-hermetically sealed pans. The sample was first heated to 20 °C over its T_g in order to remove any moisture sorbed and thermal history and then cooled to at least 50 °C below T_g at a cooling rate that equaled the subsequent heating rate. The sample was then heated at different heating rate and the onsets of T_g were recorded. All glass transition temperatures obtained were an average of three measurements.

4.3.6 Inverse gas chromatography (IGC) for surface relaxation study

The surface relaxation of the solid solutions was studied using inverse gas chromatography. The methods used were described in Section 2.2.5. Around 500 - 800 mg of sample was loaded into a pre-silanised glass column which was then tapped continuously for 15 minutes. The column was first conditioned at 25 °C and 0% RH in the column oven under He flow for 10 hours. After the conditioning process finished, the column oven temperature was immediately increased to 50 °C and then a series of decane and methane were injected continuously for 48 hours (for ball milled and melt quenched samples) and 24 hours (for spray dried samples). The data recording time for each injection was set at 15 minutes and an additional 30 minutes were allowed for sample reconditioning between each injection. The net retention volumes were calculated using IGCAnalysis2 software (Surface Measurement Systems, London, UK). For each solid solution system, 3 to 4 batches of samples were measured.

4.3.7 Isothermal microcalorimetry (IMC)

Isothermal microcalorimetry studies were carried out using a 2277 Thermal Activity Monitor (TAM) (Thermometric AB, Sweden). TAM is a very sensitive machine which could measure the heat flow of a sample in microwatt-scale. 500 mg of sample was accurately weighed into a glass ampoule fitted with rubber cap and aluminum over cap and loaded in one cell and the same amount of talc was used as an inert reference loaded in another cell. Samples were kept at 50 ± 0.0001 °C for 2 days. The heat flow signal was amplified 300 folds by a connected amplifier and collected by Digitam 4.1 user interface (operating software). Data analysis was conducted using Origin software version 7.0.

4.3.8 X-ray Powder Diffraction (XRPD)

X-ray powder diffractions were performed according to the method described in Section 2.2.7.

4.3.9 Scanning electron microscopy (SEM)

Scanning electron microscopy was applied to study the morphology of the samples. The measurements were carried out as described in Section 2.2.9.

4.3.10 Atomic force microscopy (AFM)

The surface images of the melt quenched solid solutions were obtained using a multimode AFM (Veeco, Cambridge, UK). The AFM was equipped with a Nanoscope IV controller and E-type scanner (Veeco, Cambridge, UK). All images were obtained in Tapping Mode using a silicon tapping tip (NSG01, NTI-Europe, The Netherlands) with a resolution of 5 μm and a scanning rate of 1 Hz. Measurements were controlled and analyzed using Nanoscope 5.12b software (Veeco, Cambridge, UK).

4.3.11 Dynamic vapour sorption (DVS)

A DVS made by Surface Measurement System, London, UK, was used for this study. Before loading the samples, the empty glass DVS pans with flat-bottom design were

conditioned at 0% RH for 30 minutes followed by conditioning at 90% for another 30 minutes to eliminate any static charge. After drying the pans completely at 0% RH, about 10-20 mg of sample would be loaded onto one of the pans and the other empty pan was used as a reference. 600 minutes of conditioning at 0% RH were allowed to dry the sample powders before running a stepwise ramp. Afterward, RH was increased from 0-90% in the steps of 10% and returned to 0% in the same manner. At each step, a maximum of 300 minutes were allowed for the samples to sorb moisture and a dm/dt value of 0.0001 mg/min was used. Two replicates were conducted on each sample.

4.3.12 Dissolution test

A Pharma Test dissolution apparatus (Pharma Test, Germany) was used in this study. The dissolution profiles of the initial and aged solid solutions were investigated by using the modified USP paddle method at a rotation speed of 50 rpm at 37 °C and the paddles were set at 25 mm from the bottom of the vessel. Water (900mL) was used as the dissolution medium which was degassed by purging with helium for 20 minutes prior to the tests. Powder samples (containing 25 mg of indometacin) were dropped into the medium directly during experiments and UV readings were recorded every 3 minutes automatically using a Cecil CE 2020 spectrometer (Cecil Instruments, Cambridge, UK) at a wavelength of 320 nm. The dissolution tests were conducted in triplicate for each sample.

4.3.13 Evaluation of the physical stability of the solid solutions

All three solid solution systems were stored in a desiccator over saturated NaCl solution to achieve an RH of 75% at room temperature for a certain period of time. The physical stability of these samples was studied using an X-ray powder diffractometer (XRPD; PW3710 Philips, Holland). The X-ray patterns were obtained using a step of 0.02° in a 2θ range of 5-40°, with a rate of one second per step, and the copper radiation $K_{\alpha 1}$ and $K_{\alpha 2}$ with tube power of 45kV voltage and 30 mA current.

4.4 Results and discussion

4.4.1 Physical properties of the solid solutions

XRPD and DSC measurements were carried out to confirm the amorphicity of the solid solutions prepared by different methods. All systems were completely amorphous according to the XRPD and DSC results. Figure 4.1 shows the XRPD pattern of the spray dried sample (XRPD patterns of the ball milled and melt quenched solid solutions were shown in Chapter 3).

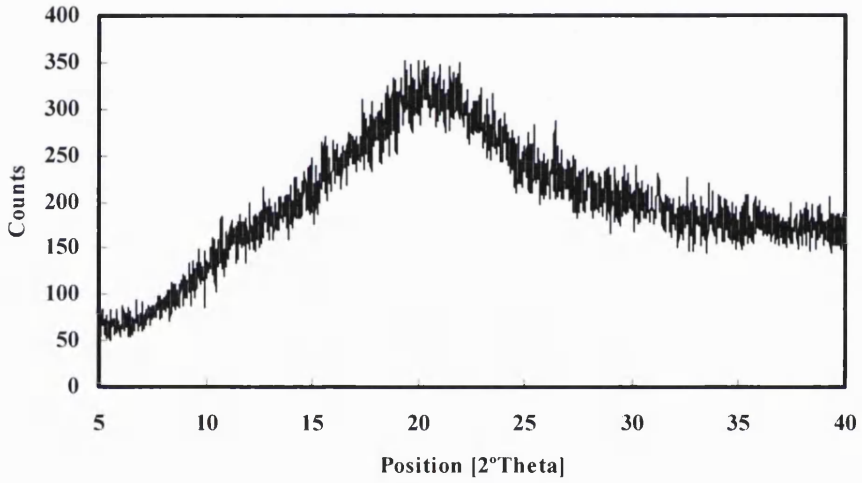

Figure 4.1: *XRPD pattern of spray dried indometacin:PVP (70%:30%) solid solution.*

a b

Figure 4.2: *SEM images of spray dired indometacin:PVP (70%:30%) solid solution (a, 20 µm and b, 5 µm).*

Scanning electron microscopy (SEM) images of the spray dried sample are shown in Figure 4.2. The spray dried particles were spherical in shape with a size of less than 5 μm. Compared to the SEM images of the melt quenched and ball milled samples (Figure 3.1 and 3.8), it is shown that the size order of the samples were melt quenched > ball milled > spray dried. Furthermore, different preparation methods could generate a different particle surface. Spray dried particles were relatively smooth without any obvious cracks while ball milled particles were the roughest. This was probably due to the massive mechanical impact applied during planetary ball milling.

Samples	T_g (onset)	ΔCp (J/g °C)	Loss on drying (% w/w)
Ball milled solid solution	64.0±1.47	0.26±0.03	0.44±0.04
Melt quenched solid solution	67.3±0.58	0.25±0.01	0.35±0.05
Spray dried solid solution	64.7±1.81	0.29±0.05	0.63±0.11

Table 4.1: *Glass transition temperature and heat capacity of the solid solutions determined by Step-scan DSC and the loss on drying determined by TGA (n=3).*

The glass transition temperature and the heat capacity change at T_g of each solid solution system were measured by Step-scan DSC (Table 4.1). There was only one T_g observed for each system which indicates the formation of solid solutions (Figure 4.3). The T_g of the samples were similar to each other while the melt quenched sample had the highest value and the ball milled one had the lowest. Moreover, the ΔC_p of all three solid solutions were close to each other indicating the magnitudes of amorphicity of the samples were similar regardless of the preparation method. It is expected that the particle size of a sample might affect its T_g in DSC studies. If the sample mass is

constant, it is expected to see that an increase in particle size will result in a higher T_g value, because a larger particle size might have a higher extent of thermal lag caused by the thicker sample and the resolution of T_g would be reduced. Furthermore, a larger particle size might have a worse contact with the bottom of the DSC pan. All these factors would play an important role for an increased T_g. Therefore, all solid solutions were sieved through a 90 μm sieve in order to break down any lumps or agglomerates formed during preparation to guarantee a relatively homogenous and smaller distribution of sample size.

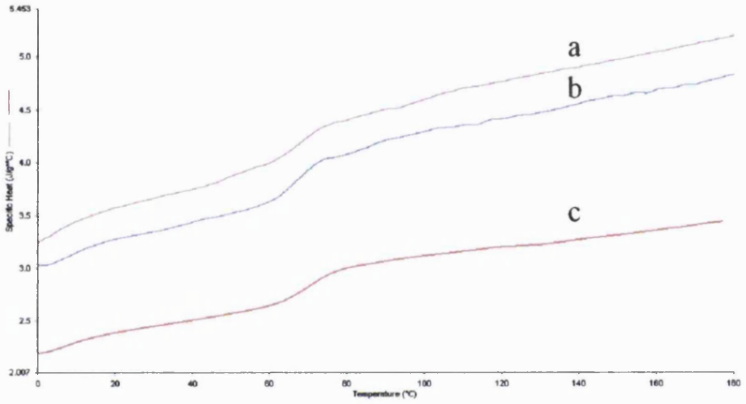

Figure 4.3: *Step-scan DSC traces of the spray dried (a), melt quenched (b) and ball milled (c) solid solutions (an indometacin to PVP ratio of 70%:30%).*

Moisture content or any residual organic solvent would affect the relaxation behaviour of a sample greatly because they can act as a plasticiser to reduce the T_g of the sample and increase its molecular mobility. Therefore, before the freshly prepared solid solutions were tested by different techniques, two hours were allowed to dry them in a vacuum desiccator over P_2O_5 to minimise any moisture or organic solvent residual coming from spray drying. Thermal gravimetric analysis (TGA) results of the solid solutions after drying are shown in Table 4.1. All systems have shown a relatively low loss on drying level. The spray dried sample had a slightly higher loss of weight than the others probably due to its lower density and porous structure which would tend to sorb more moisture or solvents.

4.4.2 Relaxation evaluation using Step-scan DSC

Many researchers have applied DSC to determine the relaxation of amorphous materials. Hancock *et al.* (1995) used conventional-DSC to compare relaxation behaviours between a small molecular weight pharmaceutical glass and some large molecular weight polymers. Van den Mooter *et al.* (1999) used relaxation data obtained using conventional-DSC to predict the physical stability of three amorphous pharmaceutical compounds. During a DSC scan, an aged sample shows an endothermic relaxation peak, which is usually referred to as an enthalpy recovery, and its intensity is dependent on the aging conditions such as time and temperature. This endothermic peak accompanies the T_g and it is also called an overshoot peak (Van den Mooter *et al.*, 1999). A disadvantage of the conventional-DSC method in relaxation study is that the endothermic peak is usually associated with the heat capacity change in a scan signal and sometimes it is difficult for the analyzer to perform an accurate calculation. In order to solve this problem, Craig *et al.* (2000) tried to use modulated-temperature DSC (MTDSC) as a means to determine the relaxation of amorphous lactose. The advantage of MTDSC is its capability of separating the apparent heat capacity change at T_g from the enthalpy recovery (Kawakami and Pikal, 2005), hence greatly helping the accurate assessment of T_g, heat capacity and relaxation endotherms.

SSDSC is a technique which is similar to the MTDSC. Instead of heating and cooling a sample repeatedly, the sample under SSDSC examination is heated and held isothermally in each step and this procedure is repeated until the sample reaches a temperature required by the study. In a SSDSC, the relaxation endothermic peak can also be separated from the apparent heat capacity. Figures 4.4 to 4.6 have shown the enthalpy recoveries of aged solid solutions prepared by ball milling melt quenching and spray drying respectively after aging for different periods.

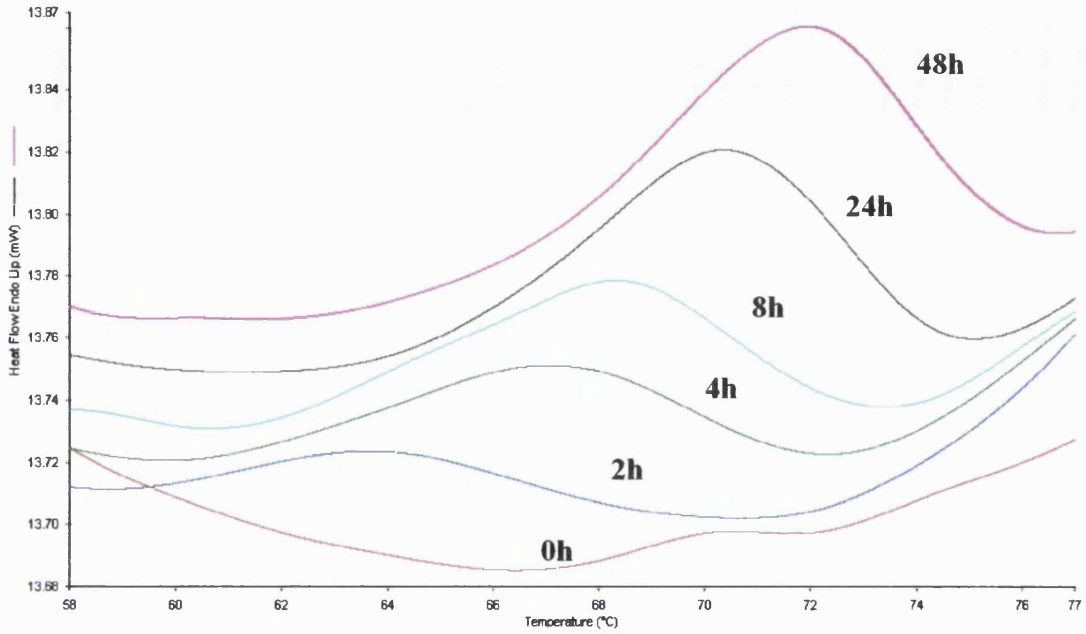

Figure 4.4: *Changes of the endothermic peaks of ball milled solid solution (an indometacin to PVP ratio of 70%:30%) aged at 50 °C for 0, 2, 4, 8, 24 and 48 hours.*

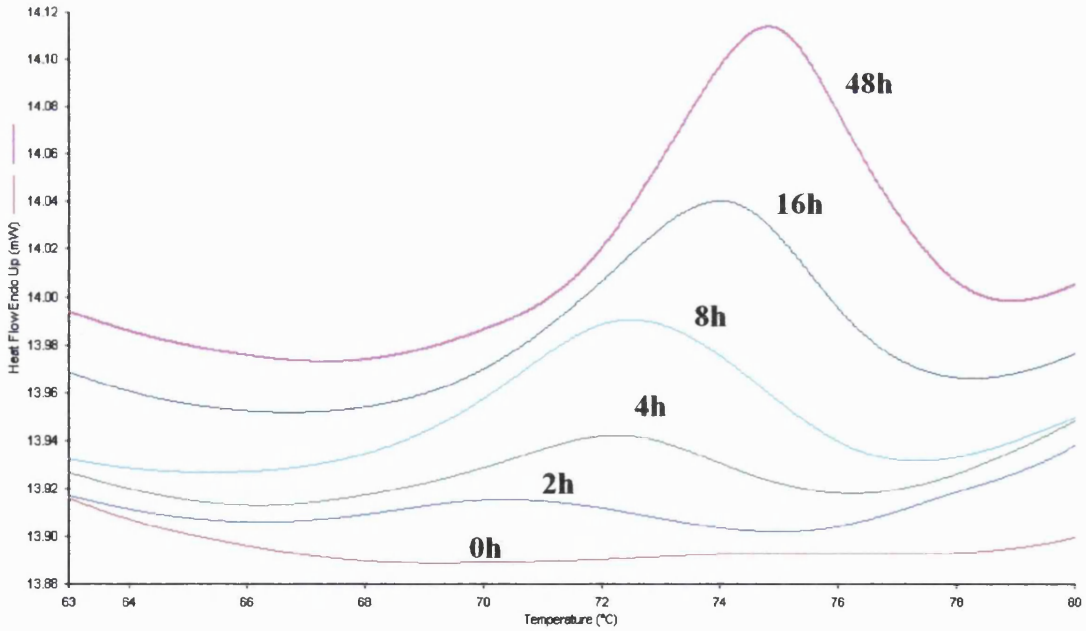

Figure 4.5: *Changes of the endothermic peaks of melt quenched solid solution (an indometacin to PVP ratio of 70%:30%) aged at 50 °C for 0, 2, 4, 8, 16 and 48 hours.*

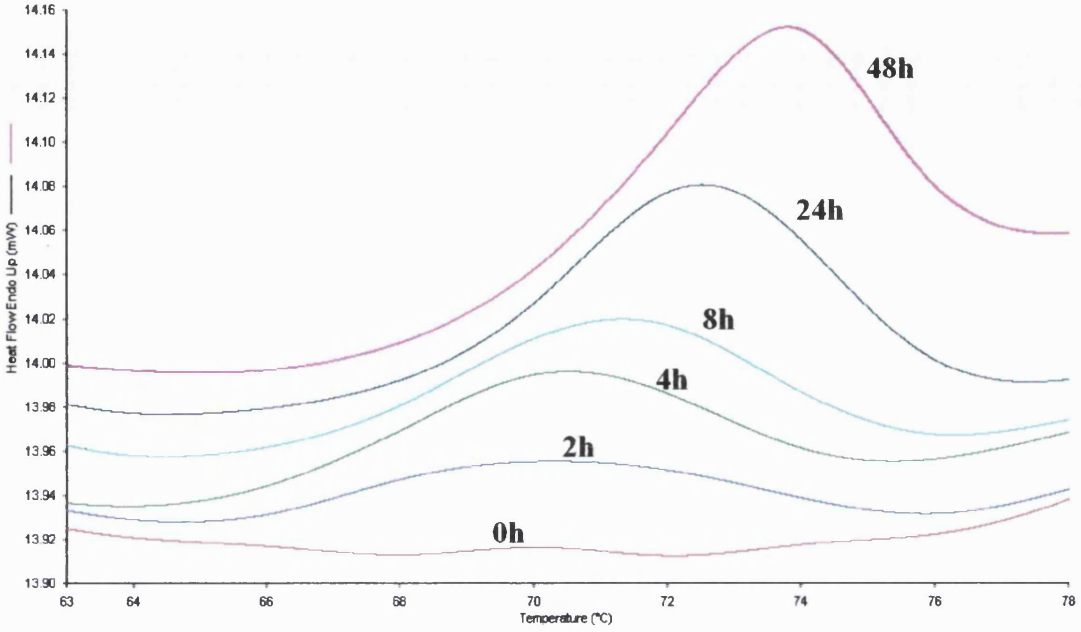

Figure 4.6: *Changes of the endothermic peaks of spray dried solid solution (an indometacin to PVP ratio of 70%:30%) aged at 50 °C for 0, 2, 4, 8, 24 and 48 hours.*

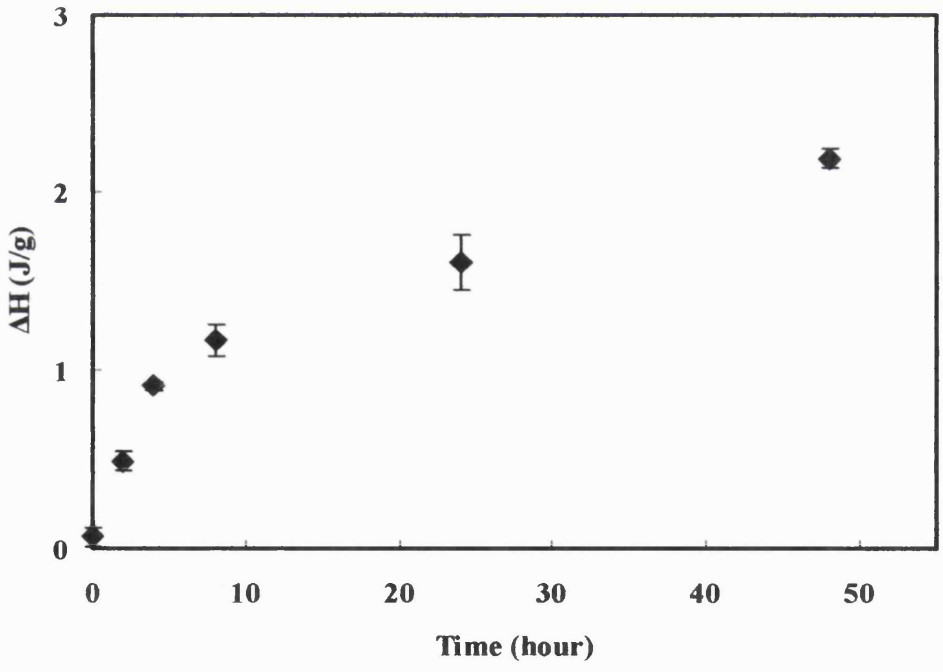

Figure 4.7: *Enthalpy recovery of ball milled solid solution (an indometacin to PVP ratio of 70%:30%) aged at 50 °C as a function of time, determined by SSDSC (n=3).*

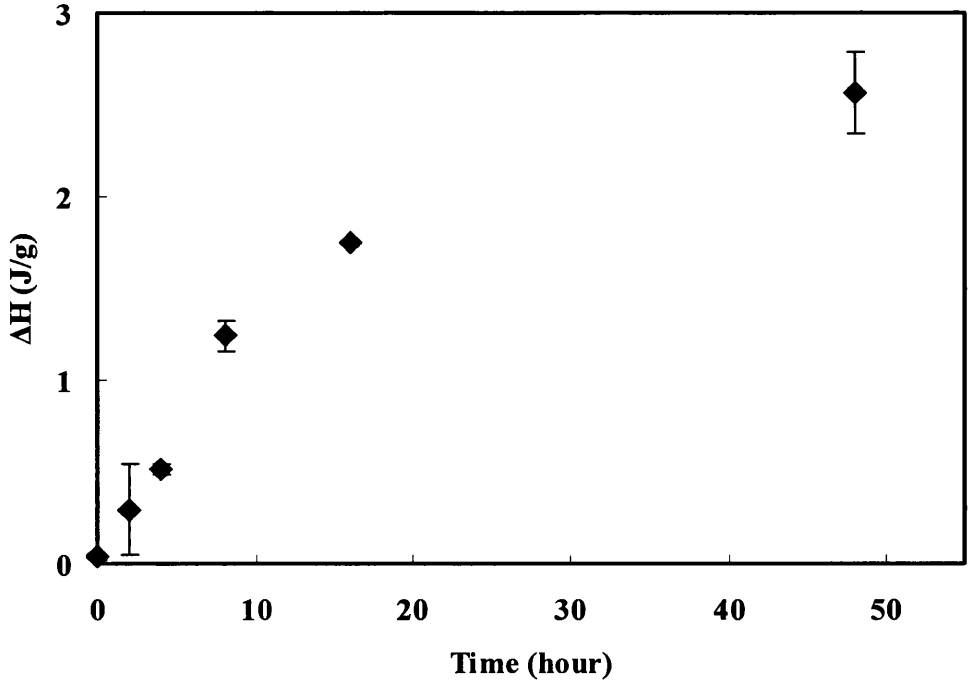

Figure 4.8: *Enthalpy recovery of melt quenched solid solution (an indometacin to PVP ratio of 70%:30%) aged at 50 °C as a function of time, determined by SSDSC (n=3).*

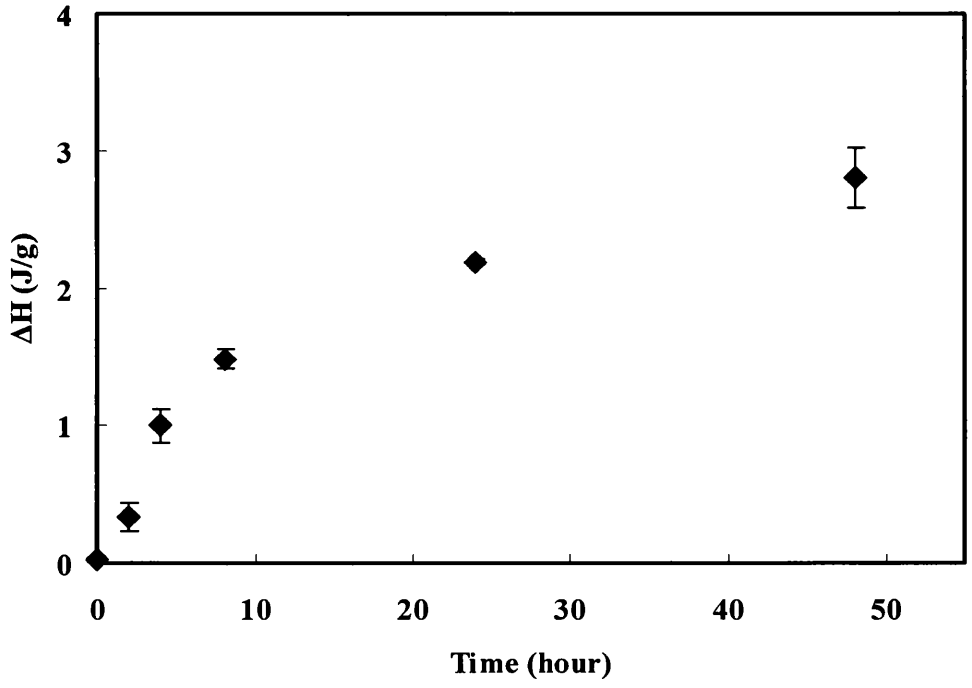

Figure 4.9: *Enthalpy recovery of melt quenched solid solution (an indometacin to PVP ratio of 70%:30%) aged at 50 °C as a function of time, determined by SSDSC (n=3).*

As can be seen from Figures 4.7 to 4.9, no matter which preparation method was used, the solid solutions have all shown a gradual increase of the enthalpy recovery as aging time increased. This indicated that the structural rearrangement of the glassy sample towards the equilibrium state.

Although MTDSC or SSDSC can measure the enthalpy recovery in a more accurate extent than conventional DSC, its value is not necessarily the same as enthalpy relaxation because factors such as the "frequency effect" and "temperature scan effect" may also contribute to the endotherm measured near T_g. These factors might probably be the reason why the solid solutions at time zero display a small enthalpy peak. The "frequency effect" in some cases, can make a significant impact to the endotherm even though it is not related to enthalpy relaxation or recovery. Therefore, miscalculation of enthalpy recovery might be made if it is not taken into account (Kawakami and Pikal, 2005). It needs to be pointed out that the "frequency effect" at different aging time or temperature would remain constant as long as the same batch of sample with a similar particle size and density is used. On the other hand, the "temperature scan effect" is caused by the lower scan rate of MTDSC or SSDSC (compared to a conventional DSC experiment). This slow heating procedure might allow the sample to relax even during the temperature scans. Therefore, the enthalpy loss caused by a temperature scan and the frequency effect must be addressed in order to obtain an accurate relaxation enthalpy. A well accepted method is to subtract the raw endotherm data of different aging times by the enthalpy recovery value obtained with the zero one (Liu *et al.*, 2002; Kawakami and Pikal, 2005).

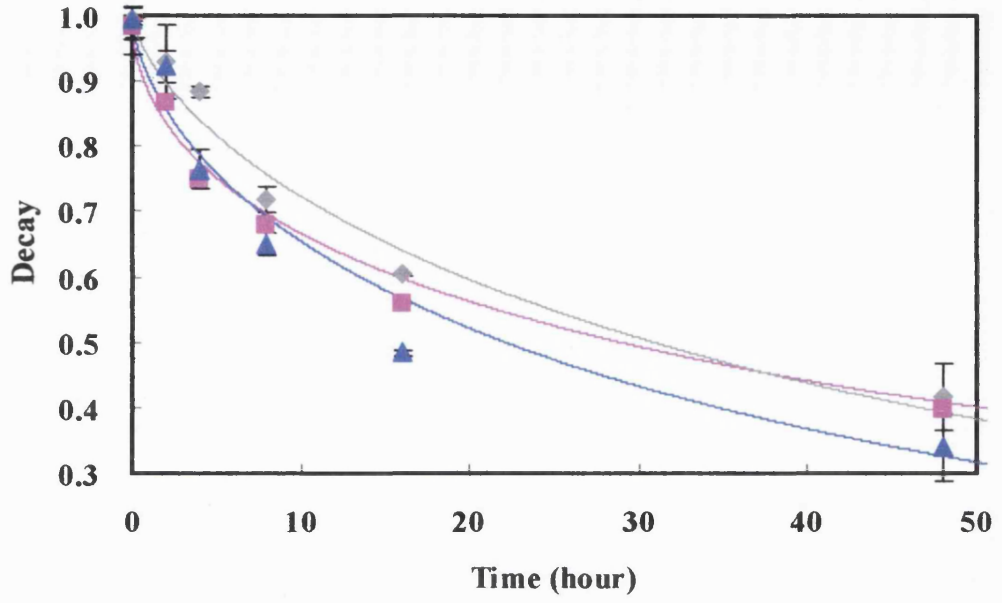

Figure 4.10: *Structural relaxation decay function of ball milled (■), spray dried (▲) and melt quenched (◆) solid solutions(an indometacin to PVP ratio of 70%:30%) determined by enthalpy recovery method, with KWW fitting shown as solid lines (n=3).*

Samples	τ (day)	β	τ^{β} (day)	Chi^2 DoF	R^2
Ball milled solid solution	58.6	0.50	7.9	0.0016	0.9733
Melt quenched solid solution	47.7	0.71	15.6	0.0008	0.9865
Spray dried solid solution	39.9	0.62	9.8	0.0017	0.9785

Table 4.2: *Relaxation parameters obtained from DSC data for different solid solutions containing indometacin:PVP of 70%:30% (R^2, coefficient of determination, and Chi^2/DoF, reduced Chi^2 value).*

The enthalpy relaxation data of the solid solutions were normalised using Equation 3.11

and fitted to the Kohlraush-Williams-Watts (KWW) equation in order to obtain the τ and β values according to the method described in Chapter 3. Figure 4.10 shows the fraction of sample that relaxed after a certain period of time and Table 4.2 shows the relaxation parameters obtained after fitting to the equation.

As expected, the solid solutions prepared by different methods have shown different relaxation behaviours (Table 4.2). The relaxation time constant, τ^{β} was used to evaluate the relaxation rate of these three systems. The molecular mobility of the systems was in the order of melt quenched, spray dried and ball milled solid solutions from low to high. In a study, Liu *et al.* (2002) mentioned that during structural relaxation, a sample starts to deviate from its initial glassy state, where the configurations were "frozen in" during processing, towards the equilibrium supercooled liquid state. Hence the relaxation would be expected to be dependent on the preparation methods. The τ^{β} of the spray dried solid solution is in good correlation with the value of a spray dried indometacin and PVP system (10.0 hours) obtained by Matsumoto and Zografi (1999). Furthermore, the β values of the solid solutions were also different to each other while the melt quenched sample has the most homogeneous distribution of relaxation and the ball milled one has the least. This large distribution in relaxation of the ball milled sample might be due to its heterogeneity. The ball milled solid solution was found to be less homogenous than the spray dried and melt quenched ones as indicated by the larger width of its T_g, because a broad T_g might be a result of some heterogeneous regions within the amorphous sample or some extra compounds generated by chemical degradation. Patterson *et al.* (2007) tried to study the effect of different preparation methods on the physical properties of some pharmaceutical APIs compounded with PVP and it was found that the ball milled carbamasipine and PVP was less homogenous than the melt quenched and spray dried ones. Though MTDSC only detected a single T_g on the ball milled carbamasipine and PVP system, Raman mapping data had indicated that there was evidence for small clusters of carbamasepine rich areas.

In some previous studies, it has been discovered that preparation methods can play an

important influence on the pharmaceutically related properties of the resulted product. Surana *et al.* (2004) found that the method used to prepare amorphous trehalose can affect the enthalpy relaxation, crystallisation behaviours and the rate or extent of water sorption to the material. In another case amorphous tri-*O*-methyl-β-cyclodextrin prepared by different methods also displayed differences in the crystallisation and relaxation though their glass transition temperature and heat capacity change were similar (Tsukushi *et al.*, 1994). These findings give support to what was observed in this study; indometacin-PVP solid solutions prepared by different methods have a different relaxation profile.

4.4.3 Relaxation evaluation using the retention volume of decane

In Chapter 3, an IGC method based on the use of the retention volume (V_{max}) of decane was developed to study the surface relaxation of the melt quenched solid solution. In this section this method was further applied to determine the surface relaxation of the other two solid solution systems at 50 °C in order to compare them to the DSC relaxation data. Ball milled and melt quenched solid solutions were first conditioned at 25 °C and 0% RH in the column oven under He flow for 10 hours and then the temperature was increased to 50 °C followed by a series injection of decane and methane for up to 48 or 24 hours respectively in order to obtain the V_{max} information as a function of aging time.

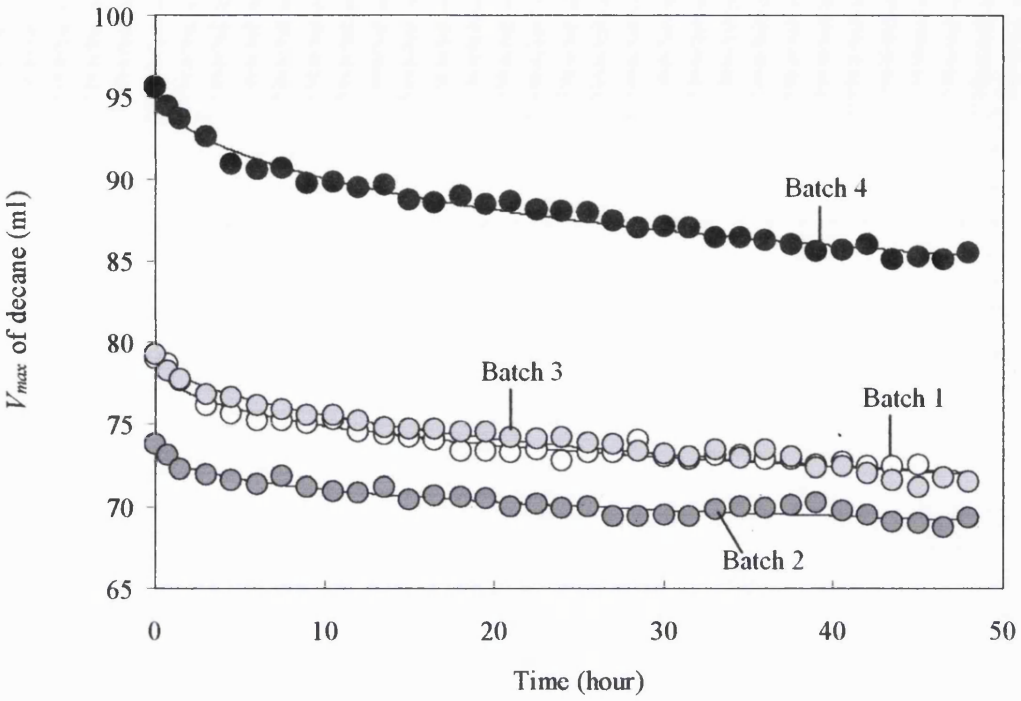

Figure 4.11: *Decrease of decane V_{max} on four different batches of ball milled solid solution (an indometacin to PVP ratio of 70%:30%) as a function of time at 50 ℃.*

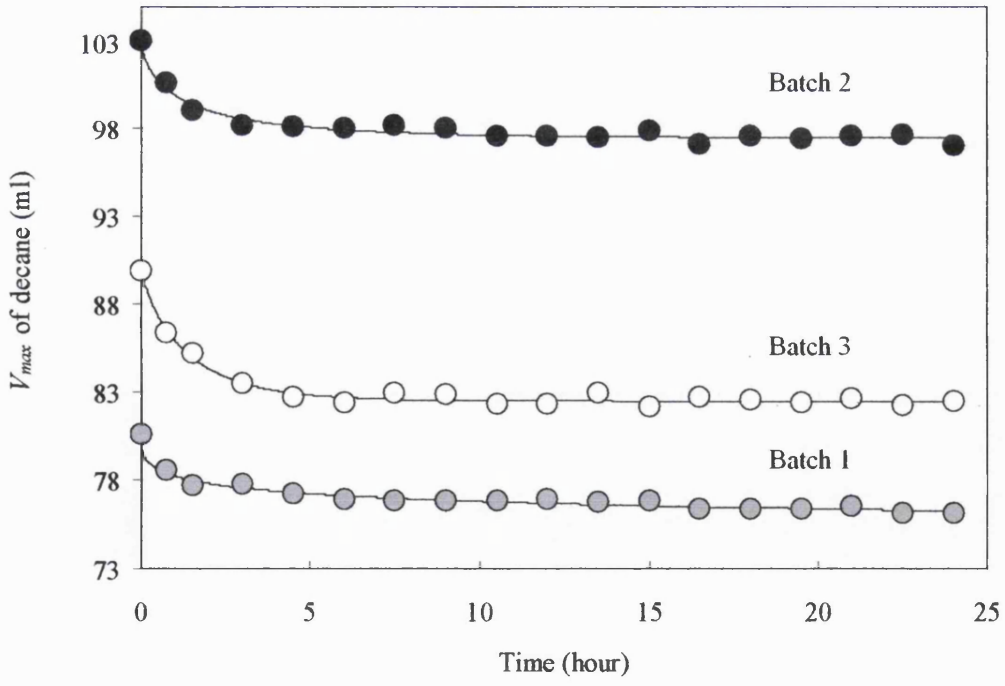

Figure 4.12: *Decrease of decane V_{max} on three different batches of spray dried solid solution (an indometacin to PVP ratio of 70%:30%) as a function of time at 50 ℃.*

The V_{max} changes of the ball milled and melt quenched solid solutions aged at 50 °C are shown in Figures 4.11 and 4.12. The V_{max} change of the melt quenched solid solution has already been shown in Chapter 3 (Figure 3.25). For all samples, V_{max} of decane decreased as the aging time increased. The spray dried solid solution displayed a steep drop of V_{max} in the first 3-5 hours followed by a slower decrease later on. In the case of ball milled solid solution the decrease of V_{max} was much slower. The spray dried solid solution relaxed in a faster manner than the ball milled and melt quenched ones. In order to have a clear view of the relaxation behaviours, the V_{max} data obtained were normalised using the method developed in Chapter 3 in order to perform a KWW fitting. Once the surface relaxation parameters were acquired, they were compared to the bulk relaxation data obtained by DSC study. Figures 4.13 to 4.15 show the comparison of the KWW fitting obtained using IGC and DSC relaxation data.

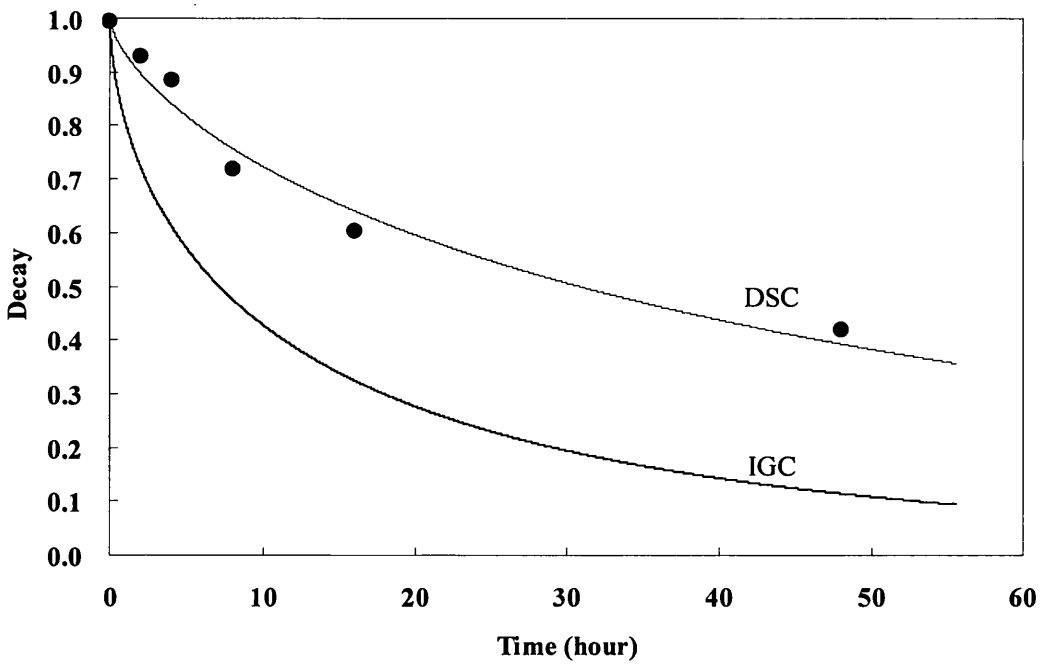

***Figure 4.13**: KWW fitting of the IGC and DSC data of the melt quenched solid solution (an indometacin to PVP ratio of 70%:30%) aged at 50 °C.*

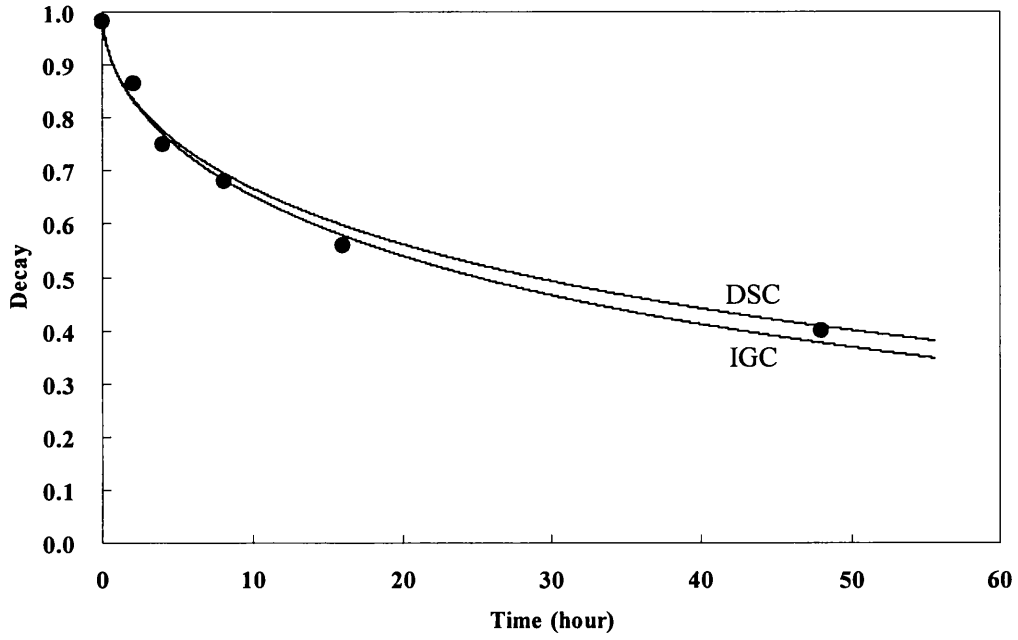

***Figure 4.14**: KWW fitting of the IGC and DSC data of the ball milled solid solution (an indometacin to PVP ratio of 70%:30%) aged at 50 °C.*

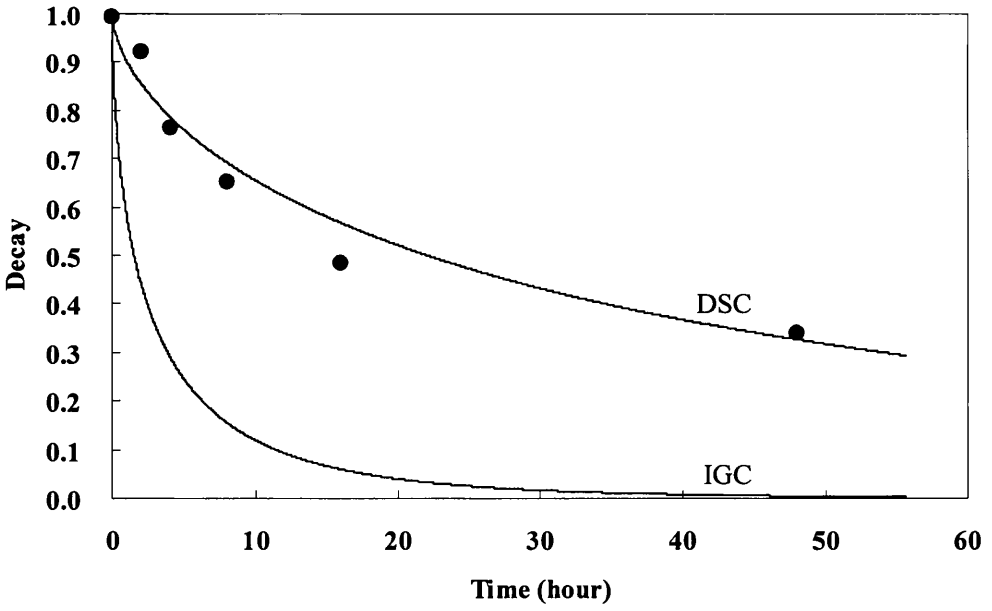

***Figure 4.15**: KWW fitting of the IGC and DSC data of the spray dried solid solution (an indometacin to PVP ratio of 70%:30%) aged at 50 °C.*

Preparation method	IGC (surface)					SSDSC (bulk)				
	$\tau(h)$	β	$\tau^{\beta}(h)$	Chi^2 /DoF	R^2	$\tau(h)$	β	$\tau^{\beta}(h)$	Chi^2 /DoF	R^2
Melt quenching	13.1	0.60	4.6	0.0032	0.9904	47.7	0.71	15.6	0.0016	0.9733
Ball milling	50.8	0.50	7.1	0.0015	0.9575	59.6	0.50	7.9	0.0008	0.9865
Spray drying	2.8	0.60	1.8	0.0015	0.9756	39.9	0.62	9.8	0.0017	0.9785

Table 4.3: *A comparison of the surface (IGC) and bulk (DSC) relaxation (R^2, coefficient of determination, and Chi^2/DoF, reduced Chi^2 value).*

Table 4.3 shows τ, β and τ^{β} of relaxation at the surface determined using IGC and that of the bulk relaxation determined using SSDSC. It has been proven by many researchers that the surface and bulk of some amorphous materials behave very differently. For example, Wu and Yu (2006) have studied the surface crystallisation of amorphous indometacin and discovered that its surface crystallised faster than its bulk and displayed different crystallisation kinetics. In polymer science, Fakhraai and Forrest (2008) studied the surface relaxation of polystyrene using atomic force microscopy and the surface relaxation was observed at all temperatures studied from 4 to 96 °C with enhanced surface mobility relative to the bulk. These match well with what was observed in this study: higher molecule mobility discovered at the surface of the amorphous solid solution. Furthermore, the β values of the bulk and surface relaxation were surprisingly close to each other which indicated a similar distribution of relaxation time through out the bulk and the surface.

The preparation methods resulted in different surface relaxation. The surface of the melt quenched sample was the most stable but the spray dried sample relaxed the fastest. The surface morphology might have played an important role on the surface relaxation. The

difference between the surface and bulk relaxation is very significant in melt quenched and spray dried samples. However, in the case of ball milled sample, the difference was very limited. During ball milling, mechanical force was applied on the surface of the particles to facilitate crystalline indometacin dissolving into the rubbery PVP. The amorphous region of these two components was mainly located on the surface and left the core of the sample either a small amount of PVP or crystalline indometacin (none of them would give any relaxation response). Though SSDSC was obtaining the relaxation information of the whole sample, this relaxation was mainly from the outer layer. Therefore it has similar relaxation profile to the IGC detected relaxations. This case in another way proved the capability of IGC in detecting surface relaxation.

Furthermore, AFM was used to study whether surface relaxation could cause any change on the roughness of the sample. The melt quenched system was investigated here and this sample was unground, therefore it appeared as a flat cake which was feasible for the roughness measurement using AFM. The melt quenched samples that were ground appeared as particles with a very small size and it was difficult to measure the roughness at the surface of a single particle. The ball milled and spray dried samples which also appeared as fine particles were not studied here for the same reason. The melt quenched sample was aged at 50 °C for 48 hours and the root-mean-square roughness (R_q) of the initial and the aged samples was measured according to the AFM amplitude images (Figure 4.16). To correct the scanner bow, each image was treated using the third order plane fit command of the control software in both y and x direction. The root-mean-square roughness was calculated using Equation 4.1:

$$R_q = \sqrt{\frac{1}{n_p}\sum_{i=1}^{n} y_i^2} \qquad \text{Equation 4.1}$$

where y_i is the distance of point i from the centre line and n_p is the number of points taken. However, no apparent change of the roughness on the sample was noticed after aging (Table 4.4). On the other hand, phase images of the samples indicated a good

homogeneity on the surface and no phase separation occurred after aging for 48 hours.

n	R_q (Initial)	R_q (Aged at 50 °C for 48 hours)
1	0.365	0.470
2	0.439	0.427
3	0.496	0.416
4	0.435	0.337
5	0.477	0.411
Average (std)	0.442 (0.050)	0.412 (0.048)

Table 4.4: *Root-mean-square roughness of the initial and aged solid solution measured from the amplitude images.*

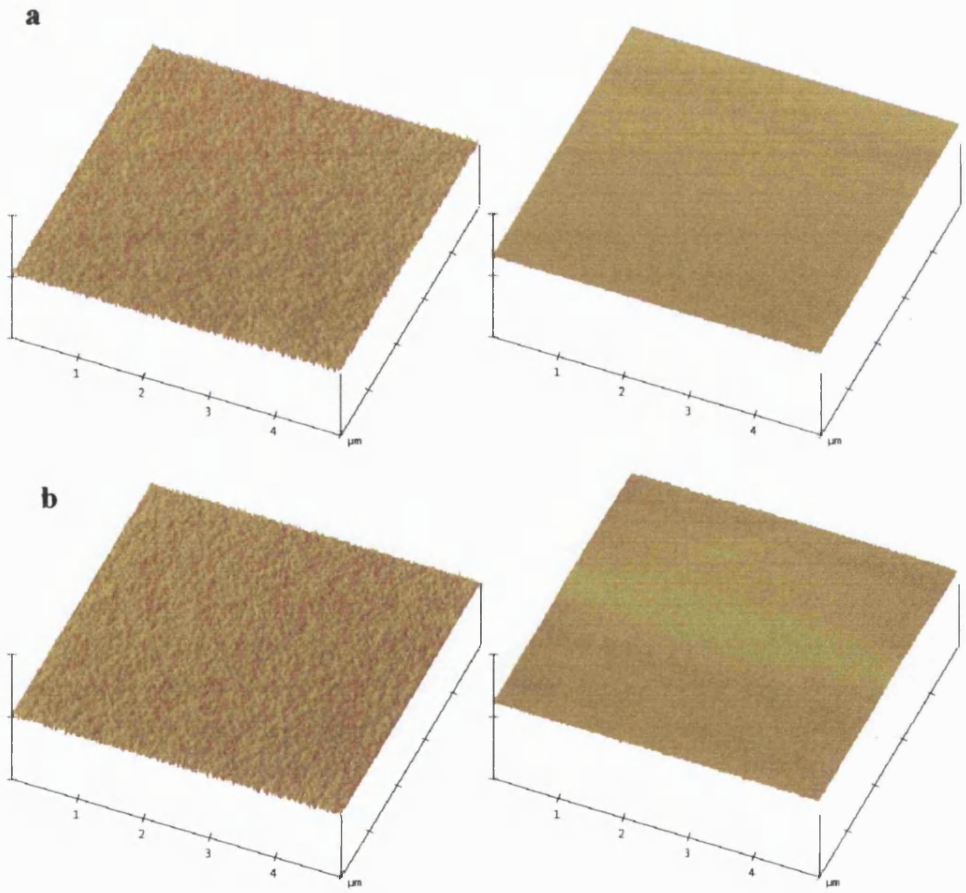

Figure 4.16: *Tapping-mode AFM images: a) initial sample and b) sample aged at 50 °C for 48 hours (left, amplitude image; right, phase image).*

4.4.4 Relaxation evaluation using isothermal microcalorimetry

In this section, isothermal microcalorimetry was used to study the relaxation behaviours of the solid solutions. IMC is a technique which can be used to directly measure the rates of enthalpy relaxation (Liu *et al.*, 2002). IMC can continuously record heat production rate during enthalpy relaxation which can provide more data points than DSC which measures cumulative change. IMC is considered to be more sensitive than DSC in measuring slow relaxation (Liu *et al.*, 2002).

IMC measures the heat flow to or from the sample. An equation was differentiated from the KWW equation (Equation 3.9) to obtain the expression for heat power P per gram of sample used, μW/g (Liu *et al.*, 2002). This equation was used in order to fit the signal measured by IMC to obtain the relaxation parameters (Liu *et al.*, 2002):

$$P = 277.8 \cdot \Delta H_{\infty} \cdot (\frac{\beta}{\tau}) \cdot (\frac{t}{\tau})^{\beta-1} \cdot \exp\left[-(\frac{t}{\tau})^{\beta}\right] \qquad \text{Equation 4.2}$$

where P is the heat power, ΔH_{∞} is the relaxation enthalpy at time infinite, t is time in hour and the other parameters are the same as stated previously. 277.8 in the equation is a result of unit conversions due to differentiating KWW equation to Equation 4.2.

On the other hand, Liu *et al.* (2002) have suggested using another equation (Equation 4.3), a modified stretched exponential function (MSE), which was originally developed for NMR relaxation, to interpret the IMC data:

$$\Phi(t) = \exp\left[-(\frac{t}{\tau_0}) \cdot (1+\frac{t}{\tau_1})^{\beta-1}\right] \quad (0 < \beta < 1) \qquad \text{Equation 4.3}$$

In order to express heat power P obtained from an IMC study, Equation 4.3 can be expressed as follow:

$$P = 277.8 \cdot \frac{\Delta H_\infty}{\tau_0} \cdot (1 + \frac{\beta t}{\tau_1}) \cdot (1 + \frac{t}{\tau_1})^{\beta-2} \cdot \exp\left[-(\frac{t}{\tau_0}) \cdot (1 + \frac{t}{\tau_1})^{\beta-1} \right] \qquad \text{Equation 4.4}$$

The relaxation time constant τ which is equivalent to the one in KWW equation can be calculated using Equation 4.5:

$$\tau = \tau_0^{1/\beta} \cdot \tau_1^{(\beta-1)/\beta} \qquad \text{Equation 4.5}$$

The main advantage of MSE equation over the KWW equation is its ability to avoid problems as time approaches zero. When t approaches zero, the power P remains finite while in the case of the KWW equation, it becomes infinite, which is physically impossible. This "time-zero" problem might create errors when analyzing Φ near time zero and introduce inaccuracies when studying very slow relaxations for short periods of time, such as a few days (Liu *et al.*, 2002). It needs to be pointed out that as experiment time increases, the MSE equation reduces to the form of KWW equation (Liu *et al.*, 2002).

The solid solutions for study were left in an isothermal microcalorimetry, Thermal Activity Monitor (TAM) at 50 °C for 48 hours. The rate of enthalpy relaxation of these samples were measured and analyzed. The heat power signals measured are shown in Figures 4.17 to 4.19.

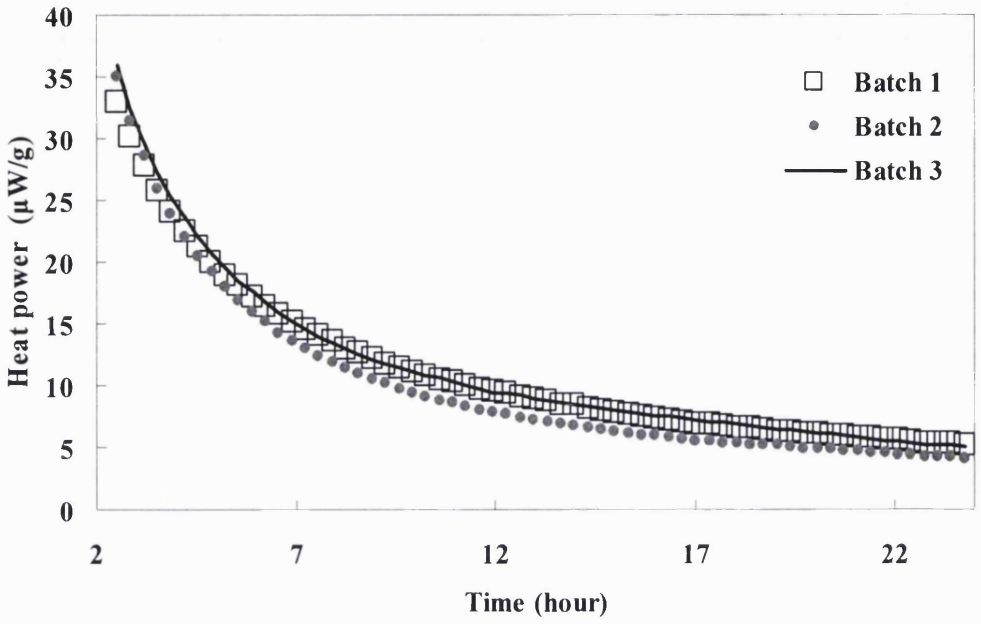

Figure 4.17: *Power time response of the ball milled solid solution (an indometacin to PVP ratio of 70%:30%) measured by IMC at 50 °C.*

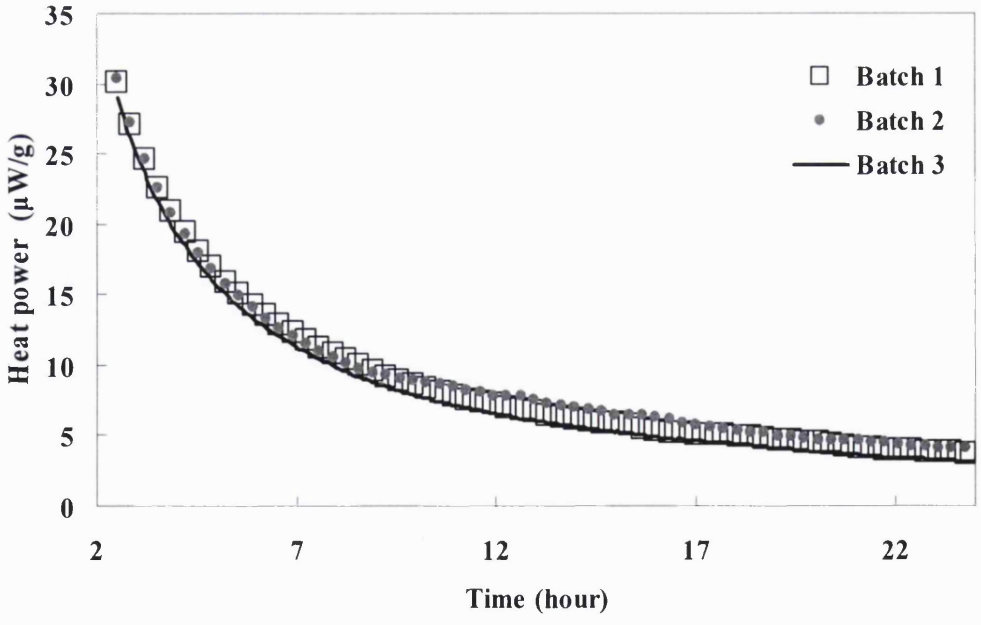

Figure 4.18: *Power time response of the melt quenched solid solution (an indometacin to PVP ratio of 70%:30%) measured by IMC at 50 °C.*

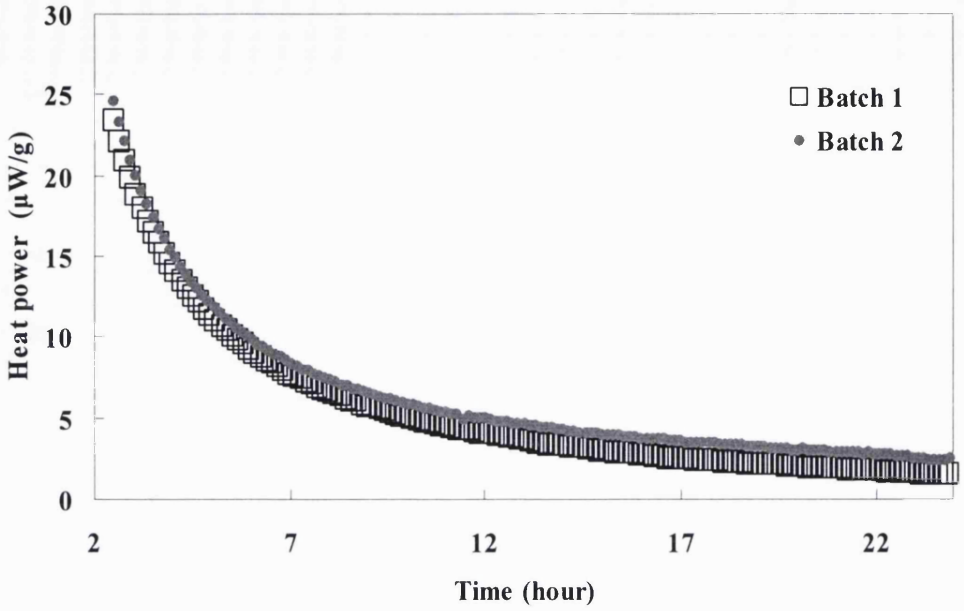

Figure 4.19: *Power time response of the spray dried solid solution (an indometacin to PVP ratio of 70%:30%) measured by IMC at 50 °C.*

Equations 4.2 and 4.4 were used to fit the power time data of the solid solutions measured by TAM. The ΔH_∞ values obtained after the fitting were compared to the ones calculated from the DSC study using Equation 3.10 (Table 4.5). A good agreement between these data was observed.

Sample	ΔH_∞(J/g)		
	MSE	KWW	SSDSC
Ball milling	3.9	4.3	3.6
Melt quenching	3.5	3.8	4.4
Spray drying	3.6	4.6	4.2

Table 4.5: *Comparison of infinite relaxation enthalpy of the solid solutions (an indometacin to PVP ratio of 70%:30%) determined by IMC and calculated according to the T_g value obtained by SSDSC.*

Preparation Method	KWW			MSE					DSC		
	τ/h	β	τ^{β}/h	τ_0/h	τ_1/h	τ/h	β	τ^{β}/h	τ/h	β	τ^{β}/h
Ball milling	9.7	0.47	3.0	1.9	0.4	10.4	0.50	3.2	59.6	0.50	7.9
Melt quenching	7.8	0.43	2.4	0.9	0.1	8.4	0.45	2.6	47.7	0.71	15.6
Spray drying	1.2	0.22	1.0	1.7	0.5	49.4	0.32	3.4	39.9	0.62	9.8

Table 4.6: *Comparison of relaxation parameters of the solid solutions (an indometacin to PVP ratio of 70%:30%) evaluated using both KWW and MSE equations in IMC study and the ones determined in DSC study (n=3).*

Relaxation parameters τ and β were calculated after fitting the IMC data to Equations 4.2 and 4.4 and compared to the ones determined using SSDSC (Table 4.6). For all three solid solutions, the τ and τ^{β} values obtained using IMC were significantly lower than those obtained using SSDSC. In a previous study, Liu *et al.* (2002) demonstrated good agreement between IMC and MTDSC. However, that comparison was only based on one hydrophilic compound, sucrose. However, in a more recent study, Bhugra *et al.* (2006) extended this study to two more compounds, indometacin (tested at 25 and 30 °C) and ketoconazole (tested at 20, 25, 30 and 35 °C), both of which are hydrophobic. The authors have found that the relaxation times obtained using IMC were significantly lower than those determined by MTDSC at all tested temperatures. Though a clear explanation on this phenomenon is still unknown, it was suggested that this difference is probably due to the high sensitivity of IMC which enables it to measure some faster modes of motion beside those which also can be measured by DSC. In another words, DSC could only measure those motions which accompanied with a change of enthalpy recovery, such as the α-relaxation (namely, structural relaxation as explained in the Introduction Chapter). Therefore, the faster relaxation times measured by IMC were probably caused by the inclusion of some faster motions or relaxation process. This reason could also be used to explain why the β value derived from IMC was smaller than the one from SSDSC.

According to the IMC relaxation data, different solid solution systems show small difference in their relaxation parameters which indicates that different preparation methods have a different impact on their relaxation behaviors as confirmed previously by both DSC and IGC studies. The relaxation parameter values determined using KWW equation were similar to the MSE ones for both ball milled and melt quenched samples. In the case of the spray dried solid solution, the values were slightly different when determined using the different equations. The reason of this is not clear; however, considering the subtleties of numerical evaluation and the relative fast relaxation rates the samples have, this difference was possible to happen.

4.4.5 Correlation of fragility, zero mobility temperature and physical stability

It is very important for pharmaceutical researchers to understand how molecular mobility of amorphous materials changes with temperature. This kind of information could help one to decide a suitable storage condition that would reduce the rates of any physical or chemical degradation to an acceptable range (Crowley and Zografi, 2001). Angell (1991) has developed a strong/fragile classification system for glasses according to the temperature dependence of relaxation time or viscosity above their T_g. When plotting relaxation or viscosity versus temperature, strong glasses yield a straight line indicating Arrhenius behaviours while fragile glasses display a significant deviation from linearity (as shown in Figure 1.6). In other words, the molecular mobility increases more rapidly in a fragile glass as the T_g is approached during the heating or cooling procedure. For example, the rate of molecular mobility of sorbitol, a fragile glass, changes by about one order of magnitude for a temperature change of 10 °C (Bohmer *et al.*, 1993), while for a strong glass, such as $ZnCl_2$, the same level of change happens every 25 °C (Bohmer *et al.*, 1993).

In this study, the dependence of glass transition temperature on heating rate was evaluated using DSC to study the fragility of the solid solution systems. The solid solution sample was first heated to 20 °C above their T_g followed by cooling down to at least 50 °C lower than it. The cooling rate has to be identical to the subsequent heating otherwise an error would happen in the measurement of activation enthalpy (Moynihan *et al.*, 1974 and 1976; Crichton and Moynihan, 1988). Subsequently, the sample was scanned at heating rates of 2, 5, 10, 20 and 40 °C/min^{-1} and the onsets of T_g were recorded for calculation later. This range of heating rate was chosen because it is not so slow that the sensitivity of a scan is compromised, while significant thermal lags which usually happen at fast heating rate can be avoided (Crowley and Zografi, 2001). Figure 4.20 shows the DSC scans of the solid solutions.

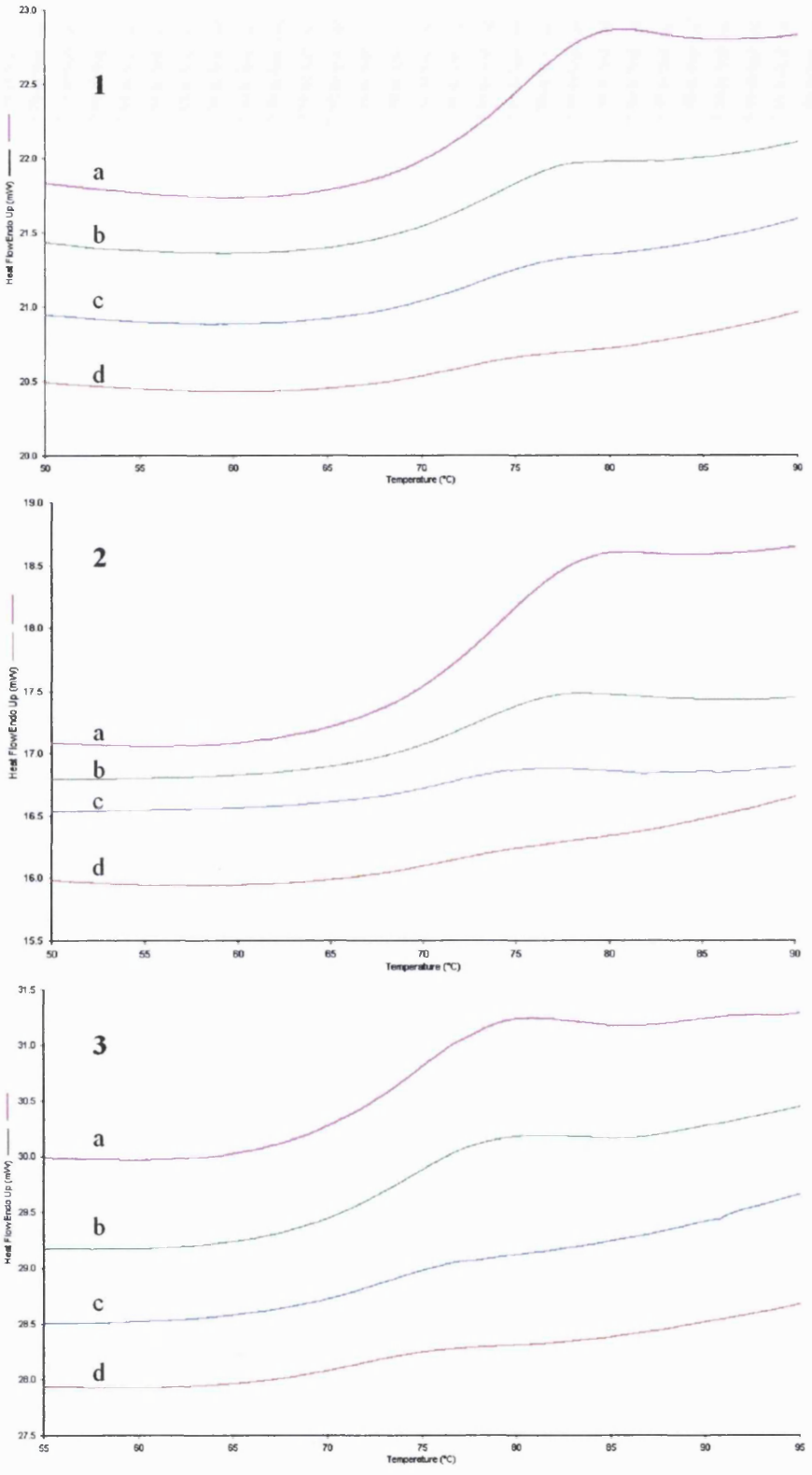

Figure 4.20: *DSC traces (each trace is a representative of three measurements) of the ball milled (1), melt quenched (2) and spray dried (3) samples (an indometacin to PVP ratio of 70%:30%) scanned at 40 (a), 20 (b), 10 (c) and 5 (d) °C/min.*

The activation enthalpy of structural relaxation ΔE_{Tg} at T_g of the sample can be calculated using the heating rate dependence of T_g (ΔE_{Tg} can be obtained from the slope of a plot of $1/T_{gon}$ against lnq) according to an equation applied by Moynihan *et al.* (1974):

$$-\frac{\Delta E_{T_g}}{R} = \frac{d(\ln q)}{d(1/T_g)} \qquad \text{Equation 4.6}$$

where R is the gas constant (R=8.3145 J · K^{-1} · mol^{-1}) and q is the heating/cooling rate. Fragile glasses which display non-Arrhenius behaviour usually have a large ΔE_{Tg} close to T_g and therefore a less significant effect of heating rate on T_g (Crowley and Zografi, 2001).

The fragility parameter, m, defined as the slope of the $log\tau$ versus T_g/T line at the glass transition temperature (T=T_g), can be expressed in the following equation:

$$m = \left[\frac{d\log_{10}\tau(T)}{d(T_g/T)}\right]_{T=T_g} \qquad \text{Equation 4.7}$$

where τ is the relaxation time constant and it would slow down to 100 s at T_g (Zallen, 1983). Equation 4.7 can also be expressed in terms of the temperature dependent apparent activation energy ΔE^* (which can be replaced by ΔE_{Tg}):

$$m = \frac{\Delta E_{T_g}}{(\ln 10)RT_g} \qquad \text{Equation 4.8}$$

A large value of m indicates a fragile glass and a small value indicates a strong one. The strength parameter D in Vogel-Tammann-Fulcher (VTF) equation can be calculated using m based on Equation 4.9. In this case, a value of D more than 30 indicates a strong glass, and if it is lower than 10 the glass displays fragile behaviour.

$$D = \frac{(\ln 10)m_{\min}^2}{m - m_{\min}}$$ Equation 4.9

where m_{min} is the minimum value of m and it is defined as $m_{min}=log\ (\tau_{Tg}/\tau_0)$. As described before τ_{Tg} is approximate 100 s, with τ_0 which is the timescale of vibration motions being 10^{-14} s, m_{min} can be calculated to be 16. Moreover, T_0, the temperature at which the molecular mobility (also the configuration entropy) reaches zero, can be calculated according to the following equation (Yoshioka and Aso, 2005):

$$T_0 = T_g(1 - \frac{m_{\min}}{m})$$ Equation 4.10

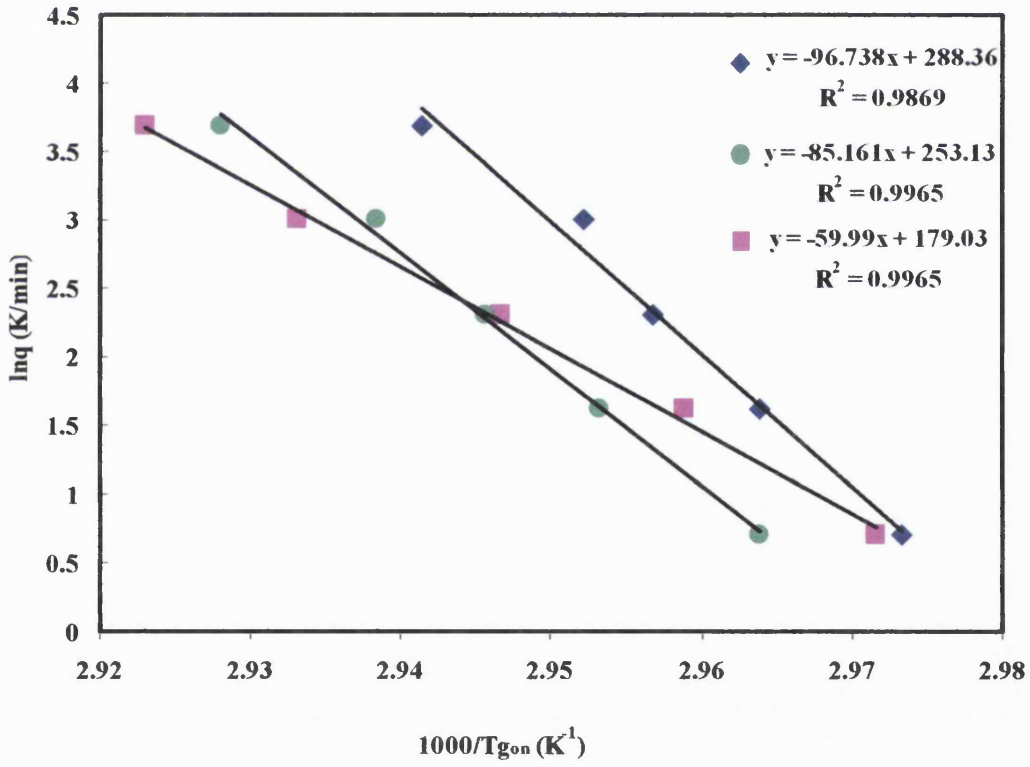

Figure 4.21: *Plot logarithm of heating rate as a function of $1/T_{gon}$ of the ball milled (■), spray dried (●) and melt quenched (◆) solid solutions (an indometacin to PVP ratio of 70%:30%). The regression straight lines and coefficients of determination are shown (n=3).*

After plotting *ln* (heating rate) versus reciprocal glass transition temperature of the three different solid solutions (Figure 4.21), based on the slopes of the regression straight lines, the activation enthalpy, fragility parameters and other related parameters of the solid solutions can be obtained (values are listed in Table 4.7). The regression straight lines of the data points produced very good coefficients of determination (R^2) which are around 0.99 for all three systems.

Preparation method	*T_g (q=10 °C/min)	ΔE_{Tg} (kJ/mol)	m	D	T_0(°C)	T_g-T_0 (°C)
Ball milling	66.4±0.4	498.8	77	9.7	-4.2	70.6
Melt quenching	65.2±0.7	804.3	124	5.5	21.6	43.6
Spray drying	66.5±1.1	708.1	109	6.3	16.7	49.8

Table 4.7: *A table of fragility and other related values of the solid solutions (an indometacin to PVP ratio of 70%:30%) prepared by different methods (T_g values are mean ± s.d., n=3).*

The difference in the slope of the regression linearity led to very different activation enthalpy of the solid solutions. The melt quenched solid solution had the highest ΔE_{Tg} which was 804.3 kJ/mol and the ball milled one had the lowest, 498.8 kJ/mol. All of them were higher than the ΔE_{Tg} of pure indometacin, which was 385 kJ/mol as determined in a previous study (Hancock *et al.*, 1998). Although all systems had very similar T_g, this difference in ΔE_{Tg} ultimately led to difference in their fragility parameters and strength parameters. The D values indicated the fragile nature of the

solid solutions (D<10), and both D and m values indicated the melt quenched solid solution was the most fragile glass among the three while the spray dried one being the next and the ball milled one being the least. Different preparation methods seemed to have different impacts on the fragility of the solid solutions. Interestingly, the m value of ball milled sample matched well with the one reported for amorphous indometacin (m=77; Hancock *et al.*, 1998). Considering that the process of ball milling does not require any heat or solvent as needed by the other two methods which include complete melting or dissolution of indometacin and PVP, the fragility of the ball milled sample was expected to be the closest to the pure indometacin or PVP (m=46; Buckton *et al.*, 2006). Therefore, this result further demonstrates the fragility of a product can largely be affected by the way it is prepared.

The zero mobility temperature T_0 of the solid solutions was calculated according to Equation 4.10. The values of the melt quenched, spray dried and ball milled samples were 21.6, 16.7 and -4.2 °C respectively. The accuracy of this calculation method has been validated previously. Hatley (1997) found that the T_g-T_0 of sucrose was 61.5 °C obtained using this method, which was in good agreement with the value 60 °C determined by Hancock *et al.* (1995) who based on a more direct approach using enthalpy relaxation.

Glass transition temperature T_g is considered to be an important factor deciding the stability of a glass, and the higher the T_g value the more stable the glass would be at a particular storage temperature. However, some studies have proven that this is not necessary the case (Tarelli *et al.*, 1994; Hatley and Colaco, 1997). T_0 instead, was considered to be a better measure of stability than T_g. Although the T_g of the solid solutions studied here were very similar to each other, enthalpy relaxation studies done by SSDSC indicated that the melt quenched solid solution was the most stable product, the spray dried one being the next and the ball milled one the last. The T_0 and T_g-T_0 values were found to be in good correlation with the SSDSC relaxation studies. It can be seen from Equation 4.10 that a fragile glass would have a small T_g-T_0 while a

strong glass would have the opposite and this is also what is observed based on the T_g-T_0 data of the solid solutions. Therefore, a fragile glass would have more stability advantage than the stronger one when below T_g, because the viscosity of a fragile glass increases more drastically at a given range of temperature drop. So if the samples have similar T_g, at the same aging temperature, the fragile sample would appear to be more stable than the strong one. In the case when the temperature is around or above T_g, the fragile glass is more sensitive to temperature changes than a strong one. Therefore, when a fragile glass is undergoing glass transition, softening happens much faster as the temperature increases compared to stronger glasses, and it is expected that the fragile glass would crystallise more easily. However, a study indicated that the fragile glass trehalose showed less crystallisation tendency than the stronger glass sucrose (Hatley, 1997) when above their T_g. In fact, Pikal *et al.* (1995) suggested that a higher fragility might provide a better stability if the glass transition temperatures are the same. This finding matches well with what was observed in this study.

To further confirm the relation between the fragility, zero mobility temperature, and the stability, a physical stability study was conducted on the solid solutions. The solid solutions were stored at room temperature at 70% RH and after a period of time, samples were taken out for XRPD study. As can be seen in Figure 4.22, the ball milled sample recrystallised in 70 days, followed by the spray dried one recrystallised in 188 days as characteristic peaks of crystalline indometacin were observed. The XRPD patterns of the melt quenched solid sample did not show any significant change after storage of 188 days indicating the sample might still remain in its amorphous form. The physical stability order here coincides with the DSC relaxation data and also the T_0 values obtained from the fragility parameters. Therefore, the fragility and zero mobility temperature are two important factors which must be taken into account in prediction of stability study of amorphous materials.

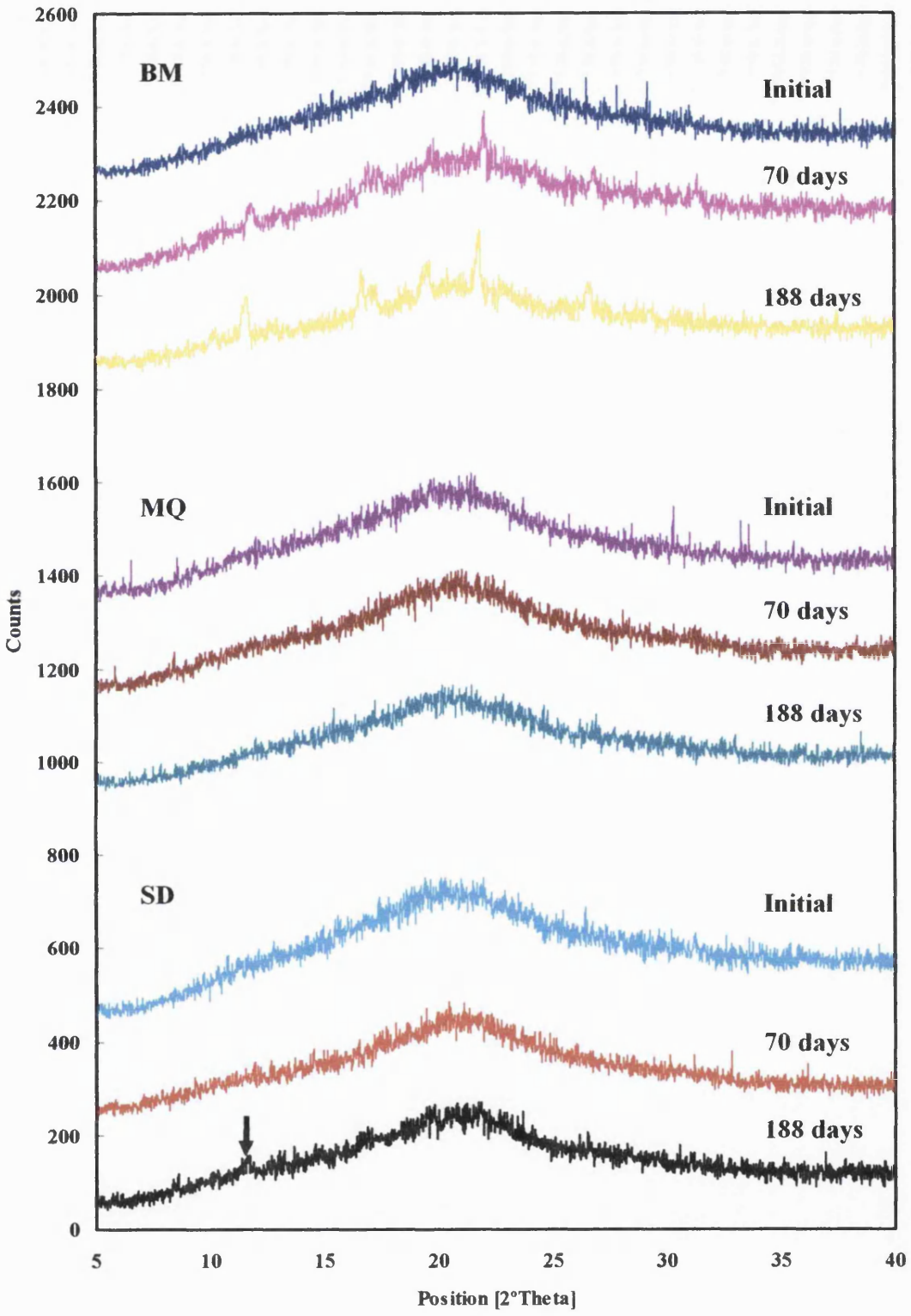

Figure 4.22: *XRPD patterns of the ball milled (BM), melt quenched (MQ) and spray dried (SD) solid solutions (an indometacin to PVP ratio of 70%:30%) stored at room temperature and 75% RH for 0, 70 and 188 days.*

4.4.6 Effect of relaxation on the dissolution behaviour of the solid solutions

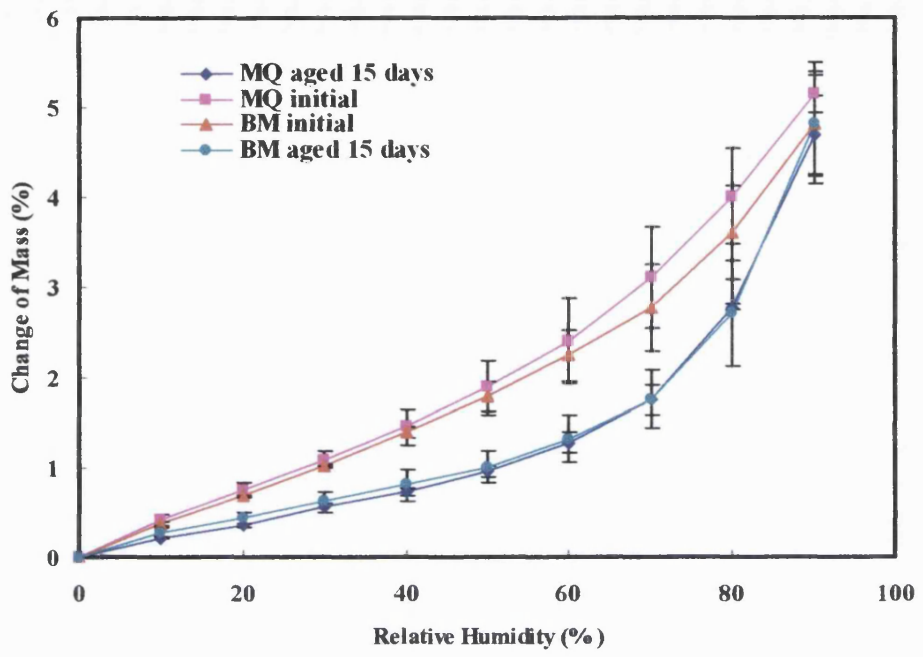

Figure 4.23: *Water vapour sorption isotherms for the unaged and aged (15 days at 50 ℃) melt quenched and ball milled solid solutions of indometacin and PVP (70%:30%).*

Dynamic vapour sorption (DVS) studies were carried out on the initial solid solutions and the ones aged for 15 days at 50 ℃ to evaluate the water sorption behaviours of the solid solutions. About 10-20 mg of powders were first loaded onto the sample pan, after conditioning at 0% RH, RH was increased from 0% to 90% in a step of 10%. Amorphous materials have better apparent solubility and faster dissolution rate than their crystal forms. But if the amorphous products recrystallise during storage and their dissolution rate would probably decrease, as a consequence their bioavailability would be jeopardised, as indicated by some studies (Leuner and Dressman, 2000). It is interesting to investigate whether the physical aging process would affect the water sorption or dissolution behaviours even though a sample has not started to recrystallise. Figure 4.23 shows the water vapour sorption isotherms of the aged and unaged solid solutions which indicate different water uptake behaviour between the samples. All isotherms show an inflection at 10% RH and another one can be seen at

around 60-70% RH. This type of shape is similar to a type-II Brunauer-Emmett-Teller (BET) isotherm which shows an initial linear adsorption followed by an inflection caused by monolayer coverage of the gas molecules and then a rapid increasing curvature caused by multilayered adsorption or condensation. Type-II BET isotherm is usually used to describe adsorption on macroporous adsorbents with strong adsorbate-adsorbent interactions. However, it needs to be borne in mind that the BET classification does not account for any change in the physical properties of the adsorbent (Ambarkhane, 2005); it only takes into account the type of adsorbent and adsorbate, and intermolecular interactions between the surfaces. Physical change such as glass transition can affect the shape of the isotherm. A glass material even though it has a T_g higher than the experimental temperature, when it sorbs enough amount of water which can act as a plasticiser, its molecular mobility can be largely increased and its dry T_g might be lowered to the experimental temperature. Therefore, the glass could be in a rubbery state and it would display different water uptake behaviour.

From Figure 4.23, it could be seen that the preparation methods did not give an obvious difference on the shape of the isotherms of either the aged or unaged solid solutions. However, the isotherms between the aged and unaged samples were significantly different. Aging affected both the extent and the rate of water sorption. In unaged samples, the rate of water sorption was more rapid with a nearly linear increase in the amount of sorption while the aged samples showed an obvious sigmoidal shape and sorbed less water. It is known that the surface area or morphology would affect the rate of sorption of a sample, but in this case, aging did not cause any discernible change on the particle size and surface morphology, hence these different water sorption behaviours are a result of relaxation which accompanies decrease of free volume and/or increase of density. An interesting phenomenon was observed here, though the difference of water sorption between aged and unaged samples became more and more pronounced in the range from 10% to 70% RH, above 70% the sorption rate of the aged samples became faster than the unaged ones. As a consequence, the sorption profiles of the aged samples gradually approached that

of the unaged ones and at 90% RH point. Therefore, it is reasonable to believe that at 90% RH, the water sorption behaviour was independent of its thermal history, which means the thermal history was erased. One possible reason for this is that the T_g of the aged samples was lowered by the sorbed water because of the plasticising effect, and the samples were in the rubbery state starting to sorb a large amount of water (This sudden change of water sorption profile is similar to the enthalpy recovery around T_g in the DSC study). Another explanation suggested by Surana *et al.* (2004) is that the reversal of aging is caused by the volume expansion during water sorption in the amorphous structure. After aging, the free volume of the amorphous material would decrease accompanied by increase in density. However, the sorbed water might be able to expand the structure as a result to increase its free volume. When the water is dried at a low temperature, the amorphous structure does not have enough molecular mobility to relax again and it would stay expanded, thereby, the effect of aging can be reversed.

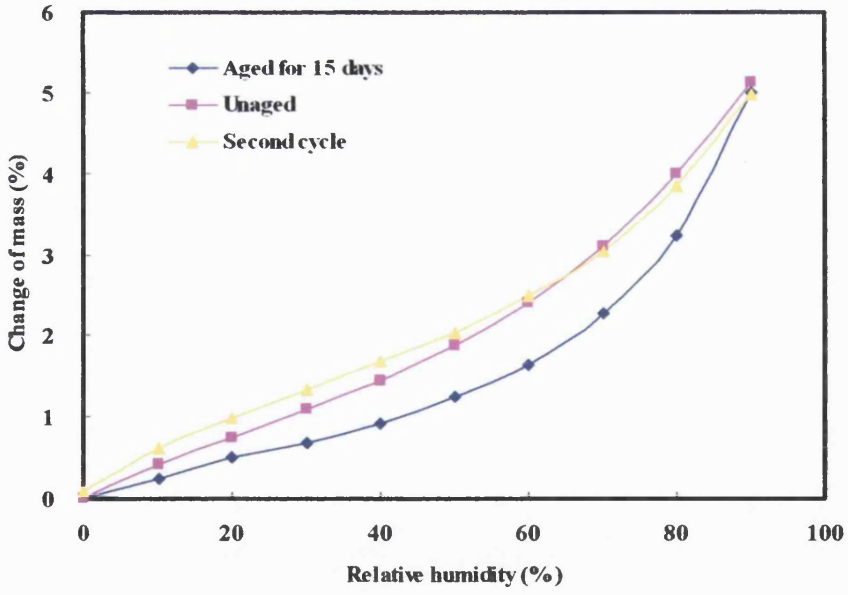

Figure 4.24: *Water sorption profiles of the unaged melt quenched solid solution of indometacin and PVP (70%:30%), the one aged for 15 days at 50 ℃ and the second cycle of the aged sample.*

In order to confirm the effect of the water sorption on the removal of thermal history, the melt quenched solid solution sample which had been aged for 15 days at 50 °C was subjected to two RH cycles and the mass change of the sample of the second cycle was compared to the initial unaged sample. Figure 4.24 shows that after the first RH cycling, the water sorption ability of the sample has increased dramatically in the second cycle and its sorption profile is similar to that of the initial unaged sample. This indicated that the effect of relaxation was removed during the RH cycling treatment.

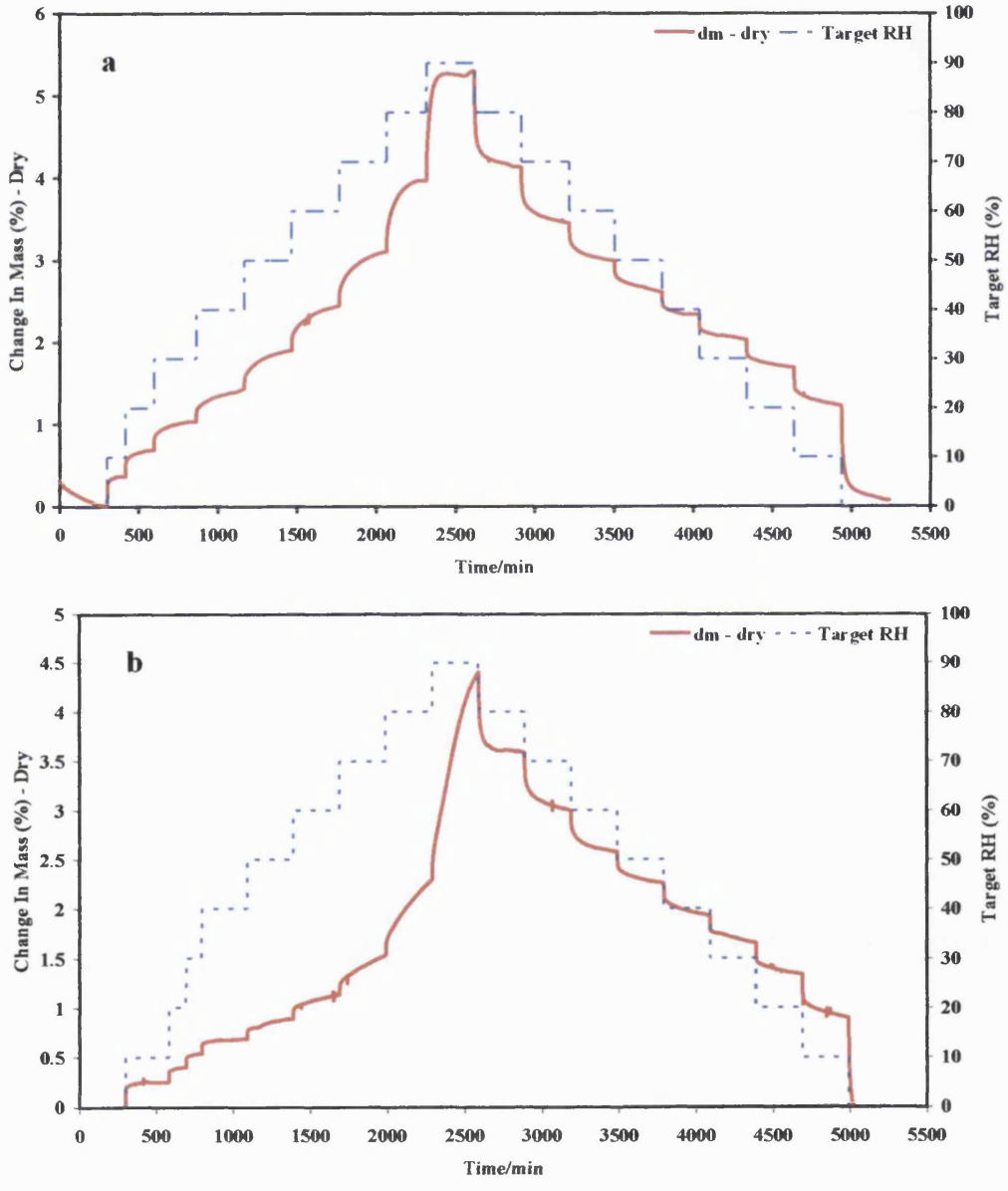

Figure 4.25: *Dynamic vapour sorption traces of the ball milled solid solutions: a) unaged sample and b) sample aged for 15 days at 50 °C.*

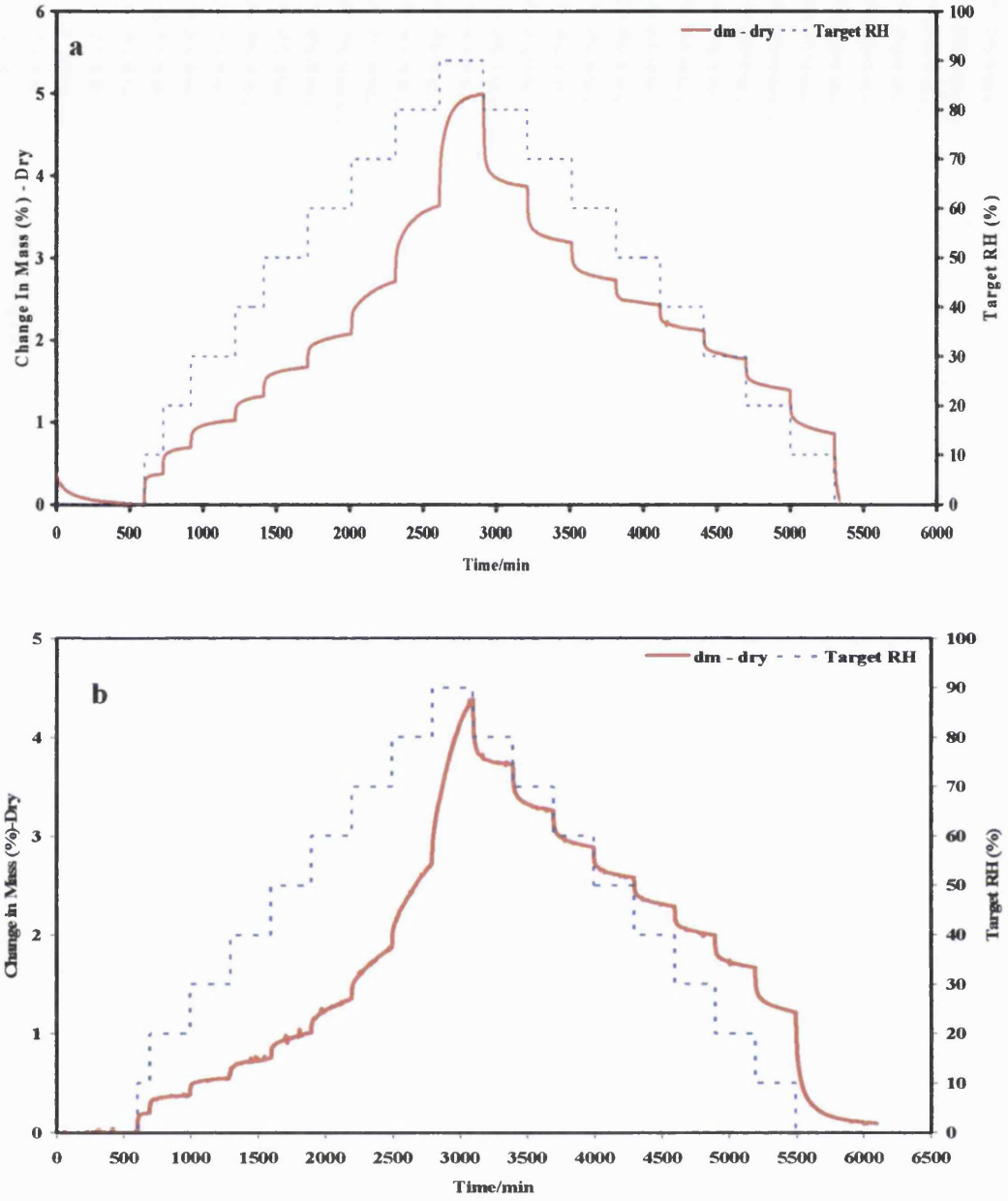

Figure 4.26: *Dynamic vapour sorption traces of the melt quenched solid solutions: a) unaged sample and b) sample aged for 15 days at 50 ℃.*

Figures 4.25 and 4.26 give a clear view of the dynamic vapour sorption traces of the solid solutions. Correlating with the change of mass plot in Figure 4.23, the aged solid solutions show small water sorption but rapid equilibrium from 10% to 30% RH. Above 30%, 300 minutes were not enough for the samples to reach equilibrium state. In the region of 70% to 90% RH, the water sorption rate has significantly increased

compared to the unaged sample. During DVS experiments, instant NIR spectra were obtained to monitor any potential transition which could happen to the samples, but no apparent change in the spectra was found on the samples before and after exposure to different relative humilities. Furthermore, both the aged and unaged samples after DVS experiments were tested by DSC and it was confirmed that they were still in amorphous form.

Studies were taken further to investigate whether the difference in the water sorption behaviours caused by relaxation would reflect on the dissolution profiles of the solid solutions. The fresh and aged solid solutions prepared by ball milling and melt quenching were tested (Figure 4.27).

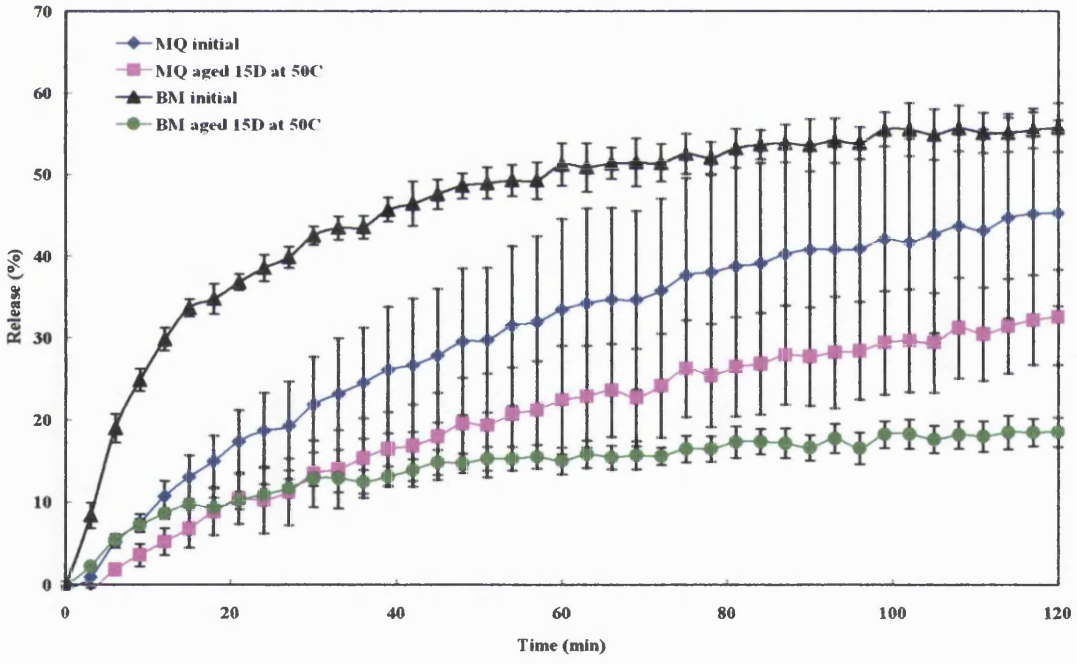

Figure 4.27: *The dissolution profiles of the unaged and aged solid solutions (an indometacin to PVP ratio of 70%:30%) prepared by ball milling and melt quenching (n=3).*

Preparation methods have played an important role on the dissolution profiles of the solid solutions. Though there is no difference in their water sorption behaviours, the

fresh ball milled sample dissolved much faster than the fresh melt quenched one. The ball milled sample showed a rapid release in the initial state followed by a gradual approach to equilibrium and after 2 hours it reached around 56 % of release. In the case of the melt quenching sample, the dissolution rate was much slower and the release profile did not reach equilibrium. Only 45% of indometacin was released after 2 hours, lower than that of the ball milled one. The higher dissolution rate of the ball milled sample was probably because of its rougher surface and smaller particle size and therefore, it would have a higher surface area, i.e. better wettability.

It seems that the solid solution prepared by ball milling was superior to that of the melt quenched one in both the dissolution rate and extent of release. However, the dissolution profile of the ball milled sample was more sensitive to the aging process. As shown in Table 4.8, both t_{20} and t_{120} of the aged ball milled sample dropped in a larger extent compared to the aged melt quenched one. This result correlated well with the DSC relaxation data, in which it was indicated that the melt quenched solid solution relaxed slower than the ball milled one which means a smaller fraction of sample would have relaxed after aging for 15 days, thereby, the change in the dissolution profile would also be milder. In addition, though the aged ball milled sample still showed a faster initial release than the aged melt quenched one, it quickly reached equilibrium after about 30 minutes while the aged melt quenched sample kept on releasing and reached around 33 % in 2 hours. The fast equilibrium in the ball milled sample was probably accounted to the recrystallisation of the amorphous indometacin, because both the relaxation and the physical stability data have proven that the ball milled sample was less stable compared to the melt quenched one.

It is usually considered that the dissolution rate would only be jeopardised if the amorphous content of a product has recrystallised during storage. The studies here have given evidence that relaxation would also affect the dissolution profile of a product even though it is still in amorphous state. Hopefully, this finding would give a better understanding when preparing a stable amorphous formulation.

Sample	t_{20}	t_{120}
Ball milled (unaged)	36%	56%
Ball milled (aged)	10%	19%
Melt quenched (unaged)	17%	45%
Melt quenched (aged)	10%	33%

Table 4.8: *Percentage release of indometacin from the solid solutions (an indometacin to PVP ratio of 70%:30%) at 20 min (t_{20}) and 120 min (t_{120}) (n=3).*

4.5 Conclusion

Decane V_{max} method has been shown to be very useful in detecting surface relaxation and this method was applied to study the surface relaxation of the PVP-indometacin solid solutions prepared by ball milling melt quench and spray drying. The surface relaxation was then compared to the bulk relaxation obtained from the enthalpy relaxation detected by SSDSC and it was found that the surface relaxes faster than the bulk, irrelevant of how the sample was prepared. However, different preparation methods appeared to have a significant impact on the relaxation kinetics irrespective of whether at the surface or in the bulk. If the preparation processes were different, the configuration of the products are frozen into a different initial glassy state, therefore, how the amorphous product deviate from this state would be affected. The β values of the surface and the bulk were very similar for all three solid solutions, which demonstrate a similar distribution of relaxation times between the surface and the bulk. The IMC study further proved the influence of preparation methods on relaxation. The high sensitivity of IMC enables it to measure some faster modes of motion rather than structural relaxation alone, and therefore, difference of relaxation data obtained by SSDSC and IMC were observed.

The glass fragility of the solid solutions was measured using the heating rate dependence of glass transition temperature. According to the fragility parameter, the zero mobility temperature of the samples was obtained. Similarly, preparation methods were shown to be influential to these values. Ball milling generates amorphous forms through solid state while spray drying and melt quenching use a more disorder liquid phase. Hence it was reasonable to observe that the fragility parameter of the ball milled sample was closer to that of the individual indometacin and PVP.

The physical stability data showed good correlation with the bulk relaxation data obtained by SSDSC, which has confirmed the feasibility of predicting the shelf life of products by comparing their molecular mobility. Furthermore, the fragility and zero

mobility temperature were also very useful in predicting the physical stability of an amorphous sample. Though the T_g of the solid solutions were very similar, their T_0 can be very different and the rank order of T_0 matched well with the physical stability data. Therefore, T_0 might act as a better indicator than T_g in predicting the stability of an amorphous sample. All these parameters can provide some guidance when preparing a stable amorphous product.

Physical aging was found to be able to affect the water sorption behaviours of the amorphous solid solutions according to DVS experiment, and as a result their dissolution properties were affected. The aged samples showed a decrease of dissolution rate and the extent of decrease was correlated to the relaxation rate. The ball milled solid solution which relaxed faster than the melt quenched one showed a larger extent of decrease in its dissolution rate. Furthermore, the dissolution property of the solid solutions was found to be dependent on the preparation method.

Chapter 5

Effect of preparation methods and formulations on the dissolution rate and stability of solid dispersion/solutions

5.1 Introduction

In recent years, as high throughput screening is becoming more and more useful, increased amounts of poorly water-soluble drugs have been developed from the discovery pipeline. Therefore, solutions are demanded to solve the low aqueous solubility of these compounds. A commonly used strategy is to turn the drug into the amorphous form to improve its dissolution rate and hence bioavailability. But in many cases, the application of the amorphous form is compromised by its poor physical stability. Some researchers have tried to use additional carriers to form a solid dispersion/solution with the amorphous drug in order to slow down its conversion to the crystalline form for an enhancement in the stability (Boldyrev *et al.*, 1994; Matsumoto and Zografi, 1999; Watanabe *et al.*, 2003). However, when a solid dispersion/solution is made, two questions would arise immediately: what carrier should be used, since there are many available; and which preparation method is more suitable for the drug and carrier combination? In the present study, different types of carriers are used to form solid dispersion/solutions with the model drug indometacin using different preparation methods. The stability and dissolution properties of the products were investigated. Indometacin, being a proton donor with a carboxylic acid group, could interact with many carriers which makes it a very useful model for this study.

The carriers used in this study can be divided into two categories, those which are immiscible with the model drug and those which are miscible. Usually, a carrier which is miscible with a drug is preferred when preparing a solid dispersion/solution because it could help to form a one-phase system. The T_g of the unstable drug could be improved by forming a molecular dispersion with a high T_g carrier. The molecular dispersion of the drug within the carrier matrix is important for separating the drug molecules from each other. However, these factors are not enough to guarantee a stable amorphous formulation if intermolecular interactions are not present. The hypothesis here is trying to show that no matter whether the carrier and drug are miscible or not, strong intermolecular interactions are vital for the physical stability of a solid dispersion/solution.

Sometimes, even though a carrier has been shown to be effective in improving the stability of an amorphous drug, it might not result in a good dissolution profile. A ternary solid dispersion is therefore prepared which contains a carrier capable of strong intermolecular interaction and a carrier capable of rapid wettability, and a good stability and dissolution balance is achieved.

5.2 Chapter outline

The following issues are studied in this chapter: 1) how ball milling parameters could affect the amorphisation rate of crystalline indometacin and its physical stability; 2) the stabilisation and solubilising effects of the carriers on the model drug; 3) the effect of Polyvinylpyrrolidone (PVP) and Hydroxypropyl methylcellulose acetate succinate (HPMCAS) on the improvement of the dissolution rate and stability of indometacin; 4) the effect of different preparative methods on the dissolution and stability properties of the solid dispersion/solution systems; 5) the possibility to prepare a ternary solid dispersion system which could produce a good balance of stability and dissolution properties.

5.3 Methods

5.3.1 Spray drying

A GEA Niro SD MICRO™ was used for spray drying purpose. For indometacin and PVP (25%:75%), 4 g of materials were dissolved into 200 mL of absolute ethanol (a feed concentration of 2%) and for indometacin and HPMCAS (25%:75%), 3 g of materials were dissolved into 200 mL of acetone and water (80%:20%). 30 minutes were allowed for the samples to dissolve completely into the solvents. The solution prepared was then spray dried using the parameters listed as follow:

atomiser gas flow: 2.5 kg/h
chamber inlet flow: 30.0 kg/h
inlet temperature: 80 °C
feeding rate: 20%

Spray dried samples were collected from the collection bottle and cyclone, passed through 500 μm and then stored in a vacuumed desiccator over phosphorus pentoxide (P_2O_5) at room temperature for at least 1 day before further use.

5.3.2 Ball milling

Ball milling was used as described in Section 2.2.2 to prepare different samples required for this study. To prepare solid dispersion/solution samples, Different carriers were milled with crystalline indometacin using a planetary miller (Pulverisette 5-Fritsch). 5 g of powders with a drug to carrier ratio of 75% to 25% were weighed and loaded into a 250 mL ZrO_2 jar. The ZrO_2 balls (Ø=15mm) to sample weight ratio was 16:1 (about 45 milling balls). The powders were milled for 6 hours at a pot rotation speed of 300 rpm. The milled products were passed through a 500 μm sieve in order to break down any lumps. The product prepared was stored in a vacuumed desiccator over P_2O_5 at room temperature before further use.

5.3.3 Thermal gravimetric analysis (TGA)

Thermal gravimetric analysis was performed to study the moisture content of the samples. The operating conditions were described in Section 2.2.9. For each sample, 3 measurements were conducted.

5.3.4 Differential scanning calorimetry (DSC)

Differential scanning calorimetry studies were performed using a Perkin Elmer Pyris 1 DSC to detect any glass transition, crystallisation or melting of indometacin within the samples. Step scan, hyper scan and conventional scan modes were used as described in Section 2.2.6.

5.3.5 X-ray Powder Diffraction (XRPD)

X-ray powder diffractions were performed as described in Section 2.2.7 using a Philip PW3710 X-ray diffractometer. XRPD was applied for characterisation of the amorphous or crystalline samples.

5.3.6 Fourier transform infrared spectroscopy (FTIR)

Fourier transform infrared spectroscopy was used as described in Section 2.2.9 to study the intermolecular interactions between the drug and the carriers.

5.3.7 Scanning electron microscopy (SEM)

Scanning electron microscopy images of the samples were obtained as describe in Section 2.2.9.

5.3.8 Dissolution test

A Pharma Test automatic dissolution apparatus (Pharma Test, Germany) was used. Samples (containing 25 mg of indometacin) were first loaded in size 1 gelatin capsules and then their dissolution profiles were obtained using the modified USP paddle method at a rotation speed of 100 rpm at 37 °C. The paddles were set at 25 mm from the bottom of the vessel. Degassed phosphate buffer (pH of 6.8) was used as dissolution medium

(900 mL for each vessel). UV readings were recorded automatically by a Cecil CE 2020 spectrometric (Cecil Instruments, Cambridge, UK) at intervals of 5 minutes. The wavelength used was at 320 nm. Three capsules were tested for each sample.

5.3.9 Contact angle measurement

Wettability of the samples was studied by measuring their contact angles. All samples were compressed into flat-faced discs (3 discs tested for each sample) using a hydraulic press (5 bars), followed by applying 20 μl of distilled water on their surface. Images were taken at one second after the contact of the droplet and the surface by a digital camera and analysed using ImageJ analysis software.

5.3.10 Physical stability studies of the solid dispersion/solutions

The solid dispersion/solutions were stored at conditions with different temperatures and RH (30 °C 11% RH; 30 °C 75% RH; 40 °C 11% RH and 40 °C 75% RH). The crystallinity of indometacin in the solid dispersion/solutions was tested using X-ray powder diffraction (XRPD) and differential scanning calorimetry (DSC), and the moisture content was measured using thermal gravimetric analysis (TGA) after certain periods of time. RH of 75% and 11% were achieved using saturated NaCl and LiCl solutions respectively.

5.4 Results and discussion

5.4.1 Effect of milling conditions on the amorphisation rate of indometacin

Mixtures of crystalline indometacin and 10% PVP were milled under different conditions in order to investigate how milling parameters could affect the amorphisation rate of indometacin. The reason of adding a small amount of PVP to indometacin was because indometacin on its own recrystallised very quickly during milling. After 15 minutes of milling without any additive, the enthalpy of melting of indometacin decreased slightly and remained on a similar level even though the milling time was prolonged to a longer period. Indometacin was reported to be miscible with PVP at a concentration as low as 5% w/w (Matsumoto and Zografi, 1999). Interactions such as van der Waal's force and hydrogen bonding between indometacin and PVP could help to greatly reduce the mobility of the drug as a result of slowing down the recrystallisation rate.

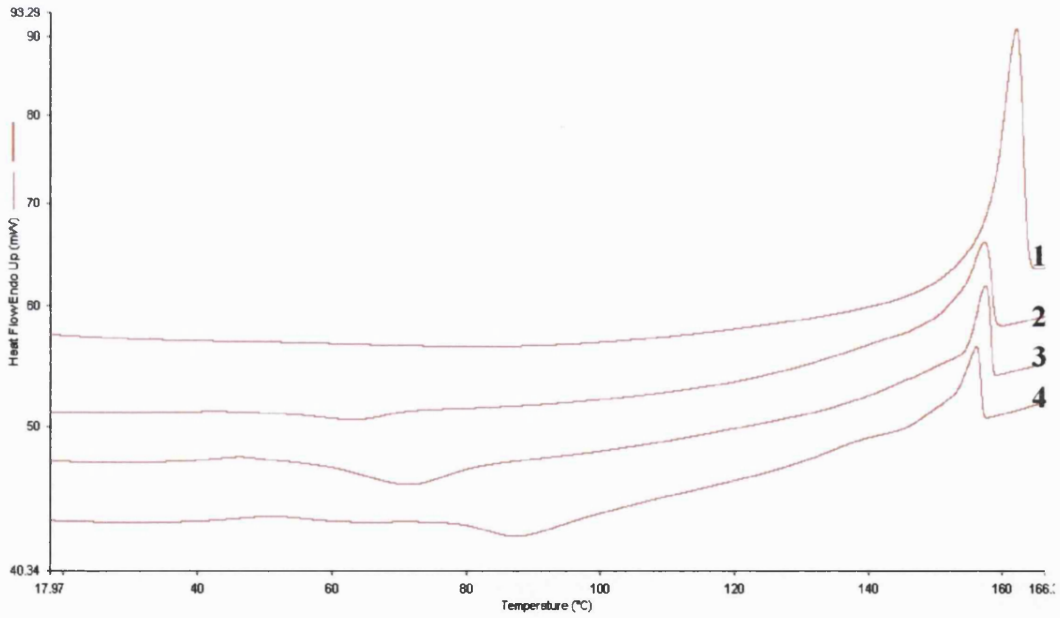

Figure 5.1: *DSC scans of indometacin:PVP (90%:10%) physical mixture (1), the mixture that milled for 1 hour at 200 rpm (2), 2 hours at 200 rpm (3), and 2 hours at 300 rpm (4).*

The amount of the crystalline content in the milling products was determined using

DSC. A comparison of the DSC scans for a physical mixture of PVP-indometacin and the ones milled at different conditions is shown in Figure 5.1. The big endothermic peak at around 157 °C in the physical mixture was related to the melting of crystalline indometacin. In the ball milled products the melting peak decreased indicating a decrease of crystallinity, and also the exothermic peak started to appear at around 40 to 60 °C corresponding to the recrystallisation of the amorphous indometacin. The onset of recrystallisation shifted to a higher temperature as the milling time and the milling rate increased, and this reflected that the amorphous phase produced by ball milling was becoming thermodynamically more stable and the presence of nuclei of crystallisation probably was decreasing.

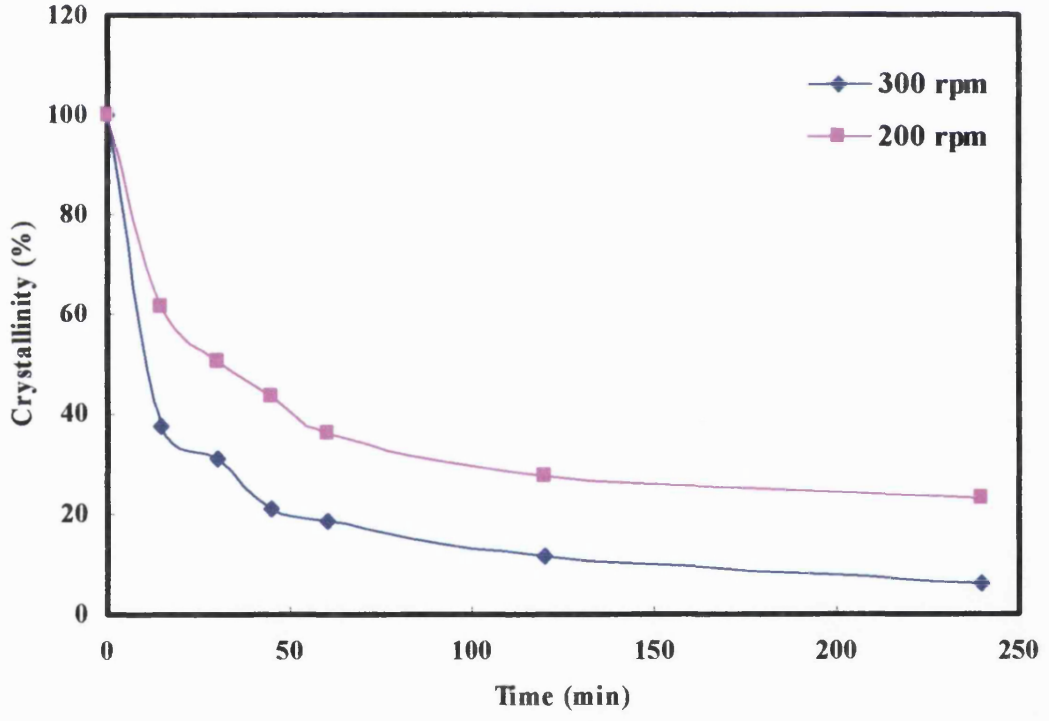

Figure 5.2: *Effect of milling time on the crystalline indometacin content of the ball milled product at two rotation speed: 300 rpm and 200 rpm.*

Figure 5.2 shows the effect of milling time and rotation speed on the amorphisation rate of crystalline indometacin. The crystallinity of the sample decreased as a function of

milling time. The amorphisation rate of milling at 300 rpm appeared to be faster than the one at 200 rpm. Especially in the first 15 minutes, the percentage of crystallinity dropped to around 37% milled at 300 rpm compared to 61% milled at 200 rpm. After continuous milling for one hour, the amorphisation rate at both rotation speeds became significantly slower. The amorphisation effect is determined by the competition between recrystallisation rate of the amorphous phase and the amorphisation rate of ball milling. After progressive milling, mechanical energy from the colliding balls generates defects and destruction of the crystalline phase, but on the other hand, a part of this energy gradually transform into heat which increases the temperature inside the milling pot. Therefore, in the local contact region between the balls and the sample, temperature may increase to a level which could cause the amorphous phase start to crystallise. Also after continuously receiving large amounts of energy, molecular mobility of the amorphous phase would increase and recrystallisation could happen much easier. Consequently ball milling is more efficient at making material amorphous in the early stage but as milling time increases, the rate of conversion to amorphous state tends to equal the recrystallisation rate.

A clearer comparison of the milling rotation speed on the amorphisation effect of the sample is shown in Figure 5.3. The milling duration was fixed at 2 hours and as the rotation speed increased the crystallinity of the sample dropped down. However, the efficiency of amorphisation decreased as the rotation speed increased. By increasing the speed from 100 rpm to 200 rpm, the crystallinity dropped from 90% to around 27%, but when it was increased further to 350 rpm, the decrease of crystallinity became milder. Ksiazek *et al.* (2007) studied the amorphisation rate of selenium in relation with different milling conditions, and found that the crystallinity level reached a plateau when the rotation speed increased to a certain point. A faster rotation speed might increase the temperature further in the pot and adversely compromise the amorphisation effect. These sets of studies provide some guidance in deciding the milling conditions for preparing solid dispersion/solutions in the later sections. It is not always favourable to mill something longer or more intensively. A suitable condition should be carefully

decided in order to reach the maximum efficiency.

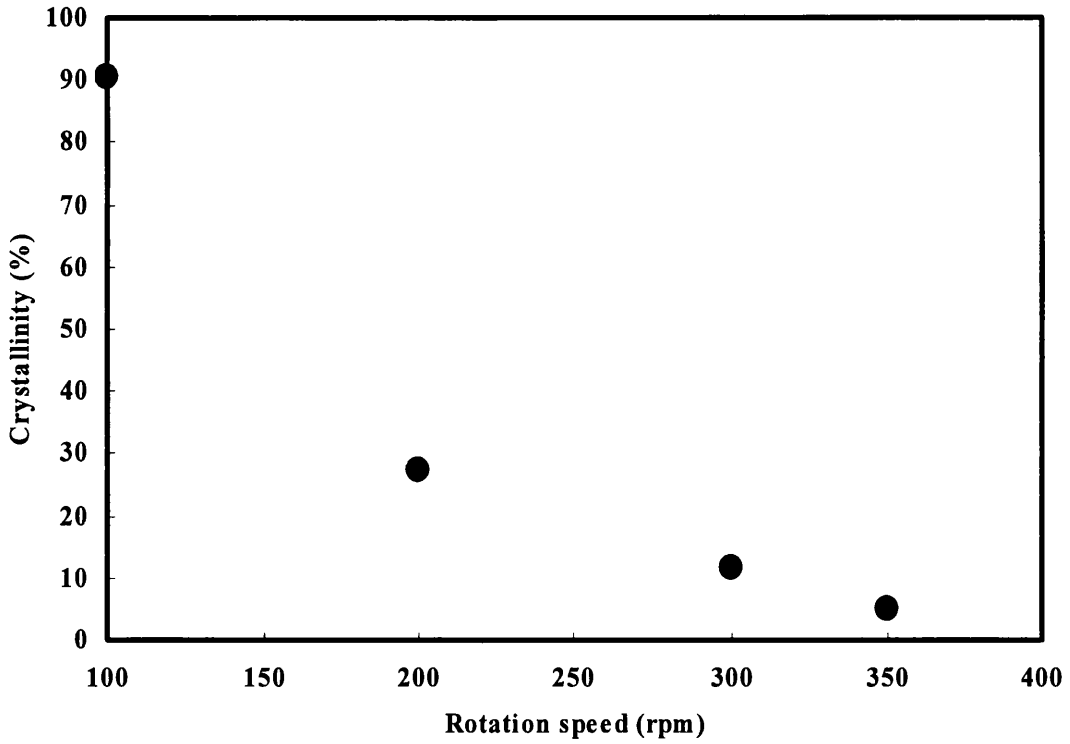

Figure 5.3: *Effect of rotation speed on the crystalline indometacin content of the ball milled product. Milling duration was fixed at 2 hours.*

5.4.2 Carriers which are immiscible with the model drug

5.4.2.1 Physical properties of the solid dispersions

In this section, Neusilin and cellulose derivatives microcrystalline cellulose (MCC) and silicified microcrystalline cellulose (SMCC) were milled with indometacin (the drug and carrier ratio was 25% to 75%), a hydrophobic drug which would recrystallise from its amorphous form easily when milled on its own. MCC is widely used as a filler and binder and it was rated as the most useful filler for direct compression tabletting by Shangraw and Demarest (1993). However, it has some limitations such as low bulk density, high lubricant sensitivity, poor flow characteristics and the influence of moisture on the compression characteristics (Bolhuis and Chowhan, 1996). To address these problems, SMCC was developed by a process of 'silicification' which leads to the deposition of SiO_2 on the surface of the particles. Though it was proven that the

fundamental chemical properties of SMCC are very similar to that of its parental material (Tobyn *et al.*, 1998; Buckton *et al.*, 1999), SMCC was found to have many advantages over MCC (Sherwood *et al.*, 1996; Khalaf *et al.*, 1997). Our focus in the study was this extra compound on the surface of the carriers. The hydrogen-bonding potential of silanols on silica surfaces has been found to be able to improve the physical stability of some amorphous compounds (Chuang and Maciel, 1996, 1997; Watanabe *et al.*, 2001). The question is whether this silica on the surface of SMCC could help to stabilise indometacin in its amorphous form and produce better dissolution properties? Therefore, carriers with different amounts of silica: MCC (0%) and SMCC (2%, 5% and 10%) were milled with indometacin in order to study the effect of different amounts of silica on the physical and dissolution properties of indometacin. In addition, as a comparison, indometacin was also milled with Neusilin, a compound that contains 29.2%-35.5% of silica on the surface.

Surface morphology of the pure materials was characterised using scanning electron microscopy (SEM) as shown in Figure 5.4. Pure indometacin appeared as long polyhedral particles with sharp edges and smooth surfaces. Neusilin particles were spheroid in form with a rougher surface. Neusilin was reported to consist of amorphous microporous granules of magnesium alumina silicate with a specific surface area of ~300 m^2/g (Gupta *et al.*, 2003). The images of SMCC containing 2% of silica and MCC showed similar shape, but a close up of the surface of SMCC appeared rougher than that of MCC, presumably, as noted by Tobyn *et al.* (1998): it is due to the silica on the surface. This 2% of silica was able to increase the specific surface area of SMCC fivefold as compared to MCC (Muzikova and Novakova, 2007). The images of SMCC containing 5% and 10% silica did not show any significant difference to the one containing 2% of silica.

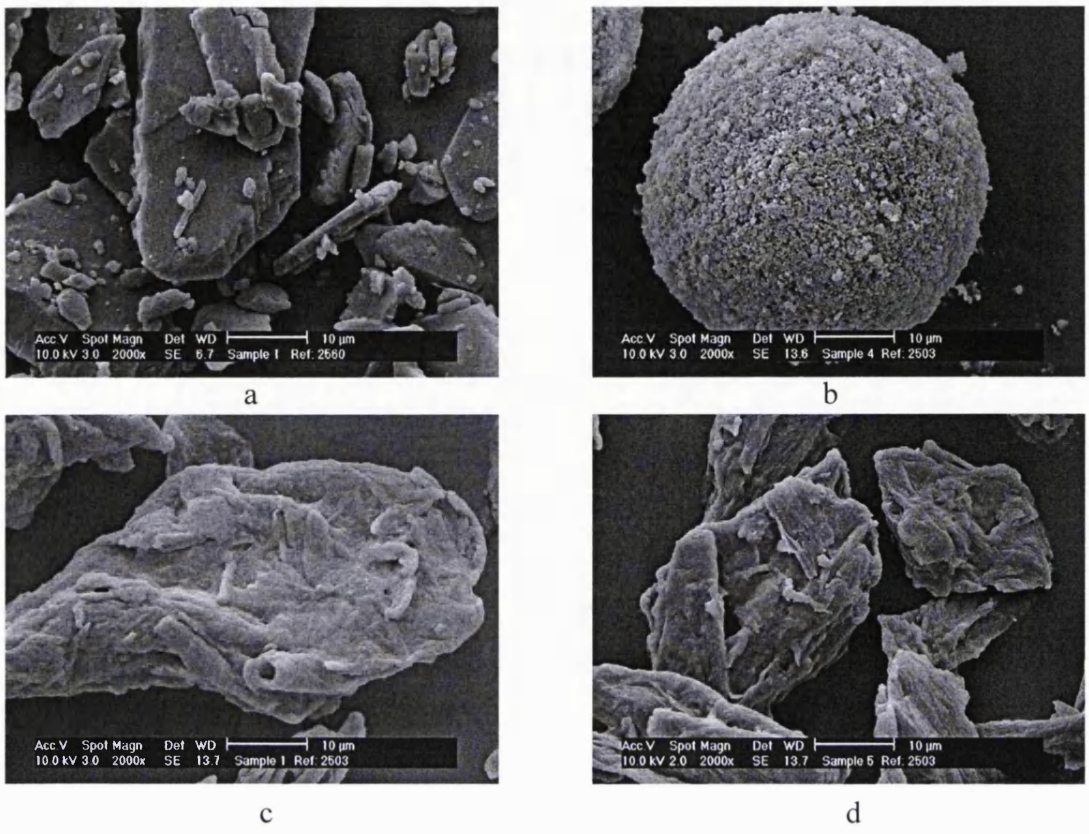

Figure 5.4: *SEM images of a) crystalline indometacin; b) pure Neusilin; c) pure SMCC 2%; and d) pure MCC.*

Indometacin was then milled with the carriers. At intervals of 5, 15, 30, 60, 120, 240 and 360 minutes, samples were withdrawn and characterised using XRPD in order to investigate the extent of amorphisation of indometacin (XRPD patterns are shown in Figure 5.5).

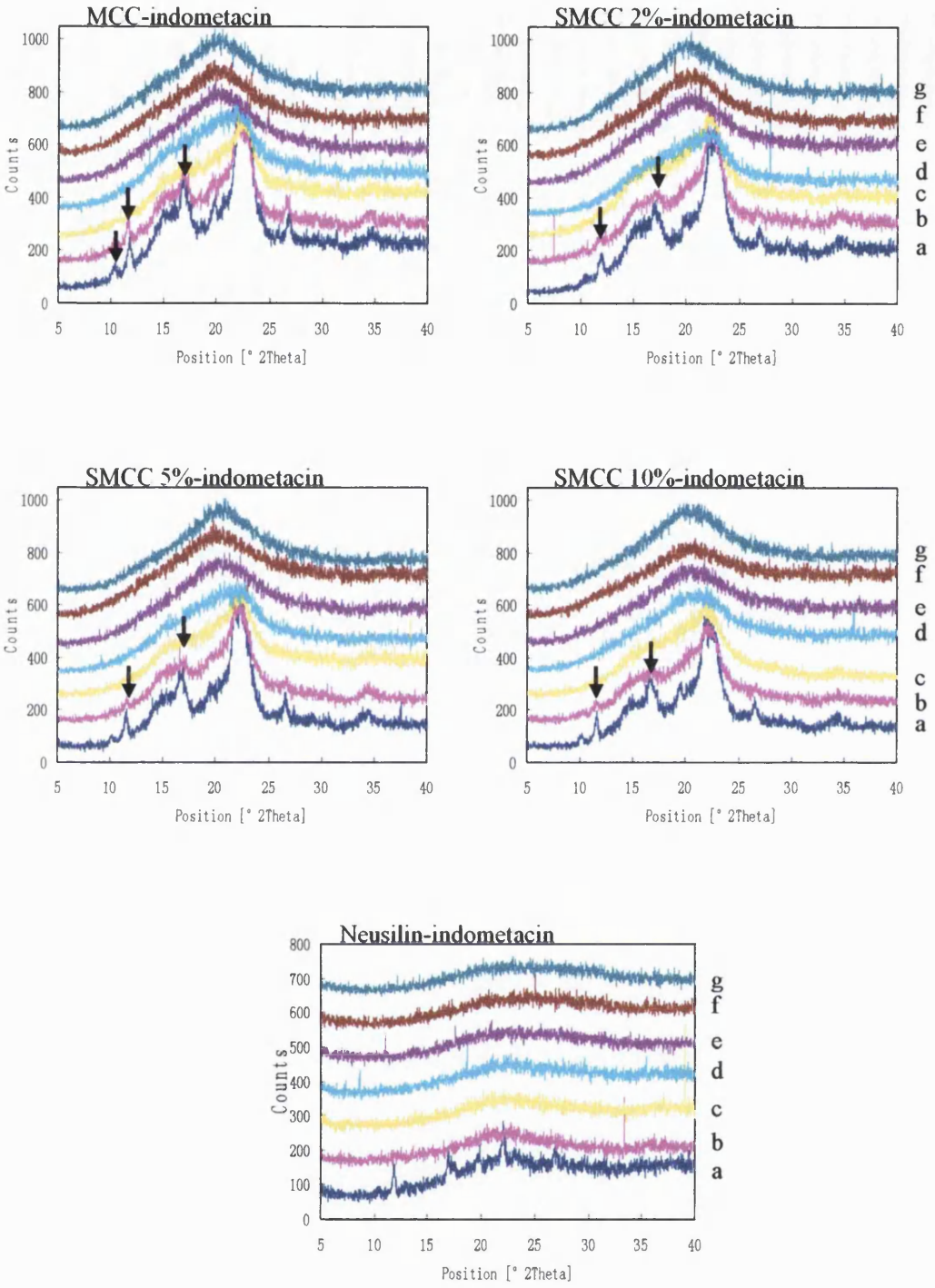

Figure 5.5: *XRPD patterns of indometacin milled with different carriers (durg:carrier, 25%:75%) for 5 (a), 15 (b), 30 (c), 60 (d), 120 (e), 240 (f), and 360 (g) minutes.*

Indometacin appeared amorphous by XRPD after milling with all the carriers, but a difference in the amorphisation rate was noticed. After milling together with Neusilin, which has the highest amount of silica at the surface for only 15 minutes, indometacin

became XRPD amorphous, indicating a strong interaction between the drug and the carrier. SMCC showed a slightly faster amorphisation rate of indometacin than that of MCC. As shown by the arrows in Figure 5.5, the intensity of the peaks belonging to crystalline indometacin decreased to a larger extent when milled with SMCC after 15 minutes than milled with MCC. Considering that the only difference between SMCC and MCC is the silica, this extra compound at the surface of SMCC might help to increase the interaction between the carriers and indometacin. However, among the three types of SMCC containing different amount of silica, no significant difference on the amorphisation rate was observed.

It is interesting to point out that as well as the influence of the carriers, the melting temperature of the compounds could also affect its rate of conversion to amorphous state. In a previous study, Gupta *et al.* (2003) tried to turn four different drugs into amorphous by milling them with Neusilin, and it was found that the amorphisation time related to the melting temperature of the drug. A higher melting temperature might require a higher energy to demolish the crystal lattice structure.

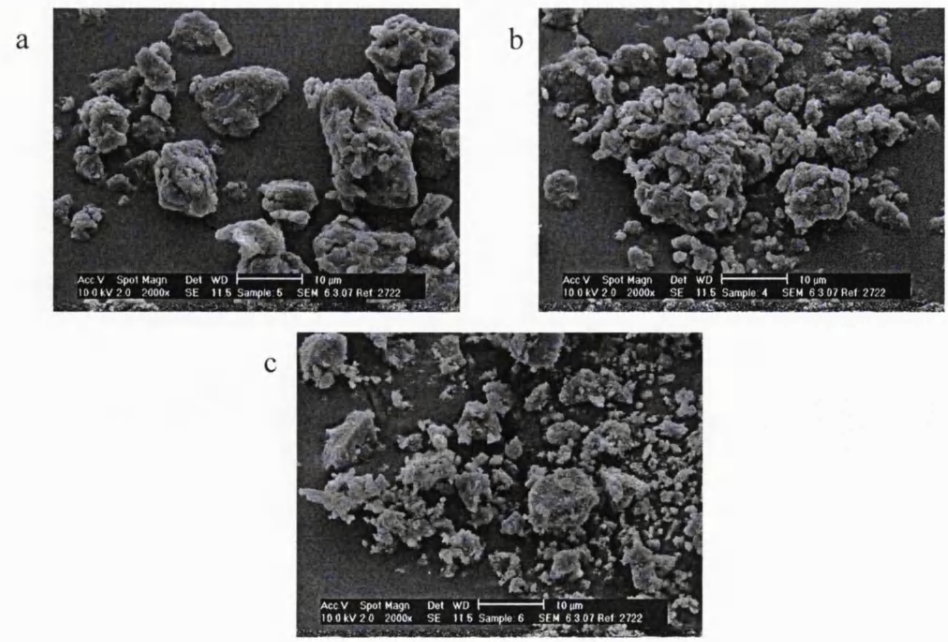

Figure 5.6: *SEM images of indometacin milled with a) MCC, b) SMCC, and c) Neusilin for 6 hours with a drug to carrier ratio of 25%:75%.*

The SEM images of the solid dispersions are shown in Figure 5.6. Post milling, the particle size of all samples decreased. Indometacin-Neusilin particles had the smallest particle size (less than 5 μm). The solid dispersions containing SMCC and MCC also decreased to a size of ca. 15 μm. The particle size reduction was due to the impact force received during ball milling. Moreover, in the SEM images, there is no sign of any crystalline structures, indicating the crystalline indometacin has been broken down by milling.

Step-scan DSC studies were conducted to investigate the glass transition temperature or any possible fusion of melting of the solid dispersions. It is noticed that all indometacin solid dispersions containing SMCC or MCC showed a small endothermic peak at around 150 °C, which is the melting point of indometacin. However, prior to the endotherm, a broad and shallow exothermic peak could be seen between 95 to 140 °C. Considered the slow heating rate and constant isothermal holding within a step scan, this endotherm was very likely caused by the recrystallisation of amorphous indometacin. It was unclear whether the melting of indometacin was coming from the initial solid dispersions or recrystallisation during the step scan. Therefore, conventional DSC and Hyper-DSC scans were conducted to clarify this question. The high heating rate of Hyper-DSC has been claimed to be able to minimise any undesired phase transition during a DSC scan and also it enables a higher sensitivity for detecting small thermal events (McGregor *et al.*, 2004; Saunders *et al.*, 2004). No melting of indometacin was detected in either type of DSC scans confirming the amorphous state of indometacin. SSDSC, conventional DSC and Hyper-DSC scans of Neusilin solid dispersions did not show any sign of melting which indicated that the solid dispersions were amorphous. The recrystallisation of indometacin in the SMCC or MCC solid dispersions during the SSDSC experiment might indicate a less extent of interaction between the drug and carriers compared to that of the Neusilin.

The glass transition temperatures of the solid dispersions are listed in Table 5.1. SMCC-indometacin and MCC-indometacin systems have a similar T_g in the range

between 46 to 49 °C which was slightly higher than that of the amorphous indometacin (42 °C). Therefore, it was expected that a certain level of interaction between the drug and the carriers existed which helped to raise the T_g. The T_g of the Neusilin-indometacin solid dispersion was not detected and the exact reason is unknown. The moisture levels of the solid dispersions were tested by TGA (Table 5.1). Neusilin-indometacin tended to absorb the most moisture probably due to its high porosity and high specific surface area. Both the SMCC and MCC systems showed similar moisture levels. A previous study has shown that SMCC and MCC have similar porosity regardless of the silica content (Tobyn *et al.*, 1998), and in two other studies, dynamic vapour sorption measurements on pure SMCC and MCC indicated similar hygroscopicity (Buckton *et al.*, 1999; Aljaberi *et al.*, 2009). Therefore, it is reasonable for the SMCC and MCC systems here to sorb similar amount of moisture.

Sample ID	T_g (°C, onset)	Moisture content (% w/w)
Neusilin-indometacin	N/A	5.10
MCC-indometacin	48	4.27
SMCC 2%-indometacin	49	3.77
SMCC 5%-indometacin	49	4.36
SMCC 10%-indometacin	46	4.01

Table 5.1: *Glass transition temperature and moisture content of the solid dispersions of indometacin and Neusilin, SMCC (contain different amount of silica) or MCC.*

As discussed in the Introduction Chapter, the term solid dispersion is generally used to describe a matrix formed by two solids, in many cases, a hydrophobic drug and a hydrophilic carrier. Depending on the physical status of these two components, such as crystalline or amorphous, a solid dispersion can be divided into many subtypes. But in general, amorphous systems can be defined as solid dispersions or solid solutions.

Though it could be used for a wider meaning, solid dispersion here is used to particularly represent a system where amorphous drug is dispersed in the carrier matrix, but the drug and the carrier are immiscible. In this case, the solid dispersion means the formation of a two-phase system. Meanwhile, solid solution indicates that the amorphous drug is miscible with the carrier and they are molecularly dispersed into each other forming a one phase system. The solubility parameter (δ) can be used as a powerful tool to compare the miscibility between two solids. Compounds with similar solubility parameter values are easy to mix because of the energy of mixing released by intramolecular interactions is equaled by the energy released by intermolecular interactions (Greenhalgh *et al.*, 1999). Greenhalgh *et al.* (1999) also demonstrated that compounds with a $\Delta\delta$ less than 7.0 $MPa^{1/2}$ are likely to be miscible, while if the $\Delta\delta$ is more than 10 $MPa^{1/2}$, the compounds are likely to be immiscible. Table 5.2 has shown that both MCC and silica have a $\Delta\delta$ value of more than 10 $MPa^{1/2}$ with indometacin. Therefore, indometacin is not miscible with either MCC or SMCC.

Material	V (cm^3/mol)	δ_t	δ_d	δ_p	δ_h	Method/Reference
Indometacin	229.8[a]	25.9	23.4	6.0	9.4	VH[b]/this study
Indometacin	275.0[c]	23.6	20.9	6.5	8.8	MMP[d]/Dwan'Isa *et al.* (2005)
MCC	216.0	39.3	19.4	12.7	31.3	IGC/Huu-Phuoc *et al.* (1987)
Silica	26.1	35.3	12.2	N/A	N/A	IGC/Rowe (1988)

Table 5.2: *Hansan solubility parameters of indometacin, MCC and silica. a) The molar volume was obtained according to Fedors' method (Fedors, 1974), b) The calculation of the partial solubility parameter was based on (VH) van Krevelen and Hoftyzer's method (van Krevelen and Hoftyzer, 1976); c) The molar volume was calculated by molecular weight/true density; and d) Molecular Modeling Pro (MMP) software (Chem SW Inc., Fairfield, CA).*

SMCC and MCC in their pure forms are mainly crystalline and their percentage crystallinities are shown in Table 5.3. In the DSC scans, SMCC and MCC would tend to degrade before any melting peak starts to appear; therefore, it is difficult to confirm the solid properties of these carriers in the solid dispersions using DSC. Polar light microscopy was used here to confirm the amorphous state of the carriers and it was found that after intensive milling together with indometacin, a small amount of crystalline SMCC or MCC content still existed. Therefore, the indometacin-MCC and indometacin-SMCC systems should be characterised as solid dispersions which have two phases. For a solid dispersion, its physical stability relies on immobilisation and isolation of the labile amorphous drug in the carrier matrix. Therefore, interactions between the drug and the carrier would be critical for an improved stability of solid dispersion. Strong interactions could help to immobilise the amorphous drug molecules and prevent them getting back together to form nuclei sites. The interaction between indometacin and MCC, SMCC or Neusilin and the physical stabilities of these solid dispersions will be discussed in the next section.

Sample	% Crystallinity
MCC	86
SMCC	85
MCC+silica (Dry mix)	85
MCC+silica (Wet mix)	86

Table 5.3: *Percentage crystallinities of SMCC, MCC and MCC-silica mixtures (adapted from Tobyn et al., 1998).*

5.4.2.2 Drug-carrier interaction determined by FTIR

Interactions between the carriers and indometacin were studied using Fourier transform infrared (FTIR). Indometacin is a non-steroidal anti-inflammatory drug which has a carboxylic group and a benzoyl carbonyl group. These two groups were the major focus

in this section of the work. Like many carboxylic acid containing drugs, crystalline indometacin exhibited a dimer peak at 1715 cm^{-1} and a benzoyl carbonyl peak at 1690 cm^{-1}. When it was melt quenched (made amorphous), the acid dimer and benzoyl carbonyl peaks shifted to 1708 and 1682 cm^{-1} respectively, in addition, a third peak which was related to the free acid carbonyl appeared at 1735 cm^{-1} (Figure 5.7). A blue shift (shift to a larger wavenumber) was noticed when indometacin transferred from amorphous to the crystalline state which indicated that hydrogen bond was not preferred during crystallisation.

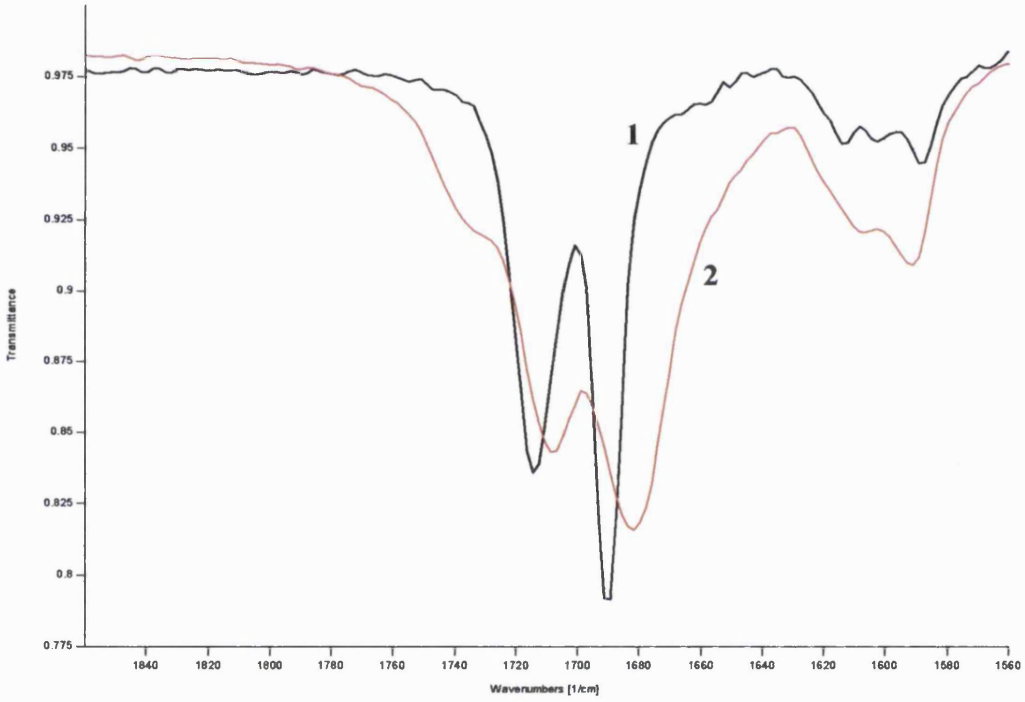

Figure 5.7: *FTIR spectra of (1) crystalline and (2) amorphous indometacin.*

The FTIR spectra of pure MCC and SMCC, their physical mixtures with indometacin and solid dispersions are shown in Figure 5.8. The small peaks of SMCC and MCC at 1635 cm^{-1} are related to the O-H symmetric stretching, but they would not interfere with the interpretation of the characteristic peaks of indometacin. Other characteristic peaks of SMCC and MCC were at 2900 cm^{-1} related to C-H symmetric stretching, and bands between 1000-1200 cm^{-1} related to C-C and C-O stretching. Silica has a strong peak at

1070 cm^{-1} but no difference was found in this region between SMCC and MCC. Tobyn *et al.* (1998) have compared the FTIR spectra of SMCC, MCC and MCC with silica physical mixtures, and no evidence of spectral difference in their characteristic regions was found, which means that the silification process did not cause any change on the spectra of MCC.

The physical mixtures of indometacin and SMCC/MCC were similar to each other and the characteristic peaks of indometacin did not change indicating an absence of interaction between the drug and carriers. After milling with SMCC to form solid dispersions, the dimer peak of indometacin was greatly reduced and shifted to 1709 cm^{-1} indicating the disruption of intermolecular interaction associated with crystalline indometacin. Meanwhile, the carbonyl peak became broader and shifted to 1682 cm^{-1}, indicating increasing amorphisation of indometacin. The melt quenched indometacin has a characteristic peak at 1735 cm^{-1} which relates to its free acid carbonyl peak. The spectra of indometacin-SMCC solid dispersions show that this peak has disappeared, which indicates there was a certain level of interaction between the drug and the carriers. However, the dimer peak of indometacin was still shown, which meant that there was some indometacin that was not interacting with SMCC. The solid dispersions of SMCC and MCC with different grades of silica on the surface did not show any difference in their FTIR spectra; therefore, it seems that silica did not play a significant impact on the interaction between indometacin and the carriers.

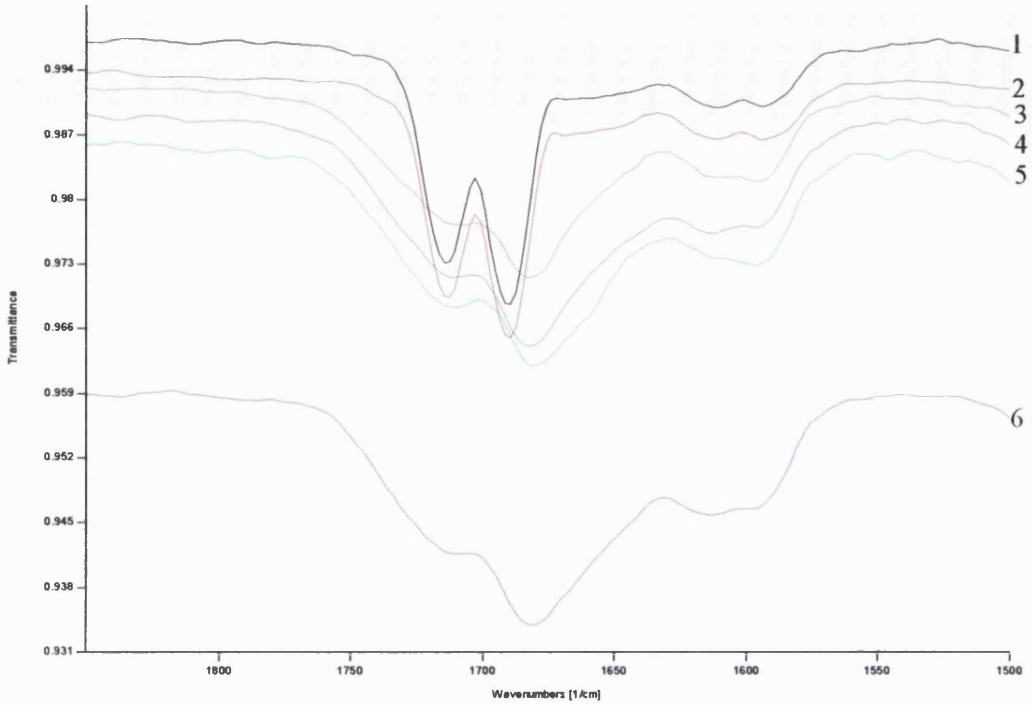

Figure 5.8: *FTIR spectra of physical mixtures of 1) MCC-indometacin, 2) SMCC 2%-indometacin, and solid dispersions of 3) MCC-indometacin, 4) SMCC 2%-indometacin, 5) SMCC 5%-indometacin and 6) SMCC 10%-indometacin.*

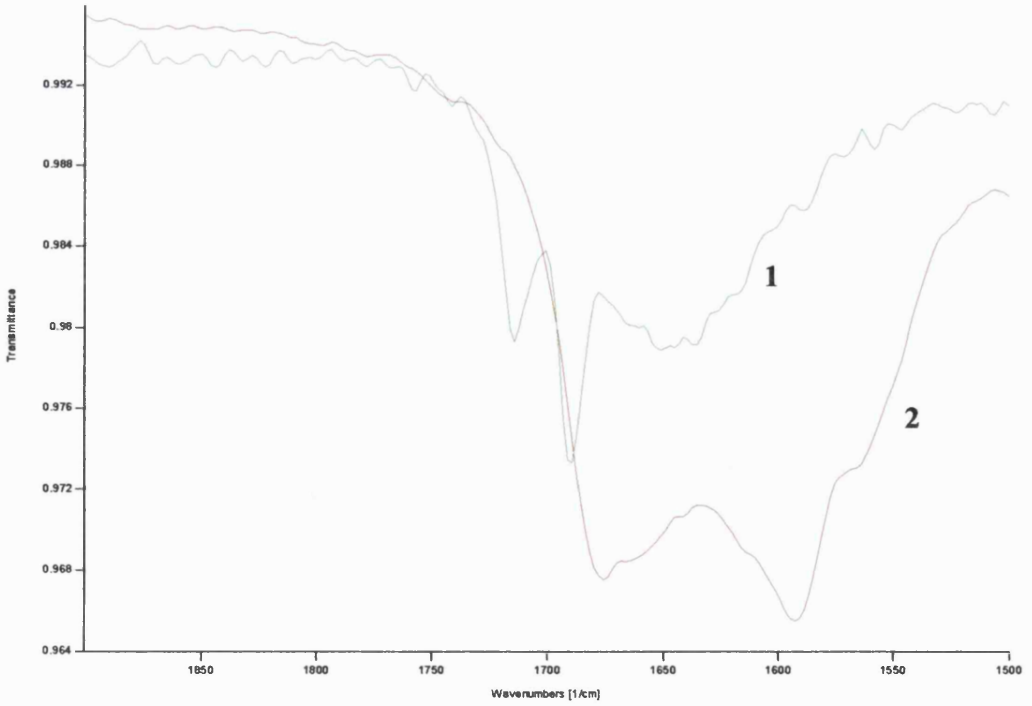

Figure 5.9: *FTIR spectra of Neusilin-indometacin physical mixture (1) and solid dispersion (2).*

Figure 5.9 shows the FTIR spectra of Neusilin-indometacin physical mixture and solid dispersion. After milling for 6 hours, the dimer peak of crystalline indometacin at 1715 cm^{-1} and the free acid carbonyl of amorphous indometacin disappeared completely. The planetary ball milling technique seems to be very efficient in facilitating strong interaction between the drug and the carrier in the solid state even after a few hours of milling. In fact this technique has been widely used in chemistry studies to cause mechanochemical phenomena (Lin and Nadiv, 1979; Jiang *et al.*, 1998) and mechanical alloying (McCormick, 1995) on a ground product because of the high energy generated during milling.

Watanabe *et al.* (2002) have found that due to the similar pKa value between silica and indometacin, the silanol group from silica may act as a Bronsted acid or a Bronsted base to form acid-base interaction between indometacin. Though Neusilin was reported to be neutral in water with a pH of 7.4, Gupta *et al.* (2003) found that the titration curves of Neusilin were more characteristic of a universal buffer and the OH groups associated with Si, Mg and Al in Neusilin could be amophoteric. Therefore, Neusilin was able to form an acid-base interaction with the acidic indometacin. Kararli *et al.* (1989) have reported the formation of the magnesium salt of ibuprofen with MgO; their FTIR data showed a reduction of the carbonyl peak intensity of ibuprofen at 1700 cm^{-1} and the appearance of a new carboxylate peak at 1590 cm^{-1}. Similarly, the FTIR data here for indometacin-Neusilin show the appearance of a carboxylate peak at around 1592 cm^{-1}, indicating a salt formation between them. These results compare favorably with the work of Gupta *et al.* (2003), who investigated the possibility of an acid-base interaction between different carboxylic acid containing drugs and Neusilin. The silanol groups in Neusilin might also be able to interact with proton-donating and proton accepting drugs through hydrogen bonding.

The silica compositions in Neusilin and SMCC are 29.2-35.6%, 2%-10% respectively, and zero for MCC. It appears that the high silica content, Mg^{2+} and Al^{3+} are responsible for the strong interaction to the carboxylic group of indometacin. Watanabe *et al.* (2001)

reported that though in the ratio of 1:1, the percentage of silica which reacted with amorphous indometacin was not more than 4% after milling for 180 minutes according to the T_g increment of indometacin and calculation using the Gordan-Taylor equation (Gordon and Taylor, 1952). Though SMCC has a maximum 10% of silica on the surface, it might still be not enough for any apparent interaction with indometacin to occur. Therefore, higher silica content of SMCC probably as much as that of Neusilin might be needed in order to result in any difference compared to MCC.

5.4.2.3 Physical stability studies of the solid dispersions

5.4.2.3.1 Effect of silica content on the physical stability

As already discussed in the previous section, Neusilin, SMCC and MCC have different amount of silica ranging from c.a. 0% to 30% and Neusilin with the highest amount of silica showed a strong interaction with indometacin compared to SMCC and MCC in the FTIR study. It would be interesting to investigate whether the different amounts of silica could result in a different physical stability. Therefore, the solid dispersions of indometacin and Neusilin, SMCC, and MCC were kept at 30 °C, 11% RH and 40 °C, 75% RH for different periods of time and then samples were taken out for XRPD test to evaluate their physical stability.

Andronis *et al.* (1997) have studied the effects of sorbed water on the crystallisation of indometacin from the amorphous state at 30 °C. It was found that at this particular temperature, when the RH is below 43%, only the stable γ crystal form appears, whereas at higher RH, only the metastable α crystal form appears. The crystallisation mechanism of the γ form changed from surface-initiated to bulk-initiated crystallisation at 21% RH, and the crystallisation rates of the γ form were higher when crystallisation was surface-initiated. It was also found by Andronis *et al.* (1997) that amorphous indometacin stored in 11% RH gave the fastest crystallisation rate of the γ form. Hence the storage condition of 30 °C, 11% RH was chosen here as one of the storage conditions. Melt quenched indometacin without any additive recrystallised in 2 days after storing at 30 °C, 11% RH (Figure 5.10). Two major characteristic peaks which are

corresponding to γ-indometacin (11.5° and 21.8°) could be observed indicating a certain amount of amorphous indometacin had crystallised. After compounding with the carriers, it remained amorphous for at least 6 months. A halo was still be seen on the XRPD diffraction patterns of the solid dispersions (Figure 5.11).

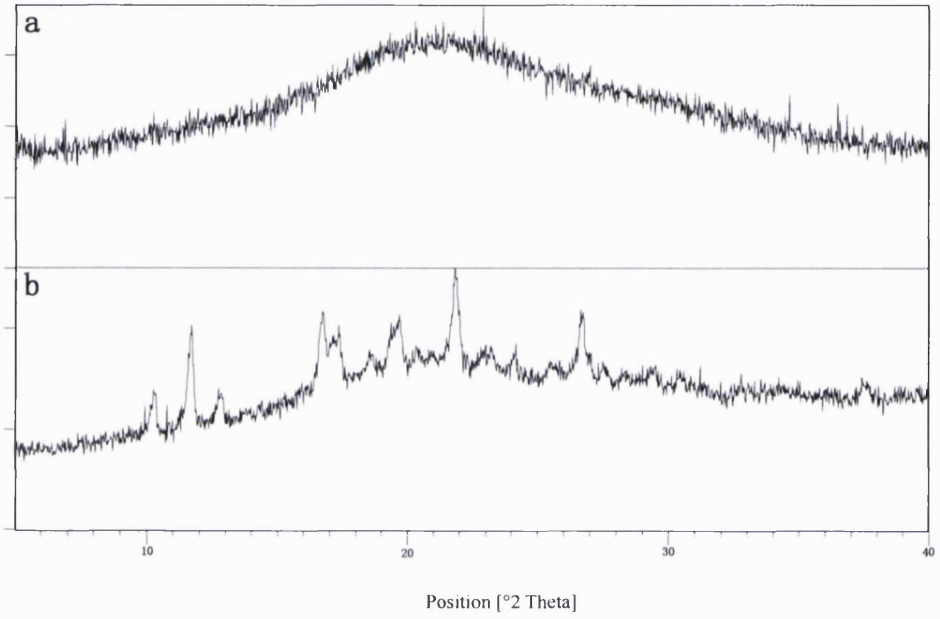

Figure 5.10: *XRPD of a) melt-quenched indometacin and b) melt-quenched indometacin, stored for 2 days at 30 °C 11% RH.*

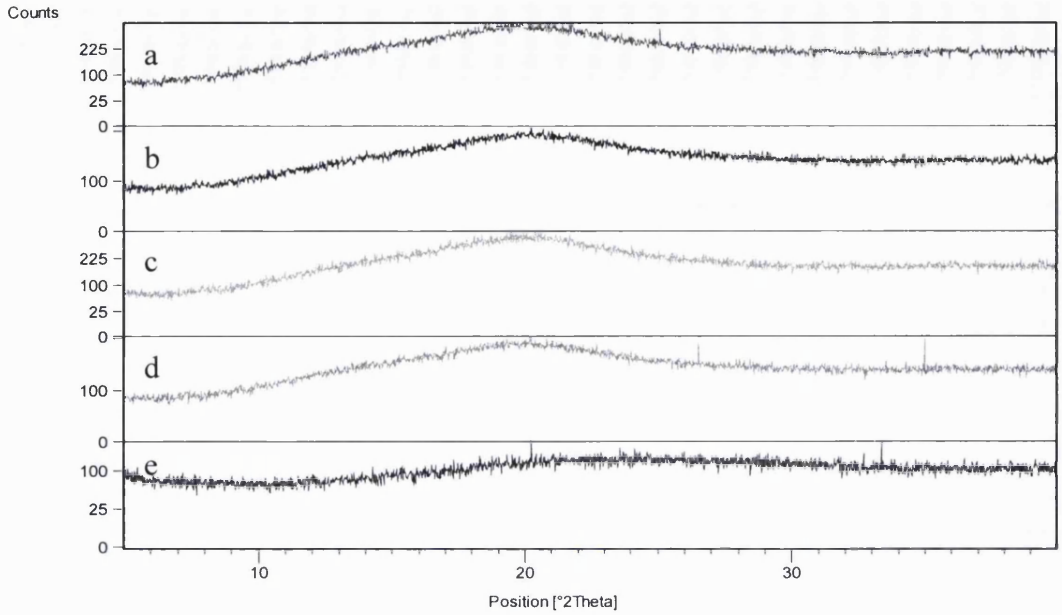

Figure 5.11: *XRPD of solid dispersions of indometacin with MCC (a), SMCC 2% (b), SMCC 5% (c), SMCC 10% (d) or Neusilin (e) after storage at 30 °C 11% RH for 6 months (a drug to carrier ratio of 25%:75%).*

The indometacin solid dispersions were also stored at 40 °C, 75% RH, a commonly used condition for physical stability studies, and the drug showed different recrystallisation tendencies. SMCC and MCC containing solid dispersions recrystallised after two weeks while Neusilin-indometacin system stayed amorphous for more than 6 months. The higher stability of Neusilin-indometacin can be attributed to the better hydrogen bonding ability between the silanol groups of Neusilin and the carboxylic group of indometacin. Meanwhile, the salt formation between the indometacin carboxylic group and Mg^{2+} and Al^{3+} of Neusilin might also be responsible for enhancing stability. The equivalent stability of SMCC-indometacin and MCC-indometacin solid dispersions indicated that the different amount of silica on the surface of SMCC did not give a substantial impact on retarding the recrystallisation of indometacin to SMCC.

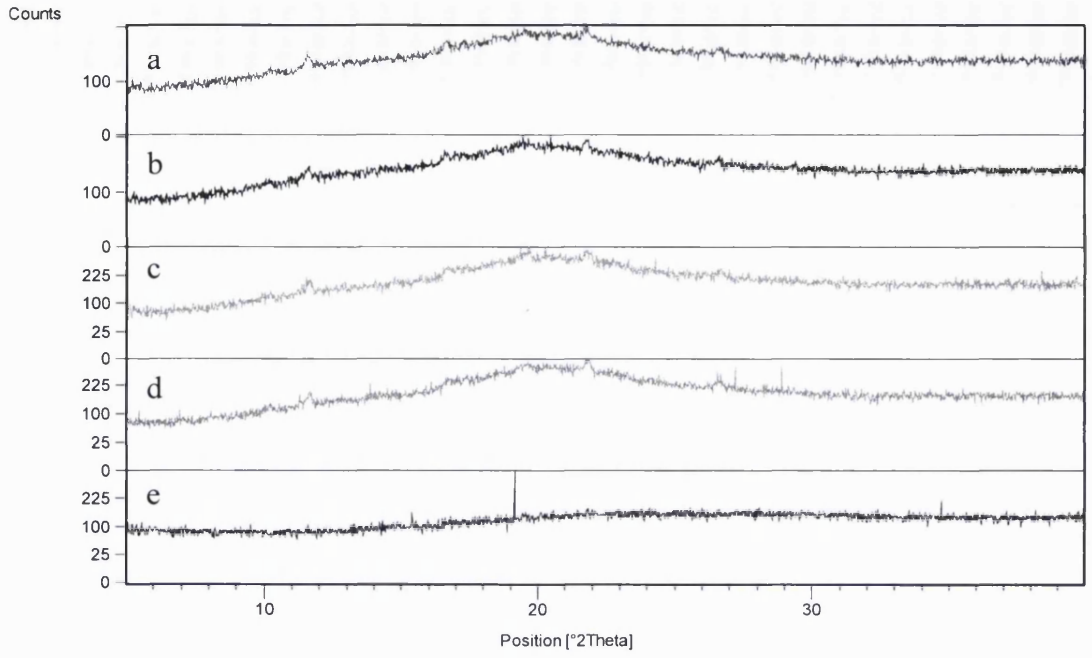

Figure 5.12: *XRPD of solid dispersions of indometacin with MCC (a), SMCC 2% (b), SMCC 5% (c), SMCC 10% (d) or Neusilin (e) after storage at 40 ºC 75% RH (a drug to carrier ratio of 25%:75%).*

The molecular arrangement in an amorphous solid is not totally random, as in the gas phase, but features short-range molecular order similar to that in a crystalline solid. However, unlike crystals, an amorphous solid lacks the long-range order of molecular packing (Yu, 2001). Hence it is easy to understand that an amorphous solid will be in a higher energy state and has a higher mobility. This force will drive the solid to recrystallise in order to become more stable. At a high relative humidity and high temperature storage condition, water will act as a plasticiser together with heat received from high temperature to largely enhance the mobility of an amorphous material. This is the reason why melt quenched indometacin became crystalline again in a very short period time. In the milled samples, because of van der Waal's force, hydrogen bonding, and acid-base interactions between the drug and the carriers, the mobility of the drug is greatly reduced as a result of retarding its recrystallisation rate and enhancing its kinetic

stability.

5.4.2.3.2 Effect of milling duration on the physical stability

It has been shown that a longer milling time could render a higher level of amorphous content. Therefore, indometacin was milled with SMCC (2%) in a drug to carrier ratio of 25%:75% for 2, 4, 6 and 24 hours and then placed at 30 °C 11% RH to investigate the effect of milling duration on the physical stability of the solid dispersions. A different milling ball to sample weight ratio was used here (5:1, approximately 15 balls).

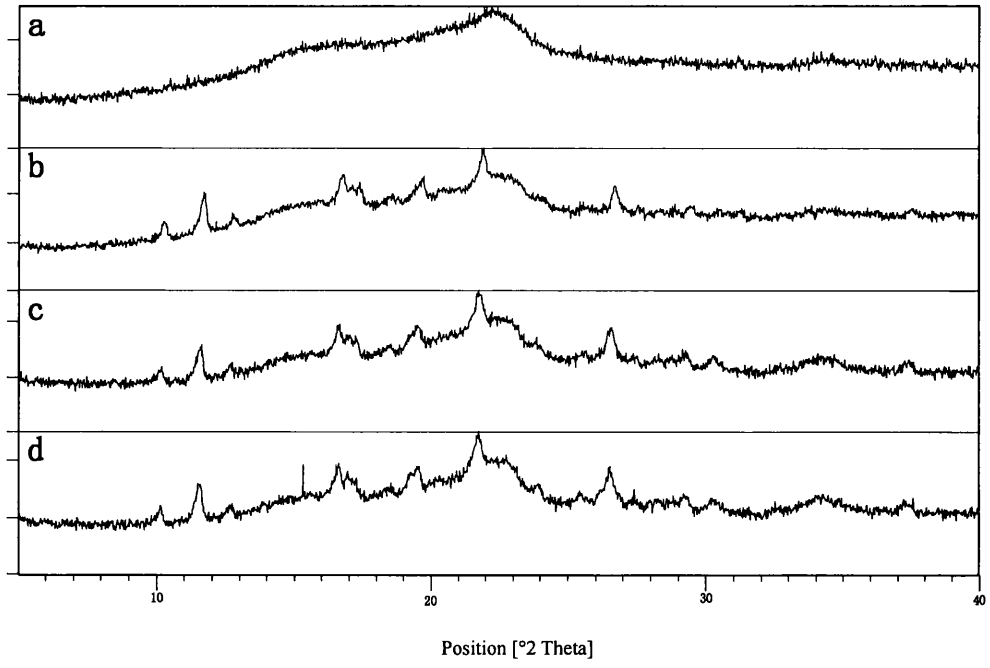

Figure 5.13: *Indometacin-SMCC (25%:75%) milled for 2 hours and stored at 30 °C, 11% RH for a) 0 day, b) 1 week, c) 2 weeks and d) 4 weeks.*

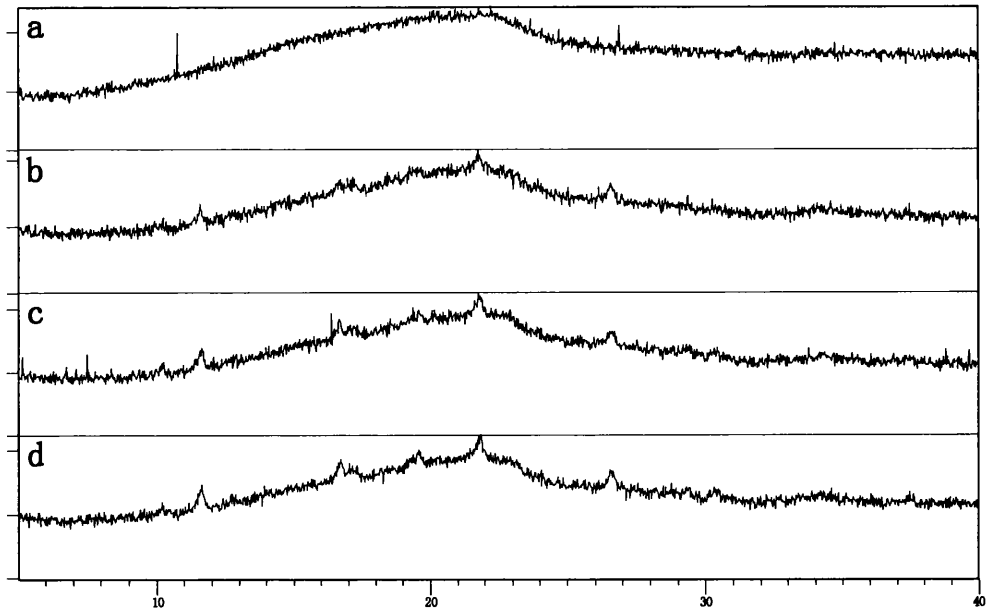

Figure 5.14: *Indometacin-SMCC (25%:75%) milled for 4 hours and stored at 30 °C, 11% RH for a) 0 day, b) 1 week, c) 2 weeks and d) 4 weeks.*

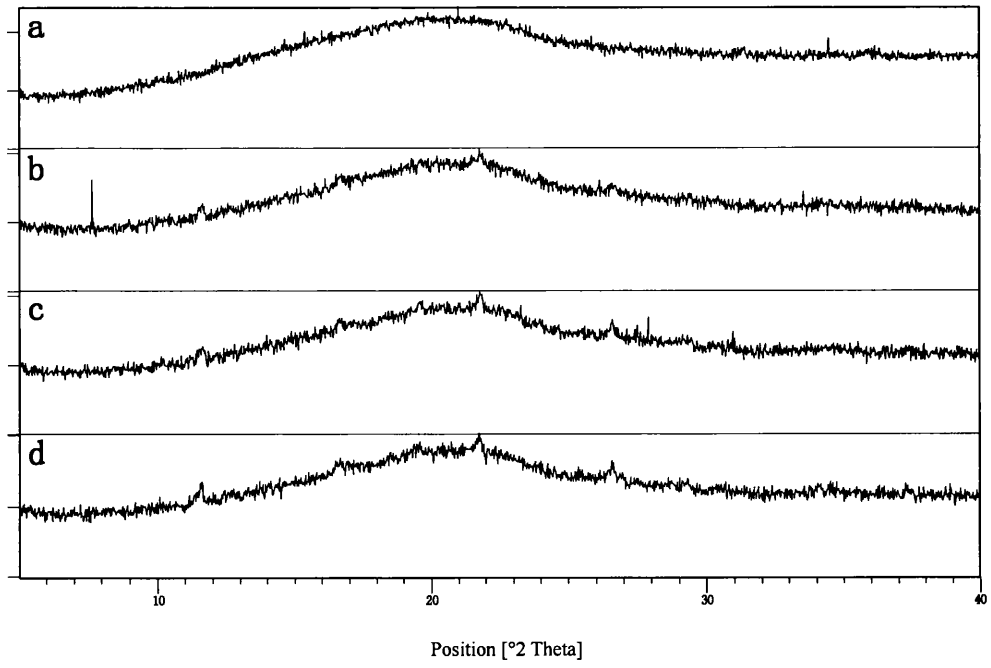

Figure 5.15: *Indometacin-SMCC (25%:75%) milled for 6 hours and stored at 30 °C, 11% RH for a) 0 day, b) 1 week, c) 2 weeks and d) 4 weeks.*

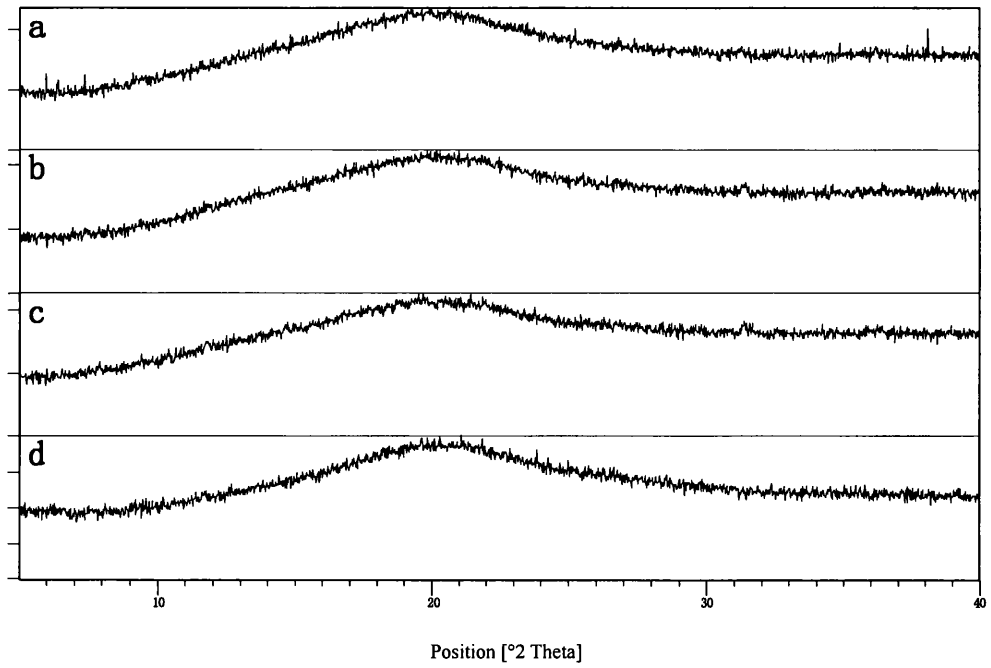

Figure 5.16: *SMCC Indometacin-SMCC (25%:75%) milled for 24 hours and stored at 30 °C, 11% RH for a) 0 day, b) 4 weeks, c) 2 months and d) 4 months.*

Figures 5.13 to 5.16 show that the samples which were milled for 2 hours recrystallised in 1 week, and the intensities of the characteristic peaks of indometacin increased as the storage time prolonged. The samples milled for 4 and 6 hours also recrystallised in 1 week, though the intensities of the peaks were not as significant and after storage for a longer period of time, the intensities of the peaks remained nearly the same. It was indicated that the milling time can be a variable which can affect the stability of the resultant samples. This was further proved by the samples which were milled for 24 hours. There is not any obvious peak shown and the samples remained amorphous after storing for 4 months. The higher mechanical force generated by a longer milling time could help the materials interact with each other in a larger extent. It is known that hydrogen bonding, salt formation or van der Waal's forces are the important factors for keeping the materials stable, and a reasonably long milling time can help the bonding and interaction develop, resulting in improved kinetic stability. The nucleation effect is important for an amorphous material to recrystallise. In this case if the interaction

between the drug and the carrier is large enough to avoid the aggregation, the nucleation effect can be retarded hence the stability can be increased.

Together with the milling time and rotation speed, the number of milling balls could also affect the milling outcome. The lower amount of balls used here (instead of 45 used in the previous sections) could decrease the impact and friction forces resulting at a slower amorphisation rate. Therefore, under the same milling durations, the sample milled using fewer milling balls probably contains more nucleation sites which could act as a trigger for crystallisation. For example, both milled for 6 hours, the one milled by 15 balls recrystallised in one week, but the one milled by 45 balls stayed amorphous for more than half a year. Hence, when the milling temperature is not too high to cause any crystallisation or the milling intensity is not too extreme to cause any potential degradation, by adjusting the rotation speed, milling time, and the milling balls, one could control the amorphous content and physical stability of the final products. Of course, the material or size of the milling balls could also influence the milling effect. This study demonstrates that milling conditions could greatly influence the stability of the amorphous products.

5.4.2.4 Dissolution properties of the solid dispersions

The dissolution properties of the solid dispersions were studied in pH 6.8 phosphate buffer and compared to that of the amorphous and crystalline indometacin. No matter what sample was used for investigation, a dose of 25 mg of indometacin was fixed to guarantee the sink conditions. Sink conditions mean that the dissolution of the drug will not be affected by its saturation solubility and it is very important for a dissolution experiment to be carried out in this condition.

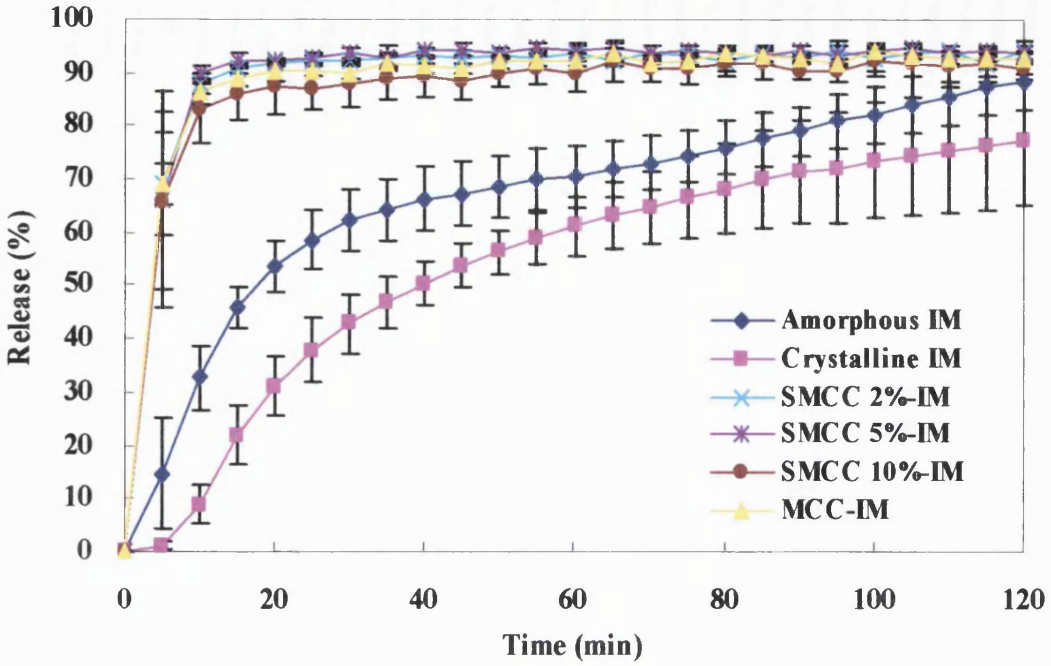

Figure 5.17: *Dissolution profiles of crystalline, amorphous indometacin (IM) and the SMCC and MCC solid dispersions (with a drug to carrier ratio of 25%:75%) at pH 6.8 phosphate buffer (37 °C).*

Figure 5.17 shows the dissolution profiles of crystalline, amorphous indometacin, MCC-indometacin and different SMCC-indometacin systems. As expected, crystalline indometacin showed the slowest dissolution rate compared to the others and amorphous indometacin was the second slowest. This matches well with the understanding that an amorphous material would have some dissolution advantages compared to its crystalline form because of its higher energy state. All indometacin solid dispersions displayed a significant improvement in the dissolution rate. The systems reached nearly 100% of release in only 10 minutes and stay in a plateau throughout the two-hour test. Both SMCC and MCC are excellent fillers for direct compression in tabletting and they are also good disintegrants which help the powders disperse well into the medium to prevent aggregation. Also, because of their hydrophilic nature, the powders were wetted very easily which helped to increase the dissolution rate. SMCC solid dispersions did not show any difference compared to the MCC one despite having a higher surface area.

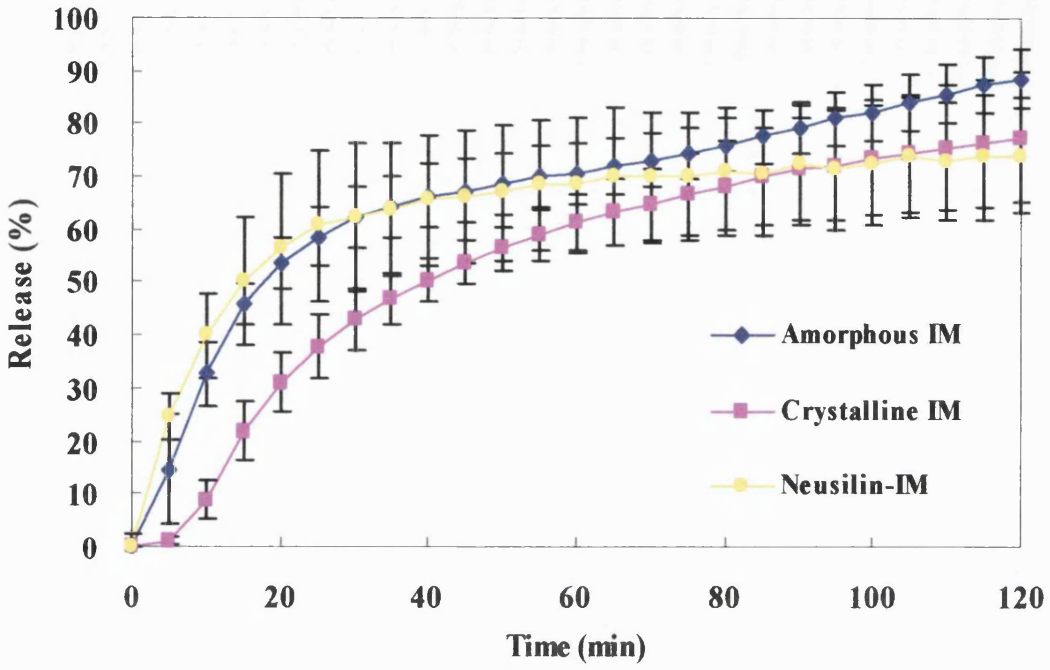

Figure 5.18: *Dissolution profiles of crystalline, amorphous indometacin and indometacin-Neusilin (25%:75%) solid dispersion at pH 6.8 phosphate buffer (37 ℃).*

The dissolution profile of Neusilin-indometacin solid dispersion is shown in Figure 5.18. The system also displayed a faster dissolution rate compared to the crystalline indometacin. However compared to the amorphous indometacin, the dissolution improvement is very small. In the first 40 minutes, Neusilin-indometacin dissolved slightly faster but after that the dissolution rate became milder and slower than that of the amorphous indometacin.

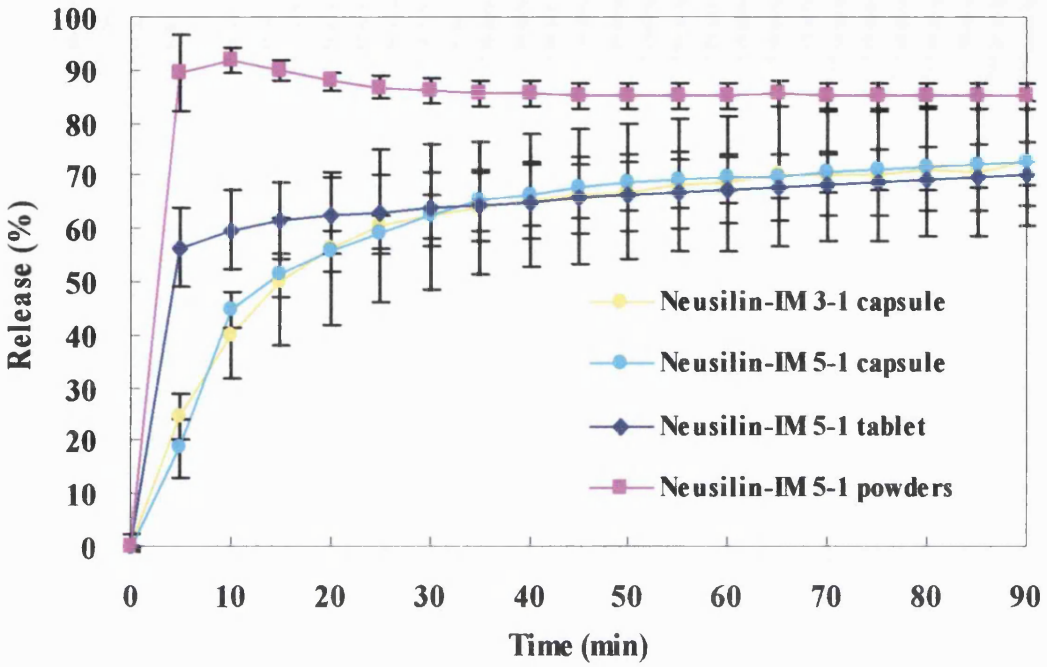

Figure 5.19: *Dissolution profiles of Neusilin-indometacin solid dispersions with different carrier to drug ratios and the samples were introduced to the pH 6.8 phosphate buffer (37 ℃) via different ways.*

Some previous studies have shown that a higher carrier ratio might help to increase the dissolution rate of solid dispersions (Leonardi *et al.*, 2007). Therefore the Neusilin to indometacin ratio was increased from 3:1 to 5:1 to investigate the effect of Neusilin concentration on the dissolution rate of indometacin. However, no obvious change of dissolution rate was noticed between the samples with different ratios (as shown in Figure 5.19). For both samples, small aggregates were observed in the medium during dissolution experiments. It was suspected that the poor dispersion of the powders in the medium as a result limited the dissolution performance of the solid dispersion. Therefore, the sample powders were introduced to the dissolution medium in two other ways during dissolution experiments: 1) the powders were compressed into tablets and then added to the medium; and 2) powders were directly added to the medium. In either case, the solid dispersion powders dispersed well into the medium and hence their dissolution rates have improved (Figure 5.19). Especially when powders were directly

introduced, a rapid release of drug (~90%) was detected in 5 minutes.

An amorphous solid dispersion could not only benefit from the amorphous state of the drug, but also the smaller particle size and the increased wettability of the hydrophilic carriers. Figure 5.20 has shown the contact angle of crystalline indometacin in comparison with its solid dispersions. As expected, SMCC-indometacin and MCC-indometacin systems showed smallest angle values indicating the best wettability of the samples. The contact angle of Neusilin and indometacin solid dispersion was just slightly lower than that of the crystalline one, which might be able to explain why the dissolution rate improvement of Neusilin was not as much as SMCC and MCC.

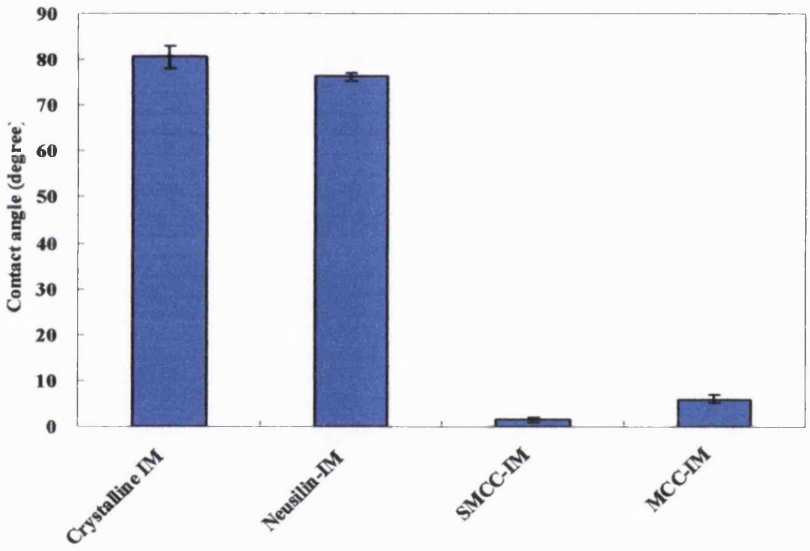

Figure 5.20: *Contact angle of crystalline indometacin and the solid dispersions of indometacin with Neusilin, SMCC or MCC (a drug to carrier ratio of 25%:75%).*

An excellent carrier should not only have good interaction ability with a drug in solid state but also be able to maintain the apparent solubility of the drug at a high level in the dissolution medium. Indometacin on its own and the solid dispersions of MCC, SMCC 2%, Neusilin with indometacin were placed in the pH 6.8 phosphate buffer and continuous shaking was maintained for 24 hours. Thereafter, the solutions were taken out for assessment of the concentration of indometacin. Neusilin system did not show

significant improvement of the apparent solubility of indometacin compared to the amorphous indometacin alone, but both MCC and SMCC were able to increase the apparent solubility of the drug by about two fold. The dissolution test did not show any difference between the MCC and SMCC systems, SMCC indeed was shown to be able to maintain a higher apparent solubility than MCC.

Sample	Apparent solubility of indometacin (μg/mL) in 24 hours
MCC-indometacin	1467
SMCC 2%-indometacin	2310
Neusilin-indometacin	968
Indometacin (amorphous)	911
Indometacin (crystalline)	719

Table 5.4: *Effect of carrier species on the apparent solubility of indometacin compared with that of indometacin along (pH 6.8 phosphate buffer at 37 °C) in 24 hours.*

5.4.2.5 Preparing the solid dispersions by spray drying

The possibility of preparing indometacin solid dispersions with MCC and Neusilin was investigated using spray drying as an alternative method. Normally, in a spray drying preparation, drug and carrier are completely dissolved in solvents in order to achieve a clear solution for a better feeding efficiency. However, since MCC and Neusilin are not soluble in any common laboratory solvent used for spray drying, suspensions of the carriers with completely dissolved indometacin in ethanol were made. The nozzle size of the GEA Niro spray dryer is ~500 μm, therefore, Neusilin with a particle size around 15 μm would be no problem for passing through the nozzle. But since MCC has an average particle size of around 50 μm, blockage of the nozzle would be expected during spray drying. To solve this problem, the particle size of MCC was reduced to around 15

μm using an air jet mill. A relatively higher feeding rate was also used as a precaution to prevent any blockage of the nozzle. After spray drying, indometacin still remained crystalline in the MCC systems, albeit XRPD patterns indicated a decrease of the characteristic peaks of crystalline indometacin. Indometacin and Neusilin spray dried sample appeared to be amorphous by XRPD. The SEM images of the spray dried samples are shown in Figure 5.21. On the surface of the MCC-indometacin particles, some needle shape particles can be seen which is related to the crystalline drug. Neusilin-indometacin particles showed no sign of any crystalline material. However, by visual observation, both spray dried samples turned from slightly yellow to white after storing at 30 °C 11%RH in one week indicating a poor physical stability compared to their ball milled samples.

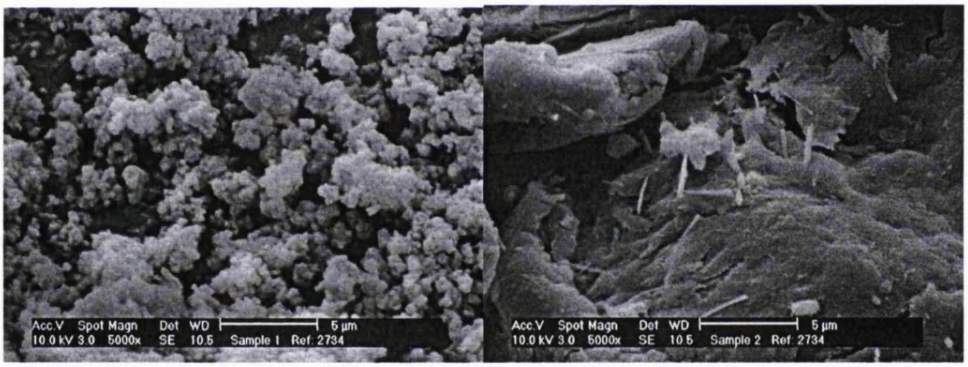

a b

Figure 5.21: *SEM images of spray dried indometacin with Neusilin (a) or MCC (b) with a drug to carrier ratio of 25%:75%.*

5.4.3 Carriers which are miscible with the model drug

In the previous section, carriers which are immiscible with indometacin were used to form solid dispersions with indometacin. Interactions between the drug and the carriers have been shown to be crucial to the physical stability of the systems as shown by the FTIR and accelerated stability studies. The planetary ball milling technique has been shown to be very useful to facilitate this solid-solid interaction between the drug and the carriers. In this section, PVP and HPMCAS, two carriers which should be miscible with indometacin according to their solubility parameters (Table 5.5) were used to form solid

solutions with the drug (the drug to carrier ratio was 75% to 25%). The solubility parameter differences between indometacin and PVP or HPMCAS are 3.4 and 2.1 $MPa^{1/2}$ respectively, which fall in the category of $\Delta\delta$<7.0 $MPa^{1/2}$ (Table 5.5). Thereby, indometacin is expected to be miscible with both of the carriers. Two different methods, planetary ball milling and spray drying were used to prepare the solid solutions and the effects of the preparation methods were studied.

Material	V (cm^3/mol)	δ_t	δ_d	δ_p	δ_h	Method/Reference
Indometacin	229.8[a]	25.9	23.4	6.0	9.4	VH[b]/this study
PVP	89.2[a]	22.5	16.5	12.4	8.9	VH[b]/this study
HPMCAS	N/A	23.8	N/A	N/A	N/A	MMP[d]/Ghebremeskel *et al.* (2007)
Griseofulvin	223.9[a]	23.9	21.3	6.5	8.6	VH[b]/this study

Table 5.5: *Hansan solubility parameters of the drugs and carriers.*

a. The molar volume was obtained according to Fedors' method (Fedors, 1974).

b. The calculation of the partial solubility parameter was based on van Krevelen and Hoftyzer's method (van Krevelen and Hoftyzer, 1976).

c. The molar volume was calculated by molecular weight/true density.

d. Molecular Modeling Pro software (Chem SW Inc., Fairfield, CA).

5.4.3.1 Preparation of the solid solutions by spray drying

There are many studies (Wang and Wang, 2002; Lin and Gentry, 2003; Godbee *et al.*, 2004) available if one needs more information about the physical properties and morphology of the particles in relation to the spray drying variables. In the current spray drying experiment, the main concern was how to improve the yield of the final product by optimising some spray drying variables. The GEA Niro spray dryer used for this study is a middle-scale laboratory spray dryer which is designed for spray drying liters

of liquid feed. However, the amount of solution used in the study was usually not more than 300 mL which would lead to a very low product yield. Therefore, 9 batches of PVP and indometacin (3:1) solutions (200 mL, 3% w/v loading) were spray dried using different spray drying variables in order to find out the most suitable setting.

Table 5.6 has shown the spray drying variables of 9 different batches. Throughout the 9 batches, the concentration of the solution, nozzle pressure, and atomisation gas flow were fixed to maintain a relatively constant particle size. The variables altered were chamber inlet flow, inlet temperature, pumping rate and the solvent types. In the first 3 batches, the inlet temperature was gradually increased and it seemed that at 80 °C the product has a higher yield than the other two temperatures. If the inlet temperature is too low, it might not provide enough heat to dry the droplets properly leading to formation of slurries with bad flowability; meanwhile if the inlet temperature is too high, the outlet temperature would be too close to the T_g of the particles and they would stick to the inner wall of the chamber. In both situations, product yield would be hampered. 80 °C appeared to be a suitable temperature for the PVP and indometacin system. In batch 4 the chamber inlet flow was increased to 30 kg/h (the maximum flow rate the spray dryer could achieve). A significantly increase in the product yield was noticed.

Batch	1	2	3	4	5	6	7	8	9
Atomisation gas flow (kg/h)	2.5	2.5	2.5	2.5	2.5	2.5	2.5	2.5	2.5
Chamber inlet flow (kg/h)	25	25	25	30	20	30	25	25	30
Nozzle pressure (bar)	1.5	1.5	1.5	1.5	1.5	1.5	1.5	1.5	1.5
Inlet Temperature (°C)	60	80	100	80	80	80	80	120	80
Pumping rate (%)	20	20	20	20	20	30	20	20	20
Solvent type	EtOH	EtOH	EtOH	EtOH	EtOH	EtOH	EtOH:Water 2:1	EtOH:Water 2:1	EtOH:Water 2:1
Final product weight (g)	0.3777	0.5421	0.3909	1.7432	0.666	0.9403	0.4647	0.2516	0.3962
Yield	6.29%	9.96%	6.52%	29.03%	11.09%	15.66%	7.74%	4.19%	6.60%

Table 5.6: *List of the spray drying parameters used for different batches of operations and their final yields.*

A higher chamber inlet flow might enable a better drying effect on the particles and also facilitate the transportation of the particles to the collection point in favour of a better yield. In contrast, when the chamber inlet flow was reduced in batch 5, a decrease in the product yield was noticed. A decrease was also found on batch 6 when the pumping rate was increased. Because as the chamber inlet flow was fixed, a higher pumping rate would reduce the drying effect and the moisture content in the particles would be raised. All batches using ethanol and water mixtures as the dissolution medium gave relatively poor product yield, because water with a higher boiling temperature than ethanol would reduce the drying effect when other parameters are the same. In this case increasing the inlet temperature would help to increase the drying of the particles but the outlet temperature would be too close to their T_g resulting in a decrease in the final yield. Therefore, batch 4 appeared to be the most suitable setting here for the spray drying experiment of PVP and indometacin.

The setting used in batch 4 PVP-indometacin solid solution was also applied to prepare the HPMCAS-indometacin solid solutions, except that the solvent was changed to acetone: water (80%:20%) because HPMCAS is insoluble in pure water, acetone or ethanol. An acceptable yield at around 15% was achieved.

The SEM images of the spray dried particles of PVP-indometacin and HPMCAS-indometacin solid solutions are shown in Figure 5.22. PVP-indometacin sample appeared to be spherical while the HPMCAS-indometacin particles were deformed spheres. The irregular shape of the HPMCAS-indometacin particles might be due to the high viscosity of the polymer solution. It was found that solvent evaporation rate and viscosity could be correlated with morphology of particles (Al-Obaidi, 2007). The different solvent system and the viscosity of the polymer solution could all play an important role on the morphology of the particles. All the particles have a size of less than 5 μm.

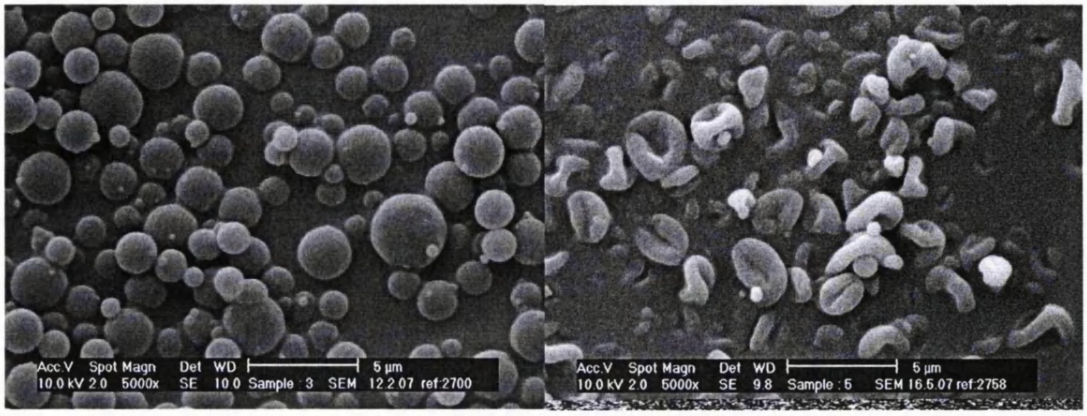

a b

Figure 5.22: *SEM images of spray dried indometacin with PVP (a) or HPMCAS (b), with a drug to carrier ratio of 25%:75%.*

XRPD assessments were conducted to investigate the crystallinity of spray dried PVP-indometacin and HPMCAS-indometacin samples. No characteristic peaks of indometacin were observed in the XRPD patterns (Figure 5.23) indicating that the samples were completely amorphous after preparation. Furthermore, DSC was applied to confirm the amorphous state of the systems. SSDSC showed a single T_g of PVP-indometacin and HPMCAS-indometacin at 100 and 58 °C respectively, indicating the complete miscibility between the drug and the carriers and the formation of solid solutions (Figure 5.24). Conventional DSC at 20 °C/min scan rate also confirmed this finding by only showing one T_g for the systems.

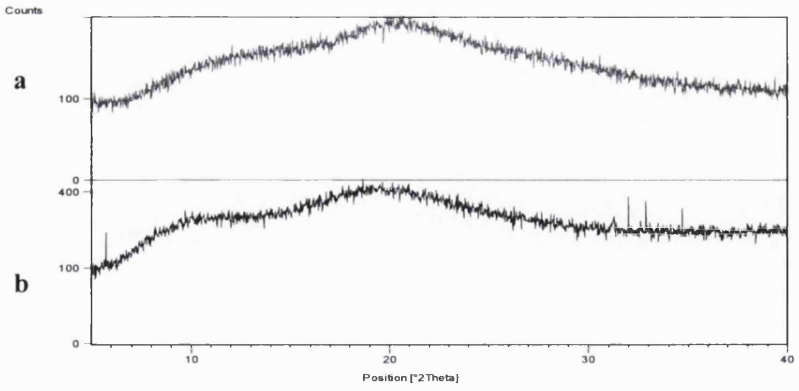

Figure 5.23: *XRPD patterns of spray dried indometacin with PVP (a) or HPMCAS (b), with a drug to carrier ratio of 25%:75%.*

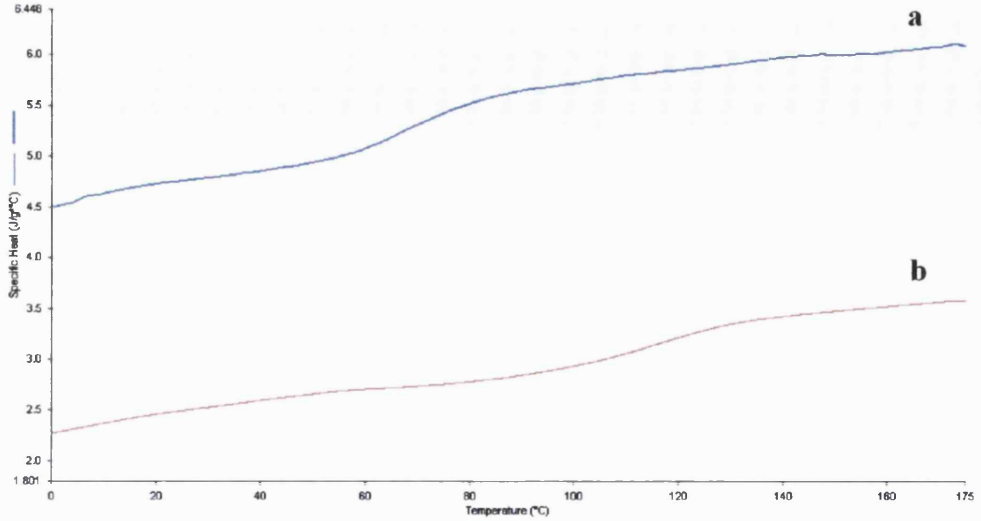

Figure 5.24: *DSC scans of spray dried indometacin with HPMCAS (a) or PVP (b), with a drug to carrier ratio of 25%:75%.*

5.4.3.2 Preparation of the solid solutions by ball milling

Indometacin and PVP or HPMCAS with a ratio of 1:3 were milled for 5, 15, 30, 60, 120, 240 and 360 minutes. Samples were withdrawn and characterised using XRPD to study the amorphous state conversion rate of indometacin (Figure 5.25). By milling with PVP and HPMCAS, indometacin was able to achieve amorphous in 30 and 60 minutes respectively. SEM studies were conducted to investigate the morphology of the ball milled samples and the images were shown in Figure 5.26. The ball milled samples were assessed by SSDSC and conventional DSC studies. Both PVP-indometacin and HPMCAS-indometacin systems had a single T_g no matter what scanning mode was used, indicating one-phase systems were formed. In SSDSC measurements, the T_g were 101 °C for PVP-indometacin and 58 °C for HPMCAS-indometacin (Figure 5.27). This result showed that the formation of solid solution by ball milling is possible. During ball milling, heat was generated which would help to dissolve indometacin into PVP or HPMCAS. Of course, the presupposition is that the carrier will have a certain level of solubility for the drug which was predicted by the solubility parameters of the drug and the carriers (Table 5.5).

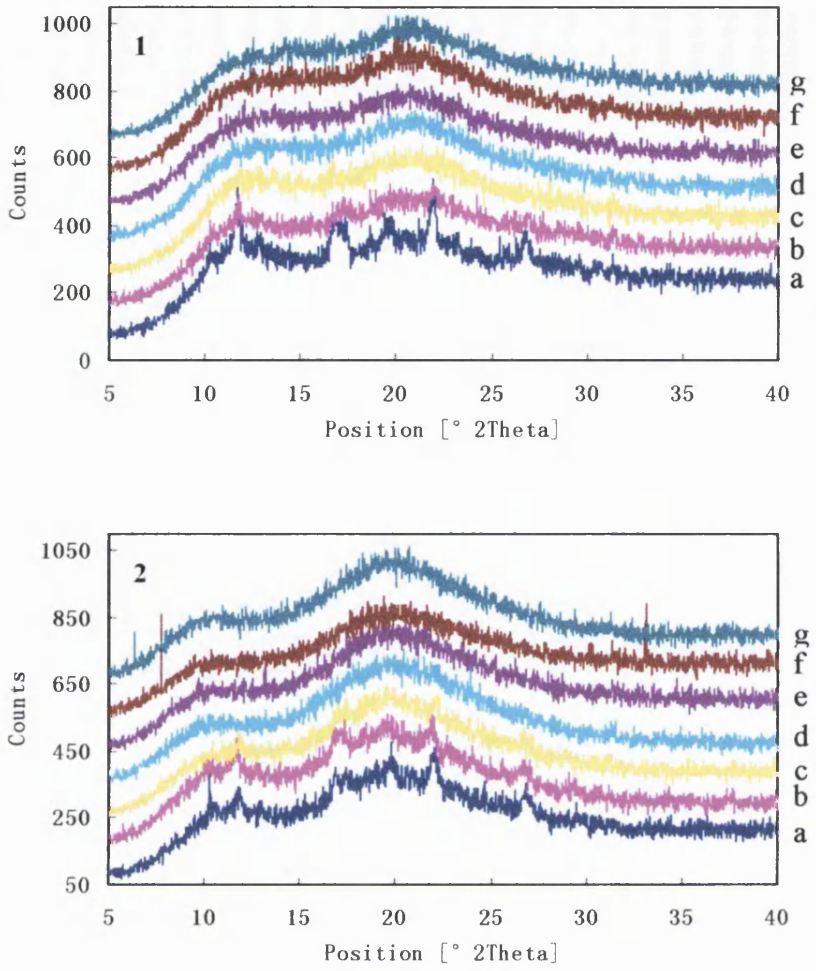

Figure 5.25: *XRPD patterns of indometacin milled with PVP (1) or HPMCAS (2) for 5 (a), 15 (b), 30 (c), 60 (d), 120 (e), 240 (f), and 360 (g) minutes.*

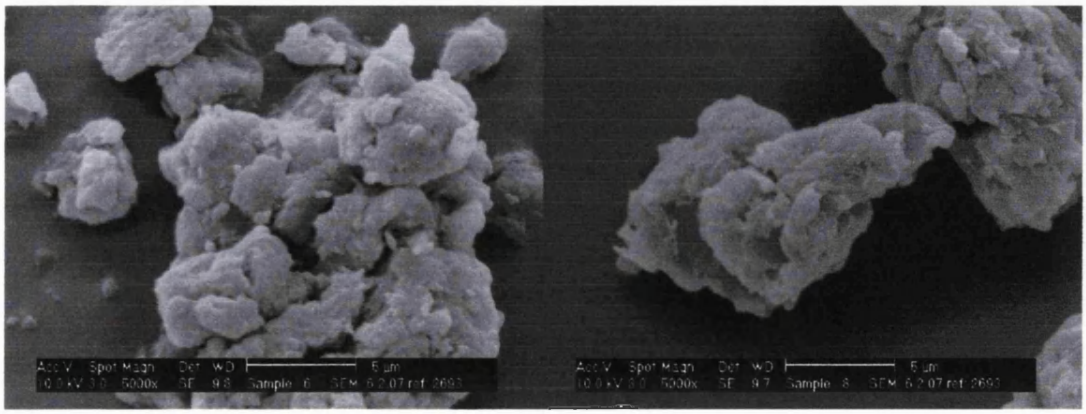

a b

Figure 5.26: *SEM images of ball milled indometacin with PVP (a) or HPMCAS (b), with a drug to carrier ratio of 25%:75%.*

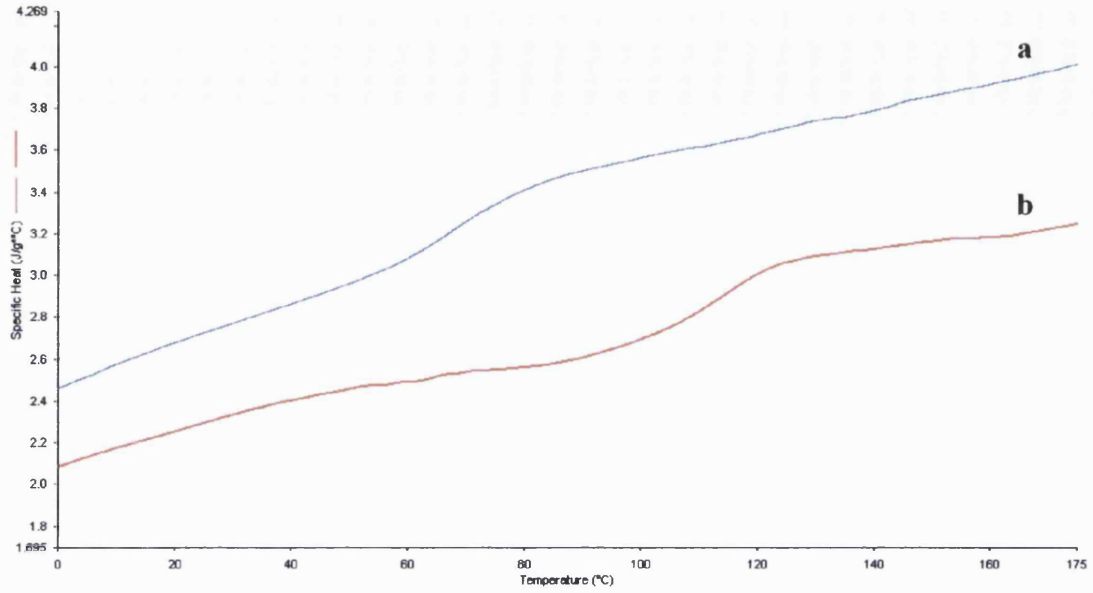

Figure 5.27: *DSC scans of ball milled indometacin with HPMCAS (a) or PVP (b), with a drug to carrier ratio of 25%:75%.*

5.4.3.3 Hydrogen bonding between the drug and the carriers

FTIR studies were conducted to investigate the drug and carrier interactions. Figure 5.28 shows the FTIR spectra of PVP and indometacin physical mixtures and the solid solutions prepared by ball milling and spray drying. In the physical mixtures, the peak at around 1662 cm^{-1} was related to the non-hydrogen bonded carbonyl group of PVP, and the other two peaks were related to crystalline indometacin as described in the previous section. After compounding with PVP using both methods, the dimer peak of indometacin at 1715 cm^{-1} disappeared, indicating the absence of any intramolecular interaction of indometacin molecules and the formation of amorphous indometacin. Meanwhile, a band started to show at around 1724 cm^{-1} which was related to the hydrogen bonding between the indometacin carboxyl and the PVP carbonyl group (Taylor and Zografi, 1997). Furthermore, the shift of the carbonyl group of PVP also indicated increased conjugation between PVP and indometacin.

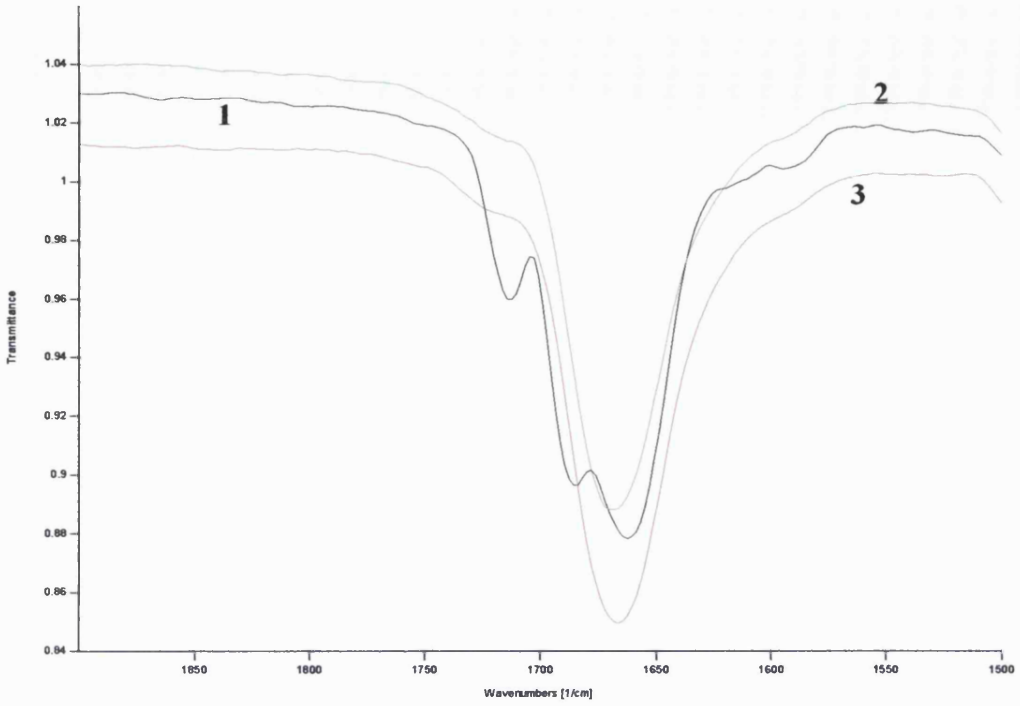

Figure 5.28: *FTIR spectra of indometacin and PVP physical mixture (1) and their spray dried (2) and ball milled (3) samples.*

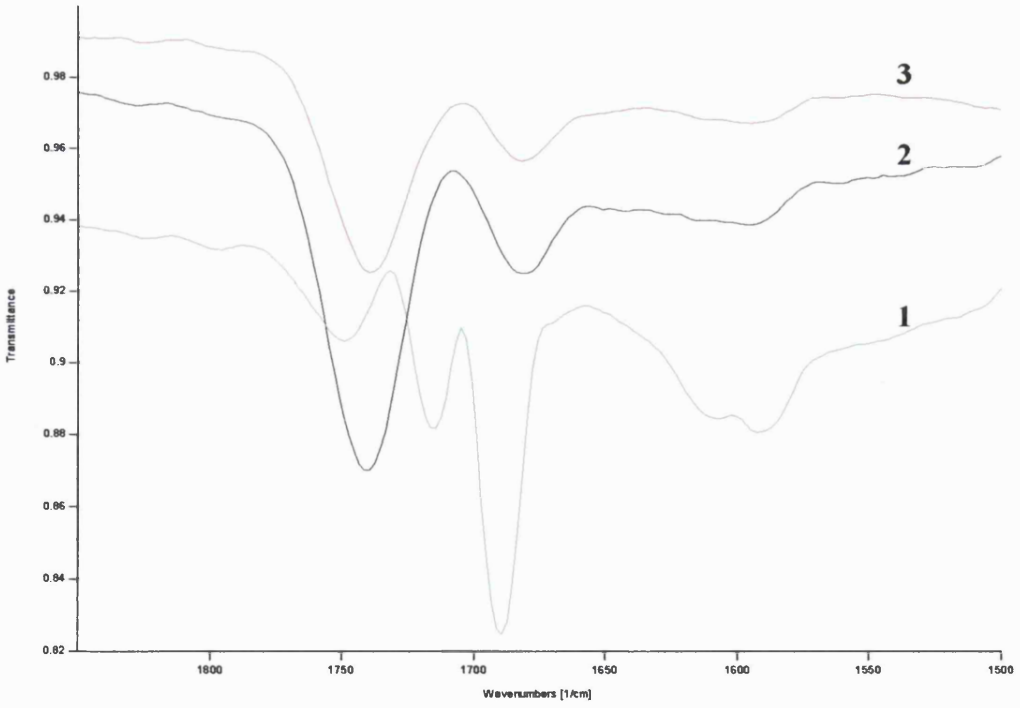

Figure 5.29: *FTIR spectra of indometacin and HPMCAS physical mixture (1) and their spray dried (2) and ball milled (3) samples.*

The FTIR spectra of HPMCAS and indometacin related systems are shown in Figure 5.29. The peak at 1750 cm^{-1} in the physical mixtures corresponded to the carbonyl groups in succinoyl and acetyl groups of HPMCAS (Fukui *et al.*, 2001). In the spectra of solid solutions prepared by ball milling and spray drying, the carbonyl peak of HPMCAS shifted to a lower wavenumber, together with the disappearance of indometacin dimer peak and shift of indometacin carbonyl peak. These changes indicate strong hydrogen bonding between the drug and the carrier.

Both PVP-indometacin and HPMCAS-indometacin systems have displayed strong hydrogen bonding between the drug and the carriers. Preparation techniques did not seem to have an impact on the hydrogen bonding results. It is important to point out that hydrogen bonding is an important factor for the formation of the solid solutions because interactions between the drug and carriers can increase the likelihood of molecular dispersions (Patterson *et al.*, 2007). Sekizaki *et al.* (1995) have shown that a certain degree of solid solution formation was achieved by merely physical mixing two compounds which are capable of forming strong hydrogen bond.

5.4.3.4 Physical stability of the solid solutions

PVP-indometacin and HPMCAS-indometacin solid solutions were stored at 30 °C 11% RH and 40 °C 75% RH for 2 months to investigate their physical stabilities. After storage, the samples were taken out for XRPD or DSC assessments. TGA studies were also conducted to monitor the change of moisture content of the samples (Table 5.7). Increased physical stabilities were achieved by all solid solutions since no recrystallisation of indometacin was noticed as determined by either XRPD or DSC tests. This improvement of physical stability of the sample is due to the strong hydrogen bonding between the two components and the solubility of indometacin into the carrier matrix which could prevent the drug molecules getting back together to form nucleation sites.

Carrier	Method	Initial water content % (w/w)	30 °C 11% RH		40 °C 75% RH	
			Solid state	Water content % (W/W)	Solid state	Water content % (W/W)
PVP	Spray drying	1.76	Amorphous	2.39	Amorphous	10.30
HPMCAS	Spray drying	0.50	Amorphous	0.28	Amorphous	3.77
PVP	Ball milling	4.14	Amorphous	3.16	Amorphous	12.60
HPMCAS	Ball milling	0.85	Amorphous	0.59	Amorphous	2.19

Table 5.7: *Physical stability of the solid solutions (a drug to carrier ratio of 25%:75%) stored for 2 months in different conditions as determined by XRPD or DSC.*

It was observed that both ball milled and spray dried PVP-indometacin samples have displayed a change of shape after storage at 40 °C 75% RH for 2 months. The particles looked like they have been melted and became a glass-like cake. It was difficult to assess these samples using XRPD, because unlike powders, they were very difficult to be flattened onto an XRPD sample plate. DSC measurements thereby were conducted to detect any possible change to the samples. Phase separation or crystallisation was not detected, since there was only one T_g detected and no endothermic peak of crystalline indometacin was observed. Indometacin remained amorphous in the samples. Hasegawa *et al.* (2005) in a study had developed a closed melting method to prepare solid solution of troglitazone and PVP. To lower the degradation tendency of the drug, troglitazone and PVP physical mixtures were placed over saturated salt solution to obtain a certain amount of water which could

help to lower the T_g of the materials and enable the preparation of amorphous solid solutions by heating below the melting of the drug. The change of shape of the PVP-indometacin solid solutions at 40 °C 75% RH was probably due to the large amount of water sorbed to the samples (Table 5.7) which acted like a plasticiser to lower the T_g of the samples down to the studied temperature. Therefore, without heating the samples over their T_g, the samples could still enter their rubbery state resulting in melting of the drug in the PVP. The PVP-indometacin solid solutions stored at 30 °C 11% RH remained powder like, because the water sorbed was limited. HPMCAS-indometacin solid solutions did not show any apparent change in the shape or morphology after storage at both conditions, which might imply a better stability over the PVP solid solutions.

5.4.3.5 Dissolution properties of the solid solutions

The dissolution profiles of the PVP-indometacin and HPMCAS-indometacin solid solutions were studied at pH 6.8 phosphate buffer and the results are shown in Figures 5.30 and 5.31. The effect of preparation method on the dissolution properties was also investigated.

Solid solutions of PVP and indometacin prepared by both techniques showed a significant improvement of the dissolution rate of indometacin compared to its pure crystalline and amorphous samples. The preparation techniques seem to have very little influence on the dissolution profiles, though the spray dried sample did show a slightly faster dissolution rate (Figure 5.30). However, the preparation technique appeared to play an important role in the HPMCAS-indometacin system. After 10 minutes, the spray dried sample showed a faster dissolution rate then amorphous indometacin while the ball milled sample was slower. This faster dissolution might be caused by the smaller particle size of the spray dried sample compared to the ball milled one which enables a higher surface area for the carrier to dissolve in a faster manner. The ball milled HPMCAS-indometacin did show an advantage in the dissolution rate compared to amorphous indometacin after 60 minutes as shown in

Table 5.8. The effect of preparation methods on the dissolution rate of indometacin appeared to be depended on the type of carrier.

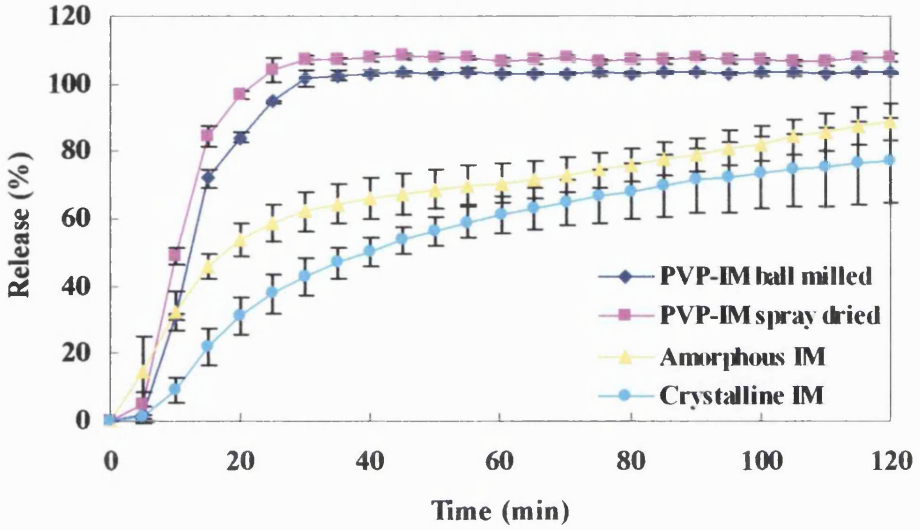

Figure 5.30: *Dissolution profiles of crystalline, amorphous indometacin and indometacin-PVP (25%:75%) solid solutions prepared by ball milling and spray drying, studied at pH 6.8 phosphate buffer (37 ℃).*

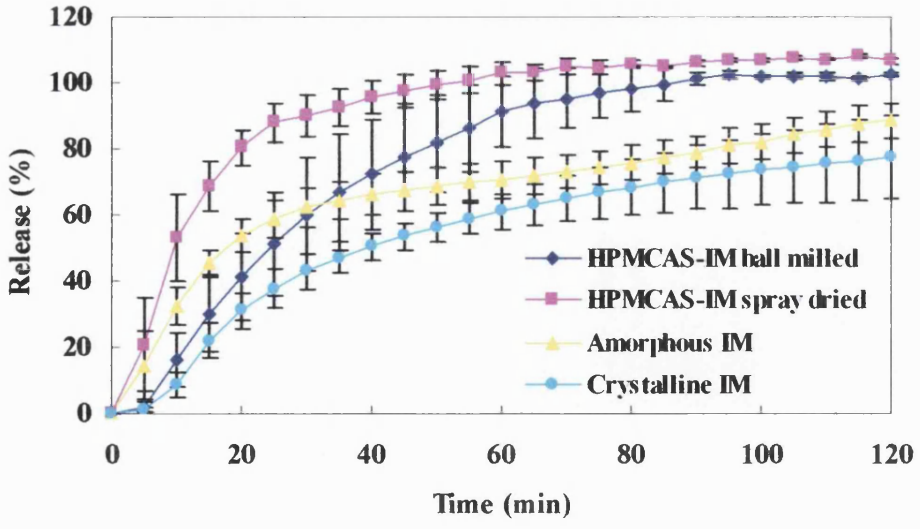

Figure 5.31: *Dissolution profiles of crystalline, amorphous indometacin and indometacin-HPMCAS (25%:75%) solid solutions prepared by ball milling and spray drying, studied at pH 6.8 phosphate buffer (37 ℃).*

Sample	t_{10}	t_{60}	Increased fold compared to crystalline indometacin	
			t_{10}	t_{60}
Ball milled HPMCAS-indometacin	16.2%	91.2%	1.8	1.5
Spray dried HPMCAS-indometacin	53.2%	102.8%	6.0	1.7
Amorphous indometacin	32.3%	70.4%	3.6	1.2
Crystalline indometacin	8.9%	61.1%	1	1

Table 5.8: *Release percentage of indometacin-HPMCAS (25%:75%) solid solutions, and crystalline and amorphous indometacin at 10 minutes (t_{10}) and 60 minutes (t_{60}).*

5.5 General discussion

Two types of methods have been widely used for preparing solid dispersion/solutions: one is a melting related method such as the melt quenching, melt extrusion methods and so forth; while the other is solvent evaporation. The melting method may not be well suited to some systems due to degradation. For example PVP was found to be unstable when exposed at a temperature over 150 °C for a certain period of time (Wade and Weller, 1994), but there are many drugs which have a melting temperature of over 200 °C. Chemical degradation might happen if these two components are heated together at a temperature over 200 °C. Therefore, solvent methods such as spray drying could be used as an alternative way for thermo-sensitive compounds. One of the advantages of the solvent methods is the convenience of scaling up which help them find large interests in industries. However, the involvement of large amount of solvents might cause handling and environmental issues.

Ball milling is a technique which is also very useful for preparation of amorphous materials and it is fundamentally different to the melting and solvent methods. Both melting and solvent methods generate amorphous forms through the liquid phase, such as solution or melt, which is more disordered compared to ball milling. During ball milling, highly structured crystalline compound changes to the disordered amorphous state while the product remains as a solid. This advantage helps ball milling to be more useful in preparation of solid dispersion/solution using those carriers which either have an extremely high melting point (i.e. Neusilin) or would degrade upon heating (i.e. SMCC and MCC). Also, it is useful for carriers which are not soluble in any commonly used laboratory solvents. MCC and Neusilin are not soluble in methanol, ethanol, acetone, water and other usual spray drying solvents, therefore, suspensions could only be made for spray drying. The ball milled MCC-indometacin and Neusilin-indometacin showed excellent physical stability when stored at 30 °C 11% RH, the spray dried product recrystallised within one week under the same condition. When prepared into suspensions, interactions between the drug and carrier might not happen as much as those in solutions. In solutions, the

entanglement of carrier chains might help to expose some functional groups which could interact with a drug easily. In ball milling, the mechanical force generated could help to facilitate solid-solid interactions regardless of whether the carriers are soluble or not. In comparison to the melting and solvent methods, the high-energy milling technique, such as planetary ball milling, has not received much attention in the preparation of solid solutions. However, the tremendous energy generated by a planetary mill, makes it more efficient than the conventional ball milling techniques and even enables the preparation of one-phase systems or the formation of drug-carrier miscible regions (Boldyrev *et al.*, 1994; Friedrich *et al.*, 2005). In a previous study Gupta *et al.* (2003) used a roller ball mill to prepare indometacin and Neusilin solid dispersion using a ratio of 1:5, but FTIR studies indicated that dimer peak of indometacin still existed after 24 hours of continuous milling. However, the planetary ball mill used here was able to turn indometacin 100% amorphous in less than 6 hours using a low drug to carrier ratio (1:3). No dimer peak of indometacin was shown as tested by FTIR. Also, in this study, indometacin was able to form solid solutions with PVP and HPMCAS using a planetary ball mill, and the samples showed similar glass transition temperature and physical stability compared to the spray dried systems. Though the ball milled samples showed slower dissolution rate compared to the spray dried ones, they did show obvious improvements compared to the amorphous and crystalline drug. All these positive results indicate that planetary ball milling is a very convenient technique. Either solid dispersions or solid solutions could be made by ball milling according to the miscibility between the drug and the carriers.

The solubility parameter is a very useful indicator for evaluation of the miscibility (solubility) between low molecular weight drugs and carriers. Many studies have demonstrated how to use solubility parameter as a predictor for the selection of carriers to prepare solid dispersions or solutions (Greenhalgh *et al.*, 1999). However, good miscibility between the drug and the carrier does not necessarily lead to a good physical stability. Table 5.5 shows that griseofulvin has a solubility parameter close to

that of PVP ($\Delta\delta$<7.0 $MPa^{1/2}$), and they are expected to be completely miscible with each other. Some previous studies have proven the formation of solid solution between griseofulvin and PVP (Mayersohn and Gibaldi, 1966; Al-Obaidi, 2007). Though an increased dissolution rate was achieved, griseofulvin recrystallised after less than 2 weeks at room temperature (Al-Obaidi, 2007). This rapid recrystallisation is due to lack of interaction between griseofulvin and PVP as both of them are proton acceptors. Indometacin has a similar solubility parameter to griseofulvin, but its carboxyl group makes it a proton donor enabling the formation of hydrogen bonding with the carbonyl group of PVP. Improvements of the physical stability of indometacin-PVP solid solutions were shown after storage at 30 °C 11% RH and 40 °C 75% RH. Intermolecular interaction seems to be a key factor to be considered when choosing a carrier for preparing stable solid solutions but not only the miscibility. Intermolecular interaction is also important to carriers which are immiscible with the drug. SMCC, MCC and Neusilin, could all interact with indometacin as indicated by the FTIR results. Instead of the reduction and small shift that was seen for the SMCC-indometacin and MCC-indometacin systems the dimer peak of indometacin disappeared after compounding with Neusilin indicating a stronger interaction. The strong acid-base interaction and hydrogen bonding between indometacin and Neusilin made the system more stable then the SMCC and MCC ones as shown by the stability test data. Therefore, when choosing a carrier to form solid dispersion/solution with a drug, the interaction potency between the components should be carefully evaluated, such as whether they are a proton donor, proton acceptor or capable of both, and whether they can form a salt through acid-base reaction.

Improving the physical properties of an amorphous drug is one of the main reasons for preparing solid dispersions/solutions however, if the dissolution property of the drug can not be improved, this formulation would be worthless. For example, PHPMA contains a hydroxyl and carbonyl group can act as a proton donor or proton acceptor in favour of hydrogen bonding with many drugs and it has been proved to be

able to stabilise griseofulvin for a long period of time (Al-Obaidi, 2007). In this study, PHPMA milled with indometacin and the solid dispersion was found stable after storage at 30 °C 75% RH for four weeks. However, during dissolution, PHPMA formed a hydrogel which prevents the release of indometacin leading to a very poor dissolution profile (Figure 5.32). In order to solve this problem, a ternary system was developed. MCC which has been shown to significantly increase the dissolution rate of indometacin in the binary system was added. PHPMA was first milled with indometacin to allow them interact with each other completely and then MCC was added and milled for another period of time.

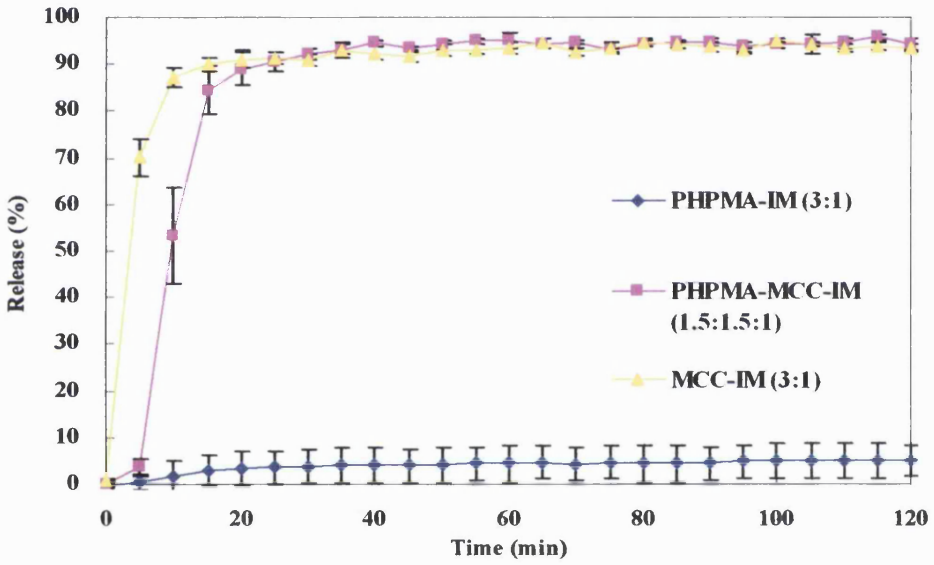

Figure 5.32: *Dissolution profiles of the solid dispersions of PHPMA-MCC-indometacin, PHPMA-indometacin and MCC-indometacin.*

The purpose of using two carriers here is to utilise the stabilisation effect of PHPMA and the excellent solubilising effect of MCC to provide a system with combined advantages of their both. Figure 5.32 shows that the dissolution rate of PHPMA-MCC-indometacin system has significantly increased. The PHPMA-MCC-indometacin system also showed an increase in the physical stability compared to the MCC-indometacin one after storing at 30 °C 75% RH for 4 weeks

(Figure 5.33). Hence ternary solid dispersion can be a very useful approach to prepare a solid dispersion/solution for a poorly soluble drug.

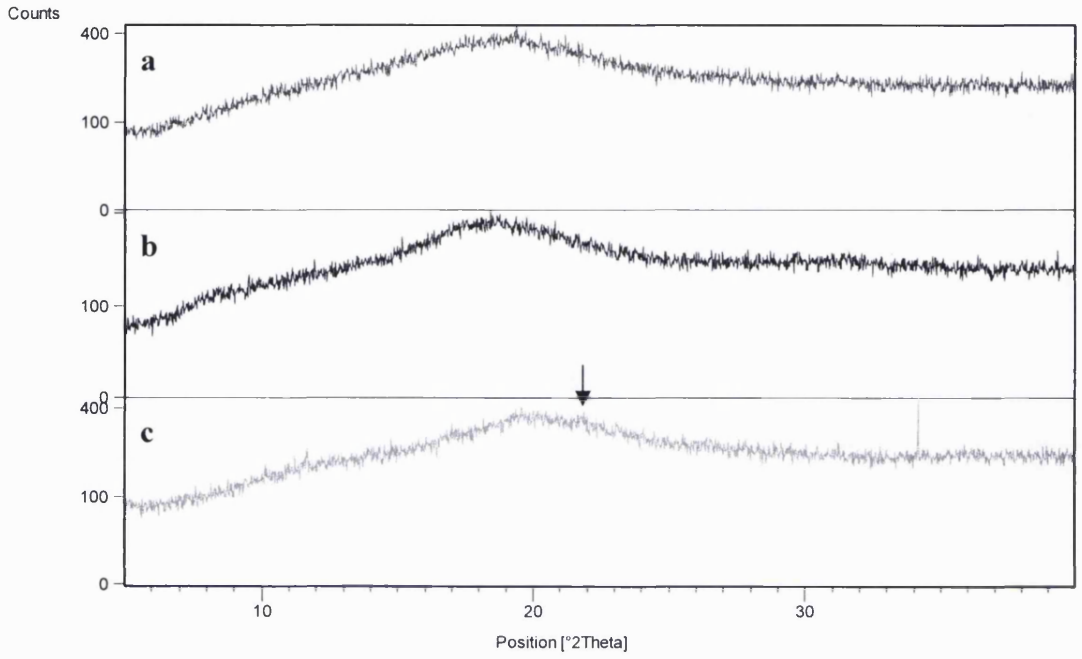

Figure 5.33: *XRPD patterns of solid dispersions of a) PHPMA-MCC-indometacin (1.5:1.5:1), b) PHPMA-indometacin (3:1) and c) MCC-indometacin (3:1) stored at 30 °C 75% for 4 weeks.*

5.6 Conclusion

In this study, it was found that the rate of crystalline indometacin to the amorphous state depends on the milling parameters such as the milling duration and milling intensity. There are two processes competing during amorphisation: the generation of amorphous phase caused by the mechanical energy of colliding balls and the conversion of the amorphous phase back to crystalline caused by increasing temperature in the milling pot during intensive collision. After prolonged milling, the rate of generation of amorphous phase would equal that of the formation of crystalline phase. Physical stability data indicate that longer milling time and higher milling intensity could help to increase the stability of an amorphous solid dispersion.

Carriers with different amounts of silica on the surfaces were used to prepare solid dispersions with indometacin. All carriers showed improvement in the stability and dissolution rate of indometacin. Neusilin which has the highest silica content (c.a. 30%) has shown the best stabilising effect due to its strong interaction with indometacin. SMCC has three grades of silica, 10%, 5% and 2% but the different amount of silica did not show any change in the stabilising effect of indometacin, which means that a higher amount of silica at least close to that of Neusilin on the surface is needed for an improved stability. The dissolution rate of SMCC and MCC were similar, nevertheless, SMCC indeed showed faster conversion to the amorphous state, better wettability, and higher apparent solubility of indometacin compared to MCC. Spray dried MCC or Neusilin with indometacin recrystallised very quickly which demonstrated the advantage of planetary ball milling in facilitating solid-solid interactions. Solid solutions of PVP or HPMCAS with indometacin were formed by using spray drying and ball milling methods. By using ball milling, it was possible to produce solid solutions with similar physical properties and stability with those prepared by spray drying. A difference in the dissolution properties was noticed between the two methods; however, this difference appears to be carrier specific. The dissolution profiles of the ball milled and spray dried PVP-indometacin system was very similar, while the spray dried HPMCAS-indometacin showed a faster dissolution

rate in the initial state compared to the ball milled one. Nevertheless, ball milling as an alternative method has proven to be very useful and convenient in preparing solid solution with a poorly soluble drug. Intermolecular interactions have proven to be critical for improvement of physical stability no matter whether the carrier is miscible or immiscible. Some carriers have been shown to be more effective in improvement of dissolution. According to this a ternary solid dispersion was developed using strong hydrogen bonding carrier PHPMA, and a good solubilising carrier MCC. Improved physical stability and dissolution properties were able to be achieved benefiting from the advantages of both carriers.

Chapter 6

Conclusions and future work

Conclusions

Slow dissolution and poor solubility have significantly limited the bioavailability of many poorly soluble drugs; hence it is very necessary for pharmaceutical researchers to find an efficient method to tackle this problem. Among various methods available for improvement of the dissolution property of drugs (as discussed in the introduction chapter), the formation of solid dispersions has been found to be a very useful one. In a solid dispersion, drugs can be (molecularly) dispersed into a hydrophilic carrier matrix which enables a reduction of the particle size of the drug to the molecular level. The amorphous state of the drug can provide improved dissolution rate. A major problem which greatly hampers the application of solid dispersion is the recrystallisation of the amorphous state during storage. Therefore, the aim of this thesis was to better understand some fundamental issues such as molecular mobility (both at the surface and in the bulk) and preparation method in relation to preparation of stable solid dispersions with improved dissolution rate.

Crystallisation usually happens at the surface initially; therefore molecular mobility at the surface of the solid dispersions was first to be studied. The hypothesis based here was that molecular mobility can be represented by the relaxation time which could be determined by the change of some related physical properties during physical aging. Since relaxation also accompanies with a decrease in energy, the decrease of the dispersive surface free energy of the amorphous samples could probably provide useful information about the surface molecular mobility. Indometacin and PVP with a weight ratio of 70% to 30% were melt quenched and ball milled, and DSC studies have confirmed the formation of solid solutions. Planetary ball milling was shown to be efficient in generation of complete miscibility between PVP and indometacin with a concentration of PVP as low as 30%. The glass transition of the ball milled sample was 64 °C which was close to that of the melt quenched one (67 °C). In addition, FTIR studies confirmed the hydrogen bonding interaction between the drug and the carrier, and preparation method did not seem to have a significant effect on the interaction.

The dispersive surface free energy of indometacin increased after compounding with PVP as determined by inverse gas chromatography which shows the possibility to increase wettability of a hydrophobic drug by dispersing it in a hydrophilic carrier matrix. The melt quenched solid solution was aged at 40, 50 and 60 °C at 0% RH for 18 days and samples were taken out at different time points for IGC measurements to monitor the change of the dispersive surface free energy. XRPD, DSC and FTIR measurements confirmed that the sample did not show any change and remained in the amorphous state. IGC measurements have shown that the dispersive surface free energy of the sample decreased after aging and after fitting the surface energy data to the KWW equation, relaxation times of the sample were able to be obtained for direct comparison. The relaxation showed temperature dependence with the sample aged at 40 °C having the slowest relaxation time while the one aged at 60 °C the fastest. The sample aged at a higher temperature might tend to recrystallise first since it had the highest surface molecular mobility. In addition, the melt quenched solid solution with a higher PVP content (50% w/w) was aged at 40, 60 and 70 °C to study the effect of carrier ratio on the surface molecular mobility. At 60 °C the relaxation time was slower than that of 70 °C, and at 40 °C decrease of surface energy was absent when the carrier content was increased. Therefore, for the stability point of view, a higher carrier concentration is favoured because the drug molecules could be trapped further apart within the carrier matrix, and higher carrier content could allow higher extent of carrier-drug interaction and further improvement of glass transition temperature.

The dispersive surface free energy did not change in the case of the ball milled solid solution after aging at 50 and 60 °C for 14 days; however the retention volume of decane decreased indicating a decrease of interaction tendency between the surface and the vapour probe which also showed temperature dependence. This decrease of interaction tendency indicated a decrease of energy state at the surface. The acid-base parameters of the ball milled sample indicated a reorientation of polar surface groups which would affect its adhesion-cohesion force balance. Decane V_{max} was found to be more sensitive than the dispersive surface free energy in measuring the change of

energy state. Furthermore, it could measure the decrease of energy state with a shorter measuring time.

The newly developed decane V_{max} method was applied to study the surface molecular mobility of the melt quenched and ball milled solid solutions aged at 50 °C at 0% RH, moreover a spray dried solid solution with the same drug and carrier composition was added into comparison (the T_g of the spray dried sample was 65 °C which was also close to that of the other two samples). The decane V_{max} obtained were fitted to a modified KWW equation to obtain the minimum retention volume of decane and with these data, KWW fitting was able to perform to obtain the relaxation parameters of these samples. The solid solution prepared by spray drying showed the highest molecular mobility while the melt quenched one was the slowest. The surface molecular mobility was then compared to the bulk molecular mobility measured using the DSC relaxation enthalpy recovery method. The hypothesis here was that since crystallisation is mainly surface initiated, the molecular mobility at the surface should be higher than that of the bulk. The results shown here have verified this hypothesis. For all solid solutions regardless of the preparation method used, surface relaxation is faster than that of the bulk. Surface molecular mobility should be therefore distinguished from the bulk molecular mobility in the preparation of amorphous solid dispersions. Preparation methods have shown significant influence on the molecular mobility both at the surface and in the bulk. Therefore, the effect of preparation method should be another important factor to consider in solid dispersion preparation. The surface relaxation data of the ball milled solid solution was very close to the bulk ones which might suggest that the drug and carrier miscible regions are mainly located on the outer surface of the sample. The relaxation time distribution constant suggested that the ball milled sample had a less homogeneity than the melt quenched one, which might have negative effect for the physical stability of the sample.

The activation energy of the solid solutions was studied using the scanning rate dependence of glass transition temperature method and thereby, the fragility parameters

of the systems were calculated. Preparation methods also showed great influence on the fragility of the final products whereas the melt quenched sample was the most fragile and the ball milled one was the least. According to the fragility parameters, the zero mobility temperature of the solid solutions could be obtained. The T_0 appeared to be correlated to the molecular mobility and fragility of the samples. The more fragile the sample was, the smaller the T_g-T_0 value was. This finding might suggest that when the glass transition temperatures are the same, the more fragile sample is preferred since it might have a higher T_0 which is positive for the physical stability of the products during storage. A physical stability test was performed by storing the solid solutions at room temperature at 75% RH. The ball milled sample showed the fastest crystallisation whereas the melt quenched one showed the slowest. This result was in good correlation with the T_0 and molecular mobility data. T_0 appeared to be a better indicator than T_g for prediction of the physical stability of an amorphous product.

The water sorption and dissolution behaviour of the freshly prepared and aged solid solutions prepared by melt quenching and ball milling were also investigated. After aging at 50 °C for 15 days, the water uptake ability of the solid solutions decreased which was caused by the decrease of molecular mobility and internal energy. In the dissolution test, the dissolution rate of the aged samples also decreased significantly. Preparation method appeared to have a significant effect on the dissolution rate: the initial ball milled sample had a faster dissolution rate than the initial melt quenched one. The decrease tendency of the dissolution rate of the solid solutions after physical aging was also depending on the preparation method. The ball milled sample which had the faster bulk relaxation rate showed a larger decreasing extent than the melt quenched one. The studies here demonstrated the importance of molecular mobility and preparation method in relation to the dissolution performance of the solid solutions.

Carriers which are miscible and immiscible with indometacin were prepared into solid dispersions with the model drug using ball milling and spray drying. The immiscible carriers used were SMCC, MCC and Neusilin which contain different amount of silica

at the surface. All carriers showed significant improvement of physical stability and dissolution rate compared to amorphous or crystalline indometacin. Neusilin (c.a. 30%) which has the highest concentration of silica displayed the fastest rate of conversion to the amorphous phase. Neusilin also had the best stabilisation effect of amorphous indometacin which was due to the largest carrier-drug interaction (acid-base interaction and hydrogen bonding) as confirmed by FTIR. SMCC carriers (2%, 5%, and 10%) which have slightly higher silica content showed a faster rate of conversion than MCC (0%), however, they did not show any significant difference in the physical and dissolution properties compared to MCC. FTIR studies also confirmed that SMCC and MCC had similar hydrogen bonding tendency to indometacin. Spray drying was used to prepare solid dispersions of indometacin and Neusilin or MCC. The hypothesis was that carrier-drug interaction could happen easier through the liquid state than solid state interactions. However, the spray dried solid dispersions recrystallised within one week under the same storage condition. For immiscible carriers, ball milling showed an advantage over spray drying in facilitating solid-solid interactions. It is very important to choose the right preparation method for a particular type of carrier in order to reach the maximum stabilisation effect. Furthermore, solid solutions of PVP or HPMCAS (miscible carriers) with indometacin were prepared by ball milling and spray drying. Both solid solution systems showed significant improvement of stability and dissolution performance of indometacin. Preparation method seemed to have an impact on the dissolution properties of the solid solutions and the extent of impact was carrier dependent. Ball milling was shown to be very useful and convenient in preparing solid solutions for both types of carriers. All studies here indicated the importance of intermolecular interaction in relation to the physical stability of the amorphous solid dispersions no matter whether the carrier is miscible or immiscible. Therefore, intermolecular interactions should be one of the main concerns when designing a solid dispersion formulation. Meanwhile, the formation of a ternary solid dispersion was found to be a useful strategy for both dissolution and stability improvement. In a ternary solid dispersion, carriers which have the advantage of rapid dissolution or intermolecular interaction could be used as a combination and improved dissolution and

stability are able to be achieved making use of the advantages of the individual carrier.

Future work

According to the finding obtained in this study there are some interesting points which could be studied further in the future: the decane V_{max} method has been found to be very useful in measuring surface molecular mobility, hence it would be very interesting to apply it for the study of the surface molecular mobility of amorphous materials at different relative humidity. It would also be interesting to study the surface molecular mobility of a solid dispersion with different carrier species. Other surface measuring techniques such as atomic force microscopy could be used to study the surface of a sample in correlation with the IGC study. A preliminary study has indicated that the decane V_{max} method is also useful to measure the onset and rate of crystallisation at the surface. More experiments should be conducted in order to complete this study. The decane V_{max} method could then be applied to study the onset and rate of surface crystallisation (under different temperatures and relative humidities) in comparison with the bulk crystallisation studied using isothermal microcalorimetry, XRPD or DSC. Furthermore, the decane V_{max} method focuses on the surface characterisation, however, the definition of surface is unknown. It would be necessary to investigate how far into the bulk the IGC method is actually probing. Finally, intermolecular interaction has been shown to be very important for stability improvement. It would be interesting to compare the stability of two solid dispersion systems which containing the same carrier and drug composition with similar T_g but different intermolecular interaction levels.

Bibliography

Al-Obaidi, H. (2007). "Optimization of drug carrier interactions in spray dried solid dispersions." The School of Pharmacy, University of London. Thesis.

Aljaberi, A., Chatterji, A., Shah, N. H. and Sandhu, H. K. (2009). "Functional performance of silicified microcrystalline cellulose versus microcrystalline cellulose: a case study." Drug Dev. Ind. Pharm.: 1-6.

Ambarkhane, A. (2005). "Characterisation of the amorphous solid state using solvent vapour induced transitions." The School of Pharmacy, University of London. Thesis.

Amidon, G. L., Lennernas, H., Shah, V. P. and Crison, J. R. (1995). "A theoretical basis for a biopharmaceutic drug classification: the correlation of in vitro drug product dissolution and in vivo bioavailability." Pharm. Res. 12(3): 413-420.

Andronis, V., Yoshioka, M. and Zografi, G. (1997). "Effects of sorbed water on the crystallization of indomethacin from the amorphous state." J. Pharm. Sci. 86(3): 346-351.

Andronis, V. and Zografi, G. (1997). "Molecular mobility of supercooled amorphous indomethacin, determined by dynamic mechanical analysis." Pharm. Res. 14(4): 410-414.

Andronis, V. and Zografi, G. (1998). "The molecular mobility of supercooled amorphous indomethacin as a function of temperature and relative humidity." Pharm. Res. 15(6): 835-842.

Andronis, V. and Zografi, G. (2000). "Crystal nucleation and growth of indomethacin polymorphs from the amorphous state." J. of Non-Cryst. Solid 271(3): 236-248.

Angell, C. A. (1988). "Structural instability and relaxation in liquid and glassy phases near the fragile liquid limit." J. of Non-Cryst. Solid 102(1-3): 205-221.

Angell, C. A. (1991). "Relaxation in liquids, polymers and plastic crystals - strong fragile patterns and problems." J. of Non-Cryst. Solid 131: 13-31.

Angell, C. A. (1995). "Formation of glasses from liquids and biopolymers." Science 267: 1924-1935.

Aso, Y. and Yoshioka, S. (2006). "Molecular mobility of nifedipine-PVP and phenobarbital-PVP solid dispersions as measured by C-13-NMR spin-lattice relaxation time." J. Pharm. Sci. 95(2): 318-325.

Aso, Y., Yoshioka, S. and Kojima, S. (2000). "Relationship between the crystallization rates of amorphous nifedipine, phenobarbital, and flopropione, and their molecular mobility as measured by their enthalpy relaxation and H-1 NMR relaxation times." J. Pharm. Sci. 89(3): 408-416.

Aso, Y., Yoshioka, S. and Kojima, S. (2004). "Molecular mobility-based estimation of the crystallization rates of amorphous nifedipine and phenobarbital in poly(vinylpyrrolidone) solid dispersions." J. Pharm. Sci. 93(2): 384-391.

Atkinson, R. M., Bedford, C., Child, K. J. and Tomich, E. G. (1962). "The effect of griseofulvin particle size on blood levels in man." Antibiot. Chemother. 12: 232-238.

Augsburger, L. L. and Hoag, S. W. (2008). "Pharmaceutical dosage forms: tablets." New York; London, Informa Healthcare.

Bachrach, W. H. (1959). "Reserpine, gastric secretion, and peptic ulcer." Am. J. Dig. Dis. 4(2): 117-124.

Bajdik, J., Pintye-Hodi, K., Planinsek, O., Tuske, Z., Tasic, L., Regdon, G., Srcic, S. and Eros, I. (2004). "Surface treatment of indomethacin agglomerates with Eudragit." Drug Dev. Ind. Pharm.30 (4): 381-388.

Bauer, G., Rieckmann, P. and Schaumann, W. (1962). "Effect of particle sizes and detergents on the absorption of spironolactone from the gastrointestinal tract." Arzneimittelforschung 12: 487-489.

Benet, L. Z., Greither, A. and Meister, W. (1976). "Gastrointestinal absorption of drugs in patients with cardiac failure." in "The effect of disease states on pharmacokinetics of drugs." Washington, D.C., American Pharmaceutical Association.

Bhugra, C. and Pikal, M. J. (2008). "Role of thermodynamic, molecular, and kinetic factors in crystallization from the amorphous state." J. Pharm. Sci. 97(4): 1329-1349.

Bhugra, C., Rambhatla, S., Bakri, A., Duddu, S. P., Miller, D. P., Pikal, M. J. and Lechuga-Ballesteros, D. (2007). "Prediction of the onset of crystallization of amorphous sucrose below the calorimetric glass transition temperature from correlations with mobility." J. Pharm. Sci. 96(5): 1258-1269.

Bhugra, C., Shmeis, R., Krill, S. L. and Pikal, M. J. (2006). "Predictions of onset of crystallization from experimental relaxation times I-correlation of molecular mobility from temperatures above the glass transition to temperatures below the glass transition." Pharm. Res. 23(10): 2277-2290.

Bhugra, C., Shmeis, R., Krill, S. L. and Pikal, M. J. (2008a). "Different measures of molecular mobility: Comparison between calorimetric and thermally stimulated current relaxation times below T_g and correlation with dielectric relaxation times above T_g." J. Pharm. Sci. 97(10): 4498-4515.

Bhugra, C., Shmeis, R., Krill, S. L. and Pikal, M. J. (2008b). "Prediction of onset of crystallization from experimental relaxation times. II. Comparison between predicted and experimental onset times." J. Pharm. Sci. 97(1): 455-472.

Bohmer, R., Ngai, K. L., Angell, C. A. and Plazek, D. J. (1993). "Nonexponential relaxations in strong and fragile glass formers." J. Chem. Phys. 99(5): 4201-4209.

Boldyrev, V. V., Shakhtshneider, T. P., Burleva, L. P. and Severtsev, V. A. (1994). "Preparation of the Disperse Systems of Sulfathiazole-Polyvinylpyrrolidone by Mechanical Activation." Drug Dev. Ind. Pharm. 20(6): 1103-1114.

Bolhuis, G. K. and Chowhan, Z. T. (1996). "Materials for direct compaction." In "Pharmaceutical powder compaction technology." New York, Marcel Dekker.

Breitenbach, J. and Lewis, J. (2003). "Two concepts, one technology: controlled release and solid dispersion with meltrex." In "Modified-Release Drug Delivery Technology." New York; London, Informa Healthcare.

Broman, E., Khoo, C. and Taylor, L. S. (2001). "A comparison of alternative polymer excipients and processing methods for making solid dispersions of a poorly water soluble drug." Int. J. Pharm. 222(1): 139-151.

Bruning, R. and Samwer, K. (1992). "Glass transition on long time scales." Phys. Rev. B 46(18): 11318-11322.

Buckton, G. (1995). "Interfacial phenomena in drug delivery and targeting." Chur, Switzerland, Harwood Academic Publishers.

Buckton, G., Adeniyi, A. A., Saunders, M. and Ambarkhane, A. (2006). "HyperDSC studies of amorphous polyvinylpyrrolidone in a model wet granulation system." Int. J. Pharm. 312(1-2): 61-65.

Buckton, G., Ambarkhane, A. and Pincott, K. (2004). "The use of inverse phase gas chromatography to study the glass transition temperature of a powder surface." Pharm. Res. 21(9): 1554-1557.

Buckton, G. and Darcy, P. (1999). "Assessment of disorder in crystalline powders - a review of analytical techniques and their application." Int. J. Pharm. 179(2): 141-158.

Buckton, G. and Gill, H. (2007). "The importance of surface energetics of powders for drug delivery and the establishment of inverse gas chromatography." Adv. Drug Del. Rev. 59(14): 1474-1479.

Buckton, G., Yonemochi, E., Yoon, W. L. and Moffat, A. C. (1999). "Water sorption and near IR spectroscopy to study the differences between microcrystalline cellulose and silicified microcrystalline cellulose before and after wet granulation." Int. J. Pharm. 181(1): 41-47.

Byrn, S. R., Pfeiffer, R. R. and Stowell, J. G. (1999). "Solid-state chemistry of drugs." New York, Academic Press.

Carroll, P. J. and Patterson, G. D. (1985). "The distribution of relaxation frequencies from photon-correlation spectroscopy near the glass-transition." J. Chem. Phys. 82(1): 9-13.

Chadwick, K., Davey, R. and Cross, W. (2007). "How does grinding produce co-crystals? Insights from the case of benzophenone and diphenylamine." Cryst. Eng. Comm. 9(9): 732-734.

Chidavaenzi, O. C., Buckton, G., Koosha, F. and Pathak, R. (1997). "The use of thermal techniques to assess the impact of feed concentration on the amorphous content and polymorphic forms present in spray dried lactose." Int. J. Pharm. 159(1): 67-74.

Chiou, W. L. and Riegelman, S. (1969). "Preparation and dissolution characteristics of several fast-release solid dispersions of griseofulvin." J. Pharm. Sci. 58(12): 1505-1510.

Chiou, W. L. and Riegelman, S. (1971). "Pharmaceutical applications of solid dispersion systems." J. Pharm. Sci. 60(9): 1281-1302.

Chokshi, R. J., Sandhu, H. K., Iyer, R. M., Shah, N. H., Malick, A. W. and Zia, H. (2005). "Characterization of physico-mechanical properties of indomethacin and polymers to assess their suitability for hot-melt extrusion processs as a means to manufacture solid dispersion/solution." J. Pharm. Sci. 94(11): 2463-2474.

Chuang, I. S. and Maciel, G. E. (1996). "Probing hydrogen bonding and the local environment of silanols on silica surfaces via nuclear spin cross polarization dynamics." J. Amer. Chem. Soc. 118(2): 401-406.

Chuang, I. S. and Maciel, G. E. (1997). "A detailed model of local structure and silanol hydrogen banding of silica gel surfaces." J. Phys. Chem. B 101(16): 3052-3064.

Clas, S. D., Dalton, C. R. and Hancock, B. C. (1999). "Differential scanning calorimetry: applications in drug development." Pharm. Sci. Tech. Today 2(8): 311-320.

Coleman, N. J. and Craig, D. Q. M. (1996). "Modulated temperature differential scanning calorimetry: A novel approach to pharmaceutical thermal analysis." Int. J. Pharm. 135(1-2): 13-29.

Cowie, J. M. G., Harris, S. and McEwen, I. J. (1998). "Physical aging in poly(vinyl acetate). 2. Relative rates of volume and enthalpy relaxation." Macromolecules. 31(8): 2611-2615.

Craig, D. Q., Royall, P. G., Kett, V. L. and Hopton, M. L. (1999). "The relevance of the amorphous state to pharmaceutical dosage forms: glassy drugs and freeze dried systems." Int. J. Pharm. 179(2): 179-207.

Craig, D. Q. M., Barsnes, M., Royall, P. G. and Kett, V. L. (2000). "An evaluation of the use of modulated temperature DSC as a means of assessing the relaxation behaviour of amorphous

lactose." Pharm. Res. 17(6): 696-700.

Craig, D. Q. M., Kett, V. L., Andrews, C. S. and Royall, P. G. (2002). "Pharmaceutical applications of micro-thermal analysis." J. Pharm. Sci. 91(5): 1201-1213.

Crichton, S. N. and Moynihan, C. T. (1988). "Dependence of the glass-transition temperature on heating rate." J. Non-Cryst. Solid 99(2-3): 413-417.

Crowley, K. J. and Zografi, G. (2001). "The use of thermal methods for predicting glass-former fragility." Thermochim. Acta 380(2): 79-93.

Crowley, K. J. and Zografi, G. (2002). "Cryogenic grinding of indomethacin polymorphs and solvates: Assessment of amorphous phase formation and amorphous phase physical stability." J. Pharm. Sci. 91(2): 492-507.

Crowley, K. J. and Zografi, G. (2003). "The effect of low concentrations of molecularly dispersed poly(vinylpyrrolidone) on indomethacin crystallization from the amorphous state." Pharm. Res. 20(9): 1417-1422.

Curatolo, W. (1998). "Physical chemical properties of oral drug candidates in the discovery and exploratory development settings." Pharm. Sci. Tech. Today 1(9): 387-393.

Dannenfelser, R. M., He, H., Joshi, Y., Bateman, S. and Serajuddin, A. T. M. (2004). "Development of clinical dosage forms for a poorly water soluble drug I: Application of polyethylene glycol-polysorbate 80 solid dispersion carrier system." J. Pharm. Sci. 93(5): 1165-1175.

Davenport, H. W. (1971). "Physiology of the Digestive Tract." Chicago, Year Book Medical Publishers Ltd.

Debenedetti, P. G. (1996). "Metastable liquids: concepts and principles." Princeton, N.J.; Chichester, Princeton University Press.

Debenedetti, P. G. and Stillinger, F. H. (2001). "Supercooled liquids and the glass transition." Nature 410(6825): 259-267.

DeMaggio, G. B., Frieze, W. E., Gidley, D. W., Zhu, M., Hristov, H. A. and Yee, A. F. (1997). "Interface and surface effects on the glass transition in thin polystyrene films." Phys. Rev. Lett. 78(8): 1524-1527.

Dove, J. W., Buckton, G. and Doherty, C. (1996). "A comparison of two contact angle measurement methods and inverse gas chromatography to assess the surface energies of theophylline and caffeine." Int. J. Pharm. 138(2): 199-206.

Dwan'Isa, J. L., Dinguizli, M., Preat, V., Arien, A. and Brewster, M. (2005). "Qualitative prediction of solubilization of highly hydrophobic drugs in block copolymer micelles." J. Contr. Rel. 101(1-3): 366-368.

Fakhraai, Z. and Forrest, J. A. (2008). "Measuring the surface dynamics of glassy polymers." Science 319(5863): 600-604.

Fedors, R. F. (1974). "Method for estimating both solubility parameters and molar volumes of liquids." Poly. Eng. Sci. 14(2): 147-154.

Ford, J. L. (1986). "The current status of solid dispersions." Pharm. A. Hel. 61(3): 69-88.

Forster, A., Hempenstall, J. and Rades, T. (2001). "Characterization of glass solutions of poorly water-soluble drugs produced by melt extrusion with hydrophilic amorphous polymers." J. Pharm. Pharmaco. 53(3): 303-315.

Fowkes, F. M. (1964). "Attractive forces at interfaces." Ind. Eng. Chem. 56(12): 40-52.

Friedrich, H., Nada, A. and Bodmeier, R. (2005). "Solid state and dissolution rate characterization of co-ground mixtures of nifedipine and hydrophilic carriers." Drug Dev. Ind. Pharm. 31(8): 719-728.

Fujii, M., Okada, H., Shibata, Y., Teramachi, H., Kondoh, M. and Watanabe, Y. (2005). "Preparation, characterization, and tableting of a solid dispersion of indomethacin with crospovidone." Int. J. Pharm. 293(1-2): 145-153.

Fukui, E., Miyamura, N. and Kobayashi, M. (2001). "Effect of magnesium stearate or calcium stearate as additives on dissolution profiles of diltiazem hydrochloride from press-coated tablets with hydroxypropylmethylcellulose acetate succinate in the outer shell." Int. J. Pharm. 216(1-2): 137-146.

Gaisford, S. and Buckton, G. (2001). "Potential applications of microcalorimetry for the study of physical processes in pharmaceuticals." Thermochim. Acta 380(2): 185-198.

Ghebremeskel, A. N., Vernavarapu, C. and Lodaya, M. (2007). "Use of surfactants as plasticizers in preparing solid dispersions of poorly soluble API: Selection of polymer-surfactant combinations using solubility parameters and testing the processability." Int. J. Pharm. 328(2): 119-129.

Godbee, J., Scott, E., Pattamunuch, P., Chen, S. and Mathiowitz, E. (2004). "Role of solvent/non-solvent ratio on microsphere formation using the solvent removal method." J. Microencapsul. 21(2): 151-160.

Gong, K., Viboonkiat, R., Rehman, I. U., Buckton, G. and Darr, J. A. (2005). "Formation and characterization of porous indomethacin-PVP coprecipitates prepared using solvent-free supercritical fluid processing." J. Pharm. Sci. 94(12): 2583-2590.

Gordon, M. and Taylor, J. S. (1952). "Ideal copolymers and the second-order transitions of synthetic rubbers, 1: non-crystalline copolymers." J. Appl. Chem. 2: 493-498.

Greenhalgh, D. J., Williams, A. C., Timmins, P. and York, P. (1999). "Solubility parameters as predictors of miscibility in solid dispersions." J. Pharm. Sci. 88(11): 1182-1190.

Grimsey, I. M., Feeley, J. C. and York, P. (2002). "Analysis of the surface energy of pharmaceutical powders by inverse gas chromatography." J. Pharm. Sci. 91(2): 571-583.

Guo, Y., Byrn, S. R. and Zografi, G. (2000). "Physical characteristics and chemical degradation of amorphous quinapril hydrochloride." J. Pharm. Sci. 89(1): 128-143.

Gupta, M. K., Tseng, Y. C., Goldman, D. and Bogner, R. H. (2002). "Hydrogen bonding with adsorbent during storage governs drug dissolution from solid-dispersion granules." Pharm. Res. 19(11): 1663-1672.

Gupta, M. K., Vanwert, A. and Bogner, R. H. (2003). "Formation of physically stable amorphous drugs by milling with neusilin." J. Pharm. Sci. 92(3): 536-551.

Gutmann, V. (1978). "The donor-acceptor approach to molecular interactions." New York; London, Plenum Press.

Hammerschmidt, J. A., Gladfelter, W. L. and Haugstad, G. (1999). "Probing polymer viscoelastic relaxations with temperature-controlled friction force microscopy." Macromolecules 32(10): 3360-3367.

Hancock, B. C., Dalton, C. R., Pikal, M. J. and Shamblin, S. L. (1998). "A pragmatic test of a simple calorimetric method for determining the fragility of some amorphous pharmaceutical materials." Pharm. Res. 15(5): 762-767.

Hancock, B. C. and Parks, M. (2000). "What is the true solubility advantage for amorphous pharmaceuticals?" Pharm. Res. 17(4): 397-404.

Hancock, B. C., Shamblin, S. L. and Zografi, G. (1995). "Molecular mobility of amorphous pharmaceutical solids below their glass-transition temperatures." Pharm. Res. 12(6): 799-806.

Hancock, B. C. and Zografi, G. (1997). "Characteristics and significance of the amorphous state in pharmaceutical systems." J. Pharm. Sci. 86(1): 1-12.

Hasegawa, S., Hamaura, T., Furuyama, N., Kusai, A., Yonemochi, E. and Terada, K. (2005). "Effects of water content in physical mixture and heating temperature on crystallinity of troglitazone-PVP K30 solid dispersions prepared by closed melting method." Int. J. Pharm. 302(1-2): 103-112.

Hatley, R. H. (1997). "Glass fragility and the stability of pharmaceutical preparations--excipient selection." Pharm. Dev. Technol. 2(3): 257-264.

Hatley, R. H. and Colaco, C. A. (1997). "Stabilisation of biological molecules, cells and organisms. Protein Labelling: Bioconjugation techniques for the biomedical sciences." London, Macmillan Press.

Hilden, L. R. and Morris, K. R. (2004). "Physics of amorphous solids." J. Pharm. Sci. 93(1): 3-12.

Hogan, S. E. and Buckton, G. (2001). "Water sorption/desorption - near IR and calorimetric study of crystalline and amorphous raffinose." Int. J. Pharm. 227(1-2): 57-69.

Huang, J. J., Wigent, R. J., Bentzley, C. M. and Schwartz, J. B. (2006). "Nifedipine solid dispersion in microparticles of ammonio methacrylate copolymer and ethylcellulose binary blend for controlled drug delivery - Effect of drug loading on release kinetics." Int. J. of Pharm. 319(1-2): 44-54.

Hutchinson, J. M. (1995). "Physical aging of polymers." Prog. Poly. Sci. 20(4): 703-760.

Huu-Phuoc, N., Nam-Tran, H., Buchmann, M. and Kesselring, U. W. (1987). "Experimentally optimized determination of the partial and total cohesion parameters of an insoluble polymer (microcrystalline cellulose) by gas-solid chromatography." Int. J. Pharm. 34(3): 217-223.

Imaizumi, H., Nambu, N. and Nagai, T. (1980). "Stability and several physical properties of amorphous and crystalline form of indomethacin." Chem. Pharm. Bull. 28(9): 2565-2569.

Jiang, J. Z., Larsen, R. K., Lin, R., Morup, S., Chorkendorff, I., Nielsen, K., Hansen, K. and West, K. (1998). "Mechanochemical synthesis of Fe-S materials." J. Sol. State Chem. 138(1): 114-125.

Kajiyama, T., Tanaka, K. and Takahara, A. (1997). "Surface molecular motion of the monodisperse polystyrene films." Macromolecules 30(2): 280-285.

Kanig, J. L. (1964). "Properties of fused mannitol in compressed tablets." J. Pharm. Sci. 53: 188-192.

Kararli, T. T., Needham, T. E., Seul, C. J. and Finnegan, P. M. (1989). "Solid-state interaction of magnesium-oxide and ibuprofen to form a salt." Pharm. Res. 6(9): 804-808.

Karavas, E., Ktistis, G., Xenakis, A. and Georgarakis, E. (2006). "Effect of hydrogen bonding interactions on the release mechanism of felodipine from nanodispersions with polyvinylpyrrolidone." Eur. J. Pharm. Biopharm. 63(2): 103-114.

Karki, S., Friscic, T., Jones, W. and Motherwell, W. D. S. (2007). "Screening for pharmaceutical

cocrystal hydrates via neat and liquid-assisted grinding." Mol. Pharm. 4(3): 347-354.

Kaushal, A. M., Gupta, P. and Bansal, A. K. (2004). "Amorphous drug delivery systems: molecular aspects, design, and performance." Crit. Rev. Ther. Drug Carrier Syst. 21(3): 133-193.

Kawakami, K. and Pikal, M. J. (2005). "Calorimetric investigation of the structural relaxation of amorphous materials: Evaluating validity of the methodologies." J. Pharm. Sci. 94(5): 948-965.

Kerc, J. and Srcic, S. (1995). "Thermal-analysis of glassy pharmaceuticals." Thermochim. Acta 248: 81-95.

Kerle, T., Lin, Z. Q., Kim, H. C. and Russell, T. P. (2001). "Mobility of polymers at the air/polymer interface." Macromolecules 34(10): 3484-3492.

Kerr, W. L., Lim, M. H., Reid, D. S. and Chen, H. (1993). "Chemical reaction kinetics in relation to glass temperatures in frozen food polymer solutions." J. Sci. Food Agric. 61: 51-56.

Khalaf, A. S., Tobyn, M. J. and Staniforth, J. N. (1997). "Measurement of the flow properties of silicified microcrystalline cellulose." AAPS conference, Seattle, WA.

Khalid, A. (2006). "Characterisation of spray-dried trehalose/alkaline phosphatase formulations." The School of Pharmacy, University of London. Thesis.

Khougaz, K. and Clas, S. D. (2000). "Crystallization inhibition in solid dispersions of MK-0591 and poly(vinylpyrrolidone) polymers." J. Pharm. Sci. 89(10): 1325-1334.

Kiselev, A. V. and Yashin, Y. J. (1969). "Gas-adsorption chromatography." New York; London, Plenum Press.

Konno, H. and Taylor, L. S. (2006). "Influence of different polymers on the crystallization tendency of molecularly dispersed amorphous felodipine." J. Pharm. Sci. 95(12): 2692-2705.

Ksiazek, K., Wacke, S., Gorecki, T. and Gorecki, C. (2007). "Effect of the milling conditions on the degree of amorphization of selenium by milling in a planetary ball mill - art. no. 012037." XIII International Seminar on Physics and Chemistry of Solids 79: 12037-12037
12250.

Leonardi, D., Barrera, M. G., Lamas, M. C. and Salomon, C. J. (2007). "Development of prednisone: polyethylene glycol 6000 fast-release yablets from solid dispersions: solid-state characterization, dissolution behavior, and formulation parameters." AAPS PharmSciTech 8(4) E1-E8.

Leuner, C. and Dressman, J. (2000). "Improving drug solubility for oral delivery using solid

dispersions." Eur. J. Pharm. Biopharm. 50(1): 47-60.

Levy, G., Antkowiak, J. M., Procknal, J. A. and White, D. C. (1963). "Effect of certain tablet formulation factors on dissolution rate of the active ingredient. II. granule size, starch concentration, and compression pressure." J. Pharm. Sci. 52: 1047-1051.

Lin, I. J. and Nadiv, S. (1979). "Review of the phase-transformation and synthesis of inorganic solids obtained by mechanical treatment (mechanochemical reactions)." Mat. Sci. Eng. 39(2): 193-209.

Lin, J. C. and Gentry, J. W. (2003). "Spray drying drop morphology: Experimental study." Aerosol Sci. Techn. 37(1): 15-32.

Lin, S. L., Menig, J. and Lachman, L. (1968). "Interdependence of physiological surfactant and drug particle size on the dissolution behavior of water insoluble drugs." J. Pharm. Sci. 57(12): 2143-2148.

Liu, J. S., Rigsbee, D. R., Stotz, C. and Pikal, M. J. (2002). "Dynamics of pharmaceutical amorphous solids: The study of enthalpy relaxation by isothermal microcalorimetry." J. Pharm. Sci. 91(8): 1853-1862.

Liu, Y., Russell, T. P., Samant, M. G., Stohr, J., Brown, H. R., Cossy-Favre, A. and Diaz, J. (1997). "Surface relaxations in polymers." Macromolecules 30(25): 7768-7771.

Loftsson, T. and Brewster, M. E. (1996). "Pharmaceutical applications of cyclodextrins. 1. Drug solubilization and stabilization." J. Pharm. Sci. 85(10): 1017-1025.

Majerik, V., Charbit, G., Badens, E., Horvath, G., Szokonya, L., Bosc, N. and Teillaud, E. (2007). "Bioavailability enhancement of an active substance by supercritical antisolvent precipitation." J. Supercr. Fluids 40(1): 101-110.

Marshall, W. R. and Seltzer, E. (1950). "Principles of spray drying. Part I. Fundamentals of spray-dryer operation." Chem. Eng. Prog. 46: 501-508.

Masters, K. (1972). "Spray drying: an introduction to principles, operational practice and applications." London, L. Hill.

Matsumoto, T. and Zografi, G. (1999). "Physical properties of solid molecular dispersions of indomethacin with poly(vinylpyrrolidone) and poly(vinylpyrrolidone-co-vinylacetate) in relation to indomethacin crystallization." Pharm. Res. 16(11): 1722-1728.

Maury, M., Murphy, K., Kumar, S., Shi, L. and Lee, G. (2005). "Effects of process variables on the powder yield of spray-dried trehalose on a laboratory spray-dryer." Eur. J. Pharm. Biopharm. 59(3): 565-573.

Mayersohn, M. and Gibaldi, M. (1966). "New method of solid-state dispersion for increasing dissolution rates." J. Pharm. Sci. 55(11): 1323-1324.

Mccormick, P. G. (1995). "Application of mechanical alloying to chemical refining." Mat. Trans. JIM 36(2): 161-169.

McGregor, C., Saunders, M. H., Buckton, G. and Saklatvala, R. D. (2004). "The use of high-speed differential scanning calorimetry (hyper-DSC^{TM}) to study the thermal properties of carbamazepine polymorphs." Thermochim. Acta 417(2): 231-237.

Merisko-Liversidge, E. (2002). "Nanocrystals: resolving pharmaceutical formulation issues associated with poorly water-soluble compounds." Particles. Orlando/Florida, Marcel Dekker: 49.

Mio, H., Kano, J., Saito, F. and Kaneko, K. (2002). "Effects of rotational direction and rotation-to-revolution speed ratio in planetary ball milling." Materials Science and Engineering a-Structural Materials Properties Microstructure and Processing 332(1-2): 75-80.

Moynihan, C. T., Easteal, A. J., Debolt, M. A. and Tucker, J. (1976). "Dependence of fictive temperature of glass on cooling rate." J. Amer. Cer. Soc. 59(1-2): 12-16.

Moynihan, C. T., Easteal, A. J., Wilder, J. and Tucker, J. (1974). "Dependence of glass-transition temperature on heating and cooling rate." J. Phys. Chem. 78(26): 2673-2677.

Muzikova, J. and Novakova, P. (2007). "A study of the properties of compacts from silicified micro crystalline celluloses." Drug Dev. Ind. Pharm. 33(7): 775-781.

Nakamichi, K., Nakano, T., Yasuura, H., Izumi, S. and Kawashima, Y. (2002). "The role of the kneading paddle and the effects of screw revolution speed and water content on the preparation of solid dispersions using a twin-screw extruder." Int. J. Pharm. 241(2): 203-211.

Nardin, M. and Papirer, E. (1990). "Relationship between vapor-pressure and surface-energy of liquids - application to inverse gas-chromatography." J. Colloid and Interface Sci. 137(2): 534-545.

Newell, H. E. and Buckton, G. (2004). "Inverse gas chromatography: Investigating whether the technique preferentially probes high energy sites for mixtures of crystalline and amorphous lactose." Pharm. Res. 21(8): 1440-1444.

Newell, H. E., Buckton, G., Butler, D. A., Thielmann, F. and Williams, D. R. (2001a). "The use of inverse phase gas chromatography to measure the surface energy of crystalline, amorphous, and recently milled lactose." Pharm. Res. 18(5): 662-666.

Newell, H. E., Buckton, G., Butler, D. A., Thielmann, F. and Williams, D. R. (2001b). "The use of inverse phase gas chromatography to study the change of surface energy of amorphous lactose as a

function of relative humidity and the processes of collapse and crystallisation." Int. J. Pharm. 217(1-2): 45-56.

Oguchi, T., Matsumoto, K., Yonemochi, E., Nakai, Y. and Yamamoto, K. (1995). "Dissolution studies in organic-solvents for evaluating hydrogen-bond matrix of cellulose in the ground mixture." Int. J. Pharm. 113(1): 97-102.

Ohta, M. and Buckton, G. (2004). "The use of inverse gas chromatography to assess the acid-base contributions to surface energies of cefditoren pivoxil and methacrylate copolymers and possible links to instability." Int. J. Pharm. 272(1-2): 121-128.

Otsuka, M., Matsumoto, T. and Kaneniwa, N. (1986). "Effect of environmental temperature on polymorphic solid-state transformation of indomethacin during grinding." Chem. Pharm. Bull. 34(4): 1784-1793.

Patterson, J. E., James, M. B., Forster, A. H., Lancaster, R. W., Butler, J. M. and Rades, T. (2007). "Preparation of glass solutions of three poorly water soluble drugs by spray drying, melt extrusion and ball milling." Int. J. Pharm. 336(1): 22-34.

Pentikaninen, P. J., Wan, S. H. and Azarnoff, D. L. (1974). "Bioavailability of aminosalicylic acid and its various salts in humans IV: Comparison of four brands of the sodium salt." J. Pharm. Sci. 63(9): 1431-1434.

Petrie, S. E. B. (1972). "Thermal behavior of annealed organic glasses." J. Poly. Sci. Part A-2 10(7): 1255.

Pikal, M. J., Dellerman, K. M., Roy, M. L. and Riggin, R. M. (1991). "The effects of formulation variables on the stability of freeze-dried human growth hormone." Pharm. Res. 8: 427-436.

Pikal, M. J., Rigsbee, D. R. and Roy, M. L. (1995). "The relationship between glass transition temperature and stability of freeze-dried human growth hormone." Symposia Abstract for the 10th AAPS Annual Meeting. Miami Beach, Florida: 5-9.

Planinsek, O., Trojak, A. and Srcic, S. (2001). "The dispersive component of the surface free energy of powders assessed using inverse gas chromatography and contact angle measurements." Int. J. Pharm. 221(1-2): 211-217.

Ramos, R. (2006). "Investigation of the amorphous properties of lactose and indomethacin." The School of Pharmacy, University of London. Thesis.

Riddle, F. L. and Fowkes, F. M. (1990). "Spectral shifts in acid-base chemistry 1. van der Waals contributions to acceptor numbers." J. Amer. Chem. Soc. 112(9): 3259-3264.

Rose, H. E. (1957). "A treatise on the internal mechanics of ball, tube and rod mills." London, Constable.

Roubani-Kalantzopoulou, F. (2004). "Determination of isotherms by gas-solid chromatography Applications." J. Chromat. A 1037(1-2): 191-221.

Rowe, R. C. (1988a). "Adhesion of film coatings to tablet surfaces - a theoretical approach based on solubility parameters." Int. J. Pharm. 41(3): 219-222.

Rowe, R. C. (1988b). "Interactions in the ternary powder system microcrystalline cellulose, magnesium stearate and colloidal silica - a solubility parameter approach." Int. J. Pharm. 45(3): 259-261.

Rowe, R. C. (1989). "Surface free energy and polarity effects in the granulation of a model system." Int. J. Pharm. 53(1): 75-78.

Royall, P. G., Craig, D. Q. M. and Doherty, C. (1998). "Characterisation of the glass transition of an amorphous drug using modulated DSC." Pharm. Res. 15(7): 1117-1121.

Salekigerhardt, A., Ahlneck, C. and Zografi, G. (1994). "Assessment of disorder in crystalline solids." Int. J. Pharm. 101(3): 237-247.

Salekigerhardt, A. and Zografi, G. (1994). "Nonisothermal and isothermal crystallization of sucrose from the amorphous state." Pharm. Res. 11(8): 1166-1173.

Saunders, M., Podluii, K., Shergill, S., Buckton, G. and Royall, P. (2004). "The potential of high speed DSC (Hyper-DSC) for the detection and quantification of small amounts of amorphous content in predominantly crystalline samples." Int. J. Pharm. 274(1-2): 35-40.

Schultz, J., Lavielle, L. and Martin, C. (1987). "The role of the interface in carbon fibre-epoxy composites." J. Adh. 23(1): 45 - 60.

Sekiguchi, K. and Obi, N. (1961). "Studies on absorption of eutectic mixture. In: A behaviour eutectic mixture of sulfathiazole and that of ordinary sulfathiazole in man." Chem. Pharm. Bull. 9: 866-872.

Sekiguchi, K., Obi, N. and Ueda, Y. (1964). "Studies on absorption of eutectic mixture. II. absorption of fused conglomerates of chloramphenicol and urea in rabbits." Chem. Pharm. Bull. 12: 134-144.

Sekikawa, H., Nakano, M. and Arita, T. (1978). "Inhibitory effect of polyvinylpyrrolidone on crystallization of drugs." Chem. Pharm. Bull. 26(1): 118-126.

Sekizaki, H., Danjo, K., Eguchi, H., Yonezawa, Y., Sunada, H. and Otsuka, A. (1995). "Solid-state interaction of ibuprofen with polyvinylpyrrolidone." Chem. Pharm. Bull. 43(6): 988-993.

Serajuddin, A. T. (1999). "Solid dispersion of poorly water-soluble drugs: early promises, subsequent problems, and recent breakthroughs." J. Pharm. Sci. 88(10): 1058-1066.

Shamblin, S. L., Hancock, B. C., Dupuis, Y. and Pikal, M. J. (2000). "Interpretation of relaxation time constants for amorphous pharmaceutical systems." J. Pharm. Sci. 89(3): 417-427.

Shamblin, S. L., Tang, X. L., Chang, L. Q., Hancock, B. C. and Pikal, M. J. (1999). "Characterization of the time scales of molecular motion in pharmaceutically important glasses." J. Phys. Chem. B 103(20): 4113-4121.

Shangraw, R. F. and Demarest, D. A. (1993). "A survey of current industrial practices in the formulation and manufacture of tablets and capsules." Pharm. Technol. 17: 32-44.

Sherwood, B. E., Hunter, E. A. and Staniforth, J. N. (1996). "Silicified microcrystalline cellulose (SMCC): a new class of high functionality binders for direct compression tableting." AAPS conference, New York.

Shmeis, R. A., Wang, Z. R. and Krill, S. L. (2004). "A mechanistic investigation of an amorphous pharmaceutical and its solid dispersions, part I: A comparative analysis by thermally stimulated depolarization current and differential scanning calorimetry." Pharm. Res. 21(11): 2025-2030.

Simha, R. and Boyer, R. F. (1962). "On a general relation involving the glass temperature and coefficients of expansion of polymers." J. Chem. Phys. 37: 1003-1007.

Six, K., Verreck, G., Peeters, J., Augustijns, P., Kinget, R. and Van den Mooter, G. (2001). "Characterization of glassy itraconazole: a comparative study of its molecular mobility below T-g with that of structural analogues using MTDSC." Int. J. Pharm. 213(1-2): 163-173.

Slade, L. and Levine, H. (1991). "A food polymer science approach to structure-property relationships in aqueous food systems - nonequilibrium behavior of carbohydrate-water systems." New York, Plenum Press.

Stickel, F., Fischer, E. W. and Richert, R. (1995). "Dynamics of glass-forming liquids 1. temperature-derivative analysis of dielectric-relaxation data." J. Chem. Phys. 102(15): 6251-6257.

Surana, R., Pyne, A. and Suryanarayanan, R. (2004). "Effect of preparation method on physical properties of amorphous trehalose." Pharm. Res. 21(7): 1167-1176.

Surana, R., Randall, L., Pyne, A., Vemuri, N. M. and Suryanarayanan, R. (2003). "Determination of glass transition temperature and in situ study of the plasticizing effect of water by inverse gas

chromatography." Pharm. Res. 20(10): 1647-1654.

Tanaka, K., Taura, A., Ge, S. R., Takahara, A. and Kajiyama, T. (1996). "Molecular weight dependence of surface dynamic viscoelastic properties for the monodisperse polystyrene film." Macromolecules 29(8): 3040-3042.

Tanno, F., Nishiyama, Y., Kokubo, H. and Obara, S. (2004). "Evaluation of hypromellose acetate succinate (HPMCAS) as a carrier in solid dispersions." Drug Dev. Ind. Pharm. 30(1): 9-17.

Tarelli, E., Corran, P. H., Bingham, B. R., Mollison, H. and Wait, R. (1994). "Lysine vasopressin undergoes rapid glycation in the presence of reducing sugars." J. Pharm. Biomed. Analysis 12(11): 1355-1361.

Taylor, L. S. and Zografi, G. (1997). "Spectroscopic characterization of interactions between PVP and indomethacin in amorphous molecular dispersions." Pharm. Res. 14(12): 1691-1698.

Taylor, L. S. and Zografi, G. (1998). "Sugar-polymer hydrogen bond interactions in lyophilized amorphous mixtures." J. Pharm. Sci. 87(12): 1615-1621.

te Booy, M., de Ruiter, R. and de Meere, A. (1992). "Evaluation of the physical stability of freeze-dried sucrose-containing formulations by differential scanning calorimetry." Pharm. Res. 9: 109-114.

Telang, C., Mujumdar, S. and Mathew, M. (2009a). "Improved physical stability of amorphous state through acid base interactions." J. Pharm. Sci. 98(6): 2149-2159.

Telang, C., Mujumdar, S. and Mathew, M. (2009b). "Improved physical stability of amorphous state through acid base interactions." J. Pharm. Sci. 98(6): 2149-2159.

Thielmann, F. (2004). "Introduction into the characterisation of porous materials by inverse gas chromatography." J. Chromat. A 1037(1-2): 115-123.

Ticehurst, M. D., Rowe, R. C. and York, P. (1994). "Determination of the surface properties of two batches of salbutamol sulphate by inverse gas chromatography." Int. J. Pharm. 111(3): 241-249.

Ticehurst, M. D., York, P., Rowe, R. C. and Dwivedi, S. K. (1996). "Characterisation of the surface properties of alpha-lactose monohydrate with inverse gas chromatography, used to detect batch variation." Int. J. Pharm. 141(1-2): 93-99.

Tobyn, M. J., McCarthy, G. P., Staniforth, J. N. and Edge, S. (1998). "Physicochemical comparison between microcrystalline cellulose and silicified microcrystalline cellulose." Int. J. Pharm. 169(2): 183-194.

Tong, H., Shekunov, B., York, P. and Chow, A. (2006). "Predicting the aerosol performance of dry powder inhalation formulations by interparticulate interaction analysis using inverse gas chromatography." J. Pharm. Sci. 95(1): 228-233.

Tong, P. and Zografi, G. (1999). "Solid-state characteristics of amorphous sodium indomethacin relative to its free acid." Pharm. Res. 16(8): 1186-1192.

Tsukushi, I., Yamamuro, O. and Suga, H. (1994). "Heat-capacities and glass transitions of ground amorphous solid and liquid-quenched glass of tri-O-methyl-beta-cyclodextrin." J Non-Cryst. Solids 175(2-3): 187-194.

Turnbull, D. (1987). "Undercooled alloy phases." Warrendale, PA, The Metallurgical Society.

Van den Mooter, G., Augustijns, P. and Kinget, R. (1999). "Stability prediction of amorphous benzodiazepines by calculation of the mean relaxation time constant using the Williams-Watts decay function." Eur. J. Pharm. Biopharm. 48(1): 43-48.

van Drooge, D. J. (2006). "Combining the incompatible: inulin glass dispersions for fast dissolution, stabilization and formulation of lipophilic drugs." Groningen, University of Groningen. Thesis.

van Drooge, D. J., Hinrichs, W. L. J., Visser, M. R. and Frijlink, H. W. (2006). "Characterization of the molecular distribution of drugs in glassy solid dispersions at the nano-meter scale, using differential scanning calorimetry and gravimetric water vapour sorption techniques." Int. J. Pharm. 310(1-2): 220-229.

van Krevelen, D. W. and Hoftyzer, P. J. (1976). "Properties of polymers: their estimation and correlation with chemical structure." Amsterdam; Oxford, Elsevier.

van Veen, B., Bolhuis, G. K., Wu, Y. S., Zuurman, K. and Frijlink, H. W. (2005). "Compaction mechanism and tablet strength of unlubricated and lubricated (silicified) microcrystalline cellulose." Eur. J. Pharm. Biopharm. 59(1): 133-138.

Vasanthavada, M., Tong, W. Q., Joshi, Y. and Kislalioglu, M. S. (2004). "Phase behavior of amorphous molecular dispersions I: Determination of the degree and mechanism of solid solubility." Pharm. Res. 21(9): 1598-1606.

Vasconcelos, T., Sarmento, B. and Costa, P. (2007). "Solid dispersions as strategy to improve oral bioavailability of poor water soluble drugs." Drug Dis. Today 12(23-24): 1068-1075.

Wade, A. and Weller, P. J. (1994). "Handbook of pharmaceutical excipients." Washington, American Pharmaceutical Association; London: Pharmaceutical Press.

Wang, F. J. and Wang, C. H. (2002). "Sustained release of etanidazole from spray dried microspheres

prepared by non-halogenated solvents." J. Contr. Rel. 81(3): 263-280.

Ward, S., Perkins, M., Zhang, J. X., Roberts, C. J., Madden, C. E., Luk, S. Y., Patel, N. and Ebbens, S. J. (2005). "Identifying and mapping surface amorphous domains." Pharm. Res. 22(7): 1195-1202.

Watanabe, H. (1999). "Critical rotation speed for ball-milling." Pow. Techn. 104(1): 95-99.

Watanabe, T., Hasegawa, S., Wakiyama, N., Kusai, A. and Senna, M. (2003). "Comparison between polyvinylpyrrolidone and silica nanoparticles as carriers for indomethacin in a solid state dispersion." Int. J. Pharm. 250(1): 283-286.

Watanabe, T., Hasegawa, S., Wakiyama, N., Usui, F., Kusai, A., Isobe, T. and Senna, M. (2002). "Solid state radical recombination and charge transfer across the boundary between indomethacin and silica under mechanical stress." J. Sol. State Chem. 164(1): 27-33.

Watanabe, T., Wakiyama, N., Usui, F., Ikeda, M., Isobe, T. and Senna, M. (2001). "Stability of amorphous indomethacin compounded with silica." Int. J. Pharm. 226(1-2): 81-91.

Willart, J. F. and Descamps, M. (2008). "Solid state amorphization of pharmaceuticals." Mol. Pharm. 5(6): 905-920.

Won, D. H., Kim, M. S., Lee, S., Park, J. S. and Hwang, S. J. (2005). "Improved physicochemical characteristics of felodipine solid dispersion particles by supercritical anti-solvent precipitation process." Int. J. Pharm. 301(1-2): 199-208.

Wu, S. (1971). "Calculation of interfacial tension in polymer systems." J. Polymer Sci. C-Polymer Symposium (34): 19.

Wu, T., Sun, Y., Li, N., de Villiers, M. M. and Yu, L. (2007). "Inhibiting surface crystallization of amorphous indomethacin by nanocoating." Langm. 23(9): 5148-5153.

Wu, T. and Yu, L. (2006). "Surface crystallization of indomethacin below T_g." Pharm. Res. 23(10): 2350-2355.

York, P., Ticehurst, M. D., Osborn, J. C., Roberts, R. J. and Rowe, R. C. (1998). "Characterisation of the surface energetics of milled dl-propranolol hydrochloride using inverse gas chromatography and molecular modelling." Int. J. Pharm. 174(1-2): 179-186.

Yoshioka, S. and Aso, Y. (2005). "A quantitative assessment of the significance of molecular mobility as a determinant for the stability of lyophilized insulin formulations." Pharm. Res. 22(8): 1358-1364.

Yu, L. (2001). "Amorphous pharmaceutical solids: preparation, characterization and stabilization." Adv. Drug Deliv. Rev. 48(1): 27-42.

Zallen, R. (1983). "The physics of amorphous solids." New York, Wiley.

Zhang, F., Aaltonen, J., Tian, F., Saville, D. J. and Rades, T. (2009). "Influence of particle size and preparation methods on the physical and chemical stability of amorphous simvastatin." Eur. J. Pharm. Biopharm. 71(1): 64-70.